



TNT 2010

Trends in NanoTechnology

Braga (Portugal)
September 06-10, 2010

PHANTOMS
foundations



Universidad
de Oviedo

INL
INTERNATIONAL IBERIAN
NANOTECHNOLOGY
LABORATORY

UAM
UNIVERSIDAD AUTONOMA
DE MADRID

**UNIVERSITAS
FRIBURGENSIS**

UAB

Universitat Autònoma de Barcelona



ibec Institute for Bioengineering
of Catalonia



UNIVERSITAT DE BARCELONA

leti

CIC
nanogUNE
NANOSCIENCE COOPERATIVE RESEARCH CENTER

cea

**Georgia
Tech**

dipc
Dipartimento di Fisica

NIMS
Nanomaterials Laboratory



On behalf of the International, Scientific and Technical Committees, we take great pleasure in welcoming you to Braga (Portugal) for the 11th "Trends in NanoTechnology" (TNT2010) International Conference.

TNT2010 is being held in large part due to the overwhelming success of earlier TNT Nanotechnology Conferences and will be organised in a similar way to the prior events. This edition will take place in Braga to emphasise the importance at the Portuguese and European level of the Nanoscience and Nanotechnology activity of the Northern Portugal region and in particular the launch in 2010 of the International Iberian Nanotechnology Center (INL).

This high-level scientific meeting series aims to present a broad range of current research in Nanoscience and Nanotechnology worldwide, as well as initiatives such as EU/ICT/FET, GDR-I/Nano-I, MANA, CIC nanoGUNE Consolider, Synergys, INL, etc. TNT events have demonstrated that they are particularly effective in transmitting information and promoting interaction and new contacts among workers in this field. Furthermore, this event offers visitors and sponsors an ideal opportunity to interact with each other.

One of the main objectives of the Trends in Nanotechnology conference is to provide a platform where young researchers can present their latest work and also interact with high-level scientists. For this purpose, the Organising Committee provides every year around 100 travel grants for students. In addition, this year, 19 awards (5100 Euros in total) will be given to young PhD students for their contributions presented at TNT. More than 60 senior scientists are involved in the selection process. Grants and awards are funded by the TNT Organisation in collaboration with several governmental and research institutions.

TNT is now one of the premier European conferences devoted to nanoscale science and technology with around 350-400 participants worldwide.

We are indebted to the following Scientific Institutions, Companies, Individuals and Government Agencies for their help and financial support: Phantoms Foundation, International Iberian Nanotechnology Laboratory (INL), Donostia International Physics Center (DIPC), CIC nanoGUNE Consolider, Universidad Autónoma de Madrid, Universidad Complutense de Madrid, Universidad de Oviedo, University of Purdue, Georgia Institute of Technology, CEA/LETI, Universidad de Barcelona, Institute for Bioengineering of Catalonia (IBEC), Universidad Autónoma de Barcelona, Instituto Español de Comercio Exterior (ICEX) & "españa-technology for life" program, NIMS (Nanomaterials Laboratory) and MANA (International Center for Materials and Nanoarchitectonics), University of Fribourg and frimat, Adolphe Merkle Institute, NSERC/CRSNG (Nano Innovation Platform), GDR-I/Nano-I, Centro de Investigación en Nanomateriales y Nanotecnología (CINN), Fundación Itma, Ministerio de Ciencia e Innovación, FEI Company, IJ Cambria Scientific, Fundação para a Ciência e a Tecnologia (FCT), nanoICT Coordination Action, Minatec and Wiley-VCH.

We would also like to thank the following companies and Institutions for their participation: Nanotec Electronica, Hamamatsu, Raith, Wiley-VCH, Atomic Force, Telstar, SMA/Annealsys, Phantoms Foundation, ICEX, Innovnano, Zeiss, Accelonix, Attocube Systems, Scientec, Izasa and Norconcessus.

In addition, thanks must be directed to the staff of all the organising institutions whose hard work has helped the planning and organisation of this conference.

The Organising Committee



TNT2010 ORGANISING COMMITTEE

Jose-Maria Alameda (Universidad de Oviedo, Spain)
Masakazu Aono (MANA / NIMS, Japan)
Robert Baptist (CEA / DRT / LETI, France)
Xavier Cartoixa (Universidad Autonoma de Barcelona, Spain)
Antonio Correia (Phantoms Foundation, Spain)
Pedro Echenique (Donostia International Physics Center - DICP / UPV, Spain)
Jose Maria Gonzalez Calbet (Universidad Complutense de Madrid, Spain)
Uzi Landman (Georgia Tech, USA)
Jose Maria Pitarke (CIC nanoGUNE Consolider, Spain)
Ron Reifenger (Purdue University, USA)
Jose Rivas (INL, Portugal)
Juan Jose Saenz (Universidad Autonoma de Madrid, Spain)
Josep Samitier (IBEC - Universitat de Barcelona, Spain)
Frank Scheffold (University of Fribourg, Switzerland)

*Contact person: antonio@phantomsnet.net

TNT2010 INTERNATIONAL SCIENTIFIC COMMITTEE

Masakazu Aono (MANA / NIMS, Japan)
Andreas Berger (CIC nanoGUNE Consolider, Spain)
Fernando Briones (IMM / CSIC, Spain)
Alexander Bittner (CIC nanoGUNE Consolider, Spain)
Remi Carminati (Ecole Centrale Paris, France)
Jose-Luis Costa Kramer (IMM / CSIC, Spain)
Antonio Garcia Martin (IMM / CSIC, Spain)
Pierre Legagneux (Thales, France)
Annick Loiseau (ONERA - CNRS, France)
Rodolfo Miranda (Universidad Autonoma de Madrid, Spain)
Stefan Roche (CEA / INAC, France & CIN2, Spain)
Josep Samitier (IBEC – Universitat de Barcelona, Spain)

TNT2010 TECHNICAL COMMITTEE

Carmen Chacon (Phantoms Foundation, Spain)
Viviana Estêvão (Phantoms Foundation, Spain)
Maite Fernández Jiménez (Phantoms Foundation, Spain)
Luis Froufe (ICMM / CSIC, Spain)
Paloma Garcia Escorial (Parque Científico de Madrid, Spain)
Pedro Garcia-Mochales (Universidad Autonoma de Madrid, Spain)
Adriana Gil (Nanotec, Spain)
Manuel Marques (Universidad Autonoma de Madrid, Spain)
Concepción Narros Hernández (Phantoms Foundation, Spain)
Joaquin Gaspar Ramon-Laca Maderal (Phantoms Foundation, Spain)

TNT2010 POSTER AWARDS

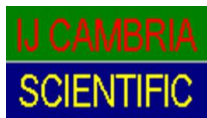
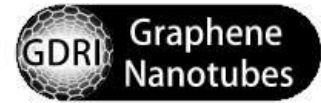
Funded by	Award
	NSERC-CRSNG (NanoIP) 300 Euros
	NSERC-CRSNG (NanoIP) 300 Euros
	NSERC-CRSNG (NanoIP) 300 Euros
	NSERC-CRSNG (NanoIP) 300 Euros
	FCT - Portugal 300 Euros
	FCT - Portugal 300 Euros
	FCT - Portugal 300 Euros
	FCT - Portugal 300 Euros
	NIMS/MANA 300 Euros
	IBEC 300 Euros
	CIC nanogUNE Consolider 250 Euros
	GDR-I on Science and Applications of Nanotubes 200 Euros
	Wiley-VCH Book voucher of 200 Euros
	PHANTOMS Foundation Ipod Nano
	PHANTOMS Foundation Ipod Nano
	PHANTOMS Foundation Ipod Nano
Private Donation	- David Prize: 300 US Dollars
Private Donation	- Keren Prize: 300 US Dollars
	TNT2010 Organisation Free registration to the 2011 Conference

TNT2010 PLATINUM SPONSORS

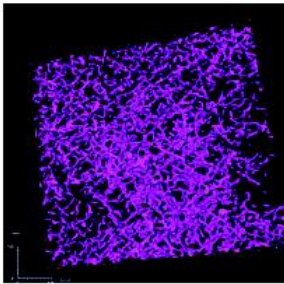


FCT Fundação para a Ciência e a Tecnologia
MINISTÉRIO DA CIÊNCIA, TECNOLOGIA E ENSINO SUPERIOR Portugal

SPONSORS

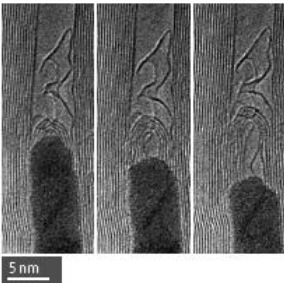


Solutions for applied Materials Research



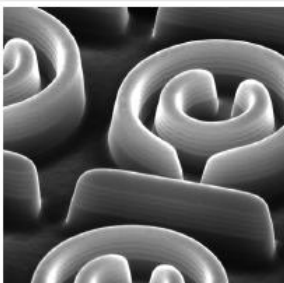
Electron tomography enables 3D visualization of nanonetworks, such as this polymer solar cell material

Courtesy of Joachim Loos, Eindhoven University of Technology, Netherlands



Materials confined within nanotubes provide an *in situ* atomic scale chemical reaction chamber in the TEM

Courtesy of Julio A. Rodriguez-Manzo, and Mauricio Terrones, IPICT, Mexico Florian Banhart, Universitaet Mainz, Germany



Split-ring resonator array with a critical dimension of 120 nm, prepared directly by FIB

3D NanoCharacterization

discover down to the atomic scale

in situ NanoProcesses

experiment down to the atomic scale

3D NanoPrototyping

create down to the nanoscale

See beyond at fei.com/research

TNT2010 EXHIBITORS



TNT2010 EXHIBITORS



Nanotec Electronica is one of the leading companies in the Nanotechnology Industry. In only ten years Nanotec Electronica has established itself as one of the strongest companies that design, manufacture and supply Scanning Probe Microscopes (SPM). Our highly qualified team uses cutting-edge technology in order to provide a cost-effective tool to gain access to the nanometer scale for both scientific and industrial communities. With its headquarters based in Spain and distributors located around the world, Nanotec ensures global presence and guarantees total customer satisfaction.

Nanotec's Cervantes FullMode Atomic Force Microscope (AFM) in its several configurations allows not only imaging samples with atomic precision but also the study of magnetic, electronic and mechanical properties at the nanoscale, making it a powerful tool for physicists, chemists, biologists and engineers willing to characterize their samples at the nanometer scale. Its robust design provides strong mechanical stability to ensure high imaging resolution, and its semi-automated and open design allows scientists to exploit the capability of SPM to its maximum for both research and academic purposes.

Nanotec Electronica also provides Dulcinea Control Systems, with an open and modular design that facilitates interfacing with any other standard AFM/SNOM/STM system available in the market. Highly versatile, it allows different modes of operation from Contact Mode to Frequency Modulation Mode and lithography ensuring a reliable and accurate performance of all SPM systems.

Nanotec has also developed and freely distributes SPM software WSxM. Its user-friendly interface ensures easy operation of SPM microscopes and data processing. WSxM is available for its free download at www.nanotec.es.

If you have any questions, or want any information about Nanotec Electronica, please contact us at:

Centro Empresarial Euronova 3
Ronda de Poniente 12, 2º C
28760 Tres Cantos (Madrid) **SPAIN**
Tel: +34-918043347
www.nanotec.es



attocube systems AG manufactures and distributes a complete line of easy-to-use scanning probe microscopes and nanopositioning systems for temperatures in the range from 300 K down to 10 mK! The innovative nanopositioners are also compatible with high vacuum and ultra high vacuum environments as well as with high magnetic fields up to 31 Tesla.

Central to our proven suite of low temperature microscopes is our powerful combination of fully automated and absolute reliable low temperature positioning devices with modular and flexible scanning probe sensors, designed specially to meet the needs of today's low temperature research. Our instruments give users the ability to analyze samples down to the atomic level, even at Milli-Kelvin temperatures.

attocube systems AG
Koeniginstr. 11a RGB
80539 Muenchen, **GERMANY**
Phone: 0049-89-2877809-0
Fax: 0049-89-2877809-19
Email: info@attocube.com
Web: www.attocube.com

HAMAMATSU

PHOTON IS OUR BUSINESS

Hamamatsu is dedicated to using photonics technologies to address the needs of mankind through practical application, as well as using photons as a tool to create scientific knowledge and explore matter, energy, distance and time.

Our manufacturing divisions support our vision by the design, manufacture and sales of products for the detection and generation of light, which our customers apply in fundamental research in diverse fields. Many sensors which were made using conventional methods need to be completely redesigned using new nanotechnologies. In addition, the possibilities of these techniques open new challenges for new application dedicated to biology, drug discovery and medical fields.

3 700 people work for Hamamatsu all over the world.

In Europe Sales offices operate in France, Germany, UK, Italy, Sweden, Belgium, Switzerland, Spain and Portugal.

HAMAMATSU

Centro de Empresas de Nuevas Tecnologías
Parque Tecnológico del Vallés
E-08290 Cerdanyola (Barcelona) **SPAIN**
Phone : +34 93 582 44 30
Fax : +34 93 582 44 31

Please contact us at spain@hamamatsu.com or visit our web page www.hamamatsu.es for more information.

norconcessus

Equipamentos de Laboratório e Científicos, Lda.

Norconcessus – Laboratory and Scientific Equipment, Lda. is a company specialized in the development of integrated turn-key solutions, providing both furniture and equipment for Laboratories and Quality Control. Norconcessus and its business partners, Concessus and Aralab, have brought up a solid corporation directed to **I&D**, with both national and international relevance, build up through the experience and technical know-how gathered along over 4 decades of existence and more than 20 years manufacturing climatic chambers and cold storage devices. Norconcessus also offers physical test machines, bioreactors, laminar flow cabinets, ovens and microscopes, among others, which are criteriously selected to meet and overcome our customer's needs and expectations, supported by a fully committed team of highly trained professionals.

To find out more about Norconcessus, please contact us at:

Trav. Monte da Bela, N. 93, Arm J
4445 – 294 Ermesinde ▪ **PORTUGAL**
Tel.: (+351) 225 420 640 ▪ Fax:(+351) 225 420 649
norcomercialsaude@nor.com.pt ▪ www.nor.com.pt

WILEY-VCH

Wiley-VCH bundles its publishing activities in the various business areas of natural and engineering sciences as well as economics. The company provides publications with the best possible distribution on an international scale, coupled with a high standard of quality. From providing students with the basic literature needed, via primary research right up to the latest laboratory methods and research results into active substances: company focus on specific areas of expertise covers the entire spectrum of human knowledge.

WEB: www.wiley-vch.de



For more than two decades Raith GmbH has been developing and selling high-tech systems in the domain of nanotechnology worldwide.

Main areas of operations are designing and manufacturing of systems enabling fabrication of superfine surface structures down to the range of less than 10 nanometers (electron and ion beam lithography) and semiconductor inspection tools for industry (defect review).

Renowned customers such as Infineon Technologies or the Massachusetts Institute of Technology in Boston avail themselves of the know-how Raith has acquired since its early being in business.

With its highly educated staff of physicists, engineers and technicians Raith offers optimum service and support for answers to technical and application related questions.

Worldwide Raith qualifies its personnel to provide fast and competent help to its customer requests.

Since 1985 Raith has pioneered the way for SEM lithography. Today complete turnkey lithography system solutions complement Raith product portfolio. These systems are used in state-of-the-art research in Physics, Electrical Engineering and other R&D related fields.

Raith GmbH
Hauert 18 - Technologiepark
44227 Dortmund **GERMANY**
Phone: +49 (0)231 / 975000-0
Fax: +49 (0)231 / 975000-5
E-mail: sales@raith.com
Web: www.raith.com



Since 1992 Suministro de Materiales y Asistencia has been founded with the finality to dedicate it to the microelectronics.

The company is dedicated to the distribution of microelectronic equipment.

Representing the most important companies specialized in this sector, like SussMicrotec, SET and Annealsys and being one of the unics companies in Spain dedicated to sale this type of equipment. Suppliers of process and testing solutions for markets as Advanced Packaging, MEMS, Nanotechnology, Compound Semiconductor, Silicon-On-Insulator and 3D Interconnect and systems for RTP, LPCVD and MOCVD.

Working with the most important private companies, universities and public institutions of Spain.

You can find more information in:
Suministro de Materiales y Asistencia SL
C/Caracas 6
28760 Tres Cantos, Madrid, **SPAIN**
Tel: +34 91 803 31 86
Fax: +34 91 803 86 85
email: smasl@arrakis.es
Web: www.smamicroelectronica.com



TELSTAR INSTRUMAT, S.L. develops high technology instrumentation sales for research and industry, offering suitable technological tools adapted to each application, in order to improve the scientific researches or productive processes of our clients. In these last few years, TELSTAR INSTRUMAT has strengthened its activities representing leading companies in Spain & Portugal in the following applications:

- Surface and material characterisation and metrology
- ThinFilm deposition systems
- Vacuum and cryogenics instrumentation and technology
- Radiometry and photometry

TELSTAR INSTRUMAT, S.L. counts amongst its customers the principal Official Organisation Investigation Centres and private customers in the microelectronic, aerospace, automotive, optical, food and pharmaceutical industries and in innovative fields such as biotechnology and nanofabrication.

Some of our principals that are specifically of interest for the attendees to this conference are listed below:

- Veeco Instruments (SPM, Optical and Mechanical Profilers)
- Sopralab (ellipsometry and thin film pororisty)
- MicroMaterials Ltd (Nanoindentation Systems)
- SPECS GmbH (Surface Analysis, XPS, AFM-STM in UHV)

The company's head office is in Sant Cugat del Vallès (Barcelona) and it also has a branch office in Madrid.

Telstar Instrumat, S.L.
Avda. Alcalde Barnils, 70, 3ª Planta
08174 Sant Cugat del Vallès **SPAIN**
Tel. +34 935 442 320
Fax. +34 935 442 911

C/ Santibáñez de Béjar, 228042 Madrid
Tel. +34 913 717 511
Fax. +34 917 477 538
Web: www.telstar-instrumat.com
E-mail: comercial@telstar-instrumat.com



The **Spanish Institute for Foreign Trade (ICEX)** ("Instituto Español de Comercio Exterior") is the Spanish Government agency serving Spanish companies to promote their exports and facilitate their international expansion, assisted by the network of Spanish Embassy's Economic and Commercial Offices and, within Spain, by the Regional and Territorial Offices.

It is part of the Spanish Ministry of Industry, Tourism and Trade ("Ministerio de Industria, Turismo y Comercio").

ICEX: www.icex.es
España, Technology for life: www.spainbusiness.com



The **Phantoms Foundation** (non-profit organisation) was established on November 26, 2002 (in Madrid, Spain) to provide high level Management profile to National and European scientific projects. The Phantoms Foundation works in close collaboration with Spanish and European Governmental Institutions such as MEC (Spanish Ministry of Science) and ICEX (Spanish Institute for Foreign Trade), or the European Commission to provide focused reports on Nanoscience & Nanotechnology related research areas (infrastructure needs, emerging research, etc.) and develop activities to stimulate commercial nanotechnology applications (Spanish Pavilion at nanotech2008).

WEB: www.phantomsnet.net



Innovnano is a young company, located in Lisbon & state of the art production plant in South of Portugal. Innovnano is part of CUF, centenary in the chemical industry. CUF being the largest Portuguese chemical group, with production facilities in Portugal & Spain. Innovnano takes advantage of its unique & innovative proprietary process for the synthesis of micro & nano particles. Our Value Proposal: Challenge our Process

- High Pressure Continuous Process
- High Purity Materials
- Quality Product Range: Nanomaterials & Advanced Ceramics
- Up-scaling, Reproducibility & Reliability
- Competitive Production Method

Philippe Guerineau
Innovnano
Lagoas Parque, Edif. 6 - Piso 2, 2740-244 Porto Salvo **PORTUGAL**
Tel: +351 9275 18558
Email: Philippe.guerineau@innovnano.pt
web: www.innovnano.pt
Phone: +34 93 309 79 16
Fax: +34 93 485 05 94
E-mail: spain@helmutfischer.com
Web: www.helmut-fischer.com



The Electron Microscopy Division is an integral part of **Carl Zeiss** developing, producing, selling and servicing SEM, TEM and Particle Beam instruments designed to set unique high quality standards and to provide customer focused solutions for the Semiconductor, Material Analysis and Life Science application fields worldwide. Development and production facilities are based in Oberkochen (Germany), Peabody, MA (USA) and Cambridge (UK).

The history of electron microscopy at Carl Zeiss dates back to 1949 when the first commercial TEM was launched. Nowadays, the company's extensive know-how also comprises ion-beam technology and e-beam based analysis technology enable us to deliver innovative solutions for your business. Our global applications and service network guarantees fast, reliable and high quality support focussed on customer requirements. Combined with dedicated upgrade strategies, this will protect your investment for its entire lifetime.

The New and Powerful Combination of FIB and GEMINI® Column: NVision 40®. and AURIGA®

For more information, please contact:

Carl Zeiss Microimaging, S.L.

c/Frederic Mompou,3

08960 Sant Just Desvern **SPAIN**

Tel.: + 34 93 480 29 52 / Fax: + 34 93 371 76 09

web: www.zeiss.es/micro



Accelonix is a fast track to the future – supplying our customers with leading edge technology and cleverly engineered advantages. Helping you stay ahead of your competitors.

We specialise in a number of key areas and are regularly developing our product lines, talking to our customers and our suppliers. So check for our latest news - and click to our products and services above to find out more.

In the Microelectronics business, speed and accuracy are key - but we understand that keeping up with your customers as well as with the speed of change can be a real challenge. So we do all we can to help you stay ahead.

We introduce innovative technologies and products to the electronics industry. We're a fast track to the future and an old-fashioned friendly hand.

We don't simply help you find a better way of doing things, we help you keep pace with technology as it evolves, pre-empting problems in good time and recommending solutions that exactly match your needs. Owning the issues with you - helping you break through barriers.

In a fast moving sector, we take time to understand your particular outlook, aims and challenges, so we can help you find that elusive solution - a better way. Then we move with you offering innovative products, thorough technical support and simple informed advice.

Our job is to keep you ahead.

For more information, please contact:

Accelonix Ibérica S.L.



ScienTec Ibérica, is the spanish branch of **ScienTec** France, its mission is to serve and attend the Iberian market from the office in Madrid.

ScienTec, as a whole, is specialized in the distribution of rigorously selected scientific equipments focused in the field of Nano-micro surface analysis, providing you a complete solution for your experimental or metrological needs

With more than 10 years experience in Nanotechnology, our sales ingeniers will help you define the right tool and configuration, our application group will teach and help you run the machines and our after sales team will preventively maintain or repair your systems.

Your investment will be back up with a perfect combination of top level instruments with the know how and tool expertise in the distribution.

By Nanocharacterization at **ScienTec** we mean:

Scanning Probe Microscopies : AFM – STM from **Agilent Technologies**

Optical Nanocaracterization: SNOM from **Nanonics**

Mechanical Nanocaracterization: **NanoIndenter** from Agilent (formerly MTS)

Digital Holographical Microscopy: from **Lyncée Tec**

Optical and mechanical profilometry : from **KLA Tencor**

Digital Fluorescence Optical Microscopy: from **Till Photonics**

Thin Film thickness: reflectrometers from **Filmetrics**

Accesories and SPM consumables.

Our main principal, Agilent Technologies, a leading player in the SPM market, provides innovative scanning probe microscopy (SPM) solutions for all academic research and industrial applications. **Agilent Technologies** Microscopes are the preferred choice to measure in liquids, temperature variation, electrochemical conditions, enviromental control or high resolution measurements. The acquisition of the Nano Instruments business have strengthen Agilent's portfolio of instrumentation for imaging, characterizing and quantifying nano-mechanical material properties.

The internal research collaboration among the differents business units at Agilent are bringing new exciting techniques to the SPM industry such as the exclusive Scanning Microwave Microscopy (SMM).

Further developments are in the pipeline.

Please contact us at:

ScienTec Ibérica

C/ Buenavista 4 Bajo

28250 Torrelodones (Madrid) **SPAIN**

Phone: +34 91-8429467

Fax: +34 902-875572

Please contact us at info@scientec.fr or visit our web page www.scientec.es for more information.



The Scientific Instrumentation Group **of IZASA** constitutes the principal Organization in Spain and Portugal specialized in distributing instruments and consumables for Industries and Research Centres, the Group supplies laboratories with high technology equipment from the most outstanding international firms.

With more than 30 years of experience and a service vocation to the Scientific Community, the Group has become a main solution provider for our customers The Group employs 129 people covering Spain and Portugal through 14 branch offices.

The Scientific Instrumentation Group develops its activities in different areas such as Research in Materials and Life Science, Industrial quality control, environmental and process monitoring, etc.

The physical Instrumentation division is focused on providing solutions for the nanostructural research. Our most important partners for this aim are:

- JEOL (Electron Optics: SEM, TEM, EPMA, AES,...)
- Rigaku (XRD, WDXRF)
- SkyScan (uCT)
- WITec (AFM, Confocal Raman Microscopy and SNOM)
- Picosun (Atomic Layer Deposition)
- Kleindiek Nanotechnik (Nanomanipulation tools)

You can find us on the internet at www.izasa.es or www.izasa.pt. Contact: dac2@izasa.es

Head offices:

IZASA S.A.
Aragoneses, 13
28108 Alcobendas (Madrid) **SPAIN**

IZASA Portugal S.A.
Rua do Proletariado, 1
Quinta do Paizinho
2795-648 Carnaxide **PORTUGAL**



in collaboration with



presents

"PASSPORT TO PRIZES" PROGRAM

At this new edition of the Trends in Nanotechnology conference we are pleased to organise the TNT2010 "Passport to Prizes" program.

How does the "Passport to Prizes" program work?

Each TNT2010 conference attendee will find a passport card inside his TNT2010 conference bag. You will take your card around the exhibit hall on Monday, Tuesday and Wednesday. Take this opportunity to visit the stands that the exhibitors have prepared, and to learn about the companies and their new products. Each exhibiting company has received a stamp with a number. Attendees will be responsible for collecting stamps from the participating exhibitors that are listed on their passport.

Once you have completed your passport card with a minimum of 13 stamps, **fill in your personal data** and take the card to the ticket tumbler located in the Registration Area. Please, do not forget to complete the passport card with your name and institution before you put it into the box.

All completed entries will be eligible for a prize drawing that will be conducted on the evening of Wednesday (08/09/2010) during the Poster Award Ceremony.

Do not miss this opportunity to win one of our **two Digital Cameras** (donated by Phantoms Foundation).

And remember that winners need to be present to win. So... see you at the conference dinner and the poster award ceremony!



SCIENTIFIC PROGRAM

TNT2010 - POSTER PRESENTATION DETAILS

Poster size: A0 format (width: 841 mm x Height: 1189 mm) (Portrait)

Posters should be installed on Monday morning and removed on Friday before 12h00



I: Invited Lecture (40 min. including discussion time)

K: Keynote Lecture (30 min. including discussion time)

O: Oral Presentation (15 min. including discussion time)

PS: Poster Session

SCIENTIFIC PROGRAM - TNT2010
Monday – September 06, 2010

08h00-09h00	REGISTRATION	
09h00-09h10	TNT2010 Opening Ceremony - Welcome and Introduction	
	Chairman: José Rivas (INL, Portugal)	
09h10-09h50	Uzi Landman (Georgia Institute of Technology, USA) <i>"Small is different: physics and chemistry in the non-scalable nano regime"</i>	I
p. 11		
09h50-10h20	Katsuhiko Ariga (MANA / NIMS, Japan) <i>"Supramolecular Materials & Hand-Operating Nanotechnology for Novel Functions"</i>	K
p. 15		
10h20-11h00	Coffee Break - Poster Session - Instrument Exhibition	
	PS	
"Nanobiotechnology" Session – Sponsored by IBEC/UB (Spain)  Chairman: Elena Martinez (IBEC, Spain)		
11h00-11h30	Janos Vörös (ETH-Zentrum, Switzerland) <i>"Nanotechnology Approaches for Enhancing the Sensitivity and Throughput of Biosensors"</i>	K
p. 63		
11h30-12h00	Valentyn Novosad (Argonne National Laboratory, United States) <i>"Spin vortices: from fundamental physics to biomedical applications"</i>	K
p. 45		
12h00-12h15	Ricardo Franco (REQUIMTE, Portugal) <i>"Malaria Diagnostics based on Antibody-Functionalized Gold Nanoparticles and Plasmodium falciparum Hsp70"</i>	O
p. 89		
12h15-12h30	Ronny Szech (Technische Universität Dresden, Germany) <i>"Diffusion of DNA polymer molecules in nanochannels"</i>	O
p. 117		
12h30-12h45	Maria Holmberg (Technical University of Denmark, Denmark) <i>"Protein Adsorption on Biomaterials - Atomic Force Microscopy and Radioactive Labeling Analysis"</i>	O
p. 95		
12h45-13h00	Dario Pisignano (Università di Lecce, Italy) <i>"Polymer Electrospun Nanofibers as Building Blocks for Nanotechnology"</i>	O
p. 113		
13h00-15h00	Lunch (*)	
"Self-Assembly" Session – Sponsored by CIC nanoGUNE (Spain)  Chairman: Alexander Bittner (nanoGUNE, Spain)		
15h00-15h40	Klaus Kern (Max-Planck-Institut für Festkörperforschung, Germany) <i>"Nanoscale electronic contacts"</i>	I
p. 9		
15h40-16h10	Ehud Gazit (Tel Aviv University, Israel) <i>"Self-Assembled Peptide Nanostructures: A New Frontier in Organic Nanotechnology"</i>	K
p. 23		
16h10-16h40	Mato Knez (Max-Planck-Institut fuer Mikrostrukturphysik, Germany) <i>"Atomic Layer Deposition - An old technique for modern nanoscience"</i>	K
p. 33		
16h40-17h10	Magali Lingenfelder (ICMAB-CSIC, Spain) <i>"Chiral recognition on surfaces: from single molecule tracking to 3d crystals"</i>	K
p. 39		
17h10-17h40	Tuomas Knowles (Nanoscience Centre – Univ. of Cambridge, UK) <i>"Protein nanofibrils"</i>	K
p. 35		
17h40-20h00	Coffee Break - Poster Session - Instrument Exhibition	
	PS	
20h00	WELCOME RECEPTION at INL	

(*) Lunch will be served at INL for those who booked

SCIENTIFIC PROGRAM - TNT2010
Tuesday – September 07, 2010

Chairman: Sebastiaan van Dijken (Aalto University, Finland)		
08h30-09h00	Kohei Uosaki (MANA / NIMS, Japan) <i>"Formation, Characterization and Catalytic Properties of Metal Nanoclusters within Molecular Layers"</i>	K
p. 59		
09h00-09h15	Eulália Pereira (REQUIMTE-Universidade do Porto, Portugal) <i>"Green Photocatalytic Synthesis of Au and Ag Nanoparticles: Size and Shape Control"</i>	O
p. 111		
09h15-09h30	Manuel Arturo Lopez Quintela (University of Santiago de Compostela, Spain) <i>"Small sub-nm metal clusters: the key missing point in many catalytic processes?"</i>	O
p. 101		
09h30-09h45	Carole Fauquet (Université de la Méditerranée, France) <i>"Combining Scanning Probe Microscopy and X-Ray Spectroscopy to Obtain Simultaneously Surface Topography and Chemical Mapping"</i>	O
p. 85		
09h45-10h00	Meiken Falke (Bruker Nano GmbH, Germany) <i>"Analysis of Carbon- and other Nano-Structures using Si Drift Detectors in Energy Dispersive X-ray Spectroscopy"</i>	O
p. 83		
10h00-11h00	Coffee Break - Poster Session - Instrument Exhibition	PS
Chairman: Andreas Berger (nanoGUNE, Spain)		
11h00-11h30	Roy Chantrell (The University of York, UK) <i>"Multiscale magnetic models of ultrafast magnetic processes"</i>	K
p. 19		
11h30-12h00	Sebastiaan van Dijken (Aalto University, Finland) <i>"Pattern Transfer and Lateral Switching Modulation in Multiferroic Heterostructures"</i>	K
p. 61		
12h00-12h15	Bertrand Raquet (LNCMI, France) <i>"Magnetic Edges Current and Disorder in Graphene Nano-Ribbons"</i>	O
p. 115		
12h15-12h30	Felix Casanova (CIC nanoGUNE, Spain) <i>"Asymmetric spin injection at high current bias in all-metallic lateral spin valves"</i>	O
p. 77		
12h30-12h45	Weisheng Zhao (IEF, CNRS/Univ. Paris Sud 11, France) <i>"A Compact Model for the Magnetic Tunnel Junction Switched by Thermally Assisted Spin Transfer Torque (STT+TAS)"</i>	O
p. 121		
12h45-13h25	David Awschalom (University of California, USA)	I
p. -		
13h25-15h30	Lunch (*)	
15h30-16h45	Parallel Session: "PhD" I	
	Parallel Session: "PhD" II	
16h45-17h45	Coffee Break - Poster Session - Instrument Exhibition	
17h45-19h30	Parallel Session: "PhD" III	
	Parallel Session: nanoResearch in Portugal	

(*) Lunch will be served at INL for those who booked

Parallel Sessions Program 

SCIENTIFIC PROGRAM - TNT2010
Tuesday – September 07, 2010

"PhD" Parallel Session I		
Chairman: Antonio Garcia Martin (IMM-CSIC, Spain)		
15h30-15h45	Si-Yu Liao (Université Bordeaux 1, France) <i>"Non-volatile memory using Optically-Gated Carbon Nanotube FET: Description of carrier mobility model in P3OT and source-drain Schottky barrier"</i>	O
p. 141		
15h45-16h00	Raquel M. Da Costa Martins (Universidad de Navarra, Spain) <i>"Bioadhesive mannosamine-loaded nanoparticles for an effective ocular vaccination against animal brucellosis"</i>	O
p. 133		
16h00-16h15	Aliaksandra Rakovich (Trinity College Dublin, Ireland) <i>"Development of Nano-Bio hybrid material based on CdTe Quantum Dots and Bacteriorhodopsin protein for future technologies"</i>	O
p. 151		
16h15-16h30	Daniel Carmona (Instituto de Nanociencia de Aragon, Spain) <i>"Silica rod-shape capsules embbebing superparamagnetic iron oxide nanoparticles"</i>	O
p. 129		
16h30-16h45	Jose Maria Porro Azpiazu (CIC nanoGUNE, Spain) <i>"Effects of asymmetric dipolar interactions between elliptical ferromagnetic nanomagnets in artificial spin-ice structures"</i>	O
p. 149		
16h45-17h45	Coffee Break - Poster Session - Instrument Exhibition	PS

SCIENTIFIC PROGRAM - TNT2010
Tuesday – September 07, 2010

"PhD" Parallel Session III		
Chairman: Pedro Garcia Mochales (UAM, Spain)		
17h45-18h00	Maria Fernanda Cardinal (University of Vigo, Spain) <i>"Modulation of Localized Surface Plasmons and SERS Response in Gold Dumbbells through Silver Coating"</i>	O
p. 127		
18h00-18h15	Marta Castro Lopez (ICFO - The Institute of Photonic Sciences, Spain) <i>"Observation of polarized multiphoton emission from resonant Al, Ag and Au nanoantennas"</i>	O
p. 131		
18h15-18h30	Aya Fujiki (Osaka university, Japan) <i>"Tunneling-current-induced light emission from PTCDI-C7 thin films on the graphite and the Au(111) surfaces"</i>	O
p. 139		
18h30-18h45	Matthew Morantz (McGill University, Canada) <i>"Synthesis, Nanostructural and Electronic Characterization of Anthracenedicarboximide Derivatives"</i>	O
p. 147		
18h45-19h00	Florent Roussel (Laboratoire Francis Perrin - CEA/DSM/IRAMIS/SPAM, France) <i>"1D polymer/CNT composite : elaboration and transport properties"</i>	O
p. 153		

SCIENTIFIC PROGRAM - TNT2010
Tuesday – September 07, 2010

Parallel Session: "PhD" Parallel Session II Chairman: Paulo Freitas (INL, Portugal)		
15h30-15h45 p. 125	Rita Branquinho (FCT-UNL/Cenimat, Portugal) <i>"Room Temperature Sputtered Ta₂O₅ for Solid State Biosensors"</i>	O
15h45-16h00 p. 143	Raquel Maia (INEB/INL, Portugal) <i>"Development of nanostructured 3D matrices to direct mesenchymal stem cells behaviour"</i>	O
16h00-16h15 p. 145	Diana Martín Becerra (IMM-CNM-CSIC, Spain) <i>"Wavelength dependence of the SPP wavevector magnetic modulation in Au/Co/Au films"</i>	O
16h15-16h30 p. 135	Laure Fabie (CEMES-CNRS, France) <i>"Nanodroplet deposition and manipulation with an AFM tip"</i>	O
16h30-16h45 p. 137	Chaoying Fu (McGill University, Canada) <i>"Self-assembly of oligothiophenecarboxylic acid monolayer by Scanning Tunneling Microscope (STM)"</i>	O
16h45-17h45	Coffee Break - Poster Session - Instrument Exhibition	PS

SCIENTIFIC PROGRAM - TNT2010
Tuesday – September 07, 2010




Parallel Session: nanoResearch in Portugal Chairman: Paulo Freitas (INL, Portugal)		
17h45-18h00 p. 165	Peter Schellenberg (University of Minho, Portugal) <i>"Visibility enhancement of Graphene on multiple substrates"</i>	O
18h00-18h15 p. 161	Teresa Monteiro (Universidade de Aveiro, Portugal) <i>"Effect of Eu-implantation and annealing on the GaN QDs excitonic recombination"</i>	O
18h15-18h30 p. 159	Gonçalo Doria (CIGMH/DCV - FCT/UNL, Portugal) <i>"Multiplex genetic characterization via noble metal nanopores"</i>	O
18h30-18h45 p. 169	Filipa Vale (Catholic University of Portugal, Portugal) <i>"Comparison of the results of the microbiologic quality of an untreated water sample using conventional culture media and a DNA chip for simultaneous detection of microorganisms"</i>	O
18h45-19h00 p. 157	Etelvina de Matos Gomes (Universidade do Minho, Portugal) <i>"Optical performance of highly oriented nanofibers of very efficiency organic nonlinear materials"</i>	O
19h00-19h15 p. 163	Carlos Rodriguez-Abreu (INL, Portugal) <i>"Fabrication of silica hollow microcoils with mesoporous walls"</i>	O
19h15-19h30 p. 167	Ricardo Simoes (University of Minho, Portugal) <i>"On the rule of disorder in the conductivity of high aspect ratio carbon filled composites in the framework of complex networks"</i>	O

SCIENTIFIC PROGRAM - TNT2010
Wednesday – September 08, 2010

Chairman: Romain Quidant (Spain)		
08h30-09h00	Diederik Wiersma (LENS, Italy) <i>"Photons, dust, and honey bees"</i>	K
p. 67		
09h00-09h30	Juan Jose Saenz (Universidad Autonoma de Madrid, Spain) <i>"Nanoparticle Dynamics in Non-Conservative Optical Fields"</i>	K
p. 53		
09h30-09h45	Elisa Mele (Italian Institute of Technology, Italy) <i>"Organic photonic devices by soft nanopatterning on active materials and nanofluids"</i>	O
p. 103		
09h45-10h00	Manfred Niehus (Universidade de Aveiro, Portugal) <i>"Coupling of photonic nanowires to k-mismatched waveguides and resonators"</i>	O
p. 109		
10h00-11h00	Coffee Break - Poster Session - Instrument Exhibition	PS
Chairman: Diederik Wiersma (LENS, Italy)		
11h00-11h30	Francisco J. Garcia Vidal (Universidad Autonoma de Madrid, Spain) <i>"Plasmonic waveguides: routers for light and efficient mediators between quantum emitters"</i>	K
p. 21		
11h30-12h00	Alexander Govorov (Ohio University, USA) <i>"Exciton-Plasmon Interactions and Fano Resonances in Nanostructures"</i>	K
p. 25		
12h00-12h30	Romain Quidant (ICFO-Inst. of Photonic Sciences, Spain) <i>"Plasmon nano-optics for Biosciences: Sensing, Trapping and hyperthermia"</i>	K
p. 49		
12h30-12h45	María Ujué González (IMM-CNM-CSIC, Spain) <i>"Increasing the modulation depth in Au/Co/Au magnetoplasmonic interferometers"</i>	O
p. 91		
12h45-13h15	Teresa Neves Petersen (Aalborg University, Denmark) <i>"Engineering biosensors and nanoparticle based drug carriers using a novel photonic technology"</i>	K
p. 43		
13h15-15h00	Lunch (*)	
Chairman: Jose-Luis Costa Kramer (IMM-CSIC, Spain)		
15h00-15h40	Masakazu Aono (NIMS / MANA, Japan) <i>"Atomic and molecular electrochemical structure control"</i>	I
p. 5		
15h40-16h10	Yuji Kuwahara (Osaka University, Japan) <i>"Optical and transport properties in molecular nanosystems observed by STM-based techniques"</i>	K
p. 37		
16h10-16h25	Alpana Nayak (National Institute for Materials Science, Japan) <i>"Kinetics underlying the switching time of a silver sulfide atomic switch"</i>	O
p. 107		
16h25-16h40	David Jacob (Max-Planck-Institut f. Mikrostrukturphysik, Germany) <i>"Dynamical Mean-Field Theory for Electronic Structure and Transport Properties of Nanoscopic Conductors"</i>	O
p. 99		
16h40-16h55	Stanislav Moshkalev (UNICAMP, Brazil) <i>"Microsensors based on multi-wall decorated carbon nanotubes and few-layer graphene"</i>	O
p. 105		
16h55-17h25	Lincoln J. Lauhon (Northwestern University, USA) <i>"Imaging of Nanoscale Form and Function: Atom Mapping and Correlated Functional Imaging of Semiconductor Nanowires"</i>	K
p. -		
17h25-18h00	Coffee Break - Poster Session - Instrument Exhibition	PS
20h30	BUS DEPARTURE (FROM INL) TO CONFERENCE DINNER	
21h00	CONFERENCE DINNER	
00h00	POSTER AWARDS CEREMONY	



(*) Lunch will be served at INL for those who booked

SCIENTIFIC PROGRAM - TNT2010
Thursday – September 9, 2010

12h00-13h00		Lunch (*)
"Colloids session" – Sponsored by Frimat (Switzerland) Chairman: Juan Jose Saenz (UAM, Spain)		
13h00-13h30	Philippe Poulin (CRPP-CNRS, France)	K
p. 47	<i>"Liquid processing of carbon nanotubes"</i>	
13h30-14h00	Jim Harden (University of Ottawa, Canada)	K
p. 27	<i>"X-ray photon correlation spectroscopy studies of slow dynamics in soft glassy materials"</i>	
14h00-14h30	Frank Scheffold (University of Fribourg, Switzerland)	K
p. -	<i>"Brush-like Interactions between Thermoresponsive Microgel Particles"</i>	
14h30-15h00	Luis M. Liz-Marzan (Universidad de Vigo, Spain)	K
p. 41	<i>"Self-Assembly and Directed Assembly of Gold Nanoparticles"</i>	
15h00-15h30		Coffee Break - Poster Session - Instrument Exhibition
"Nanotubes & Graphene" Session 1 – Sponsored by GDRI (France) Chairman: Stephan Roche (CIN2, Spain & CEA-INAC, France)		 
15h30-16h10	Andre Geim (University of Manchester, UK)	I
p. 7	<i>"Graphene: Status and Prospects"</i>	
16h10-16h40	Mark H. Rümmeli (IFW Dresden e. V., Germany)	K
p. 51	<i>"The rise of ceramic catalysts for carbon nanotube and graphene growth"</i>	
16h40-17h10	Mauricio Terrones (Carlos III Univ of Madrid, Spain & Exotic Nanocarbon Research Center, Shinshu Univ, Japan)	K
p. 57	<i>"Defect Nano-Engineering in Graphitic Materials: From Doped Carbons to Graphene"</i>	
17h10-17h25	Haldun Sevincli (Dresden University of Technology, Germany)	O
p. 119	<i>"Suppression of thermal conduction and enhanced thermoelectric figure of merit in disordered carbon systems"</i>	
17h25-17h40	Marion Cranney (Institut de Sciences des Materiaux de Mulhouse, France)	O
p. 81	<i>"Superlattice of resonators on monolayer graphene created by intercalated gold nanoclusters"</i>	
17h40-17h55	Jong-Hyun Ahn (Sungkyunkwan University, Korea)	O
p. 71	<i>"High-performance, Flexible Graphene Field Effect Transistors on Plastic substrates"</i>	
17h55-19h30		Coffee Break - Poster Session - Instrument Exhibition

(*) Lunch will be served at INL for those who booked

SCIENTIFIC PROGRAM - TNT2010
Friday – September 10, 2010

Chairman: Xavier Cartoixa (Universidad Autonoma de Barcelona, Spain)		
09h00-09h30	Clivia M Sotomayor Torres (ICN-CIN2-CSIC, Spain)	K
p. 55	<i>"Nanometrology: enabling applications of nanotechnology"</i>	
09h30-10h00	Eva M. Campo (Lehigh University, USA)	K
p. 17	<i>"Theory and modeling of optical actuation in nanocomposites through in situ electron microscopy studies"</i>	
10h00-10h15	Ricardo Ferreira (INESC-MN, Portugal)	O
p. 87	<i>"Structural modification of MgO/CoFeB using a low energy ion beam from an assisted deposition source"</i>	
10h15-10h30	Andrew Alves (University of Melbourne, Australia)	O
p. 73	<i>"The Development of Nanoscale Deterministic Ion Implants into Si and Diamond"</i>	
10h30-11h15	Coffee Break - Poster Session - Instrument Exhibition	
<p>"Nanotubes & Graphene" Session 1 – Sponsored by GDRI (France) and nanoICT CA</p> <div style="display: flex; justify-content: space-between; align-items: center;"> <div> <p>Chairman: Stephan Roche (CIN2, Spain & CEA-INAC, France)</p> </div> <div style="text-align: right;">   </div> </div>		
11h15-11h30	Paolo Bondavalli (Thales Research and Technology, France)	O
p. 75	<i>"Gas Sensor based on CNTFETs fabricated using an Original Dynamic Air-Brush technique for SWCNTs deposition"</i>	
11h30-11h45	Matthew Cole (University of Cambridge, UK)	O
p. 79	<i>"Horizontally aligned carbon nanotube networks: a route toward highly conductive, flexible & controllably transparent electrodes, field emitters and infra-red sensors"</i>	
11h45-12h00	Chang-Soo Han (Korea Institute of Machinery & Materials/Nano-Mechanics, Korea)	O
p. 93	<i>"Fast and wavelength selective photoresponse from QD/CNT hybrid"</i>	
12h00-12h15	Adelina Ilie (University of Bath, United Kingdom)	O
p. 97	<i>"Symmetry breaking and on-tube modulated surface potentials in hybrids of Single-Walled Carbon Nanotubes with encapsulated inorganic nanostructures"</i>	
12h15-12h45	Stephan Hofmann (University of Cambridge, UK)	K
p. 29	<i>"Towards an understanding of crystal growth on the nano-scale: in-situ probes for graphene, nanotube and -wire CVD"</i>	
12h45-13h15	Koji Ishibashi (RIKEN, Japan)	K
p. 31	<i>"Carbon nanotubes and graphenes for building blocks of nanodevices"</i>	
13h15-13h30	CLOSING REMARKS & TNT2011 ANNOUNCEMENT	



ABSTRACTS

(Only those abstracts received before August 23, 2010 are included in the abstracts' booklet)

INDEX - INVITED CONTRIBUTIONS

Masakazu Aono (NIMS / MANA, Japan) <i>Atomic and molecular electrochemical structure control</i>	p. 5
David Awschalom (University of California, USA) <i>Title to be confirmed</i>	p. -
Andre Geim (University of Manchester, UK) <i>Graphene: Status and Prospects</i>	p. 7
Klaus Kern (Max-Planck-Institut für Festkörperforschung, Germany) <i>Nanoscale electronic contacts</i>	p. 9
Uzi Landman (Georgia Institute of Technology, USA) <i>Small is different: physics and chemistry in the non-scalable nano regime</i>	p. 11

INDEX - KEYNOTE CONTRIBUTIONS

Katsuhiko Ariga (MANA / NIMS, Japan) <i>Supramolecular Materials & Hand-Operating Nanotechnology for Novel Functions</i>	p. 15
Eva M. Campo (Lehigh University, USA) <i>Theory and modeling of optical actuation in nanocomposites through in situ electron microscopy studies</i>	p. 17
Roy Chantrell (The University of York, UK) <i>Multiscale magnetic models of ultrafast magnetic processes</i>	p. 19
Francisco J. Garcia Vidal (Universidad Autonoma de Madrid, Spain) <i>Plasmonic waveguides: routers for light and efficient mediators between quantum emitters</i>	p. 21
Ehud Gazit (Tel Aviv University, Israel) <i>Self-Assembled Peptide Nanostructures: A New Frontier in Organic Nanotechnology</i>	p. 23
Sasha Govorov (Ohio University, USA) <i>Exciton-Plasmon Interactions and Fano Resonances in Nanostructures</i>	p. 25
Jim Harden (University of Ottawa, Canada) <i>X-ray photon correlation spectroscopy studies of slow dynamics in soft glassy materials</i>	p. 27
Stephan Hofmann (University of Cambridge, UK) <i>Towards an understanding of crystal growth on the nano-scale: in-situ probes for graphene, nanotube and -wire CVD</i>	p. 29
Koji Ishibashi (RIKEN, Japan) <i>Carbon nanotubes and graphenes for building blocks of nanodevices</i>	p. 31
Mato Knez (Max-Planck-Institut fuer Mikrostrukturphysik, Germany) <i>Atomic Layer Deposition - An old technique for modern nanoscience</i>	p. 33
Tuomas Knowles (Nanoscience Centre – Univ. of Cambridge, UK) <i>Protein nanofibrils</i>	p. 35
Yuji Kuwahara (Osaka University, Japan) <i>Optical and transport properties in molecular nanosystems observed by STM-based techniques</i>	p. 37
Lincoln J. Lauhon (Northwestern University, USA) <i>Imaging of Nanoscale Form and Function: Atom Mapping and Correlated Functional Imaging of Semiconductor Nanowires</i>	p. -
Magali Lingenfelder (ICMAB-CSIC, Spain) <i>Chiral recognition on surfaces: from single molecule tracking to 3d crystals</i>	p. 39
Luis M. Liz-Marzan (Universidad de Vigo, Spain) <i>Self-Assembly and Directed Assembly of Gold Nanoparticles</i>	p. 41
Teresa Neves Petersen (Aalborg University, Denmark) <i>Engineering biosensors and nanoparticle based drug carriers using a novel photonic technology</i>	p. 43
Valentyn Novosad (Argonne National Laboratory, United States) <i>Spin vortices: from fundamental physics to biomedical applications</i>	p. 45
Philippe Poulin (CRPP-CNRS, France) <i>Liquid processing of carbon nanotubes</i>	p. 47
Romain Quidant (ICFO-Inst. of Photonic Sciences, Spain) <i>Plasmon nano-optics for Biosciences: Sensing, Trapping and hyperthermia</i>	p. 49
Mark H. Rummeli (IFW Dresden e. V., Germany) <i>The rise of ceramic catalysts for carbon nanotube and graphene growth</i>	p. 51

Juan Jose Saenz (Universidad Autonoma de Madrid, Spain) <i>Nanoparticle Dynamics in Non-Conservative Optical Fields</i>	p. 53
Frank Scheffold (University of Fribourg, Switzerland) <i>Brush-like Interactions between Thermoresponsive Microgel Particles</i>	p. -
Clivia M Sotomayor Torres (ICN-CIN2-CSIC, Spain) <i>Nanometrology: enabling applications of nanotechnology</i>	p. 55
Mauricio Terrones (Carlos III Univ. of Madrid, Spain & Exotic Nanocarbon Research Center, Shinshu Univ, Japan) <i>Defect Nano-Engineering in Graphitic Materials: From Doped Carbons to Graphene</i>	p. 57
Kohei Uosaki (MANA / NIMS, Japan) <i>Formation, Characterization and Catalytic Properties of Metal Nanoclusters within Molecular Layers</i>	p. 59
Sebastiaan van Dijken (Aalto University, Finland) <i>Pattern Transfer and Lateral Switching Modulation in Multiferroic Heterostructures</i>	p. 61
Janos Vörös (ETH-Zentrum, Switzerland) <i>Nanotechnology Approaches for Enhancing the Sensitivity and Throughput of Biosensors</i>	p. 63
Zhiming M. Wang (University of Arkansas, USA) <i>Droplet-Patterned Epitaxial Growth: Quantum Dot Molecules and Nanoholes</i>	p. 65
Diederik Wiersma (LENS, Italy) <i>Photons, dust, and honey bees</i>	p. 67

INDEX – ORAL CONTRIBUTIONS (PLENARY SESSION)

Jong-Hyun Ahn (Sungkyunkwan University, Korea) <i>High-performance, Flexible Graphene Field Effect Transistors on Plastic substrates</i>	p. 71
Andrew Alves (University of Melbourne, Australia) <i>The Development of Nanoscale Deterministic Ion Implants into Si and Diamond</i>	p. 73
Paolo Bondavalli (Thales Research and Technology, France) <i>Gas Sensor based on CNTFETs fabricated using an Original Dynamic Air-Brush technique for SWCNTs deposition</i>	p. 75
Felix Casanova (CIC nanoGUNE, Spain) <i>Asymmetric spin injection at high current bias in all-metallic lateral spin valves</i>	p. 77
Matthew Cole (University of Cambridge, UK) <i>Horizontally aligned carbon nanotube networks: a route toward highly conductive, flexible & controllably transparent electrodes, field emitters and infra-red sensors</i>	p. 79
Marion Cranney (Institut de Sciences des Materiaux de Mulhouse, France) <i>Superlattice of resonators on monolayer graphene created by intercalated gold nanoclusters</i>	p. 81
Meiken Falke (Bruker Nano GmbH, Germany) <i>Analysis of Carbon- and other Nano-Structures using Si Drift Detectors in Energy Dispersive X-ray Spectroscopy</i>	p. 83
Carole Fauquet (Université de la Méditerranée, France) <i>Combining Scanning Probe Microscopy and X-Ray Spectroscopy to Obtain Simultaneously Surface Topography and Chemical Mapping</i>	p. 85
Ricardo Ferreira (INESC-MN, Portugal) <i>Structural modification of MgO/CoFeB using a low energy ion beam from an assisted deposition source</i>	p. 87
Ricardo Franco (REQUIMTE, Portugal) <i>Malaria Diagnostics based on Antibody-Functionalized Gold Nanoparticles and Plasmodium falciparum Hsp70</i>	p. 89
María Ujué González (IMM-CNM-CSIC, Spain) <i>Increasing the modulation depth in Au/Co/Au magnetoplasmonic interferometers</i>	p. 91
Chang-Soo Han (Korea Institute of Machinery & Materials/Nano-Mechanics, Korea) <i>Fast and wavelength selective photoresponse from QD/CNT hybrid</i>	p. 93
Maria Holmberg (Technical University of Denmark, Denmark) <i>Protein Adsorption on Biomaterials - Atomic Force Microscopy and Radioactive Labeling Analysis</i>	p. 95
Adelina Ilie (University of Bath, United Kingdom) <i>Symmetry breaking and on-tube modulated surface potentials in hybrids of Single-Walled Carbon Nanotubes with encapsulated inorganic nanostructures</i>	p. 97
David Jacob (Max-Planck-Institut f. Mikrostrukturphysik, Germany) <i>Dynamical Mean-Field Theory for Electronic Structure and Transport Properties of Nanoscopic Conductors</i>	p. 99
Manuel Arturo Lopez Quintela (University of Santiago de Compostela, Spain) <i>Small sub-nm metal clusters: the key missing point in many catalytic processes?</i>	p. 101
Elisa Mele (Italian Institute of Technology, Italy) <i>Organic photonic devices by soft nanopatterning on active materials and nanofluids</i>	p. 103
Stanislav Moshkalev (UNICAMP, Brazil) <i>Microsensors based on multi-wall decorated carbon nanotubes and few-layer graphene</i>	p. 105
Alpana Nayak (National Institute for Materials Science, Japan) <i>Kinetics underlying the switching time of a silver sulfide atomic switch</i>	p. 107
Manfred Niehus (Universidade de Aveiro, Portugal) <i>Coupling of photonic nanowires to k-mismatched waveguides and resonators</i>	p. 109
Eulália Pereira (REQUIMTE-Universidade do Porto, Portugal) <i>Green Photocatalytic Synthesis of Au and Ag Nanoparticles: Size and Shape Control</i>	p.111
Dario Pisignano (Università di Lecce, Italy) <i>Polymer Electrospun Nanofibers as Building Blocks for Nanotechnology</i>	p. 113
Bertrand Raquet (LNCMI, France) <i>Magnetic Edges Current and Disorder in Graphene Nano-Ribbons</i>	p. 115
Ronny Sczech (Technische Universität Dresden, Germany) <i>Diffusion of DNA polymer molecules in nanochannels</i>	p. 117

Haldun Sevincli (Dresden University of Technology, Germany) <i>Suppression of thermal conduction and enhanced thermoelectric figure of merit in disordered carbon systems</i>	p. 119
Weisheng Zhao (IEF, CNRS/Univ. Paris Sud 11, France) <i>A Compact Model for the Magnetic Tunnel Junction Switched by Thermally Assisted Spin Transfer Torque (STT+TAS)</i>	p. 121

INDEX – ORAL CONTRIBUTIONS (PHD - PARALLEL SESSIONS)

Rita Branquinho (FCT-UNL/Cenimat) <i>Room Temperature Sputtered Ta₂O₅ for Solid State Biosensors</i>	p. 125
Maria Fernanda Cardinal (University of Vigo, Spain) <i>Modulation of Localized Surface Plasmons and SERS Response in Gold Dumbbells through Silver Coating</i>	p. 127
Daniel Carmona (Instituto de Nanociencia de Aragon, Spain) <i>Silica rod-shape capsules embbebing superparamagnetic iron oxide nanoparticles</i>	p. 129
Marta Castro Lopez (ICFO - The Institute of Photonic Sciences, Spain) <i>Observation of polarized multiphoton emission from resonant Al, Ag and Au nanoantennas</i>	p. 131
Raquel M. Da Costa Martins (Universidad de Navarra, Spain) <i>Bioadhesive mannosamine-loaded nanoparticles for an effective ocular vaccination against animal brucellosis</i>	p. 133
Laure Fabie (CEMES-CNRS, France) <i>Nanodroplet deposition and manipulation with an AFM tip</i>	p. 135
Chaoying Fu (McGill University, Canada) <i>Self-assembly of oligothiophenecarboxylic acid monolayer by Scanning Tunneling Microscope (STM)</i>	p. 137
Aya Fujiki (Osaka university, Japan) <i>Tunneling-current-induced light emission from PTCDI-C7 thin films on the graphite and the Au(111) surfaces</i>	p. 139
Si-Yu Liao (Université Bordeaux 1, France) <i>Non-volatile memory using Optically-Gated Carbon Nanotube FET: Description of carrier mobility model in P3OT and source-drain Schottky barrier</i>	p. 141
Raquel Maia (INEB/INL, Portugal) <i>Development of nanostructured 3D matrices to direct mesenchymal stem cells behavior</i>	p. 143
Diana Martín-Becerra (IMM-CNM-CSIC, Spain) <i>Wavelength dependence of the SPP wavevector magnetic modulation in Au/Co/Au films</i>	p.145
Matthew Morantz (McGill University, Canada) <i>Synthesis, Nanostructural and Electronic Characterization of Anthracenedicarboximide Derivatives</i>	p. 147
Jose Maria Porro Azpiazu (CIC nanoGUNE, Spain) <i>Effects of asymmetric dipolar interactions between elliptical ferromagnetic nanomagnets in artificial spin-ice structure</i>	p. 149
Aliaksandra Rakovich (Trinity College Dublin, Ireland) <i>Development of Nano-Bio hybrid material based on CdTe Quantum Dots and Bacteriorhodopsin protein for future technologies</i>	p. 151
Florent Roussel (Laboratoire Francis Perrin - CEA/DSM/IRAMIS/SPAM, France) <i>1D polymer/CNT composite : elaboration and transport properties</i>	p. 153

INDEX – ORAL CONTRIBUTIONS (NANORESEARCH IN PORTUGAL - PARALLEL SESSION)

Etelvina de Matos Gomes (Universidade do Minho, Portugal) <i>Optical performance of highly oriented nanofibers of very efficiency organic nonlinear materials</i>	p. 157
Gonçalo Doria (FCT/UNL, Portugal) <i>Multiplex genetic characterization via noble metal nanoprobos</i>	p.159
Teresa Monteiro (Universidade de Aveiro, Portugal) <i>Effect of Eu-implantation and annealing on the GaN QDs excitonic recombination</i>	p. 161
Carlos Rodriguez-Abreu (INL, Portugal) <i>Fabrication of silica hollow microcoils with mesoporous walls</i>	p. 163
Peter Schellenberg (University of Minho, Portugal) <i>Visibility enhancement of Graphene on multiple substrates</i>	p. 165
Ricardo Simoes (University of Minho, Portugal) <i>On the rule of disorder in the conductivity of high aspect ratio carbon filled composites in the framework of complex networks</i>	p. 167
Filipa Vale (Catholic University of Portugal, Portugal) <i>Comparison of the results of the microbiologic quality of an untreated water sample using conventional culture media and a DNA chip for simultaneous detection of microorganisms</i>	p. 169

ALPHABETICAL ORDER

I: Invited / K: Keynote / O: Oral / PS: Parallel Session

Jong-Hyun Ahn (Sungkyunkwan University, Korea) <i>High-performance, Flexible Graphene Field Effect Transistors on Plastic substrates</i>	O	p. 71
Andrew Alves (University of Melbourne, Australia) <i>The Development of Nanoscale Deterministic Ion Implants into Si and Diamond</i>	O	p. 73
Masakazu Aono (NIMS / MANA, Japan) <i>Atomic and molecular electrochemical structure control</i>	I	p. 5
Katsuhiko Ariga (MANA, NIMS, Japan) <i>Supramolecular Materials & Hand-Operating Nanotechnology for Novel Functions</i>	K	p. 15
David Awschalom (University of California, USA) <i>Title to be confirmed</i>	I	p. -
Paolo Bondavalli (Thales Research and Technology, France) <i>Gas Sensor based on CNTFETs fabricated using an Original Dynamic Air-Brush technique for SWCNTs deposition</i>	O	p. 75
Rita Branquinho (FCT-UNL/Cenimat) <i>Room Temperature Sputtered Ta₂O₅ for Solid State Biosensors</i>	PS	p. 125
Eva M. Campo (Lehigh University, USA) <i>Theory and modeling of optical actuation in nanocomposites through in situ electron microscopy studies</i>	K	p. 17
Maria Fernanda Cardinal (University of Vigo, Spain) <i>Modulation of Localized Surface Plasmons and SERS Response in Gold Dumbbells through Silver Coating</i>	PS	p. 127
Daniel Carmona (Instituto de Nanociencia de Aragon, Spain) <i>Silica rod-shape capsules embbebing superparamagnetic iron oxide nanoparticles</i>	PS	p. 129
Felix Casanova (CIC nanoGUNE, Spain) <i>Asymmetric spin injection at high current bias in all-metallic lateral spin valves</i>	O	p. 77
Marta Castro Lopez (ICFO - The Institute of Photonic Sciences, Spain) <i>Observation of polarized multiphoton emission from resonant Al, Ag and Au nanoantennas</i>	PS	p. 131
Roy Chantrell (The University of York, UK) <i>Multiscale magnetic models of ultrafast magnetic processes</i>	K	p. 19
Matthew Cole (University of Cambridge, UK) <i>Horizontally aligned carbon nanotube networks: a route toward highly conductive, flexible & controllably transparent electrodes, field emitters and infra-red sensors</i>	O	p. 79
Marion Cranney (Institut de Sciences des Materiaux de Mulhouse, France) <i>Superlattice of resonators on monolayer graphene created by intercalated gold nanoclusters</i>	O	p. 81
Raquel M. Da Costa Martins (Universidad de Navarra, Spain) <i>Bioadhesive mannosamine-loaded nanoparticles for an effective ocular vaccination against animal brucellosis</i>	PS	p. 133
Etelvina de Matos Gomes (Universidade do Minho, Portugal) <i>Optical performance of highly oriented nanofibers of very efficiency organic nonlinear materials</i>	PS	p. 157
Gonçalo Doria (FCT/UNL, Portugal) <i>Multiplex genetic characterization via noble metal nanoprobos</i>	PS	p. 159
Laure Fabie (CEMES-CNRS, France) <i>Nanodroplet deposition and manipulation with an AFM tip</i>	PS	p. 135
Meiken Falke (Bruker Nano GmbH, Germany) <i>Analysis of Carbon- and other Nano-Structures using Si Drift Detectors in Energy Dispersive X-ray Spectroscopy</i>	O	p. 83
Carole Fauquet (Université de la Méditerranée, France) <i>Combining Scanning Probe Microscopy and X-Ray Spectroscopy to Obtain Simultaneously Surface Topography and Chemical Mapping</i>	O	p. 85
Ricardo Ferreira (INESC-MN, Portugal) <i>Structural modification of MgO/CoFeB using a low energy ion beam from an assisted deposition source</i>	O	p. 87

Ricardo Franco (REQUIMTE, Portugal) <i>Malaria Diagnostics based on Antibody-Functionalized Gold Nanoparticles and Plasmodium falciparum Hsp70</i>	O	p. 89
Chaoying Fu (McGill University, Canada) <i>Self-assembly of oligothiophenecarboxylic acid monolayer by Scanning Tunneling Microscope (STM)</i>	PS	p. 137
Aya Fujiki (Osaka university, Japan) <i>Tunneling-current-induced light emission from PTCDI-C7 thin films on the graphite and the Au(111) surfaces</i>	PS	p. 139
Francisco J. Garcia Vidal (Universidad Autonoma de Madrid, Spain) <i>Plasmonic waveguides: routers for light and efficient mediators between quantum emitters</i>	K	p. 21
Ehud Gazit (Tel Aviv University, Israel) <i>Self-Assembled Peptide Nanostructures: A New Frontier in Organic Nanotechnology</i>	K	p. 23
Andre Geim (University of Manchester, UK) <i>Graphene: Status and Prospects</i>	I	p. 7
María Ujué González (IMM-CNM-CSIC, Spain) <i>Increasing the modulation depth in Au/Co/Au magnetoplasmonic interferometers</i>	O	p. 91
Sasha Govorov (Ohio University, USA) <i>Exciton-Plasmon Interactions and Fano Resonances in Nanostructures</i>	K	p. 25
Chang-Soo Han (Korea Institute of Machinery & Materials/Nano-Mechanics, Korea) <i>Fast and wavelength selective photoresponse from QD/CNT hybrid</i>	O	p. 93
Jim Harden (University of Ottawa, Canada) <i>X-ray photon correlation spectroscopy studies of slow dynamics in soft glassy materials</i>	K	p. 27
Stephan Hofmann (University of Cambridge, UK) <i>Towards an understanding of crystal growth on the nano-scale: in-situ probes for graphene, nanotube and -wire CVD</i>	K	p. 29
Maria Holmberg (Technical University of Denmark, Denmark) <i>Protein Adsorption on Biomaterials - Atomic Force Microscopy and Radioactive Labeling Analysis</i>	O	p. 95
Adelina Ilie (University of Bath, United Kingdom) <i>Symmetry breaking and on-tube modulated surface potentials in hybrids of Single-Walled Carbon Nanotubes with encapsulated inorganic nanostructures</i>	O	p. 97
Koji Ishibashi (RIKEN, Japan) <i>Carbon nanotubes and graphenes for building blocks of nanodevices</i>	K	p. 31
David Jacob (Max-Planck-Institut f. Mikrostrukturphysik, Germany) <i>Dynamical Mean-Field Theory for Electronic Structure and Transport Properties of Nanoscopic Conductors</i>	O	p. 99
Klaus Kern (Max-Planck-Institut für Festkörperforschung, Germany) <i>Nanoscale electronic contacts</i>	I	p. 9
Mato Knez (Max-Planck-Institut fuer Mikrostrukturphysik, Germany) <i>Atomic Layer Deposition - An old technique for modern nanoscience</i>	K	p. 33
Tuomas Knowles (Nanoscience Centre – Univ. of Cambridge, UK) <i>Protein nanofibrils</i>	K	p. 35
Yuji Kuwahara (Osaka University, Japan) <i>Optical and transport properties in molecular nanosystems observed by STM-based techniques</i>	K	p. 37
Uzi Landman (Georgia Institute of Technology, USA) <i>Small is different: physics and chemistry in the non-scalable nano regime</i>	I	p. 11
Lincoln J. Lauhon (Northwestern University, USA) <i>Imaging of Nanoscale Form and Function: Atom Mapping and Correlated Functional Imaging of Semiconductor Nanowires</i>	K	p. -
Si-Yu Liao (Université Bordeaux 1, France) <i>Non-volatile memory using Optically-Gated Carbon Nanotube FET: Description of carrier mobility model in P3OT and source-drain Schottky barrier</i>	PS	p. 141
Magali Lingensfelder (ICMAB-CSIC, Spain) <i>Chiral recognition on surfaces: from single molecule tracking to 3d crystals</i>	K	p. 39
Luis M. Liz-Marzan (Universidad de Vigo, Spain) <i>Self-Assembly and Directed Assembly of Gold Nanoparticles</i>	K	p. 41
Manuel Arturo Lopez Quintela (University of Santiago de Compostela, Spain) <i>Small sub-nm metal clusters: the key missing point in many catalytic processes?</i>	O	p. 101

Raquel Maia (INEB/INL, Portugal) <i>Development of nanostructured 3D matrices to direct mesenchymal stem cells behavior</i>	PS	p. 143
Diana Martín-Becerra (IMM-CNM-CSIC, Spain) <i>Wavelength dependence of the SPP wavevector magnetic modulation in Au/Co/Au films</i>	PS	p. 145
Elisa Mele (Italian Institute of Technology, Italy) <i>Organic photonic devices by soft nanopatterning on active materials and nanofluids</i>	O	p. 103
Teresa Monteiro (Universidade de Aveiro, Portugal) <i>Effect of Eu-implantation and annealing on the GaN QDs excitonic recombination</i>	PS	p. 161
Matthew Morantz (McGill University, Canada) <i>Synthesis, Nanostructural and Electronic Characterization of Anthracenedicarboximide Derivatives</i>	PS	p. 147
Stanislav Moshkalev (UNICAMP, Brazil) <i>Microsensors based on multi-wall decorated carbon nanotubes and few-layer graphene</i>	O	p. 105
Alpana Nayak (National Institute for Materials Science, Japan) <i>Kinetics underlying the switching time of a silver sulfide atomic switch</i>	O	p. 107
Teresa Neves Petersen (Aalborg University, Denmark) <i>Engineering biosensors and nanoparticle based drug carriers using a novel photonic technology</i>	K	p. 43
Manfred Niehus (Universidade de Aveiro, Portugal) <i>Coupling of photonic nanowires to k-mismatched waveguides and resonators</i>	O	p. 109
Valentyn Novosad (Argonne National Laboratory, United States) <i>Spin vortices: from fundamental physics to biomedical applications</i>	K	p. 45
Eulália Pereira (REQUIMTE-Universidade do Porto, Portugal) <i>Green Photocatalytic Synthesis of Au and Ag Nanoparticles: Size and Shape Control</i>	O	p. 111
Dario Pisignano (Università di Lecce, Italy) <i>Polymer Electrospun Nanofibers as Building Blocks for Nanotechnology</i>	O	p. 113
Jose Maria Porro Azpiazu (CIC nanoGUNE, Spain) <i>Effects of asymmetric dipolar interactions between elliptical ferromagnetic nanomagnets in artificial spin-ice structure</i>	PS	p. 149
Philippe Poulin (CRPP-CNRS, France) <i>Liquid processing of carbon nanotubes</i>	K	p. 47
Romain Quidant (ICFO-Inst. of Photonic Sciences, Spain) <i>Plasmon nano-optics for Biosciences: Sensing, Trapping and hyperthermia</i>	K	p. 49
Aliaksandra Rakovich (Trinity College Dublin, Ireland) <i>Development of Nano-Bio hybrid material based on CdTe Quantum Dots and Bacteriorhodopsin protein for future technologies</i>	PS	p. 151
Bertrand Raquet (LNCMI, France) <i>Magnetic Edges Current and Disorder in Graphene Nano-Ribbons</i>	O	p. 115
Carlos Rodriguez-Abreu (INL, Portugal) <i>Fabrication of silica hollow microcoils with mesoporous walls</i>	PS	p. 163
Florent Roussel (Laboratoire Francis Perrin - CEA/DSM/IRAMIS/SPAM, France) <i>1D polymer/CNT composite : elaboration and transport properties</i>	PS	p. 153
Mark H. Rummeli (IFW Dresden e. V., Germany) <i>The rise of ceramic catalysts for carbon nanotube and graphene growth</i>	K	p. 51
Juan Jose Saenz (Universidad Autonoma de Madrid, Spain) <i>Nanoparticle Dynamics in Non-Conservative Optical Fields</i>	K	p. 53
Frank Scheffold (University of Fribourg, Switzerland) <i>Brush-like Interactions between Thermoresponsive Microgel Particles</i>	K	p. -
Peter Schellenberg (University of Minho, Portugal) <i>Visibility enhancement of Graphene on multiple substrates</i>	PS	p. 165
Ronny Sczech (Technische Universität Dresden, Germany) <i>Diffusion of DNA polymer molecules in nanochannels</i>	O	p. 117
Haldun Sevincli (Dresden University of Technology, Germany) <i>Suppression of thermal conduction and enhanced thermoelectric figure of merit in disordered carbon systems</i>	O	p. 119
Ricardo Simoes (University of Minho, Portugal) <i>On the rule of disorder in the conductivity of high aspect ratio carbon filled composites in the framework of complex networks</i>	PS	p. 167
Clivia M Sotomayor Torres (ICN-CIN2-CSIC, Spain) <i>Nanometrology: enabling applications of nanotechnology</i>	K	p. 55

Mauricio Terrones (Carlos III Univ of Madrid, Spain & Exotic Nanocarbon Research Center, Shinshu Univ, Japan) <i>Defect Nano-Engineering in Graphitic Materials: From Doped Carbons to Graphene</i>	K	p. 57
Kohei Uosaki (MANA, NIMS, Japan) <i>Formation, Characterization and Catalytic Properties of Metal Nanoclusters within Molecular Layers</i>	K	p. 59
Filipa Vale (Catholic University of Portugal, Portugal) <i>Comparison of the results of the microbiologic quality of an untreated water sample using conventional culture media and a DNA chip for simultaneous detection of microorganisms</i>	PS	p. 169
Sebastiaan van Dijken (Aalto University, Finland) <i>Pattern Transfer and Lateral Switching Modulation in Multiferroic Heterostructures</i>	K	p. 61
Janos Vörös (ETH-Zentrum, Switzerland) <i>Nanotechnology Approaches for Enhancing the Sensitivity and Throughput of Biosensors</i>	K	p. 63
Zhiming M. Wang (University of Arkansas, USA) <i>Droplet-Patterned Epitaxial Growth: Quantum Dot Molecules and Nanoholes</i>	K	p. 65
Diederik Wiersma (LENS, Italy) <i>Photons, dust, and honey bees</i>	K	p. 67
Weisheng Zhao (IEF, CNRS/Univ. Paris Sud 11, France) <i>A Compact Model for the Magnetic Tunnel Junction Switched by Thermally Assisted Spin Transfer Torque (STT+TAS)</i>	O	p. 121



ABSTRACTS



INVITED CONTRIBUTIONS

Atomic and molecular electrochemical structure control*

M. Aono

International Center for Materials Nanoarchitectonics (MANA)
National Institute for Materials Science (NIMS)
Tsukuba, Ibaraki, 305-0044 Japan

Local electrochemical reactions that can be controlled at the atomic and molecular scales in a reversible manner by changing the voltage applied to the local area are of great interest, since such reactions may be used to realize novel atomic and molecular devices for data processing and storage. In the present paper, we discuss the following three atomic and molecular local electrochemical reactions of interest:

- 1) Reversibly controlling the chemically unbound and bound states of a few neighbouring C₆₀ molecules by changing the polarity of applied voltage [1]. Its application to single-molecule-level ultradense data storage (~200 Tbit/in²) is discussed.
- 2) Creation of a single conductive linear polymer chain (polydiacetylene) at any designated position and its reversible control between non-metallic and metallic states by changing the magnitude of applied voltage [2]. The application of the nonmetal-metal transition to various novel electronic devices is also discussed [3].
- 3) The growth and shrinkage of a metallic atom cluster that can be controlled reversibly by changing the polarity of applied voltage; this reversible solid electrochemical reaction is the switching mechanism of the atomic switch. [4]. The application of the atomic switch to realize a novel field-programmable LSI (in collaboration with NEC Corp.) is discussed [5]. More important application to the realization of neuromorphic computational circuits using atomic switches is also discussed [6].

References

- [1] M. Nakaya et al., *Adv. Mater.* 22 (2010) 1622.
[2] Y. Okawa and M. Aono, *Nature* 409 (2001) 683; *J. Chem. Phys.* 115 (2001) 2317.
[3] Y. Okawa et al., to be published (2010).
[4] K. Terabe et al., *Nature*, 433 (2005) 47.
[5] S. Kaeriyama et al., *IEEE J. Solid-State Circuits* 40 (2005) 168.
[6] T. Hasegawa et al., *Adv. Mater.* 22 (2010) 1831.

*In collaboration with T. Nakayama, Y. Kuwahara, M. Nakaya, Y. Okawa, S. Mandal, Y. Tateyama, T. Hasegawa, K. Terabe, T. Ohno, International Center for Materials Nanoarchitectonics (MANA), National Institute for Materials Science (NIMS).

Graphene: Status and Prospects

Andre Geim

Centre for Mesoscience & Nanotechnology, University of Manchester, United Kingdom

Graphene – a free-standing atomic plane of graphite – has turned out to be a wonder material. It has already attracted many superlatives to its name. It is of course the thinnest material in the universe and arguably the strongest one ever measured. Its charge carriers exhibit the highest known intrinsic mobility, have zero effective mass and can travel micron distances without scattering at room temperature. Graphene can sustain current densities million times higher than that of copper, shows record thermal conductivity and stiffness, is impermeable to gases and reconciles such conflicting qualities as brittleness and ductility. Electron transport in graphene and its bilayer is described by massless and massive Dirac-like equations, respectively (rather than the standard Schrodinger equation), which allows the investigation of relativistic quantum phenomena in a bench-top experiment.

This will be a general talk for non-specialists introducing graphene and its fascinating properties [1]. For illustration, I will try using the results obtained by our team in Manchester during the last year or two. The new results include electron transport at the vicinity of the Dirac point in many-million-mobility devices, properties of the first stoichiometric derivative (fluorographene) and evidence for magnetic edges.

References

[1] A. K. Geim, Science 324, 1530 (2009). A. K. Geim, K. S. Novoselov, Nature Mater. 6, 183 (2007).

Nanoscale electronic contacts

Klaus Kern

Max-Planck-Institut für Festkörperforschung, Heisenbergstr. 1, D-70569 Stuttgart
and
Ecole Polytechnique Fédérale de Lausanne - EPFL, CH-1015 Lausanne, Switzerland

klaus.kern@fkf.mpg.de

Charge transport through atomic and molecular constrictions greatly affects the operation and performance of nanoscale electronic devices. Much of our understanding of the charge injection and extraction processes in these systems relies on our knowledge of the electronic structure at the contact. Despite significant experimental and theoretical advances in studying charge transport in nanoscale junctions, a microscopic understanding at the single atom/molecule level is missing.

In the present talk I will present our recent results to probe directly the nanocontact between single atoms and molecules and a metal electrode using scanning tunnelling microscopy and spectroscopy. The experiments provide unprecedented microscopic details of single molecule and atom junctions and open new avenues to study quantum critical and many body phenomena at the atomic scale.

Small is different: physics and chemistry in the non-scalable nano regime

Uzi Landman

School of physics, Georgia Institute of Technology
Atlanta, Georgia 30332 USA

Uzi.Landman@physics.gatech.edu

When the scale of materials structures is reduced to the nanoscale, emergent physical and chemical behavior often occurs, that is not commonly expected, or deduced, from knowledge learned at larger sizes. Such new behavior may be found when the size of the interrogated physical system becomes comparable to a phenomena-dependent characteristic length-scale; for example, the width of a quantum wire approaches the Fermi wave-length of the conducting electrons, or the dimensions of a liquid bridge, or a nanojet, approach the wave-length of a hydrodynamical instability underlying collapse or breakup into droplets. Using computer-based simulations [1] we highlight and illustrate such diverse emergent phenomena. Systems that we discuss include: electronic states and correlated electron quantum Hall phenomena in 2D semiconductor quantum dots and graphene, chemical nanocatalysis, charged water nanocluster droplets, liquid nanobridges and stochastic hydrodynamics, and molecular organization in lipid bilayers as well as trans-membrane transport processes investigated with large-scale molecular dynamics simulations of immersed capillary nanojet injection of a liquid through a bilayer membrane, illustrating membrane puncture and subsequent molecular self-healing processes.

References

[1] U. Landman, "Materials by Numbers: Computations as Tools of Discovery", Proc. Nat. Acad. Sci. (USA) **102**, 6671 (2005).

* Work supported by the US Department of Energy and the Air Force Office of Scientific Research.



KEYNOTE CONTRIBUTIONS

Supramolecular Materials & Hand-Operating Nanotechnology for Novel Functions

Katsuhiko Ariga

World Premier International (WPI) Research Center for Materials Nanoarchitectonics (MANA), National Institute for Materials Science (NIMS), 1-1 Namiki, Tsukuba, Ibaraki 305-0044, Japan

ARIGA.Katsuhiko@nims.go.jp

Supramolecular materials have been widely constructed via bottom-up approaches as seen in preparation of molecular complexes and organized nanostructures. Functional materials have been widely constructed via bottom-up approaches as seen in preparation of molecular patterns and complexes [1-3], organized nanostructures [4-7], and function materials [8]. These materials are used for various functions such as one-pot materials separation, selective sensing, auto-modulated drug release, and photo-energy conversions as reported in our recent researches. For example, a novel hierarchic nanostructure based on layer-by-layer (LbL) assembly and mesoporous technology, so-called mesoporous silica nanocompartment film, was reported [9]. The resulting mesoporous nanocompartment films possess special molecular encapsulation and release capabilities so that stimuli-free auto-modulated stepwise release of water or drug molecules was achieved. We also demonstrated the LbL assembly of mesoporous carbon capsules on a QCM plate and the use of the resulting structure for selective adsorption of gaseous substances [10]. The related LbL structures of mesoporous carbons were demonstrated for in situ sensor use based on highly cooperative nanopore-filling adsorption in the liquid phase [11]. Recently, we have developed preparation of zebra-type nanowires through supramolecular assembly of block copolymers (Figure 1) [6]. The obtained nanowires displayed reversible photo-current responses as photo-energy conversion capability.

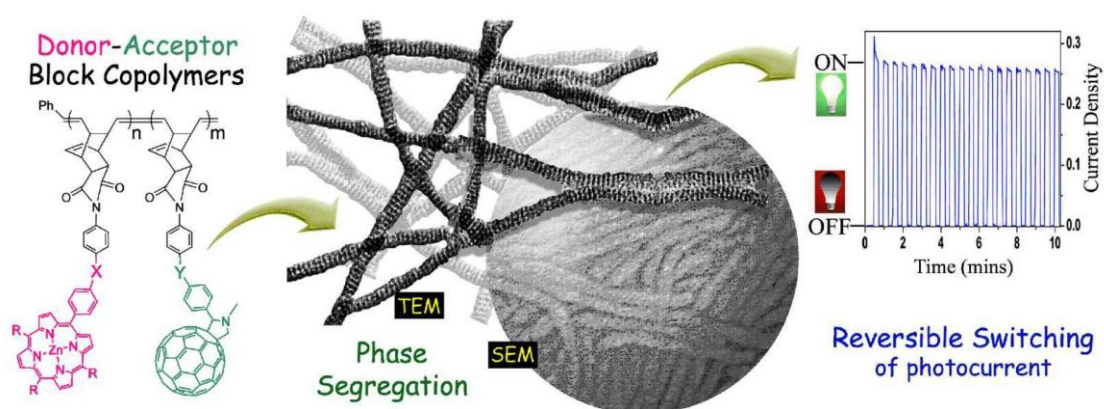


Figure 1. Zebra Nanowire for Photo-Current Switching

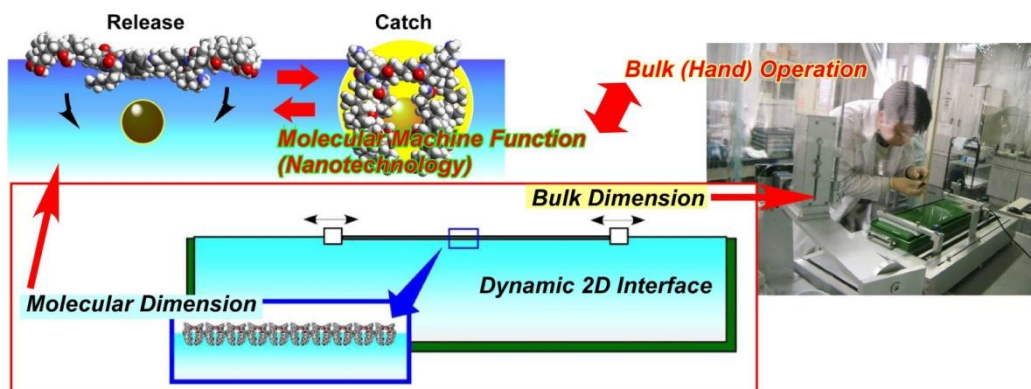


Figure 2. Hand-operating nanotechnology

Not limited to material developments, novel concepts to bridge nano (molecular) structures and bulk systems now becomes crucial in order to control real nano and molecular functions from our visible worlds. Recently, we propose a novel methodology “hand-operating nanotechnology” where molecular orientation, organization and even functions in nanometer-scale can be operated by our bulk (hand) operation. As shown in the following Figure 2, this concept can be realized at dynamic two-dimensional medium, the air-water interface because this medium possess both features of bulk and molecular dimension. For example, we successfully manipulated molecules at the air-water interface upon bulk (10-100 cm size) motion of the entire monolayer and realized “capture and release” of aqueous guest molecules using molecular machine, steroid cyclophane [12]. In addition, mechanically controlled chiral recognition by the armed cyclen monolayer was successfully demonstrated [13].

References

- [1] A. Shundo *et al.*, *J. Am. Chem. Soc.* **131**, 9494-9495 (2009). (Highlighted in *Nature Chemistry*).
- [2] S. Acharya *et al.*, *J. Am. Chem. Soc.* **131**, 11282-11283 (2009).
- [3] F. D'Souza *et al.*, *J. Am. Chem. Soc.* **131**, 16138-16146 (2009).
- [4] S. Acharya *et al.*, *J. Am. Chem. Soc.* **130**, 4594-4595 (2008).
- [5] M. Sathish *et al.*, *J. Am. Chem. Soc.* **131**, 6372-6373 (2009).
- [6] R. Charvet *et al.*, *J. Am. Chem. Soc.* **131**, 18030-18031 (2009).
- [7] N. Pradhan *et al.*, *J. Am. Chem. Soc.* **132**, 1212-1213 (2010).
- [8] K. Ariga *et al.*, *J. Am. Chem. Soc.* **129**, 11022-11023 (2007).
- [9] Q. Ji *et al.*, *J. Am. Chem. Soc.*, **130**, 2376-2377 (2008). (Highlighted in *Nature Materials*).
- [10] Q. Ji *et al.*, *J. Am. Chem. Soc.* **131**, 4220-4221 (2009).
- [11] K. Ariga *et al.*, *Angew. Chem. Int. Ed.* **47**, 7254-7257 (2008).
- [12] K. Ariga *et al.*, *J. Am. Chem. Soc.* **122**, 7835-7836 (2000).
- [13] T. Michinobu *et al.*, *J. Am. Chem. Soc.* **128**, 14478-14479 (2006).

Theory and modeling of optical actuation in nanocomposites through in situ electron microscopy studies

E.M. Campo^a, H. Campanella^a, Y. Y. Huang^b, K. Zinoviev^a, D. Yates^c, L. Rotkina^c, J. Esteve^{a*}, and E.M. Terentjev^{b*}

^aInstituto de Microelectrónica de Barcelona IMB-CNM (CSIC), Campus UAB, Barcelona, Spain

^bCavendish Laboratory, University of Cambridge, Cambridge CB3 0HE, UK

^cUniversity of Pennsylvania, Philadelphia, PA

Nano-optical mechanical actuation based on nanotube-enriched polymeric materials is a much sought-after technology. In this scheme, light sources promote mechanical actuation of polymeric materials producing a variety of nano-optical mechanical systems such as tactile displays, artificial muscles, and nano-grippers among others.

Opto-mechanical actuation is preferred to electromechanical transduction in multiple environments because it is wireless, provides low noise, and allows for electro-mechanical decoupling. It also has the potential for much higher spatial resolution. However, few materials exhibit this property. Zhang & Ijima [1] reported one of the earliest papers on single-wall carbon nanotube (SWCNT) actuation to visible light where bundles of SWCNTs are stretched, bent, or repelled reversibly by hundreds of microns when exposed to light. Despite large actuation effects, little interest was stirred into this subject.

Polymer Carbon Nanotube Composites (PCNCs) and Liquid Crystal Elastomers (LCEs) can also reversibly change their shape upon irradiation [2]. Indeed, Ahir and Terentjev[3] engineered PCNCs that could either compress or expand upon infrared irradiation and attributed actuation to nanotube alignment. The mechanism involved in opto-actuation was tentatively modelled as rigid nanotubes suffering orientational order imposed by uniaxially applied strain. In the proposed model photon absorption forms kinks, reversibly decreasing nanotube length. However, fundamental understanding of opto-actuation down to the atomic level is still missing and the suggested model is yet to be verified through direct experimental data.

We propose to examine photoactuation of polymer-carbon nanotubes (CNTs) composites by in-situ Transmission Electron Microscopy (TEM). Specific aspects of scanning electron microscopy of polymer nanocomposites as well as the suitability of different thinning techniques have been discussed recently [4]. We present the initial steps given to prepare a TEM sample by Focus Ion Beam (FIB) thinning (shown in Figure 1) and to retrofit a TEM holder as part of the in situ photonics set up. The expectation of TEM experimental results are also discussed.

Keywords: Polymer composites, Carbon nanotubes, photoactuation, in-situ TEM, FIB.

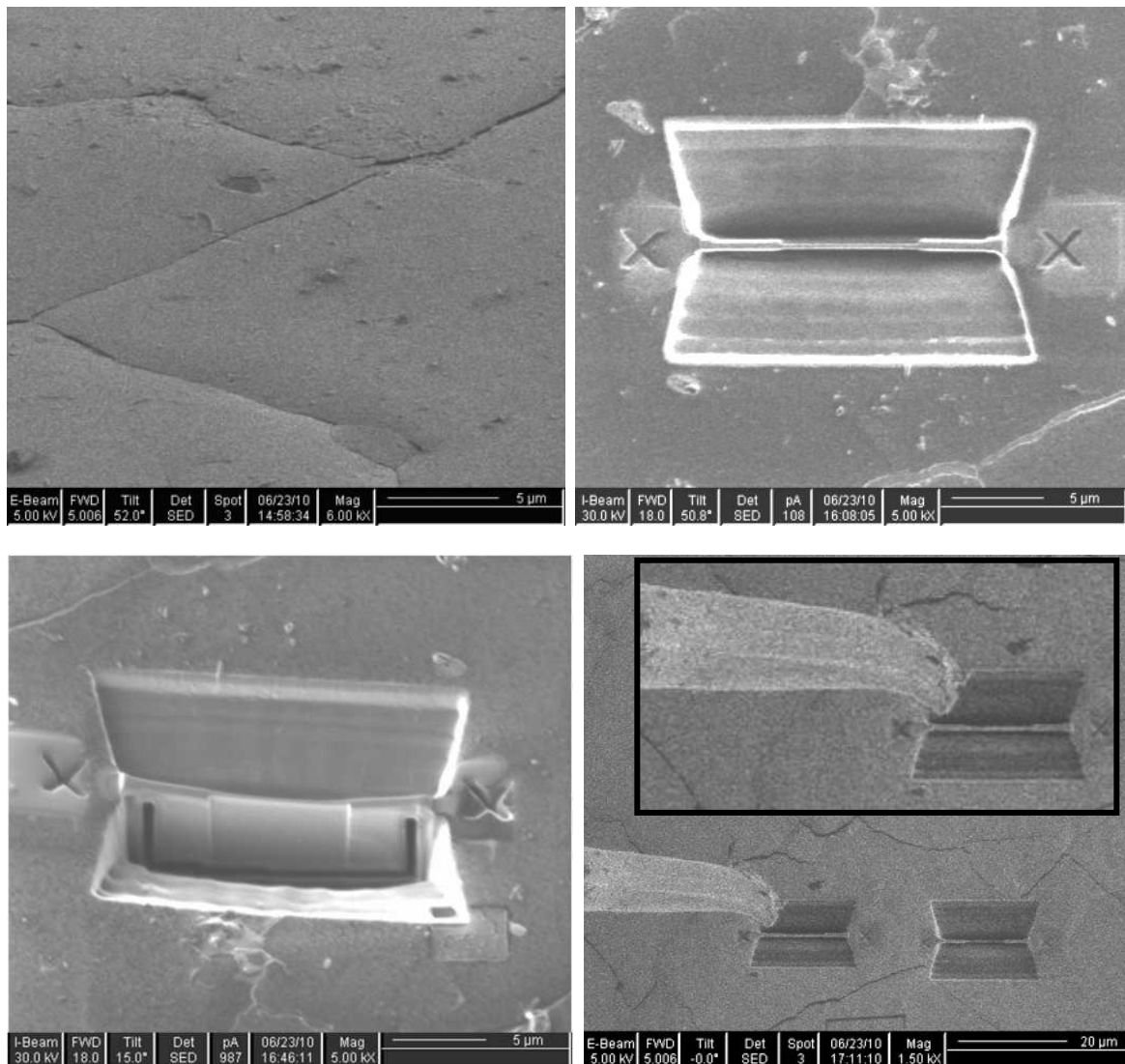


Figure 1. Focus Ion Beam Milling sequence to prepare a TEM slab for in situ experimentation. The inset shows a detailed view of the nanomanipulator in preparation for slab lift-off.

References

- [1] Zhang, Y. and Iijima, S., "Elastic Response of Carbon Nanotube Bundles to Visible Light", *Phys. Rev. Lett.* Vol. 82, No. 17 (1999)
- [2] Warner, M. and Terentjev, E.M. "Liquid Crystal Elastomers" Oxford University Press (2003)
- [3] Ahir, S.V. and Terentjev, E.M., "Photomechanical Actuation in Polymer-Nanotube composites" *Nature Materials* Vol. 4, pp 491-495, (2005)
- [4] Campo, E. M., Campanella, H., Huang, Y. Y., Zinoviev, K., Torras, N., Camargo, C., Yates, D., Rotkina, L., Esteve, J., Terentjev, E. M., "Electron microscopy of polymer-carbon nanotube composites", *SPIE Scanning Microscopy Proceedings*, Vol. 7729 (2010)

Multiscale magnetic models of ultrafast magnetic processes

Roy Chantrell

Physics Department, The University of York, UK

Magnetic materials make a vital contribution to a number of technologies, including of course magnetic recording. Increasingly, materials are structured on the nanoscale in order to produce the desired properties for specific applications. In addition, future applications may require heating of the material up to and beyond the Curie temperature characteristic of the magnetic phase transition. The important consequence is that the usual formalism, termed 'micromagnetics', cannot be used to investigate such complex phenomena. I will describe the development of new approaches linking electronic structure calculations and atomistic spin models of magnetic materials and outline applications to the fundamental understanding of ultrafast magnetisation reversal. In particular I will show that magnetisation reversal in a timescale of 300 femtoseconds is possible, and will describe the implications for heat assisted magnetic recording. Finally, I will outline recent developments which allow the bridging of the atomistic and mesoscopic lengthscales, allowing the models to be applied to the understanding of macroscopic experiments and ultimately to device design. This model will be applied to the investigation of heat assisted magnetic reversal and also opto-magnetic reversal, in which magnetisation reversal occurs in response to a pulse of circularly polarised laser light. It is shown (in agreement with experiment) that switching times on the sub-picosecond timescale are possible, with important implications for magnetic recording and spin-electronic devices.

Plasmonic waveguides: routers for light and efficient mediators between quantum emitters

Francisco J. García-Vidal

Departamento de Física Teórica de la Materia Condensada,
Universidad Autónoma de Madrid, E-28049 Madrid, Spain

Surface Plasmons (SPs) are surface electromagnetic waves that decorate metal-dielectric interfaces. Despite the inherent absorption, the propagation length of these surface waves can be as large as hundreds of microns at telecom wavelengths. Additionally, SPs provide sub-wavelength confinement in the perpendicular direction.

In the first part of the talk we will review recent developments in the search for building-up a kind of (nano)-photonic circuitry based on the aforementioned capabilities of SPs. We will put more emphasis on three routes that look very promising. 1) The so-called channel plasmons (CPs) that run in V-grooves perforated on metallic films. These surface modes were theoretically predicted almost twenty years ago but its experimental realization has only been reported very recently [1]. Moreover, the first prototypes of photonic circuits based on CPs have been also presented [2]. We will describe in detail the propagation characteristics of these surface waves and how these properties can be tailored by just tuning the geometry of the groove [3]. 2) An alternative way for light routing uses the SPs that propagate along metallic wedges, termed as wedge plasmons (WPs). We will show how these WPs present similar propagation lengths to those of CPs but they present a more pronounced subwavelength confinement [4]. 3) Very recently, we have also reported [5,6] a new type of SPs that we term as domino plasmons as they are supported by a periodic chain of metallic box-shaped elements protruding out of a metallic surface. It is shown that the dispersion relation of the corresponding electromagnetic modes is rather insensitive to the waveguide width, preserving tight confinement and reasonable absorption loss even when the waveguide transverse dimensions are well in the subwavelength regime.

In the second half we will show how both the subwavelength confinement associated with SPs and the one-dimensional character of plasmonic waveguides can be exploited to enhance the coupling between quantum emitters. Resonance energy transfer and the phenomenon of superradiance will be analyzed in three different waveguiding schemes (wires, wedges, and channels).

References

- [1] S.I. Bozhevolnyi, V.S. Volkov, E. Devaux, and T.W. Ebbesen, *Phys. Rev. Lett.* **95**, 046802 (2005).
- [2] S.I. Bozhevolnyi, V.S. Volkov, E. Devaux, J.-Y. Laluet, and T.W. Ebbesen, *Nature* **440**, 508–511 (2006).
- [3] E. Moreno, F.J. Garcia-Vidal, S.G. Rodrigo, L. Martin-Moreno, and S.I. Bozhevolnyi, *Opt. Lett.* **31**, 3447 (2006).
- [4] E. Moreno, S.G. Rodrigo, S.I. Bozhevolnyi, L. Martin-Moreno, and F.J. Garcia-Vidal, *Phys. Rev. Lett.* **100**, 023901 (2008).
- [5] M.L. Nesterov, D. Martin-Cano, A.I. Fernandez-Dominguez, E. Moreno, L. Martin-Moreno and F.J. Garcia-Vidal, *Opt. Lett.* **35**, 423 (2010).
- [6] D. Martin-Cano, M.L. Nesterov, A.I. Fernandez-Dominguez, F.J. Garcia-Vidal, L. Martin-Moreno and E. Moreno, *Opt. Express* **18**, 754 (2010).
- [7] D. Martin-Cano, L. Martin-Moreno, F.J. Garcia-Vidal and E. Moreno, *Nano Letters* (in press, 2010).

Self-Assembled Peptide Nanostructures: A New Frontier in Organic Nanotechnology

Ehud Gazit

Department Molecular Microbiology and Biotechnology, Chair of Nano-Biology, Tel Aviv University,
Tel Aviv 69978, Israel

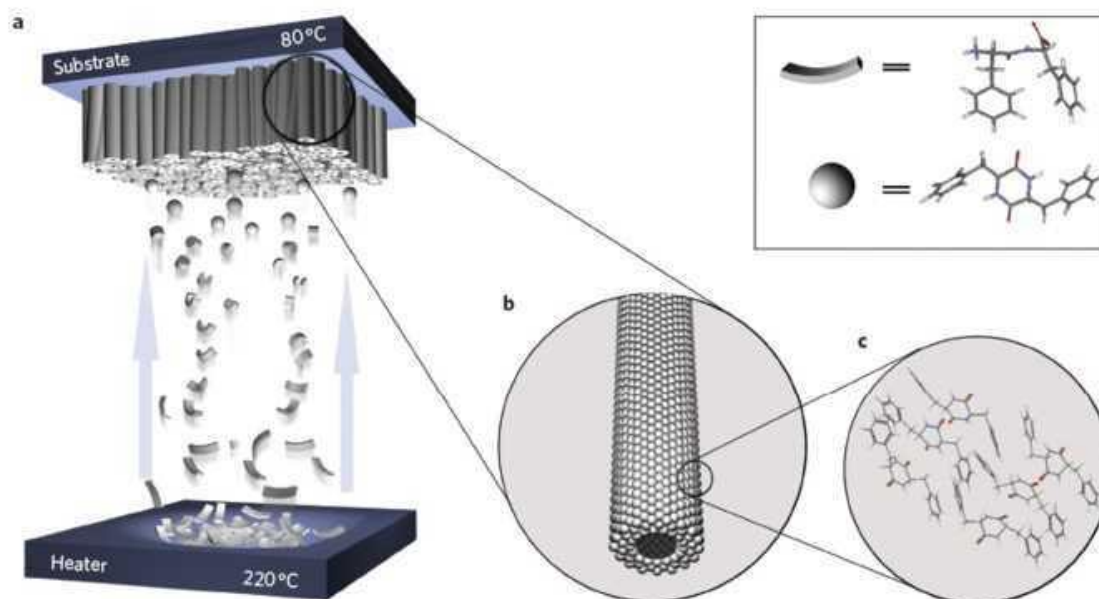
The formation of ordered amyloid fibrils is the hallmark of several diseases of unrelated origin. In spite of its grave clinical consequence, the mechanism of amyloid formation is not fully understood. We have suggested, based on experimental and bioinformatic analysis, that aromatic interactions may provide energetic contribution as well as order and directionality in the molecular-recognition and self-association processes that lead to the formation of these assemblies. This is in line with the well-known central role of aromatic-stacking interactions in self-assembly processes.

Our works on the mechanism of aromatic peptide self-assembly, lead to the discovery that the diphenylalanine recognition motif of the Alzheimer's beta-amyloid polypeptide self-assembles into ordered peptide nanotubes with a remarkable persistence length. Other aromatic homodipeptides could self-assemble in nano-spheres, nano-plates, nano-fibrils and hydrogels with nano-scale order. We demonstrated that the peptide nanostructures have unique chemical, physical and mechanical properties including ultra-rigidity as aromatic polyamides. We also demonstrated the ability to use these peptide nanostructures as casting mold for the fabrication of metallic nano-wires and coaxial nano-cables. The application of the nanostructures was demonstrated in various fields including electrochemical biosensors, tissue engineering, and molecular imaging. Finally, we had developed ways for depositing of the peptide nanostructures and their organization. We had use inkjet technology as well as vapour deposition methods to coat surface and from the peptide "nano-forests".

We are currently using this notion, as well as a novel β -breakage strategy that was developed in our laboratory, for the development of novel inhibitors of the process of amyloid formation by utilizing hetero-aromatic interactions. Our lead compound is a novel chemical entity that inhibits the formation of β -amyloid oligomers *in vitro* and protects cultured cell and isolated cortical neurons from cytotoxic effect of β -amyloid aggregates. Chronic administration of the compound was shown safe and significantly effective in preventing memory impairment in this animal model as assayed by Morris Water Maze experiments. Taken together, our hypothesis provides a new approach to understand the self-assembly mechanism that governs amyloid formation and indicates possible ways to control this process.

References

- Reches, M., & Gazit, E. (2003) Casting Metal Nanowires Within Discrete Self-Assembled Peptide Nanotubes. *Science* **300**, 625-627.
- Reches, M., & Gazit, E. (2004) Formation of Closed-Cage Nanostructures by Self-Assembly of Aromatic Dipeptides. *Nano Lett.* **4**, 581-585.
- Yemini, M., Reches, M., Rishpon, J., & Gazit, E. (2005) Novel Electrochemical Biosensing Platform Using Self-Assembled Peptide Nanotubes. *Nano Lett.* **5**, 183-186.



Proposed assembly mechanism for the formation of vertically aligned ADNTs [Taken from Adler-Abramovich et al.(2009) *Nat. Nanotech.* **4**, 849-854].

- Kol, N., Abramovich, L., Barlam, D., Shneck, R. Z., Gazit E. , & Rousso, I. (2005) Self-Assembled Peptide Nanotubes are Uniquely Rigid Bioinspired Supramolecular Structures. *Nano Lett.* **5**, 1343 - 1346.
- Mahler, A., Reches, M., Rechter, M., Cohen, S., and Gazit, E. (2006) Novel Self-Assembled Gel Biomaterial Composed of Modified Aromatic Dipeptide. *Adv. Mater.* **18**, 1365-1370.
- Carny, O., Shalev, D., and Gazit, E. (2006) Fabrication of Coaxial Metal Nanowires Using Self-Assembled Peptide Nanotube Scaffold. *Nano Lett.* **6**, 1594-1597.
- Reches, M., and Gazit, E. (2006) Controlled Patterning of Aligned Self-Assembled Peptide Nanotubes. *Nature Nanotechnol.***1**, 195-200.
- Adler-Abramovich, L., and Gazit, E. (2008) Controlled patterning of peptide nanotubes and nanospheres using inkjet printing technology. *J. Pep. Sci.* **14**, 217-223.
- Gazit, E. (2008) Bioactive nanostructures branch out. *Nature Nanotech.* **1**, 8-9
- Frydman-Marom, A. Rechter, M. Shefler, I., Bram, Y., Shalev, D. E., and Gazit, E. (2009) Cognitive Performance Recovery of Alzheimer's Disease Model Mice by Modulating Early Soluble Amyloid Assemblies. *Angew Chem Int Ed. Engl.* **48**, 1981-1986.
- Adler-Abramovich et al., and Gazit E. (2009) Self-assembled arrays of peptide nanotubes by vapour deposition. *Nature Nanotech.* **4**, 849-854.
- Ostrov, N. and Gazit, E. (2010) Genetic engineering of biomolecular scaffolds for the fabrication of organic and metallic nanowires. *Angew. Chem. Int. Ed. Engl.* **49**, 3018-3021.
- Kholkin, A., Amdursky, N., Bdikin, I., Gazit, E. & Rosenman, G. (2010) Strong Piezoelectricity in Bioinspired Peptide Nanotubes. *ACS Nano.* **2**, 610-614.
- Adler-Abramovich, L., Badihi-Mossberg, M., Gazit, E., Rishpon, J. (2010) Characterization of Peptide Nanostructures Modified Electrodes and their Application for Ultra- Sensitive Environmental Monitoring. *Small* **7**, 825-831.

Exciton-Plasmon Interactions and Fano Resonances in Nanostructures

Alexander Govorov

Department of Physics and Astronomy, Ohio University, Athens, OH, 45701;

Govorov@ohiou.edu

Coulomb and electromagnetic interactions between excitons and plasmons in nanocrystals cause several interesting effects: energy transfer between nanoparticles (NPs), plasmon enhancement, reduced exciton diffusion in nanowires (NWs), exciton energy shifts, Fano interference effect, and non-linear phenomena [1-3]. Using transport equations for excitons, we model exciton transfer in NWs and explain the origin of the blue shift of exciton emission observed during recent experiments with hybrid NW-NP assemblies [2]. We also look at optical responses of artificial light-harvesting complexes composed of chlorophylls, bacterial reaction centers, and NPs [3]. We show that, using superior optical properties of metal and semiconductor NPs, it is possible to strongly enhance the efficiency of light harvesting in such complexes [3]. An interaction between a discrete state of exciton and a continuum of plasmonic states can give rise to interference effects (Fano-like asymmetric resonances and anti-resonances). These interference effects greatly enhance visibility of relatively weak exciton signals and can be used for spectroscopy of single nanoparticle and molecules. In a nonlinear regime, the Fano effect becomes strongly amplified and results in interesting non-linear responses [4]. If an exciton-plasmon system includes chiral elements (chiral molecules or nanocrystals), the Fano-like interference effects strongly enhance the circular dichroism signals [5,6]. In conclusion, our theory explains current experimental results and also provides rationale for future experiments and applications. Potential applications of dynamic exciton-plasmon systems include sensors and light-harvesting.

References

- [1] A. O. Govorov, G. W. Bryant, W. Zhang, T. Skeini, J. Lee, N. A. Kotov, J. M. Slocik, and R. R. Naik, *Nano Letters* **6**, 984 (2006).
- [2] J. Lee, P. Hernandez, J. Lee, A. Govorov, and N. Kotov, *Nature Materials* **6**, 291 (2007).
- [3] A. O. Govorov and I. Carmeli, *Nano Letters* **7**, 620 (2007).
- [4] M. Kroner, A. O. Govorov, S. Remi, B. Biedermann, S. Seidl, A. Badolato, P. M. Petroff, W. Zhang, R. Barbour, B. D. Gerardot, R. J. Warburton, and K. Karrai, *Nature* **451**, 311 (2008).
- [5] A.O. Govorov, Z. Fan, P. Hernandez, J.M. Slocik, R.R. Naik, *Nano Letters* **10**, 1374 (2010).
- [6] Z. Fan, A.O. Govorov, *Nano Letters*, DOI: 10.1021/nl101231b (2010).

X-ray photon correlation spectroscopy studies of slow dynamics in soft glassy materials

James L. Harden

Physics Department, University of Ottawa, Ottawa, Ontario, K1N 6N5, Canada

jharden@uottawa.ca

Disordered soft solids, such as foams, gels, concentrated emulsions, and dense colloidal suspensions, exhibit apparently universal features that are characteristic of out-of-equilibrium systems. In particular these materials often display non-diffusive slow dynamics and a protracted evolution of their dynamical properties that bears strong resemblance to the phenomenon of aging seen in molecular glasses and glassy polymers, but also have features peculiar to soft systems. In an effort to understand the essential dynamical behavior of soft disordered materials at the nanoscale, we have conducted x-ray photon correlation spectroscopy (XPCS) studies on a variety of soft solids and complex fluids. The combination of large wave vectors and long time scales accessible with XPCS makes the technique uniquely well suited for elucidating the nanoscale motions in such glassy materials. In this talk, I will provide an overview of XPCS studies for a group of characteristic soft solids and complex fluids, including synthetic clay gels [1], concentrated nanoemulsions [2], nanoparticle networks [3,4], and polymer melts doped with nanoparticles [5]. For all the disordered soft solids, we observed the same generic slow dynamics characterized by an intermediate scattering function that follows a “compressed” exponential form, $g_1(Q,t) \sim \exp[-(t/\tau)^\beta]$, with $\beta \approx 1.5$ and $\tau \sim Q^{-1}$, as shown in Figure 1. Such behavior contrasts with glassy diffusion, for which correlation functions are stretched ($\beta < 1$) and $\tau \sim Q^2$. Thus, we conclude that the dynamical evolution of the disordered soft solids, while displaying signatures of aging, cannot be directly related to traditional aging phenomena in glasses. Rather, these dynamical features can be explained in terms of strain from random, highly localized stress relaxation events [6]. Interestingly, we have found that such non-diffusive dynamics may also occur transiently in complex fluid systems, such as polymer melts [5] and concentrated polymer solutions.

References

- [1] Bandyopadhyay, et al., Phys. Rev. Lett. **93**, 228302 (2004).
- [2] Guo, et al., Phys. Rev. E, **75**, 041401 (2007).
- [3] Chung, et al., Phys. Rev. Lett. **96**, 228301 (2006).
- [4] Guo, et al., Phys. Rev. E, **81**, 050401 (2010).
- [5] Guo, et al., Phys. Rev. Lett., **102**, 075702 (2009).
- [6] Cipelletti et al., Faraday Discuss. **123**, 237 (2003).

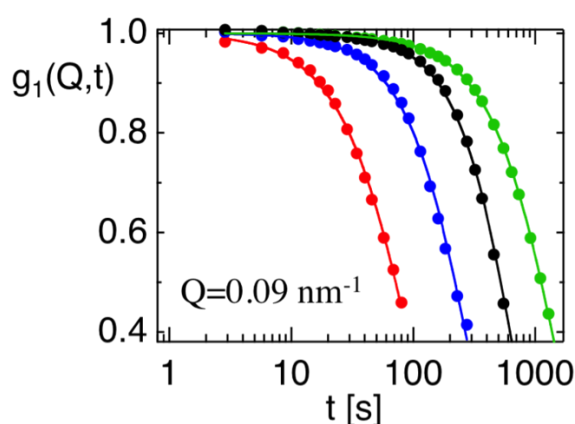


Figure 1. $g_1(Q,t)$ for nanocolloid depletion gels at times $t_s=800, 2500, 6100,$ and 13000 s after shear fluidization. Solid curves are fits to a stretched exponential form with $\beta \approx 3/2$.

Towards an understanding of crystal growth on the nano-scale: in-situ probes for graphene, nanotube and -wire CVD

S. Hofmann

Department of Engineering, University of Cambridge, Cambridge CB3 0FA, UK

sh315@cam.ac.uk

The understanding of the role of transition metal templates in the chemical vapour deposition (CVD) of nano-materials, such as graphene, carbon nanotubes and Si/Ge nanowires, remains incomplete, which limits a widespread utilisation of these materials. We investigate nanometrology that allows a monitoring of the catalytic CVD process and the contributing atomistic processes under high temperatures and reactive gas atmospheres, i.e. under typical reactor conditions. Our results aim to establish a framework for detailed growth modelling and an understanding of the materials and chemistry on the nano-scale.

We use high-pressure X-ray photoelectron spectroscopy (XPS) supported by environmental transmission electron microscopy (ETEM) and in-situ X-ray diffraction (XRD) to compare the behaviour of thick, poly-crystalline and nano-particulate catalysts during hydrocarbon exposure at temperatures ranging from 300-900°C, and during cooling to room temperature. For carbon nanotube (CNT) CVD, we find that oxide supported Fe and Ni are active as crystalline metallic nanoparticles [1,2]. For these systems, control over CNT growth is closely linked to catalyst-support interactions [3] and to pre-treatment conditions that prevent excessive coarsening and result in a suitable catalyst phase and topography [4]. On the other hand, we find that nano-particulate zirconia neither reduces to a metal nor forms a carbide while nucleating CNTs [5]. Such oxide-based catalysts or “metal-free” systems indicate a surface-based nanotube formation mechanism and/or significant deviations from bulk equilibrium phase diagrams. In order to study size- and solubility-dependent mechanisms, we compare catalyst nanoparticles with different diameters and use thick (>300 nm), poly-crystalline catalyst films, which we optimised for graphene growth. We focus on graphene nucleation and graphene domain size in relation to the catalyst grain size distribution and the C chemical potential. Time-resolved XPS allows a detailed comparison of transient states prior to graphene formation and C/metal core level signatures for CVD and bulk precipitation experiments, based on which we model the growth process.

Although it is generally agreed that the phase diagrams of nanoscale systems can be substantially different than compared to the bulk, there is very little direct experimental evidence demonstrating such size effects under growth conditions. We use Ge/Au as a model system and our ETEM data shows the formation of a liquid Au-Ge layer on sub-30 nm Au catalyst crystals, and the transition of this two-phase Au-Ge/Au coexistence to a completely liquid Au-Ge droplet during isothermal digermane exposure at temperatures far below the bulk Au-Ge eutectic temperature [6]. Upon Ge crystal nucleation and subsequent Ge nanowire growth, the catalyst either re-crystallizes or remains liquid, apparently stabilised by the Ge supersaturation. Kinetic and thermodynamic modeling gives insight into the importance of surface energies and catalyst-interface dynamics [7] to nanowire growth and geometry. We believe that such metastable nanoparticle phases are relevant to other materials systems and of key importance to controlled bottom-up crystal growth and materials design for nanotechnology.

References

- [1] Hofmann et al., Nano Lett. 7, 602 (2007)
- [2] Hofmann et al., J. Phys. Chem. C 113, 1648 (2009)
- [3] Mattevi et al., J. Phys. Chem. C 112, 12207 (2008)
- [4] Esconjauregui et al., APL 95, 173115 (2009)
- [5] Steiner et al., JACS 131, 12144 (2009)
- [6] Gamalski et al, Nano Letters, asap (2010)
- [7] Hofmann et al, Nature Materials 7, 372 (2008)

Carbon nanotubes and graphenes for building blocks of nanodevices

K. Ishibashi^{1,2}, A. Hida¹, S. Moriyama³, T. Fuse¹ and T. Yamaguchi¹

¹Advanced Device Laboratory, RIKEN Advanced Science Institute, Japan

²Interdisciplinary Graduate school of Science and Technology, Tokyo Institute of Technology, Japan
International Center for Materials Nanoarchitectonics (MANA), National Institute for Materials Science, Japan

kishiba@riken.jp

Single-wall carbon nanotubes (SWCNTs) and graphenes are grown in a self-assembled manner, and are composed by carbon. The various nanodevices could be realized with these materials due to their unique structural and physical properties. For example, they are suitable for spin-based quantum bit (qubit) with long spin coherence due to small spin orbit interaction and a natural abundance of nuclear spins in the host atom. The talk covers the following topics below.

1) Artificial atom behaviors of the SWCNT quantum dot [1-3]

It is shown that the electrons confined in the SWCNT behave those confined in the one-dimensional hard-wall potential. This makes the degeneracy of the quantum states, independent on the number of electrons or the quantum numbers. In the SWCNT quantum dots, the four or two electron shell structures are observed even with many electrons in the dot. The energy scales associated with the dot fall in a THz range, which is demonstrated by the THz photon assisted tunneling in the SWCNT single quantum dot.

2) Chemical modification of SWCNTs and their molecular scale nanostructures

Two examples of SWCNT-based molecular scale nanostructures are shown. The ring structures were fabricated with both SWCNT ends connected chemically. The scanning tunneling spectroscopy (STS) revealed a standing-wave pattern along the ring at a liquid nitrogen temperature, indicating the ballistic nature of the ring. Another example is SWCNT/molecule heterostructures. The STS study has made it possible to study the density of states and the confinement potential of a SWCNT terminated by molecules at both ends.

3) Coupled quantum dots with graphenes [4]

Graphenes quantum dots are attractive for building blocks of the spin qubit. The coupled quantum dots are basic structures for the spin qubit with a readout mechanism due to the spin blockade mechanism. The dots are formed by etching the triple-layer graphenes into the coupled dot patterns with narrow constrictions for the barriers. The coupled-dot formation has been confirmed by the charge stability diagram of the double dots.

References

- [1] K. Ishibashi, S. Moriyama, D. Tsuya, T. Fuse, M. Suzuki, "Quantum-Dot Nanodevices with Carbon Nanotubes", *J. Vac. Sci. Technol. A* **24** (4), 1349 (2006)
- [2] S. Moriyama, T. Fuse, M. Suzuki, Y. Aoyagi, K. Ishibashi, "Four-electron shell structures and an interacting two-electron system in carbon nanotube quantum dots", *Phys. Rev. Lett.* **94**, 186806 (2005)
- [3] Y. Kawano, T. Fuse, S. Toyokawa, T. Uchida, K. Ishibashi, "Terahertz photon-assisted tunneling in carbon nanotube quantum dots", *J. Appl. Phys.* **103**, 034307 (2008)
- [4] S. Moriyama, D. Tsuya, E. Watanabe, S. Uji, M. Shimizu, T. Mori, T. Yamaguchi, and K. Ishibashi, "Coupled quantum dots in a graphene-based two-dimensional semimetal", *Nano Lett.* **9**, 2891-2896 (2009)

Atomic Layer Deposition (ALD) - An Old Tool for Modern Nanoscience

Seung-Mo Lee, Adriana Szeghalmi, Eckhard Pippel, **Mato Knez**

Max Planck Institute of Microstructure Physics, Halle, Germany

Atomic layer deposition (ALD) is a thin film deposition technique which was developed in the 1970s to meet the needs for processing thin film electroluminescent displays (TFEL). Technically and chemically it is similar to chemical vapor deposition (CVD). However, in contrast to CVD, ALD incorporates as a specific feature the separation of the chemical reaction into two half-reactions. The exposure of the substrate to separate precursor vapors allows for chemical saturation of the substrate surface with a monolayer of the precursors and thus for a precise sub-Å growth control in a cycle by cycle manner. In addition, being a non-line-of-sight deposition technique, ALD allows for good coating conformality even with 3D nanostructured substrates or structures with a high aspect ratio together with a good capability for upscaling [1].

Presently, the vast majority of research performed involving ALD is based on the deposition of thin film high- κ materials, such as HfO_2 . Aside from these technological applications, an increasing number of researchers make use of the precision of ALD for fabrication or functionalization of nanostructures, optical coatings, catalytically active coatings, encapsulation, corrosion protection or even infiltration of soft materials with metals. Among these research fields, functional coatings for optics are of special interest. A combination of nanostructures and multilayer coatings can provide tunable optical filters which can be used in spectroscopy [2] (see fig. 1). Even X-ray optics can benefit from thin film nanolaminate coatings [3].

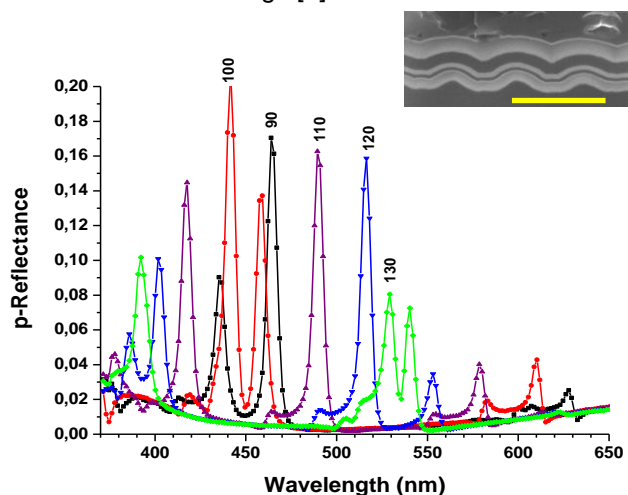


Figure 1. Selected reflection spectra as function of the rotation angle of a coated nanostructure (shown in the inset of the figure) upon irradiation with white light. The scale bar in the inset corresponds to 400 nm [2]. The most recently evolving application of ALD deals with the modification of mechanical properties of soft materials after infiltration of metals by ALD. Although the detailed chemistry behind the approach is not yet understood, biological materials, such as spider silk, collagen, or some polymers can positively or negatively alter their mechanical properties after being treated with pulsed vapors of metal precursors. The toughness of such materials increased by up to 10-fold, outperforming most manmade

materials [4] (see fig. 2). Properly adjusted, in the future this approach can potentially be used in the textile industry or the production of artificial tissues.

Most commercial ALD tools were developed for use in the microelectronics industry. Therefore, the tool design is far from being perfect for many other nanotechnology applications. Developing suitable systems for nanoparticle coatings, continuous coating systems (e.g. for fibers), or convenient tools for low-temperature or ambient pressure processing, is still a challenge.

In summary, ALD is one method-of-choice for numerous applications in nanoscale manufacturing and functionalization. Instead of being just a tool for coating, it opens numerous possibilities for research and development in various fields, from optics to electronics and even fabrics. The possibility to upscale the processes allows for a direct transition from research to development or even production, especially if 3D structures are to be produced or functionalized.

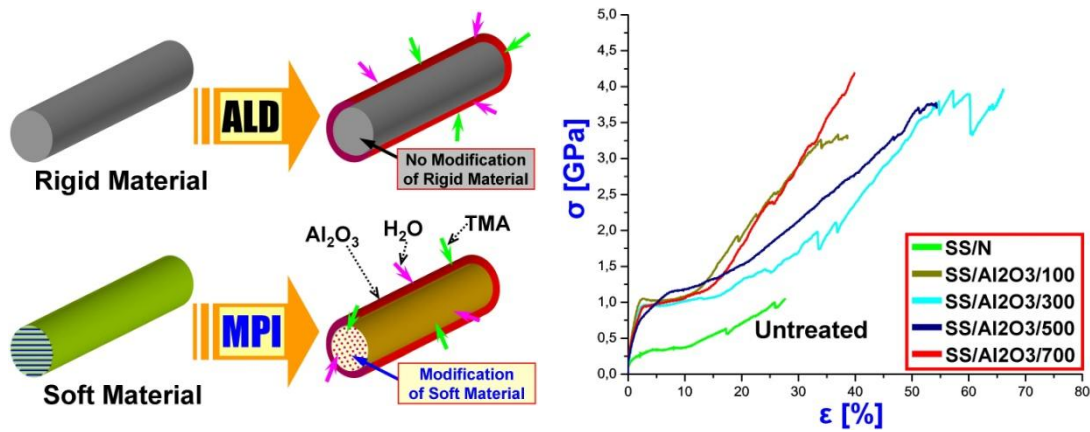


Figure 2. left: Schematic view in the difference of the classical atomic layer deposition and the infiltration occurring during ALD on some soft materials. Right: Simultaneous increase of strength and ductility (leading to a toughness increase) of spider silk after an infiltration process.

References

- [1] M. Knez, K. Nielsch, L. Niinistö, *Adv. Mater.* **2007**, 19, 3425-3438.
- [2] A. Szeghalmi, M. Helgert, R. Brunner, F. Heyroth, U. Gösele, M. Knez *Adv. Funct. Mater.* **2010**, 20, 2053-2062.
- [3] A. Szeghalmi, S. Senz, M. Bretschneider, U. Gösele, M. Knez, *Appl. Phys. Lett.* **2009**, 94, 133111.
- [4] S.-M. Lee, E. Pippel, U. Gösele, C. Dresbach, Y. Qin, C.V. Chandran, T. Bräuniger, M. Knez, *Science* **2009**, 324, 488-492.

Protein nanofibrils

Tuomas P.J. Knowles

Department of Chemistry, University of Cambridge, Lensfield Road, Cambridge CB2 1EW, UK

Many proteins possess an intrinsic susceptibility to self-assemble from their normal soluble form into elongated nanostructures, commonly known as amyloid fibrils – a process which has intricate connections with many important normal and aberrant biological pathways. This talk discusses protein nanofibrils both from a biomedical and a bionanotechnology point of view. The uncontrolled formation and growth of such amyloid structures is associated with increasingly prevalent disorders, including type II diabetes and Alzheimer's disease, but such structures are also found in functional roles in nature, including as catalytic scaffolds, functional coatings and as mediators of epigenetic information in microorganisms.

This talk presents results from the use of a range of experimental approaches, including scanning probe microscopy, biosensors and microfluidic devices, and their application to develop a quantitative understanding of the parameters which control protein self-assembly on the nanoscale.

References

- [1] Knowles et al, PRL **96**, 238301 (2006)
- [2] Knowles et al, PNAS **104** 10016 (2007)
- [3] Knowles et al, Science **21**, 318 (2008)
- [4] Knowles et al, Science **326**, 1533 (2009)
- [5] Knowles et al, Nature Nanotechnology **5**, 204 (2010)

Optical and transport properties in molecular nanosystems observed by STM-based techniques

Y. Kuwahara

¹ Department of Precision Science and Technology, Graduate School of Engineering,
Osaka University, 2-1 Yamada-oka, Suita, Osaka 565-0871, Japan

kuwahara@prec.eng.osaka-u.ac.jp

For the real progress of nanotechnology, it is indispensable to develop novel methods that can measure various physical and chemical properties of nanostructures by accessing each structure directly. From this point of view, we have developed specialized scanning tunneling microscope (STM) techniques to investigate various functionalities of nanostructures. By use of these STM techniques we evaluated and controlled functions of the molecular nanosystems fabricated on solid surfaces. In order to put the obtained information by these techniques to practical use, we verified to fabricate prototypes of electric and optical devices.

1.- Evaluation of electric transport properties in organic molecular layers

Basic science interest and potential applications in large-area, flexible electronic systems motivate research in the field of organic semiconductor systems. So far, many works aimed an understanding charge transport in organic semiconductor systems, but a well developed, microscopic investigation is still lacking. We have constructed a novel method based on STM, an independently-driven double-tip scanning tunneling microscope (DT-STM) system[1-2], which has two independently-operated tips. The two tips are used as point contact electrodes to test the performance of various prototype of organic nanoscale electric/electronic devices. We performed the direct measurement of two-dimensional electrical conductance and mobility of molecular thin films in the range of micrometer region using DT-STM. We also obtained the pronounced anisotropy of the mobility of a pentacene single crystal using DT-STM and successfully correlated the mobility anisotropy with the molecular crystal structure for the first time [3]. In addition, we fabricated nanogap flat electrodes with smooth boundaries between metal electrodes and an insulating substrate for the purpose of evaluating the electrical transport properties of a single molecule and molecular assemblies. We proposed a simple fabricating procedure that combined a lift-off process containing electron beam lithography and reactive ion etching with a mechanical grinding process. By use of the nanogap flat electrodes, high mobility in nanoscale organic-thin-film FET has been realized [4].

2.- Optoelectronic property measurement for organic molecular nanosystems

The photophysical properties of organic molecules/thin layers have been extensively investigated because of their potential applications in the field of photonics, and organic photo/electroluminescence devices. We have investigated the optoelectronic characteristics of nanomaterials, in particular, organic molecular nanosystems by use of STM-induced light emission (STM-LE) analysis [5]. Tunneling electrons from STM were used to excite photon emission from nanostructures on the surface, and the high spatial resolution of STM enables a demonstration to evaluate light emission spectra from organic molecular nanosystems in nanometer scale. Surface plasmons in the interface between a metallic/dielectric medium generate an intense electromagnetic field on the metal surface, which provides an efficient enhancement field for some optical processes. Recently, we have reported plasmon-enhanced copper phthalocyanine (CuPc) fluorescence on an Au(111) substrate by STM-LE. The quantum efficiency of the intrinsic fluorescence of CuPc is very low; however, the plasmon enhancement effect on an Au surface extensively increases fluorescence efficiency.

Considering a prospect of applications to use the plasmon enhancement effect, we fabricated a thin film organic light emission diode (OLED) on a trial base, and investigated the enhancement of electroluminescence by surface-plasmon-coupled emission [6]. Through the use of Au nanoparticles embedded in the hole transport layer, the emission intensity was increased significantly, indicating that Au nanoparticles effectively increase the internal quantum efficiency of an OLED owing to the strong coupling of excitons with localized surface plasmons of Au nanoparticles.

References

- [1] K. Takami, et al., J. Phys. Chem. B 108 (2004) 16353-16356.
- [2] K. Takami, et al., Jpn. J. Appl. Phys. 44 (2005) L120 - L122.
- [3] T. Kawanishi, et al., Appl. Phys. Lett. 93, (2008) 023303.
- [4] Y. Miki, et al. To be submitted.
- [5] T. Uemura, et al., Chem. Phys. Lett. 448 (2007) 232-236.
- [6] A. Fujike et al., Appl. Phys. Lett. 98 (2010) 043307.

Chiral recognition on surfaces: from single molecule tracking to 3D crystals

M. Lingenfelder^{1,3}, G. Tomba², G. Costantini¹, Y. Wang¹, Maarten van der Meijden⁴, Richard Kellogg⁴, A. De Vita², D. Amabilino³ and K. Kern¹

¹ Max-Planck-Institute for Solid State Research, Heisenbergstr. 1 D-70569 Stuttgart, Germany

² Physics Department, King's College London, Strand, London WC2R 2LS, United Kingdom

³ Institut de Ciència de Materials de Barcelona (CSIC) Campus Universitari 08193-Bellaterra, Spain

⁴ Syncom BV Kadijk 3 9747 AT Groningen 9704 CE Groningen, The Netherlands

The emergence of homochirality in biomolecular systems is one of the most intriguing open questions of Nature. The self-assembly and amplification of chiral subunits into higher-order species is crucial in understanding the development of homochirality in biological function. Apart from being related to the very first organic molecules synthesized on earth, understanding the basics of chiral recognition and discrimination is of high technological relevance. In fact, the chemistry and technology of production and separation of enantiomers has evolved into a branch of materials science under the name of Chirotechnology.

In this scenario, our work aims to get an insight into the fundamental aspects of chiral recognition, under the main inspiring question: How does chiral recognition take place at the single molecule level? and secondly: How can we tune the expression of chirality on a 2D template to achieve stereoselectivity for the growth of 3D crystals?

By tracking the conformational dynamics of adsorbed dipeptides on Cu(110) by scanning tunneling microscopy (STM) we have recently shown that chiral recognition takes place at the single-molecule level via the general "induced fit" mechanism developed by Pauling and Koshland more than 50 years ago.

Moreover, we can now show that fully patterned biomolecular chiral surfaces can be created by two novel methods: tuning the expression of supramolecular chirality by molecular engineering of chiral adsorption sites (footprint engineering of aminoacids) and 2D co-crystallization (mixed phases of achiral and chiral molecules) under ultra high vacuum conditions. Recent developments on diastereomeric recognition and selective crystallization at the solid/liquid interface will also be presented.

Self-Assembly and Directed Assembly of Gold Nanoparticles

Luis M. Liz-Marzán

Departamento de Química Física, Universidade de Vigo, 36310 Vigo, Spain,

The assembly of nanoparticle building blocks is a pre-requisite for the amplification of the properties of the components and/or the generation of new features unique to the ensemble. Usually, nanoparticles employed for these assemblies are spherical and lack a geometrical preference toward directional self-assembly, thus limiting their potential applications. In contrast, controlled self-assembly of non-spherical nanoparticles, such as gold nanorods, enables these arrays to form defined 1D, 2D or 3D structures with a vectorial dependence of the desired properties. We show in this communication several examples of directional nanoparticles assembly.

Standing 2D and 3D superlattices made of gold nanorods can be obtained through the use of gemini surfactants as capping agents in aqueous solution. The extreme directionality of these assemblies is reflected in the anisotropic optical properties of the crystalline superlattices¹.

On an alternative approximation, H-bonding can be exploited as the driving force to induce chain formation in functionalized nanorods. This assembly can be directed in such a way that end-to-end junctions are preferential.²

Finally, grooved PDMS surfaces will be demonstrated to serve as stamps to create long range gold nanoparticle arrays, where the specific organization depends on the groove size and periodicity. Such ordered arrays can be applied as efficient substrates for improved SERS detection.³

References

- [1] A. Guerrero-Martínez, E. Carbó-Argibay, J. Pérez-Juste, G. Tardajos, L.M. Liz-Marzán, *Angew. Chem. Int. Ed.* **2009**, *48*, 9484-9488.
- [2] W. Ni, R.A. Mosquera-Castro, J. Pérez-Juste, L.M. Liz-Marzán, *J. Phys. Chem. Lett.* **2010**, *1*, 1181-1185.
- [3] N. Pazos-Pérez, W. Ni, A. Schweikart, R.A. Alvarez-Puebla, A. Fery, L.M. Liz-Marzán, *Chem. Sci.*, in press. doi: 10.1039/c0sc00132e

Engineering biosensors and nanoparticle based drug carriers using a novel photonic technology

M.T. Neves-Petersen¹, G. Prakash Gajula¹, M. Correia¹, and S. B. Petersen^{1,2}

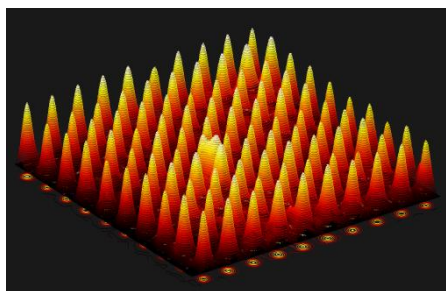
¹ NanoBiotechnology Group, Department of Physics and Nanotechnology, Aalborg University, Skjernvej 4A, Aalborg, Denmark

² University at Buffalo, The State University of New York Buffalo, The Institute for Lasers, Photonics and Biophotonics, NY 14260-3000, USA

tnp@nano.aau.dk , gp@nano.aau.dk, mc@nano.aau.dk, sp@nano.aau.dk

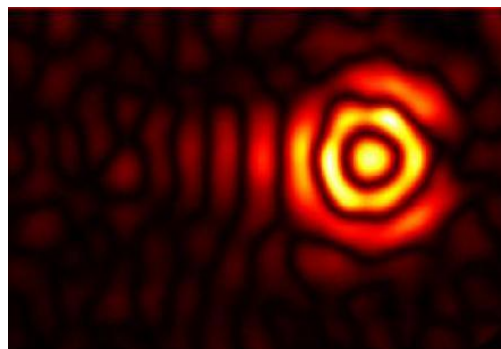
Light assisted molecular immobilisation (LAMI) is a novel technology that results in spatially localised covalent coupling of a large variety of protein molecules and other biomolecules onto thiol reactive surfaces, e.g. thiolated glass/quartz, gold or silicon [1-4]. The reaction mechanism behind the reported new technology

Protein microarray (1 μ m spots) carried out with LAMI

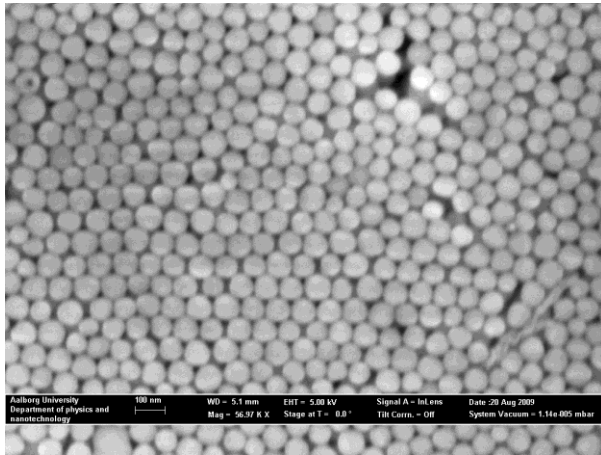


involves light-induced breakage of disulphide bridges in proteins upon UV illumination of nearby aromatic amino acids resulting in the formation of reactive molecules which will bind thiol reactive surfaces [5]. This new technology allows for dense packing of different biomolecules on a surface (enzymes, antibody Fab fragments, cancer markers such as prostate specific antigen PSA) allowing the creation of multi-potent functionalised active new materials [2, 3, 6-9]. We have recently shown that the new photonic technology combined with the Fourier-transforming properties of lenses as well as with a simple millimeter scale feature size spatial mask allows for molecular immobilisation with diffraction limited resolution, achieving ~700nm resolved patterns of immobilised biomolecules [8, 9].

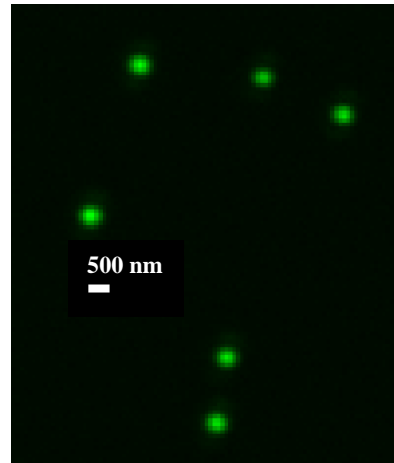
LAMI technology is ideal to couple drugs and other biomolecules to nanoparticles which can be used as carriers into cells for therapeutic purposes. We hereby show that this technique has the outstanding potential for nanomedicine allowing the creation of sensitive nanoprobe aimed at binding therapeutically interesting molecules. These nanoprobe have biological and medical applications such as bioseparation, biosensing and drug delivery. Thiol derivatised silica nanoparticles have been prepared. In order to explore the interesting magnetic properties of magnetite, superparamagnetic Fe₃O₄@SiO₂ Core-shell nanoparticles have also been prepared and functionalised with thiol groups. We have immobilised prostate specific antigen (cancer marker), human serum albumin, bovine serum albumin and insulin onto thiol derivatised nanoparticles using LAMI technology. All nanoparticles and the protein-nanoparticle bioconjugates were characterised with Dynamic Light Scattering, Scanning Electron Microscopy, Energy Dispersive X-ray spectroscopy, UV-Vis absorption and Fluorescence spectroscopy, and Fluorescence microscopy. We are currently following the interaction between insulin immobilised onto superparamagnetic nanoparticle carriers with insulin receptor protein present in muscle cells and monitoring the induced cellular metabolic changes. Since magnetite based nanoparticles are magnetic in nature, we potentially can guide the molecular carrier to a particular cellular location by means of magnetic fields, being this way able of triggering an ON-OFF cellular response (work in progress).



Fluorescence from proteins immobilised according to a diffraction pattern (700nm resolution)



SEM image of silica nanoparticles



Extrinsic fluorescence of PSA-AF555 immobilized onto thiol functionalized silica nanoparticles

References

- [1] Neves-Petersen MT, Gryczynski Z, Lakowicz J, Fojan P, Pedersen S, Petersen E, Petersen SB. **Protein Sci.** vol. 11, pp. 588-600, 2002.
- [2] Neves-Petersen MT, Snabe T, Klitgaard S, Duroux M, Petersen SB. **Protein Sci.** vol. 15, pp. 343-51, 2006.
- [3] M. Duroux, E. Skovsen, M.T. Neves-Petersen, L. Duroux, L. Gurevich, and S. B. Petersen. **Proteomics** Vol. 7, No.19, October 2007.
- [4] Jonkheijm P, Weinrich D, Schröder H, Niemeyer CM, Waldmann, H. (2008) **Angew. Chem. Int. Ed.** 47: 9618-9647.
- [5] Maria Teresa Neves-Petersen, Søren Klitgaard, Torbjørn Pascher, Esben Skovsen, Tomas Polivka, Arkady Yartsev, Villy Sundström and Steffen B. Petersen. **Biophysical Journal**, Volume 97, Issue 1, 211-226, 8 July 2009.
- [6] T. Snabe, G. A. Røder, M. T. Neves-Petersen, S. B. Petersen, S. Buus. **Biosensors and Bioelectronics**, Volume 21, Issue 8, 1553-1559, 15 February 2006.
- [7] Antonietta Parracino, Maria Teresa Neves-Petersen, Ane Kold di Gennaro, Kim Pettersson, Timo Lövgren and Steffen B. Petersen. **Protein Science** 2010, in print.
- [8] Esben Skovsen, Maria Teresa Neves-Petersen, Ane Kold, Laurent Duroux, and Steffen B. Petersen. **Journal of Nanoscience and Nanotechnology**, 9, 7, 4333–4337 (2009)
- [9] Esben Skovsen, Ane Kold, Maria Teresa Neves-Petersen, and Steffen B. Petersen. **Proteomics** 2009, 9, 1–4.

Spin Vortices: from Fundamental Physics to Biomedical Applications

V. Novosad^a, D.-H. Kim^a, E. A. Rozhkova^b, I. Ulasov^c,
M. S. Lesniak^c, T. Rajh^b, and S. D. Bader^{a,b}

^a Materials Science Division, Argonne National Laboratory, Argonne, IL, USA

^b Center for Nanoscale Materials, National Laboratory, Argonne, IL, USA

^c The University of Chicago Pritzker School of Medicine, Chicago, USA

novosad@anl.gov

The magnetic ground state of magnetically soft thin film ferromagnets in confined geometries (on the micrometer scale) consists of a curling spin configuration, known as a magnetic vortex state. The vortex is characterized by an in-plane continuous swirling closure spin structure with a core region (typically ~10 nm in diameter) where the spins tilt out of the plane, Fig. 1b, [1, 2]. The vortex state is stable because it generates minimal stray magnetic fields, with the exception of the core area, which forms to satisfy exchange energy considerations. The vortex state can be described in terms of two quantities: a core polarization that defines whether the out-of plane component of the magnetization points up or down, and a chirality that defines the in-plane curling direction (clockwise or counter-clockwise) of the spins. The characteristic reversal mechanism is via nucleation, displacement and annihilation of the vortex [3, 4]. Previous experiments examining the dynamics of the vortex core under the influence of pulsed fields [5] have detected a translational or gyrotropic eigenmode [6] consisting of sub-GHz frequency spiral-like motion of the vortex core about its equilibrium position. The sense of the core rotation is uncorrelated with the vortex chirality and that it is determined solely by the core polarization. Further, it was shown that the magnetic vortex core can be reversed using *rf* magnetic fields of very small amplitude [7], whereas up to several kOe field is required to switch the core with static field [8]. The other higher frequency (5-10 GHz) excitations [9, 10] can be understood (within some approximation) as the usual spin waves in restricted geometries [11]. Magnetic vortices in confined ferromagnets is therefore an important research topic of broad interest due its relevance to the fundamental advancement of our understanding of nanomagnetic systems. Various applications based on magnetic vortex concept include Magnetic Random Access Memories [12], spin oscillators [13, 14], and magnetic field sensors [16, 17].

Furthermore, we have recently demonstrated that the magnetic vortex microdisks (Fig. 1a) can be successfully used as multifunctional magnetic carriers for biomedicine [17]. In particular, we will report on successful interfacing of ferromagnetic nanomaterials with a spin vortex ground state and biomaterials (antibody, whole cell). Namely, the gold-coated lithographically defined microdisks with an Fe-Ni magnetic core were biofunctionalized with anti-human-IL13a2R antibody for specifically targeting human glioblastoma cells. When an alternating magnetic field is applied the vortices shift, leading to the microdisks oscillation that causes a mechanical force to be transmitted to the cell. Cytotoxicity assays, along with optical and atomic force microscopy studies, show that the spin vortex-mediated stimulus creates two dramatic effects: (a) membrane disturbance and compromising, and (b) cellular signal transduction and amplification, leading to robust DNA fragmentation and, finally, programmed cell death [18]. The experiments reveals that by employing biofunctionalized magnetic vortex microdisks the magnetic fields of low frequency of a few tens of Hz and of small amplitude of < 100 Oe applied during only 10 minutes was sufficient to achieve ~90% cancer cells destruction. For comparison, magnetic fields of few hundreds Oe, running at ~ hundreds kHz are typically needed to achieve another type of cytotoxicity, i.e. hyperthermia treatments using superparamagnetic particles. In other words, an external power supplied to the cell cultures in our experiments is ~100,000s times smaller than that applied to magnetic particles that are presently used in hyperthermia applications.

This work and the use of the Center for Nanoscale Materials at Argonne National Laboratory were supported by UChicago Argonne, LLC, Operator of Argonne National Laboratory ("Argonne"). Argonne, a U.S. Department of Energy Office of Science laboratory, is operated under Contract No. DE-AC02-06CH11357. Work at the University of Chicago is supported by the National Cancer Institute (R01-CA122930), the National Institute of Neurological Disorders and Stroke (K08-NS046430), the Alliance for Cancer Gene Therapy Young Investigator Award and the American Cancer Society (RSG-07-276-01-MGO).

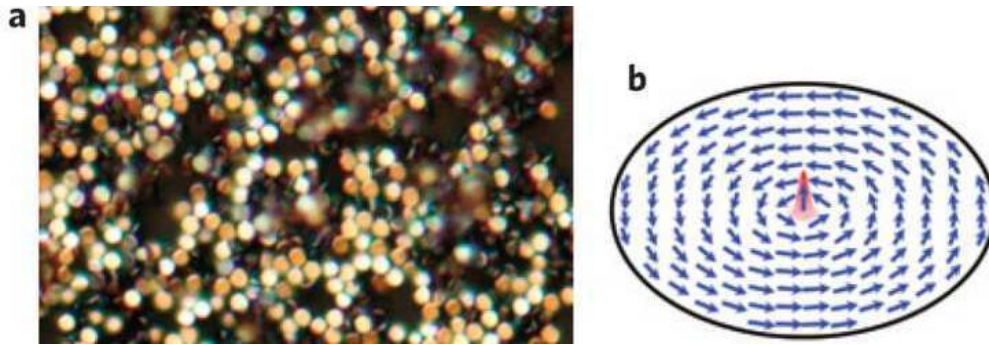


Figure 1. (a) Optical microscope image of the dried suspension of 50-nm-thick, $\sim 1 \mu\text{m}$ diameter Fe-Ni disks coated with a 5 nm of gold on each side; (b) Micromagnetic model of magnetic-vortex spin distribution.

References

- [1] T. Shinjo, *et al.*, *Science* **289** (2000) 930.
- [2] A. Wachowiak, *et al.*, *Science* **298** (2002) 577.
- [3] R. P. Cowburn, *et al.*, *Phys. Rev. Lett.*, **83** (1999) 1042.
- [4] V. Novosad, *et al.*, *IEEE Trans. Magn.*, **37** (2001) 2088.
- [5] S.-B. Choe, *et al.*, *Science* **304**(2004) 420.
- [6] A. A. Thiele, *Phys. Rev. Lett.* **30**, (1973) 230.
- [7] B. Van Waeyenberge, *et al.*, *Nature* **444** (2006) 461.
- [8] N. Kikuchi, *et al.*, *J. Appl. Phys.*, **90** (2001) 6548.
- [9] V. Novosad, *et al.*, *Phys. Rev.*, **B 66** (2002) 52407.
- [10] A. A. Awad *et al.*, *Appl. Phys. Lett.*, **96** (2010) 012503.
- [11] B. Hillebrands and K. Ounadjela, "*Spin Dynamics in Confined Magnetic Structures I*", Topics in Applied Physics, Vol. 83, Springer, Berlin, 2002.
- [12] S.-K., Kim, *et al.*, International Patent WO/2009/051442 (2009).
- [13] V. S. Pribiag, *et al.*, *Nature Physics* **3** (2007) 498.
- [14] A. Dussaux, *et al.*, *Nature Comm.*, **1**, (2010) 8.
- [15] V. Novosad and K. Buchanan, US Patent 7,697,243, 2010.
- [16] J. G. Deal, US patent Application US 2009/0117370 A1 (2009).
- [17] E. Rozhkova, *et al.*, *J. Appl. Phys.* **105**, (2009) 07B306.
- [18] D.-H. Kim, *et al.*, *Nature Materials*, **9**, 165 - 171 (2010).

Liquid processing of carbon nanotubes

P. Poulin

Centre de Recherche Paul Pascal – CNRS, Université Bordeaux I, Avenue Schweitzer,
33600 Pessac, France

poulin@crpp-bordeaux.cnrs.fr

Carbon nanotubes have to be properly spatially distributed in material to manifest their properties on macroscopic scale. Processing nanotubes in liquid states offers a variety of opportunities to control their spatial organization. The use of dispersants such as low molecular weight surfactants or polymers allows the interactions between the nanotubes to be finely tuned. As a consequence various states can be obtained from disordered dispersions with very low percolation thresholds to ordered liquid crystalline phases in which the nanotubes exhibit long range orientational ordering. Experimental observations [1-2] will be discussed and compared with recent theoretical models and simulations proposed in the literature [3, 4]. Flow of nanotube dispersions is also the opportunity to orient nanotubes and develop new processes for the fabrication of structured composites and fibers with a large fraction of carbon nanotubes. We will discuss in particular the thermomechanical properties of fibers obtained by the coagulation of nanotube dispersions in the flow of polymer solutions. Such fibers exhibit shape memory phenomena with a giant stress generation and a surprising temperature memory [5]. They can also be used as microelectrodes potentially useful for novel bio-fuel cells [6] and actuator applications [7].

References

- [1] B. Vigolo, C. Coulon, M. Maugey, C. Zakri, P. Poulin, **Science** **309**, 920-923 (2005).
- [2] C. Zakri, P. Poulin, **J. Mat. Chem.****16**, 4095-4098 (2006).
- [3] T. Schilling, S. Jungblut, M.A. Miller, **Phys Rev Lett** **98**:108303 (2007).
- [4] A. V. Kyrilyuk, P. van der Schoot **PNAS** **105**, 8221-8226 (2008).
- [5] P. Miaudet, A. Derré, M. Maugey, C. Zakri, P. Piccione, R. Inoubli, P. Poulin **Science** **318**, 1294-1296 (2007).
- [6] Gao, F.; Viry, L.; Maugey, M.; Poulin, P.; Mano, N., **Nature Communications** **1**, DOI: 10.1038 (2010)
- [7] L. Viry, C. Mercader, P. Miaudet, C. Zakri, A. Derré, A. Kuhn, M. Maugey, P. Poulin. **J. Mat. Chem.** **20**, 3487-3495 (2010)

Plasmon nano-optics for Biosciences: Sensing, Trapping and hyperthermia

R. Quidant^{1,2}

¹ ICFO-Institut de Ciències Fotòniques, Mediterranean Technology Park, 08860 Castelldefels (Barcelona), Spain

² ICREA-Institucio Catalana de Recerca i Estudis Avancats, 08010 Barcelona, Spain

In this talk, we describe our recent advances in the engineering of both the optical and thermal properties of plasmonic nanosystems and discuss their respective applications to biosciences.

Introduction

Metallic nanostructures (MN) supporting localized surface plasmon (LSP) resonances have the potential to act as efficient point-like sources of both light and heat, opening plenty of new science and applications in areas ranging from integrated optics to biomedicine. Both the optical and photothermal properties of MN can be engineered through a suitable design of their geometrical parameters, environment and illumination conditions.

Discussion

In the first part of this presentation we discuss how proper plasmon mode engineering in ensembles of electromagnetically coupled nanostructures [1] can benefit to biosensing and optical trapping. In the context of sensing, we show that shaping the sensing volume to dimensions commensurable with the target molecules to detect enables to strongly enhance the sensing sensitivity [2]. As for optical trapping, we demonstrate that plasmonic hot spots can be used to create efficient nano-optical tweezers able to trap nano-objects, including biological systems, upon moderate laser intensities [3,4].

In the second part of the talk, we discuss both theoretically and experimentally the general physical rules for optimizing heat generation in plasmonic nanostructures [5]. We then discuss the applications of functionalized point-like heat sources to the stimulation of intra cellular processes and cancer cell destruction.

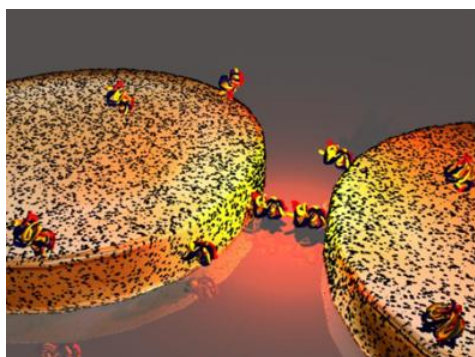


Figure 1. Artistic view of enhanced sensitivity sensing in an array of gold dimers.

References

- [1] P. Ghenuche, S. Cherukulappurath, T. Taminiau, N. F. van Hulst, R. Quidant, *Phys. Rev. Lett.* 101, 116805 (2008).
- [2] S. S. Aćimović, M. P. Kreuzer, M. U. González, R. Quidant, *ACS Nano* 3, 1231-1237 (2009).
- [3] M. Righini, P. Ghenuche, S. Cherukulappurath, V. Myroshnychenko, F. J. Garcia de Abajo, R. Quidant, *Nano Lett.* 9, 3387–3391 (2009).
- [4] M. L. Juan, R. Gordon, Y. Pang, F. Eftekhari, R. Quidant, *Nature Phys.* 5, 915-919 (2009).
- [5] G. Baffou, C. Girard, R. Quidant, *Phys. Rev. Lett.* 104, 136805 (2010).

The rise of ceramic catalysts for carbon nanotube and graphene growth

Mark H. Rummeli

IFW Dresden, Germany

Nanomaterials are of enormous fundamental interest, both from the point of view of discovering new physical phenomena as well as for their exploitation in novel devices. It is for these reasons that new nanostructures are being synthesized, functionalized and examined with respect to their special optical and electronic properties. Carbon nanotubes have a broad spectrum of interesting properties, which are relevant for technological applications. They are used for field emission and gas storage and are discussed as basic elements for future electronic devices in nanoscience and technology. Because of their nanometric dimensions and their interesting electronic properties, single walled carbon nanotubes (SWNT), in particular, are considered attractive structures to replace the semiconductor components essential in integrated circuits. The application of carbon nanotubes for producing transistors or saturable absorbers has been extensively studied; however for such applications isolated semiconducting tubes are needed. Conversely, isolated metallic nanotubes are desirable as nano-conductors. The direct synthesis of SWNT of a particular electronic form, and of a particular chirality is still lacking.

Graphene is also a remarkable material with incredible electrical and mechanical properties which was isolated more recently. This has made graphene the “new rising star” in nano-carbon based materials due to its exciting properties at the nanoscale, e.g. high charge carrier mobility. In addition, when existing as narrow strips or ribbons (ca. 10 nm wide) a band gap opens making them excellent candidates for field effect transistors. Hence, apart from the exciting possibilities in discovering new physics from these 2D structures, they offer tantalizing opportunities for the development of high speed (and even flexible) molecular electronics.

In order to integrate graphene in to electronics it needs to be fabricated in large areas or in highly defined ways (e.g. nanoribbons), better still, in a manner suited to current complimentary metal oxide semiconductor (CMOS) technology. Graphene synthesis routes which are directly compatible with current Si technology are limited.

The more popular routes to synthesize carbon nanotubes and graphene are based on the use of catalysts and these are usually metallic catalysts. Despite the success of metal catalysts they have certain drawbacks; they can be toxic and cause problems in clean room environments. In addition, in the case of nanotubes, they can be quite difficult to remove and in the process of removing them, the nanostructures themselves are often damaged. Over the last few years the use of ceramics, in particular oxide catalyst systems have begun to emerge for carbon nanotube synthesis. These exciting new catalyst systems suggest some contemporary concepts regarding their growth need re-evaluating. Moreover, many of the oxides used as catalysts are often implemented as supports in supported catalytic growth of carbon nanotubes and raise the question as to whether such supports may actually participate in the growth of the carbon nanotubes? Recent studies suggest the oxides can play an active role in the catalytic decomposition of the hydrocarbon feedstock and in the formation of sp² carbon. This latter point is particularly pertinent to graphene because it suggests the possibility of growing graphene directly on oxide surfaces. The CVD synthesis of graphene directly on oxides dispenses the need to transfer graphene after synthesis, as is the case with metal catalysts. Early investigations have shown nano-graphene can be formed directly over oxide surfaces using simple CVD routes.

To summarize, the emerging studies on ceramic catalysts, most notably oxides, suggest they have superior potential to conventional metal catalysts and open up invigorating new possibilities.

Nanoparticle Dynamics in Non-Conservative Optical Fields

Juan José Sáenz

Moving Light and Electrons (Mole) Group, Depart. Física de la Materia Condensada,
Univ. Autónoma de Madrid, Spain

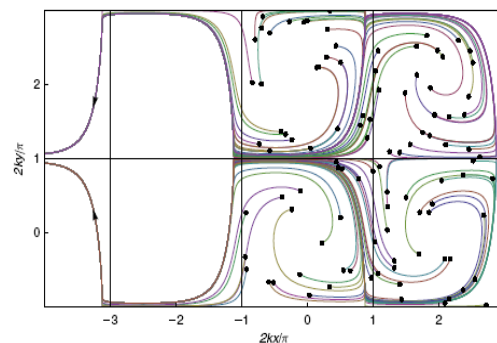
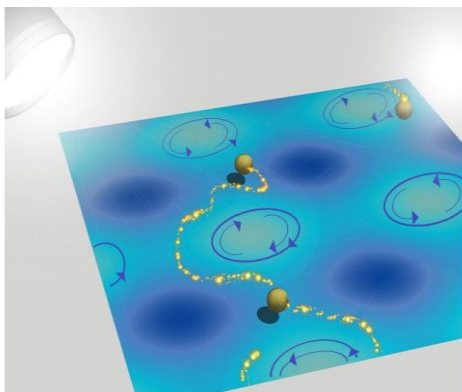
juanho.saenz@uam.es

Light forces on small (Rayleigh) particles are usually described as the sum of two terms: the dipolar or gradient force and the scattering or radiation pressure force. The scattering force is traditionally considered proportional to the Poynting vector, which gives the direction and magnitude of the momentum flow. However, as we will show, when the light field has a non-uniform spatial distribution of spin angular momentum, an additional scattering force arises as a reaction of the particle against the rotation of the spin. This non-conservative force term is proportional to the curl of the spin angular momentum of the light field [1]. We will illustrate the relevance of the spin force in the particular simple case of a 2D field geometry arising in the intersection region of two standing waves [2]. The unusual properties of the optical forces acting on particles with both electric and magnetic response will also be analyzed [3].

We will also discuss the peculiar particle dynamics in the non-conservative force field of an optical vortex lattice [4]. Radiation pressure in the whirl-light field (arising in the intersection region of two crossed optical standing waves [2]) plays an active role spinning the particles out of the whirls sites leading to a giant acceleration of free diffusion. Interestingly, we show that a simple combination of null-average conservative and non-conservative steady forces can rectify the flow of damped particles. We propose a “deterministic ratchet” stemming from purely stationary forces [4] that represents a novel concept in dynamics with considerable potential for fundamental and practical implications.

References

- [1] S. Albaladejo, M. Laroche, M. Marqués, J.J. Sáenz, **Phys. Rev. Lett.** **102**, 113602 (2009)
- [2] A. Hemmerich, T.W. Hänsch, **Phys. Rev. Lett.** **68**, 1492 (1992)
- [3] M. Nieto-Vesperinas, J.J. Sáenz, R. Gómez-Medina, L. Chantada, **Opt. Express** **18**, 1149 (2010)
- [4] S. Albaladejo, M.I. Marqués, F. Scheffold, J.J. Sáenz, **Nano Letters** **9**, 3527 (2009).
- [5] I. Zapata, S. Albaladejo, J.M. Parrondo, J.J. Sáenz, F. Sols, **Phys. Rev. Lett.** **103**, 130601 (2009)



Left: Sketch of a nanoparticle enhanced diffusion path in an optical vortex lattice [4]. **Right:** Particle trajectories in a “deterministic” optical ratchet. Initial positions are random within the chosen unit cell. All paths converge to two limit periodic trajectories which flow to the left [5].

Nanometrology: enabling applications of nanotechnology*

Clivia M Sotomayor Torres^{1,2}, T. Kehoe¹, V. Reboud¹, N. Kehagias¹, D. Dudek¹

¹ Catalan Institute of Nanotechnology, Campus de la UAB, Edifici CM3, 08193-Bellaterra (Barcelona), Spain

² Catalan Institute for Research and Advanced Studies ICREA, 08010 Barcelona, Spain

clivia.sotomayor@cin2.es

The practical application of nanotechnology, in terms of large scale production of nano-functional devices and materials, requires the development of suitable nanometrology techniques, which are tailored to (a) the features of the fabrication techniques used and (b) the parameters of the structures to be realised. After a general introduction to nanometrology, we discuss metrology techniques developed to meet the requirements of two emerging alternative patterning methods, nanoimprint lithography (NIL) and self-assembly of particles. The use of photonic and photo-acoustic effects as the basis of these metrologies ensures that they are non-contact, non-destructive and relatively quick to use.

Nanoimprint lithography (NIL) is an alternative high resolution, relatively low cost, lithography method for fabricating structures with features as small as ten nanometres, on silicon wafers up to 300 mm diameter. Sub-wavelength diffraction metrology is a new technique which has been used to characterise structures with critical dimensions as small as 50 nm, to distinguish defects [1] produced during the nanoimprint process. It is suitable for use in either inline or in situ configurations, as it requires no spectroscopic or goniometric scanning. The technique analyses a single diffraction pattern image from specially designed grating test structures, and based on the relative diffraction intensities, information can be obtained about the critical dimension, height and presence of defects in the structures. Measurements performed on a series of gratings with gradually increasing line-widths show that sensitivity to dimensional changes of at least +/- 5 nm.

Photoacoustic metrology has been used to characterize the dimensions and physical properties of polymers used in NIL. The Young's modulus of layers of PMMA and the resist mr-I 6000, of thicknesses from 586 to 13 nm, have been measured [2,3]. Acoustic phonons are generated by a 70 fs laser pulse in a pump-probe configuration (Fig. 2a). Back-scattered acoustic waves are detected at the sample surface via the change in reflectivity (Fig. 2b), and a delay line on the pump beam enables temporal resolution of 0.1 ps, with depth resolution of 10 nm. Physical parameters determine the stability of polymer nanostructures and dictate the optimum temperature, pressure and time required for NIL. Photoacoustic metrology has been used to demonstrate an increase in acoustic speed, and correspondingly Young's modulus for PMMA samples thinner than 80 nm (Fig. 2c) [3]. We are currently studying Young's modulus as a function of temperature, approaching the glass transition temperature.

Self-assembly is an emerging and highly versatile approach to nanofabrication. However, perfect crystallographic order in the plane is seldom possible. We have developed a way to obtain improved crystal ordering in the plane and in the bulk by applying acoustic fields during vertical drawing crystallisation of colloidal mesoscopic and nanoparticles [4]. The degree of crystallinity is quantitatively measured using discrete Fourier Transform analysis of the scanning electron micrograph or AFM images [5]. This approach can be extended to quantify ordering of other self-organised structures, such as micells or self-organised quantum dots. Our study covered also the 3-dimensional ordering of these structures by transmission spectroscopy [5].

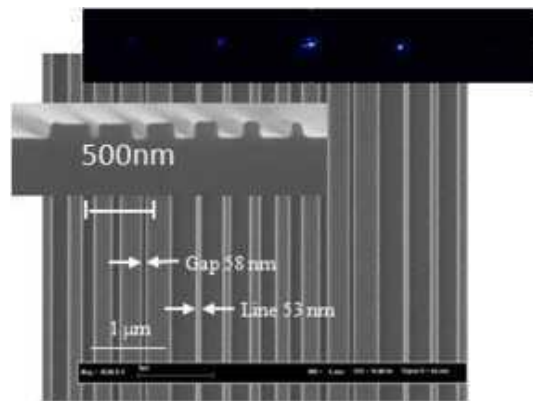
We have demonstrated new methods to characterize the structures produced by nanoimprint lithography and self-assembly, bringing these techniques closer to standardized measurements, which is a prerequisite for uptake in future applications.

Acknowledgements: Financial support of the EC Project NaPANIL (NMP2-LA-2008-214249) and of Science Foundation Ireland

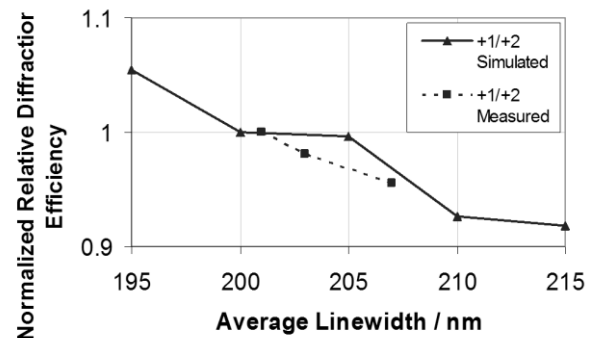
* Work done in collaboration with; R. Chauhan, J. Bryner, L. Aebi, J. Dual, all with the Institute of Mechanical Systems, ETH Zurich, CH-8092, Switzerland; with W. Khunsin now at the Max Planck Institute for Solid State Research (Stuttgart-Germany), A. Amann, E. P. O'Reilly and B. McCarthy all the Tyndall National Institute, Cork, Ireland; M. Lyschinska now at the Cork Institute of Technology, Ireland; G. Kocher now at Heriot-Watt University, Edinburgh-Scotland); with S. G. Romanov now at the Institute of Optics, Information and Photonics University of Erlangen-Nuremberg, Germany; S. Pullteap and H. C. Seat both at the ENSEIHT-INPT, Toulouse, France and with R Zentel at the für Organische Chemie, Johannes Gutenberg Universität, Mainz, Germany.

References

- [1] T Kehoe, V Reboud, C M Sotomayor Torres, *Microelectronic Engineering* **86**, (2009) 1036
 [2] J Bryner, T Kehoe, J Vollmann, L Aebi, J Dual, C M Sotomayor Torres C. M., *Proc. IEEE Ultrasonics Symposium* (2007) 1409
 [3] T Kehoe, J Bryner, V Reboud, J Vollmann, C M Sotomayor Torres, *Proc. of SPIE* **Vol. 7271** (2009) 72711V
 [4] A Amann, W Khunsin, G Kocher, C M Sotomayor Torres and E P O'Reilly, *Proc. SPIE*, **Vol. 6603**, (2007) 660321
 [5] W Khunsin, G Kocher, S G Romanov and C M Sotomayor Torres, *Advanced Functional Materials* **18** (2008) 2471

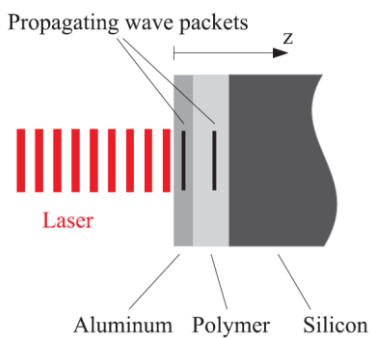


(a)

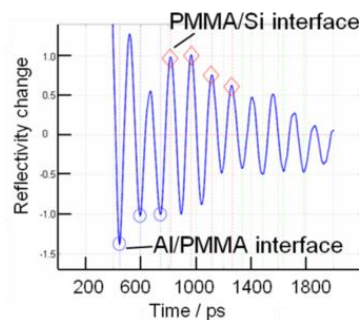


(b)

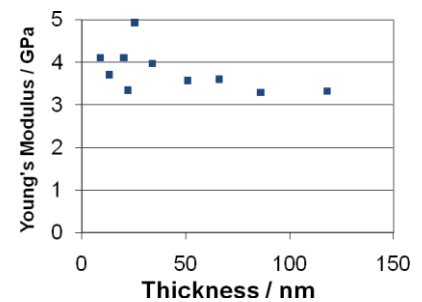
Figure 1. (a) Test gratings stamp and imprint (inset); Diffraction pattern (inset); (b) Measured and simulated relative diffraction efficiency of first and second orders, as a function of average grating linewidth



(a)

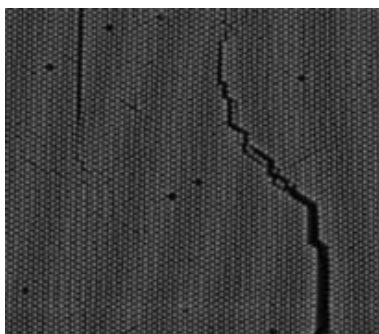


(b)

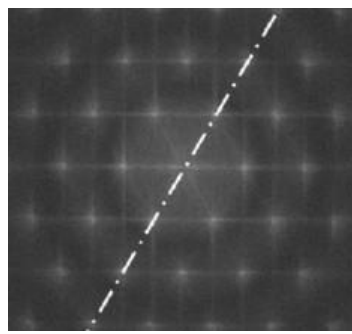


(c)

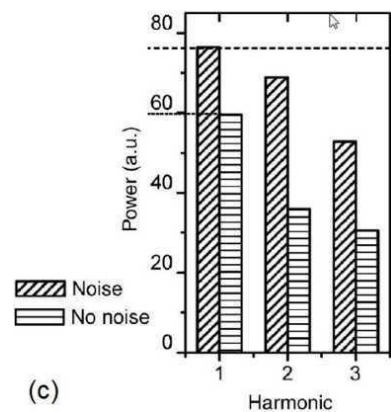
Figure 2. (a) Schematic diagram of the photoacoustic process. (b) Photoacoustic data from 51 nm thick polymer sample, showing signal from interfaces. (c) Young's modulus measured as a function of sample thickness.



(a)



(b)



(c)

Figure 3. (a) SEM image of opal film; (b) Fourier transform (FT) pattern of the SEM image; (c) Magnitudes of the first three FT harmonics, showing improvement in order due to noise

Defect Nano-Engineering in Graphitic Materials: From Doped Carbons to Graphene

Mauricio Terrones

Department of Materials Science and Engineering & Chemical Engineering, Polytechnic School, Carlos III University of Madrid, Avenida Universidad 30, 28911 Leganés, Madrid, Spain.

In this talk, defects within graphite and carbon nanotubes will be categorized in 5 different groups: 1) *Structural defects*, related to imperfections that significantly distort the curvature of the hexagonal carbon honeycomb structure; these defects are usually caused by the presence of non-hexagonal rings (e.g. pentagons, heptagons, or octagons); 2) *Topological defects*, occurring on the nanotube surface, which do not result in large curvature distortions of the tubule. In particular, these defects could be 5-7 pairs embedded in the hexagonal network or Stone-Wales (SW-type) defects that could be created by rotating a carbon bond within 4 neighboring hexagons, thus resulting in the transformation of 2 pentagons and 2 heptagons; 3) *Doping-induced defects*, arising from substitutional non-carbon atoms embedded (or incorporated) into the tubular lattice, 4) *Non- sp^2 carbon defects or edge-sites* caused the presence of highly reactive carbons such as dangling bonds, carbon chains, interstitials (free atoms trapped between SWNTs or between graphene sheets), edges (open nanotubes), add-atoms and vacancies, and 5) *Folded (or highly strained) graphene*, caused by the severe deformation of the sheets, which induces reactivity by the deformations of the sp^2 hybridized atoms.

This presentation will review recent work related to different techniques used to identify defects using HRTEM, scanning tunneling microscopy (STM), scanning tunneling spectroscopy (STS), Raman spectroscopy (RS), atomic force microscopy (AFM), thermogravimetric analyses (TGA), electron and thermal transport measurements, etc. It is important to mention that most of the time the presence of defects and their identification has been overlooked by numerous scientists. However these play a key role in the nanotubes' physico-chemical properties and biocompatibility. There are numerous challenges that will be discussed in this presentation: How do we identify defects efficiently? Could we distinguish among various defects? Would it be possible to establish a protocol able to quantify and control the amount of these defects? How many defects are necessary to fabricate robust polymer composites or 3D architectures? Could I introduce specific defects in order to make materials biocompatible? Could we promote ferromagnetism by introducing specific defects in nanostructures?, etc.

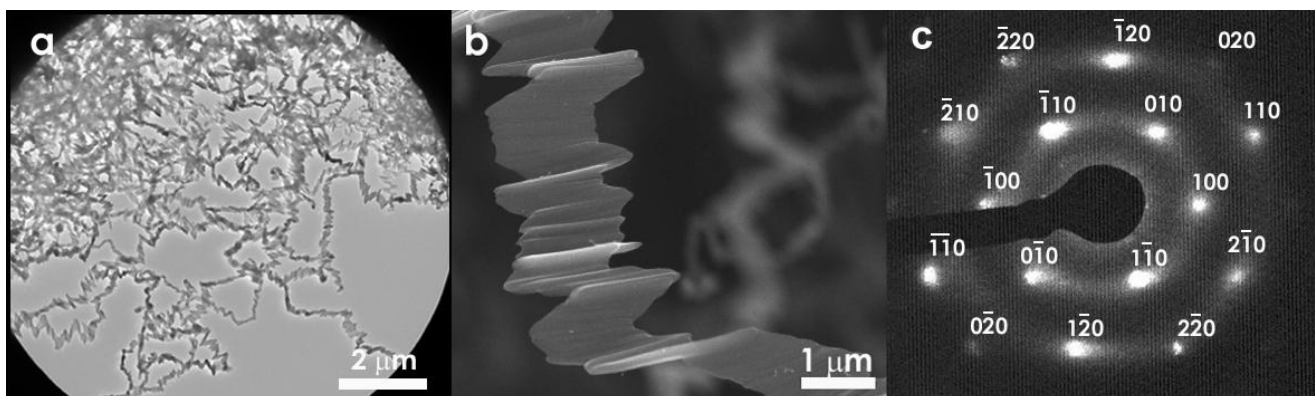


Figure 1. (a) Low and high magnification TEM image of graphene nanoribbons; (b) SEM images of an individual graphene nanoribbons, and (c) indexed electron diffraction pattern of an individual thin graphene nanoribbon (ca. 10 nm thick) showing the ABAB... stacking of the graphite structure with a 3D order.

We will also describe the use of chemical vapor deposition (CVD) for the bulk production (grams per day) of long, thin and highly crystalline graphene ribbons (<20-30 μm in length) exhibiting widths of 20-300 nm, and small thicknesses (2-40 layers; Fig. 1). These layers usually exhibit ABAB... stacking as in graphite. We also carried out transport measurements on individual nanoribbons inside the HRTEM and performed Joule heating experiments that resulted in the generation of highly crystalline graphite nanoribbons.

Finally, we will describe different methods developed by our group to obtain graphene nanoribbons based on the unzipping of multi-walled carbon nanotubes (Fig. 2). It is clear that these methods offer a

scalable route to graphene and graphitic nanoribbons. For multi-layered ribbons, exfoliation could be obtained (detachment of the layers into individual layers) as well as cutting into shorter pieces. It is clear that the ribbons and their exfoliated forms (containing several bare edges) could be used as gas storage devices, electronic wires, sensors, catalytic substrates, nanocircuits, etc. By using this new ribbon material, it is now possible to unveil new applications and novel physico-chemical properties associated with layered sp^2 hybridized carbon.

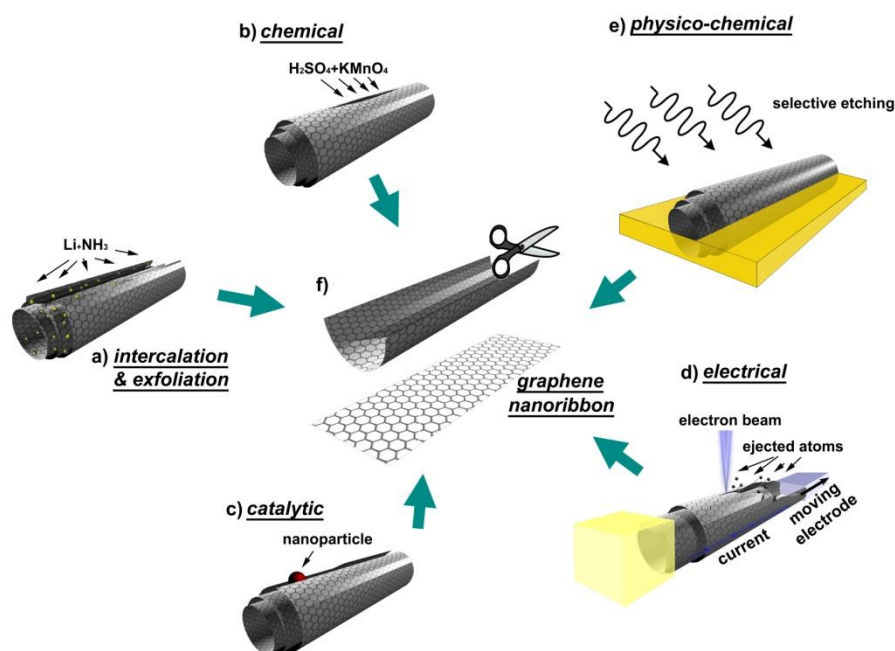


Figure 2. Sketch showing the different ways nanotubes could be unzipped to yield graphene nanoribbons (GNRs): **(a)** intercalation-exfoliation of MWCNTs, involving treatments in liquid NH_3 and Li, and subsequent exfoliation using HCl and heat treatments; **(b)** chemical route, involving acid reactions that start to break carbon-carbon bonds (e.g., H_2SO_4 and $KMnO_4$ as oxidizing agents); **(c)** catalytic approach, in which metal nanoparticles “cut” the nanotube longitudinally like a pair of scissors, **(d)** the electrical method, by passing an electric current through a nanotube physico-chemical method, and **(e)** by embedding the tubes in a polymer matrix followed by Ar plasma treatment. The resulting structures are either GNRs or graphene sheets **(f)**.

References

- [1] M. Terrones, *Int. Mat. Rev.* **49**, 325 (2004).
- [2] H. Terrones, et al., *Phys. Rev. Lett.* **84**, 1716 (2000).
- [3] X. Rocquefelte, et al. *Nano Lett.* **4**, 805, (2004).
- [4] M. Terrones, et al., *Materials Today Magazine* **7**, 30 (2004).
- [5] E. Cruz-Silva, et al. *ACS Nano* **2**, 441-448 (2008).
- [6] Y. Sato, *ACS Nano* **2**, 348-356 (2008).
- [7] J.M. Romo-Herrera, et al. *Ang. Chem. Int. Ed.* **47**, 2948-2953 (2008).
- [8] B.G. Sumpter, et al. *ACS Nano* **1**, 369-375 (2007).
- [9] X. Lepró, et al. *Nano Lett.* **7**, 2020-2026 (2007).
- [10] A. L. Elías, et al. *Small*, **3**, 1723-1729 (2007).
- [11] K.Y. Jiang, et al. *J. Mater. Chem.* **14** 37-39 (2004).
- [12] J. Campos-Delgado, et al. *Nano Letters* **8**, 2773–2778 (2008).
- [13] X. Jia, et al. *Science* **323**, 1701-1705 (2009).
- [14] M. Terrones. *Nature* **458**, 845-846 (2009).
- [15] A.G. Cano-Márquez, et al. *Nano Letters* **9**, 1527-1533 (2009).

Formation, Characterization and Catalytic Properties of Metal Nanoclusters within Molecular Layers

Kohei Uosaki

International Center for Materials Nanoarchitectonics (MANA),
National Institute for Materials Science (NIMS), 1-1 Namiki, Tsukuba 300-0044, Japan

uosaki.kohei@nims.go.jp

Metal and semiconductor nanoclusters have been attracting much attention because of their unique optical, electronic, and catalytic properties. Metal nanocluster catalysts are important not only because the ratio of surface atoms/bulk atoms increases and more metal atoms are effectively used for catalytic reactions as the size of the cluster gets smaller but also because metal nanocluster catalysts sometimes show catalytic activity that the bulk metals do not have. The origin of the unique catalytic activity of metal nanocluster catalysts is, however, not clear yet.

Hydrogen is considered to be the most important clean fuel and production of hydrogen from water using solar energy is essential for hydrogen to be widely used in future. Photoelectrochemical and photocatalytic decomposition of water has been studied for long time but many problems are not solved. Surface of semiconductor, which is the photon absorber for both photoelectrochemical and photocatalytic reactions, is usually not suitable for multi-electron reactions such as hydrogen (HER) and oxygen (OER) evolution reactions, which are the key reactions of hydrogen production from water, and, therefore, surface modification by catalytic metals are required. Direct attachment of metal onto semiconductor surface often leads to the lower efficiency due to the formation of Schottky junction and/or the introduction of surface recombination center but we have recently demonstrated that the efficient photoelectrochemical hydrogen evolution at Si electrode can be achieved by separating Pt nanoclusters (hydrogen evolution catalyst) from Si surface using organic monolayers. In this study, we followed the formation processes of Pt nanoclusters and determined the structures of the nanoclusters during HER by x-ray absorption fine structure (XAFS).

Two methods were employed to form Pt nanoclusters. In the first method, (i) a thiol-terminated organic monolayer was constructed on a hydrogen-terminated (H-) Si(111) surface by UV-induced hydrosilylation reaction, (ii) the monolayer-covered substrate was then immersed in K_2PtCl_4 aqueous solution, and (iii) finally the Pt complex attached to the monolayer was chemically or electrochemically reduced in a Pt ion free solution to form Pt clusters as shown in Scheme 1. XAFS measurements were performed at BL12C of Photon Factory after each modification step. XANES and EXAFS spectra after step (ii) show the disappearance of Pt-Cl bond and Pt coordination by more electronegative, i.e., oxygen, species. A model for the attachment of the complex to the thiol-terminated monolayer is shown in Fig. 2 (top panel). While XANES and EXAFS spectra after the chemical reduction showed the formation of Pt clusters of ca. 2 nm diameter, those after electrochemical reduction were exactly the same as those obtained before the reduction, showing the complex was not reduced, although HER is significantly accelerated at this surface compared with the surface without the Pt complex incorporation. This shows that the Pt complex is acting as HER catalyst. To see how the catalyst is working, in situ XAFS measurement is essential but not possible at this surface because the number of Pt species is too small.

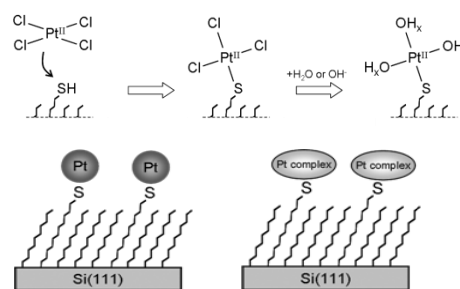
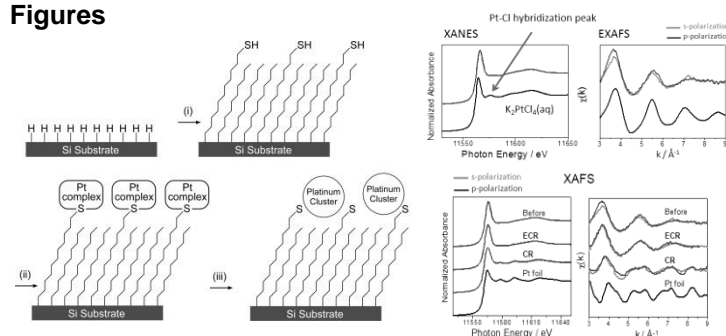
In situ XAFS study was carried out at a Si(111) electrode modified by the second method as shown in Scheme 2. After the molecular layer with viologen moiety was formed on a hydrogen-terminated Si(111) surface, the substrate was immersed in K_2PtCl_4 aqueous solution so that the Pt complex was incorporated within the molecular layer by ion exchange reaction. Figure 4 shows a series of XANES and EXAFS spectra and FT of this sample. Ex situ XANES and EXAFS spectra measured after immersion in K_2PtCl_4 solution showed typical features of $PtCl_4^{2-}$ complex. Once the sample was placed in a solution and potential was swept negatively from 0 to -0.6 V vs. Ag/AgCl, Pt-Cl hybridization peak, which appears at 11572 eV, decreased and the white line (WL) intensity increased, suggesting the exchange of Cl ligands by O species such as H_2O or OH^- . At -0.8 V, where HER vigorously took place, WL intensity decreased, indicating the reduction of Pt, but no Pt-Pt bond was observed. The WL peak also became broad as a result of Pt-H interaction as previously reported. Pt-O bond became longer at this potential. When the electrode potential was returned to 0 V, where no HER takes place, the WL peak became sharper than that at -0.8 V, suggesting the Pt-H interaction was formed only when HER is taking place. These results suggest that Pt single atom acts as HER catalyst.

In conclusion, formation of Pt single atom/molecular HER catalysts on or within organic layers.

References

- [1] T. Masuda, K. Shimazu, K. Uosaki, J. Phys. Chem. C, **112** (2008) 10923.
 [2] H. Fukumitsu, T. Masuda, D. Qu, Y. Waki, H. Noguchi, K. Shimazu and K. Uosaki, Chem. Lett., **39** (2010) 768.

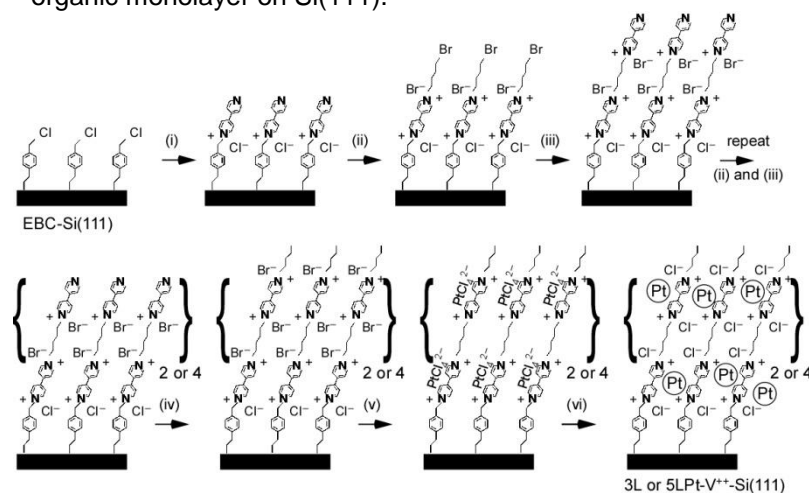
Figures



Scheme 1. Formation of thiol-terminated monolayer (i), incorporation of Pt complex (ii), and reduction of the complex (iii) to form Pt nanoclusters on organic monolayer on Si(111).

Figure 1. XANES and EXAFS spectra after step (ii) (top) and step (iii) (bottom).

Figure 2. Schematic model for complex attachment to thiol group (top) and Pt structures (bottom) after chemical (left) and electrochemical reduction (right).



Scheme 2. Formation of viologen multilayers (i-iv), incorporation of Pt complex (v), and reduction of the complex (vi) to form Pt nanoclusters within the organic layers on Si(111).

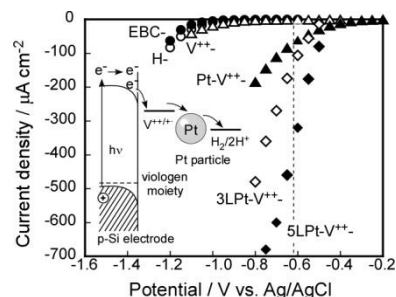


Figure 3. Steady state I-V curves of the p-type H⁻ (○), EBC⁻ (●), V⁺⁺⁻ (Δ), Pt-V⁺⁺⁻ (▲), 3LPt-V⁺⁺⁻ (◇) and 5LPt-V⁺⁺⁻ (◆) electrodes under illumination in 0.1 M Na₂SO₄ aqueous solution. Inset: Energy diagram for the HER at the p-Si(111) modified with Pt/viologen layers.

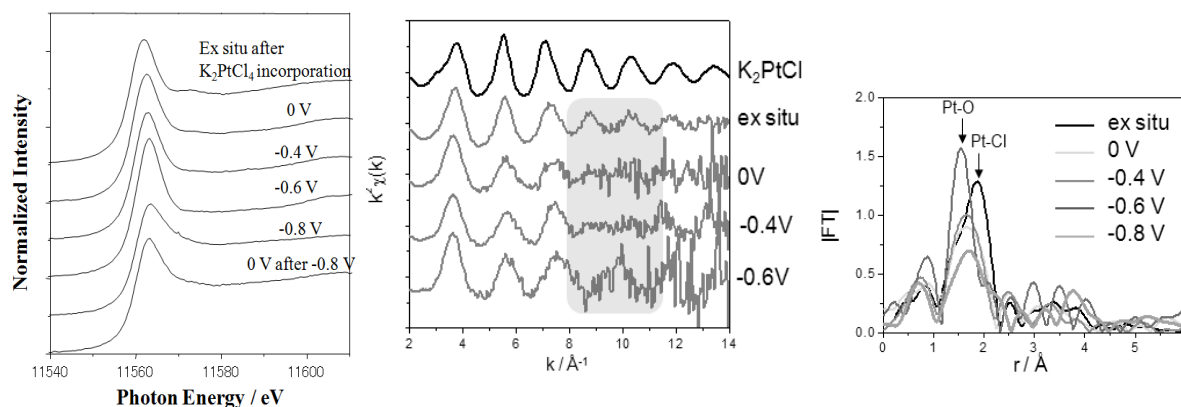


Figure 4. XANES (left) and EXAFS (middle) spectra and FT (right) obtained ex situ after immersion in K₂PtCl₄ solution and in situ at various potentials.

Pattern Transfer and Lateral Switching Modulation in Multiferroic Heterostructures

Sebastiaan van Dijken

Department of Applied Physics, Aalto University, P.O. Box 15100, FI-00076 Aalto, Finland

sebastiaan.van.dijken@hut.fi

The ability to tailor magnetic properties via coupling to ferroelectric domains is of great interest for the design of electric-field tunable magnetic devices. One-to-one imprinting of ferroelectric domains into continuous magnetic films would enable local control over magnetization dynamics but requires strong interfacial coupling to overcome exchange and magnetostatic interactions within the ferromagnet. In this paper, full pattern transfer in multiferroic heterostructures consisting of a ferroelectric substrate and a thin magnetic film with in-plane magnetization is demonstrated. Simultaneous imaging of ferroelectric and ferromagnetic domains and local magnetization reversal analysis using polarization microscopy reveals strong lateral modulations of magnetic hysteresis due to strain coupling to the underlying ferroelectric lattice. The presented experiments open up new avenues for local actuation of magnetic functionalities by external magnetic- and electric fields. Beyond this, the work provides a framework for exploring ferroelectric, ferroelastic, and ferromagnetic domain interactions in multiferroic heterostructures.

Domain formation and hysteresis in magnetic thin films depend on internal material parameters (exchange stiffness, magnetization), film thickness and shape (magnetostatics), and various other sources of magnetic anisotropy including crystal symmetry, lattice deformations (strain), and interfaces. The interplay between these film properties and an external magnetic field usually results in a laterally uniform energy landscape with random dispersions due to defects and interface roughness. The magnetic hysteresis therefore hardly depends on sample position. Area specific magnetic responses in continuous films require a local modification of the magnetic properties. This can, for example, be accomplished by the growth of ferromagnetic films onto pre-patterned substrates or local ion irradiation. In these cases, the magnetic anisotropy remains fixed after sample preparation. Interface strain coupling between ferroelectric crystals with alternating ferroelastic domains and ferromagnetic films provides an alternative route towards lateral anisotropy control in continuous magnetic media. Moreover, such multiferroic heterostructures hold the potential of electrically tunable magnetism, a phenomenon that has attracted major scientific interest in recent years.

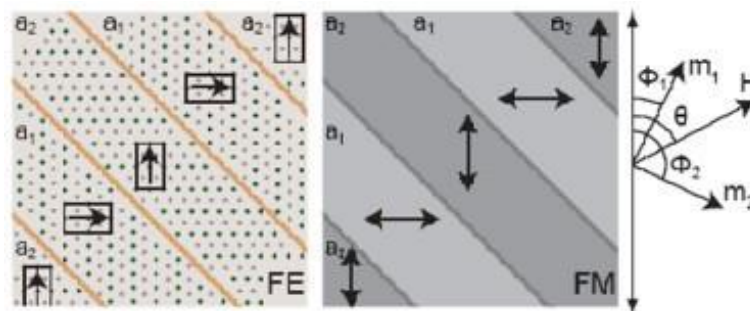


Figure 1 – Schematic illustration of the ferroelastic BaTiO_3 domain structure (FE) and the induced magnetic stripe pattern in the Fe film (FM). The arrows in FE indicate the orientation of the ferroelectric polarization and elongated c -axis in the a_1 and a_2 domains of the BaTiO_3 substrate. The uniaxial magneto-elastic easy axes in the Fe film are collinear with the ferroelectric polarization as illustrated by the arrows in FM.

In our approach to manipulate local magnetic properties we used tetragonal BaTiO_3 substrates with in-plane polarization. Stress relieve in these substrates results in a regular ferroelastic stripe pattern whereby the elongated c -axis ($c = 4.036 \text{ \AA}$, $a = b = 3.992 \text{ \AA}$) rotates by 90° in the substrate plane as illustrated in Fig. 1. Thus, the alternating a_1 and a_2 domains provide a maximum lateral strain modulation of about 1.1%. Efficient coupling of a magnetic thin film to this ferroelastic template induces

uniaxial magnetoelastic anisotropy with orthogonal magnetic easy axes in neighboring domains. A demonstration of one-to-one imprinting of BaTiO₃ domains into a continuous 10 nm thick Fe film is shown in Fig. 2. Here, strong interfacial strain coupling induces different magnetic responses in the Fe film on top of the *a*₁ and *a*₂ domains leading to an exact copy of the ferroelastic stripe pattern. Polarization analysis of the birefringent ferroelectric domains and the magnetization reversal process indicate that the ferroelectric polarization of the BaTiO₃ substrate and the strain-induced uniaxial magnetic easy axes of the Fe film are collinear. This multiferroic configuration results in coherent magnetization rotation towards the magnetic easy axes of the *a*₁ and *a*₂ domains when the applied magnetic field is reduced from saturation to zero. Thus, in the remnant state the film magnetization is laterally modulated by near 90° rotations at domain boundaries. Reversal of the applied magnetic field induces inverse domain nucleation in *a*₂ domains and more gradual magnetization reversal in *a*₁ domains. The imprinted stripe pattern in the Fe film remains visible until the magnetization is fully saturated.

The dependence of multiferroic pattern transfer on the direction and strength of the applied magnetic field, exchange and stray-field coupling between magnetic stripe domains, and other anisotropy contributions will be discussed in detail.

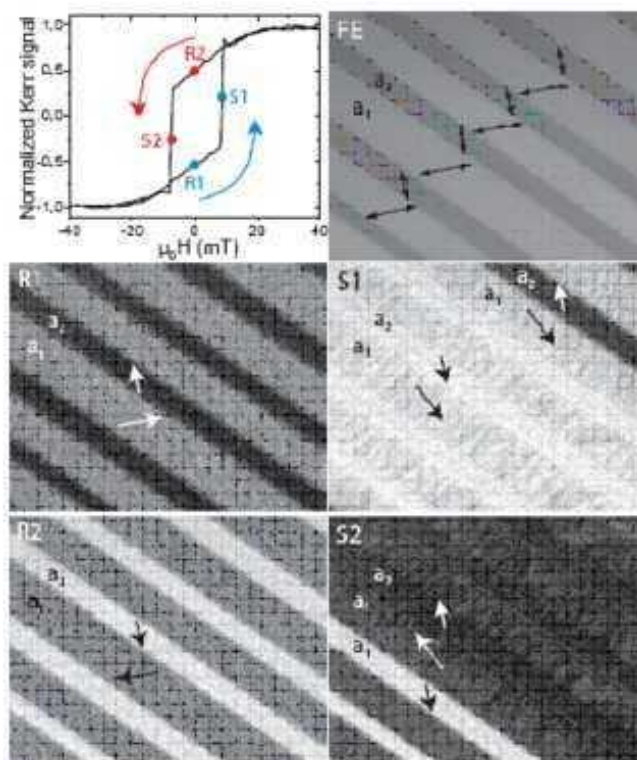


Figure 2 – Magnetic hysteresis curve and polarization microscopy images of the ferroelectric domain structure and magnetic stripe pattern during several stages of the magnetization reversal process. The figure depicts experimental data for a magnetic field angle of 10°. The hysteresis curve is a global measurement and thus an average magnetic response from several *a*₁ and *a*₂ domains. The arrows in the images indicate the orientation of ferroelectric polarization (FE) and film magnetization in the remnant state (R1 and R2) and during abrupt magnetic switching (S1 and S2).

Nanotechnology Approaches for Enhancing the Sensitivity and Throughput of Biosensors

Janos Vörös

Laboratory of Biosensors and Bioelectronics, Institute for Biomedical Engineering, ETH Zurich, Switzerland

Nanotechnology is an emerging new discipline that has brought new exciting possibilities in life sciences. Its first applications are in the area of biosensing where miniaturization is expected to bring direct benefits by improving the throughput of sensors. In addition, some of the new physical nanoscale phenomena could be utilized to develop more sensitive sensing techniques with the hope to reach the ultimate, single molecule sensitivity. This talk will outline how nanotechnology might fulfil its promises by giving selected recent examples for enhancing sensitivity and throughput of biosensors:

- 1.- Special optical properties of gold nanoparticles can be used to design biosensors based on the localized surface plasmon resonance phenomena. Adsorption events on single particles can be monitored where the shape and size of the particles determine the sensitivity.[1] The optical coupling between closely placed particles is even more interesting for biosensing because of the field enhancement that takes place between neighbouring particles. Although even single molecule sensitivity can be achieved using this concept there is still a lack of understanding about how to optimize the coupling effect.[2,3] Nevertheless applications e.g. for visualization of strain have already been demonstrated.[4]
- 2.- The electrical conductivity of gold nanoparticles provides another possibility for applications. The plasmonic properties can be combined with electrochemistry or nanowire-based sensing, giving useful additional information about interfacial ion effects such as the Stern-layer formation.[5]
- 3.- Membrane proteins are fragile and difficult to handle, but also highly important drug targets. The combination of microfabrication, polyelectrolyte multilayers, and self-assembly enabled the realization of ion-channel containing biomembranes over nanopores that are stable for weeks opening the possibility for high-throughput ion-channel screening.[6]
- 4.- One of the most successful and widespread high-throughput protein analysis tools is microarray technology. The arrays are traditionally made by spotting process. We present a robust and simple method as alternative via slicing hydrogel networks that contain the sample of interest.[7,8]

Overall, this presentation will illustrate the diverse application possibilities offered by nanotechnology highlighting the importance of combining top-down and bottom-up approaches.

References

- [1] Shape Dependent Sensitivity of Single Plasmonic Nanoparticles for Biosensing; T. Sannomiya, et al; Journal of Biomedical Optics, in press.
- [2] In situ sensing of single binding events by localized surface plasmon resonance; T. Sannomiya, et al. Nanoletters, 8(10): 3450-3455, 2008.
- [3] Biosensing by Densely Packed and Optically Coupled Plasmonic Particle Arrays; T. Sannomiya, et al. Small, 5(16): 1889-1896, 2009.
- [4] Strain mapping with optically coupled plasmonic particles embedded in a flexible substrate; T. Sannomiya, et al. Optics Letters, 34(13): 2009-2011, 2009.
- [5] Electrochemistry on a Localized Surface Plasmon Resonance Sensor; T. Sannomiya, et al., Langmuir, 2009, in press.
- [6] A gigaseal obtained with a self-assembled long-lifetime lipid bilayer on a single polyelectrolyte multilayer-filled nanopore; K. Sugihara, et al.; ACS Nano, 2010, in press.
- [7] Multilayers of Hydrogels Loaded with Microparticles: A Fast and Simple Approach for Microarray Manufacturing M. Bally, et al.; Lab Chip 10, 372-378, 2010.
- [8] Microarrays Made Easy: Biofunctionalized Hydrogel Channels for Rapid Protein Microarray Production; V. de Lange, et al., ACS Applied Materials & Interfaces, Submitted 2010.

Droplet-Patterned Epitaxial Growth: Quantum Dot Molecules and Nanoholes

Zhiming M. Wang

Institute of Nanoscale Materials Science and Engineering,
University of Arkansas, Fayetteville, AR 72701, USA

The droplet homoepitaxy is proposed as a novel approach to structure semiconductor surfaces at the nanometer scale. The nanostructured surfaces then serve as templates to engineer the growth of subsequent heterostructures such as self-assembled InAs quantum dots on GaAs substrates [1,2]. Depending on the substrate temperatures, a rich spectrum of semiconductor nanostructures is demonstrated, including quantum dot molecules [3,4] and nanoholes [5,6]. The configuration and number of quantum dots in a molecule are controllable. The drilling and filling effects of nanoholes reveal more possibilities to fabricate AlGaAs based nanostructures. Droplet-patterned epitaxy is a new concept for nanostructure growth, but fully compatible with standard equipments of molecular-beam epitaxy, therefore presents an unspoiled opportunity for nanoscale physics and devices [7,8].

References

- [1] B. L. Liang, Zh. M. Wang*, J. H. Lee, K. Sablon, Yu. I. Mazur, and G. J. Salamo, Applied Physics Letters 89, 043113 (2006).
- [2] Zhiming M. Wang, Baolai Liang, Kimberly A. Sablon, Jihoon Lee, Yuriy I. Mazur, Neil W. Strom, and Gregory J. Salamo, Small 3, 235 (2007).
- [3] J. H. Lee, Zh. M. Wang*, N. W. Strom, Yu. I. Mazur, and G. J. Salamo, Applied Physics Letters 89, 202101 (2006)
- [4] J. H. Lee, K. Sablon, Zh. M. Wang*, and G. J. Salamo, Journal of Applied Physics 103 (5), 054301 (2008)
- [5] Zh. M. Wang, B. L. Liang, K. A. Sablon, and G. J. Salamo, Applied Physics Letters 90(11), 113120 (2007)
- [6] K. A. Sablon, Zh. M. Wang*, G. J. Salamo, L. Zhou, and D. J. Smith, Nanoscale Research Letters 3 (12), 530 (2008).
- [7] B. L. Liang, Zh. M. Wang*, X. Y. Wang, J. H. Lee, Yu. I. Mazur, C. K. Shih, and G. J. Salamo, ACS Nano 2 (11), 2219 (2008).
- [8] Jiang Wu, Dali Shao, Vitaliy G. Dorogan, Alvason Z. Li, Shibin Li, Eric A. DeCuir, Jr., M. Omar Manasreh, Zhiming M. Wang*, Yuriy I. Mazure and Gregory J. Salamo, Nano Letters 10 (4), 1512–1516 (2010)

Photons, dust, and honey bees

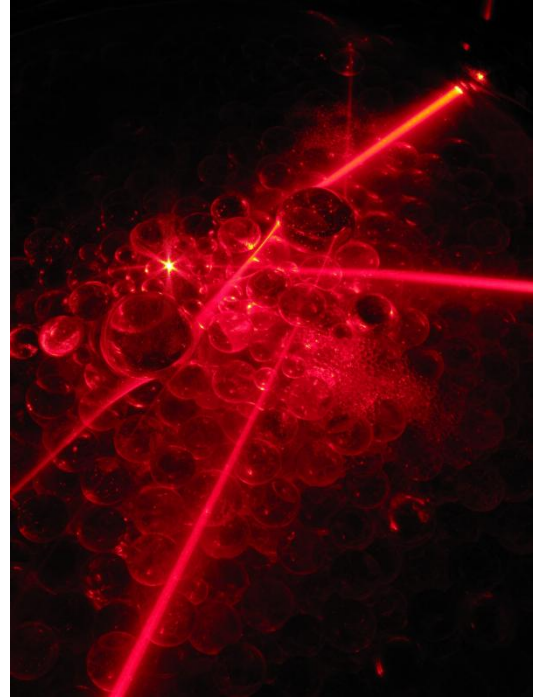
Diederik Wiersma

European Laboratory for Non Linear Spectroscopy (LENS), Univ. of Florence
National Institute for Optics, CNR
Italy

www.complexphotonics.org

People working with optics and lasers usually try to avoid dust on their equipment as much as possible. Dust particles scatter light randomly in all directions and this is often detrimental to the performance of optical devices and lasers. In this talk we will see that it is possible to turn this situation upside down and actually make use of multiple light scattering to study interesting physical phenomena. In particular, we will discuss optical Lévy flights and super diffusion, and various interference effects like weak and strong localization of light waves.

One can make use of the optical properties of disordered materials in several ways. On one side the random walk that light rays perform in such structures allows to study fundamental physical problems, including several interesting analogies between light and, for instance, electron transport. On the other side, the fact that light diffusion is quite common in daily life, allows for interesting applications. In particular, I will go in this talk into the possibility to use light trapping by disorder to create **efficient thin film solar cells**.



References

- [1] Shlesinger, M. F., Zaslavsky, G. M. & Klafter, J. *Strange kinetics*. Nature 363, 31–37 (1993).
- [2] Pierre Barthelemy, Jacopo Bertolotti, and Diederik S. Wiersma, *A Lévy flight for light*, Nature 453, 427 (2008).



ORAL CONTRIBUTIONS

(Plenary Session)

High-performance, Flexible Graphene Field Effect Transistors on Plastic substrates

Jong-Hyun Ahn, Houk Jang, Seoung-Ki Lee

SKKU Advanced Institute of Nanotechnology, Center for Human Interface Nano Technology, School of Advanced Materials Science and Engineering, Sungkyunkwan University, Suwon 440-746, Korea

ahnj@skku.edu

A high performance low-voltage graphene field-effect transistor (FET) array was fabricated on a flexible polymer substrate using solution-processable, high-capacitance ion gel gate dielectrics. The high capacitance of the ion gel, which originated from the formation of an electric double layer under the application of a gate voltage, yielded a high on-current and low voltage operation below 3 V. The graphene FETs fabricated on the plastic substrates showed a hole and electron mobility of 203 ± 57 and 91 ± 50 $\text{cm}^2/\text{V}\cdot\text{s}$, respectively, at a drain bias of -1 V. Moreover, ion gel-gated graphene FETs on the plastic substrates exhibited remarkably good mechanical flexibility. This method represents a significant step in the application of graphene to flexible and stretchable electronics.

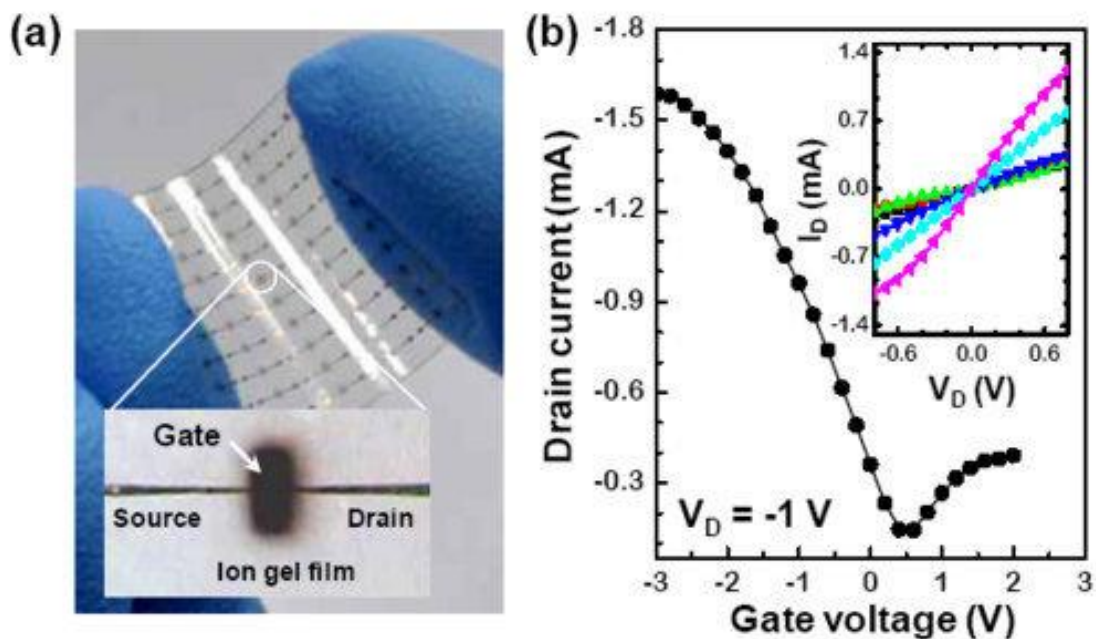


Figure. (a) Optical images of an array of devices on a plastic substrate. (b) Transfer and output characteristics of graphene FETs on plastic substrate.

The Development of Nanoscale Deterministic Ion Implants into Si and Diamond

Andrew D. C. Alves, Jessica van Donkelaar, Jonathan Newnham, Samuel Thompson, Brett Johnson
Jeffrey McCallum Kumaravelu Ganesan, Changyi Yang, Steven Prawer, David Jamieson

Australian Research Council Centre of Excellence for Quantum Computer Technology, School of
Physics, The University of Melbourne, Melbourne Victoria 3010, Australia

aalves@unimelb.edu.au

Low energy ion implantation is seen as a critical enabling technology in new electronic, spintronic and photonic devices which are being continually proposed [1-3]. The ultimate goal of the implant in this context is to reduce the implant energy and increase spatial resolution so that the implanted atom resides in an extremely well defined location. The impurity atom must be placed relative to gates controlling local electronic and magnetic fields and to couple emitted photons to optical waveguides or photonic crystals. The desired end; to load, transport, store or read out quantum states without losing the quantum encoded information to decoherence. Two popular quantum systems to be used in quantum computation and communication are the electron spin on a donor atom in Si, or a single photon emitted from a color centre in diamond. These systems rely on impurity atoms placed with nanometer scale precision inside the bulk. The preferred implant technique is to mask the substrate material with a nanometer scale aperture (Typically tens of nm wide) which can be moved relative to the substrate [4, 5].

In this paper we demonstrate the placement of both 14 keV P into Si and 14 keV N into diamond. At this energy the ion straggle is limited to a few tens of nm and one can begin to experiment with impurities one-by-one, such as measuring the spin on a single electron [6]. In the first instance donor implants are timed to demonstrate the high spatial precision of the process. Atomic force microscopy has been used to probe a Si substrate implanted with P donors and confocal microscopy has been used to image a diamond implanted with N (Fig. 1 a, b). To further understand the spatial limit of the implant process we demonstrate measurements of the amount of ion scatter from an aperture and compare this result with modeling of the ion scatter (Fig. 1 d). This modeling offers further insight into the masking process and guides the experimental conditions in a deterministic implant scenario. We also demonstrate in-situ optical alignment which allows us to align the mask with pre-existing features on the substrate.

These implants are ultimately governed by stochastic processes and the number of atoms is not precisely controlled. To implant each atom deterministically we must also detect each implant. Methods of low energy ion detection, via charge collection in a PIN structure or charge action in a MOSFET structure, have been demonstrated in Si [7, 8]. We have coupled the detection and placement aspects of deterministic implants using a higher energy 500 keV He ion beam (to ease the low noise demands on detection). This coupling of detection and placement has allowed us to register the implant to a pre existing static feature on the substrate beyond the finest spatial resolution that could be achieved with only optical alignment (Fig. 1 c).

We have also investigated the detection of single ion impacts in diamond using a metal-diamond-metal structure biased to collect ion beam induced charge in the diamond. The results show the charge collection efficiency is maximized when high purity single crystal CVD diamond is used and it is promising that low energy N implants may also be detected (Fig. 1 e).

In summary many aspects of low energy deterministic implants of single impurities into Si and diamond are investigated.

References

- [1] G.P. Lansbergen, R. Rahman, C.J. Wellard, I. Woo, J. Caro, N. Collaert, S. Biesemans, G. Klimeck, L.C.L. Hollenberg, S. Rogge, *Nature Physics*, **VOL 4** (2008) 656
- [2] B.E. Kane, *Nature*, **VOL 393** (1998) 133
- [3] J.O. Orwa, A.D. Greentree, I. Aharonovich, A.D.C. Alves, J. Van Donkelaar, A. Stacey, S. Prawer, *Journal of Luminescence*, **ARTICLE IN PRESS**
- [4] A. Persaud, S.J. Park, J.A. Liddle, T. Schenkel, J. Bokor, I. W. Rangelow, *Nano Letters* **Vol. 5, No. 6** (2005) 1087
- [5] C.D. Weis, A. Schuh, A. Batra, A. Persaud, I.W. Rangelow, J. Bokor, C.C. Lo, S. Cabrini, E. Sideras-Haddad, G.D. Fuchs, R. Hanson, D.D. Awschalom, T. Schenkel, *J. Vac. Sci. Technol. B* **26** (2008) 2596

[6] A. Morello, J.J. Pla, F.A. Zwanenburg, K.W. Chan, H. Huebl, M. Mottonen, C.D. Nugroho, C. Yang, J. A. van Donkelaar, A. Alves, D.N. Jamieson, C.C. Escott, L.C.L. Hollenberg, R.G. Clark, A.S. Dzurak, <http://arxiv.org/abs/1003.2679>

[7] D.N. Jamieson, C. Yang, T. Hopf, S.M. Hearne, C.I. Pakes, S. Praver, M. Mitic, E. Gauja, S.E. Andresen, F.E. Hudson, A.S. Dzurak, R.G. Clark, *Appl. Phys. Lett.* **86** (2005) 202101

[8] A. Batra, C.D. Weis, J. Reijonen, A. Persaud, T. Schenkel, S. Cabrini, C.C. Lo, J. Bokor, *Appl. Phys. Lett.* **91** (2007) 193502

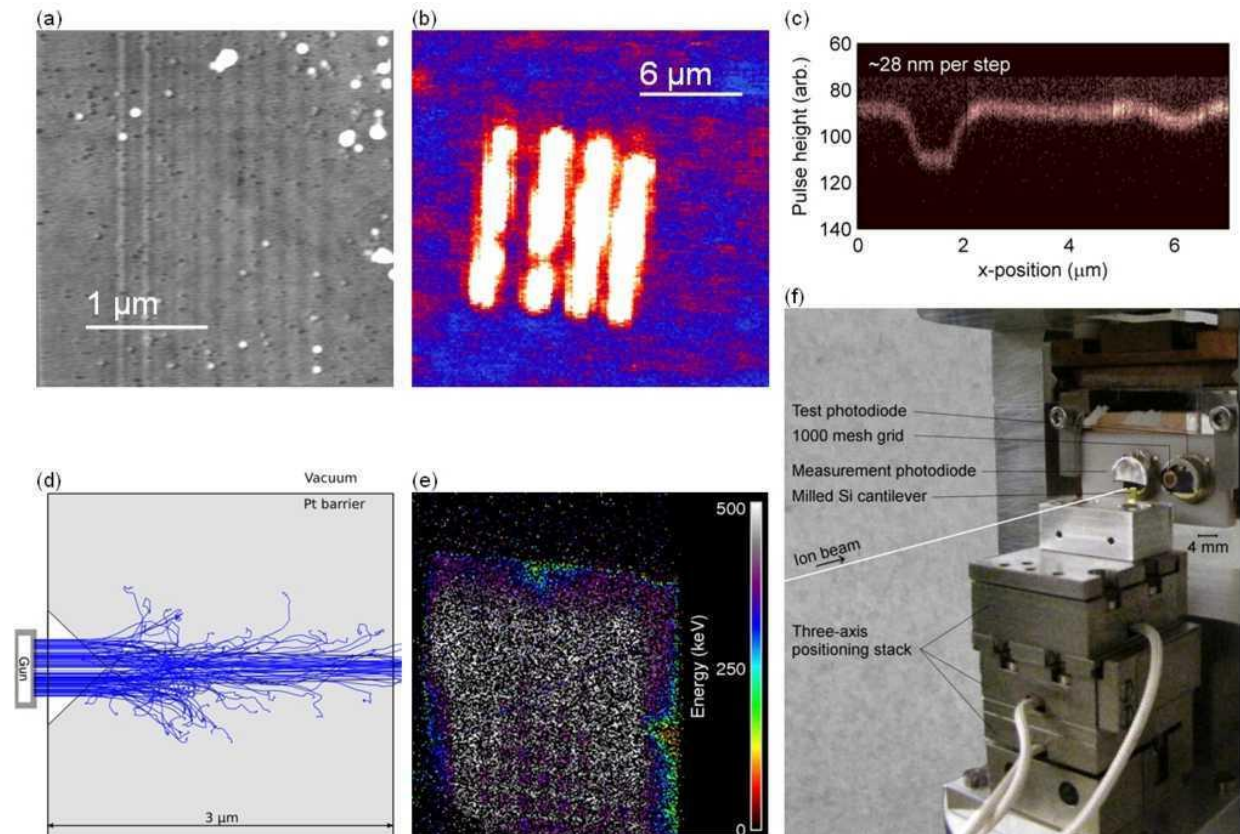


Figure 1.

(a) AFM image of 14 keV P implants into Si. The ion implants cause the Si surface to swell and to dip depending on the dose of the implant. A 60 nm wide aperture was used to define the beam and the step size of the scanned aperture was 200 nm.

(b) Confocal map of 14 keV N implants into diamond. The ion implantation results in N-V color centers after 1100 °C anneal. A 100 nm wide aperture was used to define the beam and the step size was 2000 nm. In this case the resolution of the image is not limited by the implant but rather by the confocal microscopy.

(c) A 500 keV He ion beam was scanned across a PIN detector with a patterned PMMA coating using a 100 nm wide beam defining aperture. The transmitted ions produced a pulse in the detector electronics proportional to the thickness of PMMA traversed, thus producing a map of the topography.

(d) A simulation of ion scatter from a 60 nm wide focused ion beam milled aperture. The internal geometry of the aperture has been tailored so the energy spread of exiting ions matched the measured energy spectrum during experiment. This model can be used to predict the ion scatter when attempting a deterministic implant of a low energy ion.

(e) An ion beam induced charge map of a metal-diamond-metal charged particle detector. 500 keV He ions were used to map this device and determine the noise floor for this device.

(f) The apparatus used to scan a nanoscale beam defining aperture over a PIN charged particle detector.

**CNTFETs fabricated using an
Original Dynamic Air-Brush technique for SWCNTs deposition :
Application to gas sensing and perspectives for other carbonaceous materials**

Bondavalli P.¹, Gorintin L.¹, Legagneux P., Simonato J-P², Cailler L.²

¹Nanocarb Lab, Thales Research and Technology, Palaiseau 91767, France Organization

²LITEN / DTNM / LCH, CEA-Grenoble, Grenoble 38054, France

paolo.bondavalli@thalesgroup.com

This contribution deals with Carbon Nanotubes Field Effect transistors (CNTFETs) based gas sensors fabricated using a completely new dynamic air-brush technique (patented) for SWCNTs deposition. The extreme novelty is that our technique is compatible with large surfaces, flexible substrates and allows to fabricate high performances transistors exploiting the percolation effect of the SWCNTs networks achieved with extremely reproducible characteristics. This technique is extremely interesting considering that it is suitable for industrial transfer. More precisely, we have developed a machine which allows us the dynamic deposition on heated substrates of SWCNT solutions (Fig.1), improving dramatically the uniformity of the SWCNTs mats.

The CNTFETs have been developed for gas sensing applications. Indeed we have fabricated arrays of CNTFETs achieved using different metal electrodes [1,2] (patented approach [3]) to exploit the change of metal/SWCNTs junction characteristics as a function of the gas detected (Fig.2) in order to identify a sort of electronic fingerprinting. This phenomenon is related to the change of the metal work function and so of the Schottky [1] barrier and seems to be extremely selective (see Tab.1).

Although the deposition technique has been developed to fabricate CNTFETs, this technique is extremely versatile and can be used for other kinds of applications such as fabrication of bolometers (e.g. nanotubes) [4], replacements of ITO layers (e.g. nanotubes, graphene) [5], in OLED (e.g. graphene) [6], for light and cheap ultracapacitors on flexible substrates (e.g. using carbon nanotubes or nanohorns) [7]. This technique could really allow these nanomaterials to strike the market on these applications. During the presentation examples, for all these applications, will be shown.

Results for gas sensing

We have fabricated CNTFETs using interdigitated electrodes. The distance between the fingers was 15µm. Our technique has allowed us to fabricate transistors in a reproducible way with high On/Off current ratio and on large surfaces (Fig.3). We have performed measurements of CNTFETs array before and after exposure to NH₃, NO₂, CO at concentrations, of 50ppm for Ti, Au, Ti, Pt as electrodes. The results demonstrate our concept (Fig.4). The CNTFETs permit to identify a sort of electronic fingerprinting of each gas.

This work has been performed in the frame of the ANR6 Project NANOSENSOFIN [11] for CO selective sensing, and it is a joint effort of Thales Research and Technology and CEA-LITEN teams.

References

- [1] P.Bondavalli, et al., CNTFET based gas sensors : State of the art and critical review, *Sensors and Actuators B*, 140, 1, pp 304-318, (2009)
- [2] P. Bondavalli, CNTFETs based gas sensors : patent review, *Recent Patents on Electrical Engineering*, 3 (2010)
- [3] P.Bondavalli et al Conductive nanotube or nanowire FET transistor network and corresponding electronic device, for detecting analytes., 2008 WO/2006/128828
- [4] M. Tarasov, J. Svensson, J. Weis, L. Kuzmin and E. Campbell' Carbon nanotube based bolometer, *JETP Letters*, 84, 5 (2006)
- [5] <http://www.touchuserinterface.com/2008/06/graphene-possible-replacement-for-ito.html>
- [6] J. Wu, M Agrawal, H. A. Becerril, Z. Bao, Z. Liu, Y. Chen and P. Peumans, *ACS Nano*, 4(1), 2010.
- [7] Printable Thin Film Supercapacitors Using Single-Walled Carbon Nanotubes, Martti Kaempgen, Candace K. Chan, J. Ma, Yi Cui, and George Gruner, *Nanoletters*, Vol.9 n.5 (2009)

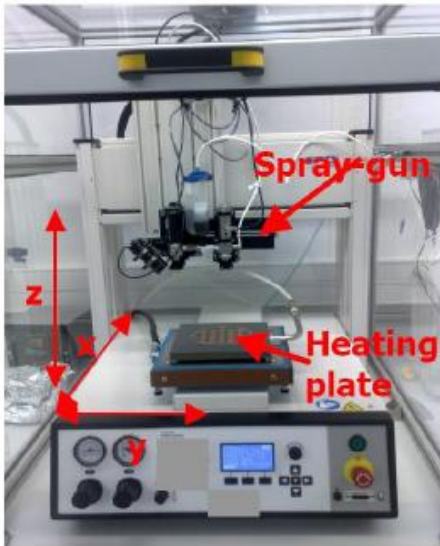


Figure 1. Machine for Dynamic Air-Brush deposition of SWCNTs.

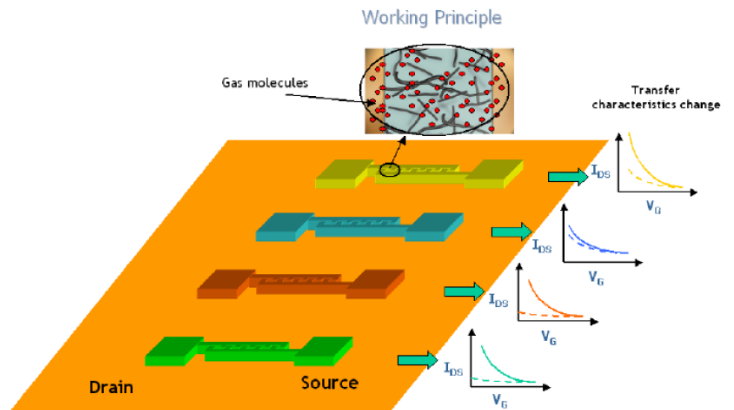


Figure 2. Gas fingerprinting concept. CNTFETs array composed by transistors with different metal electrodes (each colour). On the right: the transfer characteristics relative change after gas exposure (before, solid line and after exposure, dash line) is specific for each metal for one targeted gas.

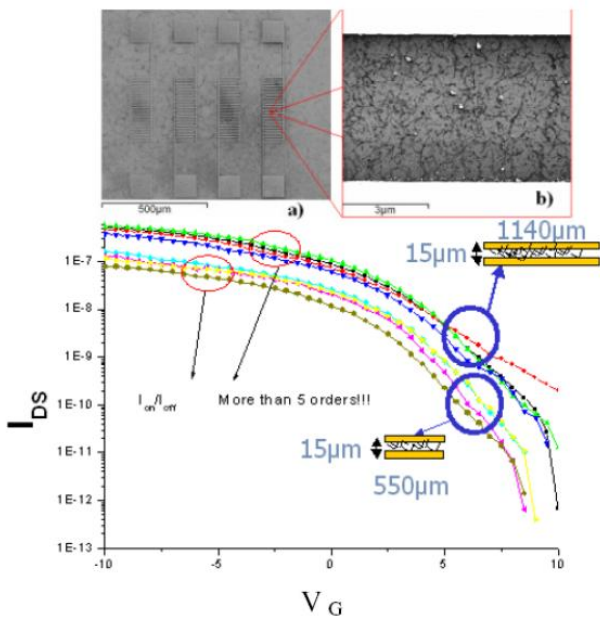


Figure 3. On the top: array of four CNTFETs with Interdigitated finger configuration and a detail (AFM picture) of the CNTs mat. On the bottom: on/off current ratio for CNTFETs with finger distance.

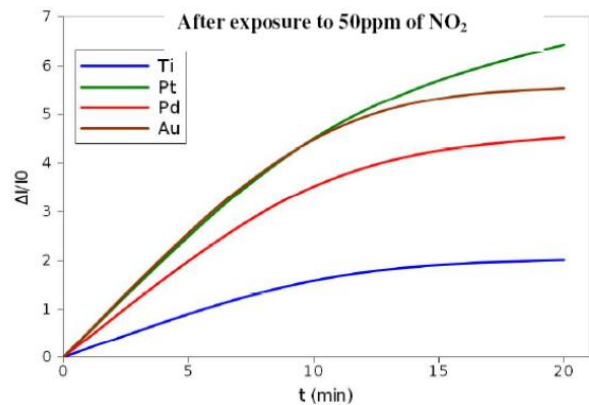


Figure 4. Current change as a function of Time, after exposure to 50ppm of NO_2 of four CNTFETs achieved using different metal as electrodes.

	CO	NH_3	NO_2
Au	65%	-30%	6600%
Ti	15%	-50%	4400%
Pd	45%	-35%	38000%
Pt	-5%	-45%	84000%

Table 1. Relative change of the current after 20 minutes of exposure to 50ppm of NO_2 , NH_3 and CO for CNTFETs achieved using Au, Pd, Ti, Pt as electrodes

Asymmetric spin injection at high current bias in all-metallic lateral spin valves

Fèlix Casanova¹, Mikhail Erekhinsky², Amos Sharoni³ and Ivan K. Schuller²

¹CIC nanoGUNE, 20018 Donostia - San Sebastian and IKERBASQUE, Basque Foundation for Science, 48011 Bilbao, Basque Country, Spain

²Physics Department, University of California-San Diego, La Jolla, CA 92093, USA

³Department of Physics, Bar Ilan University, Ramat Gan 59200, Israel

f.casanova@nanogune.eu

Creation and control of spin currents is a key ingredient in spintronics, which has as a goal the use of both the spin and charge of the electron. Ferromagnetic (FM)/non-magnetic (NM) lateral spin valves are powerful devices that decouple a pure spin current from an electrical current by using a non-local geometry (**Fig. 1**). The FM/NM interface and the materials control in an essential way the generation and manipulation of a spin current in non-local spin valves (NLSV). For this reason, we have studied the electrical spin injection and subsequent spin diffusion in metallic NLSV with transparent interfaces as a function of important experimental parameters such as injection current direction and magnitude, temperature, materials, and thickness.

Using injected DC currents we find that the spin injection is perfectly symmetric when applying low currents from the FM (spin injection) or into the FM (spin extraction), reversing exactly the polarity of the spin current in the NM [1]. This provides means for a pure electrical manipulation of the spin current polarity. Very recently, we have observed a breaking of symmetry between spin injection and spin extraction at high current bias, which, unlike other systems such as semiconductors [2,3], tunnel barriers [4] or graphene [5,6], is not expected in metallic junctions. A systematic study shows that the spin diffusion length of the NM is independent of current direction, whereas the effective spin polarization of the FM appears to be larger for spin injection and smaller for spin extraction. Possible explanations for this behavior will be discussed.

The injection and diffusion of the spin current into the NM is studied by comparing the experiments with a spin-diffusion model. We identify the effect of the surface and the interface on the spin diffusion length and injection efficiency, due to an enhanced spin-flip scattering [7]. These experiments have important implications for the physics of spin currents and for the development of devices based on these phenomena.

Work supported by the US-DOE.

References

- [1] F. Casanova, A. Sharoni, M. Erekhinsky, I. K. Schuller, *Phys. Rev. B* **79**, 184415 (2009).
- [2] X. Lou et al., *Nature Phys.* **3**, 197 (2007).
- [3] S.P. Dash et al., *Nature* **462**, 491 (2009).
- [4] S. O. Valenzuela et al, *Phys. Rev. Lett.* **94**, 196601 (2005).
- [5] W. Han et al., *Phys. Rev. Lett.* **102**, 137205 (2009)
- [6] M. Shiraishi et al., *Adv. Funct. Mater.* **19**, 3711 (2009).
- [7] M. Erekhinsky, A. Sharoni, F. Casanova, I. K. Schuller, *Appl. Phys. Lett.* **96**, 022513 (2010).

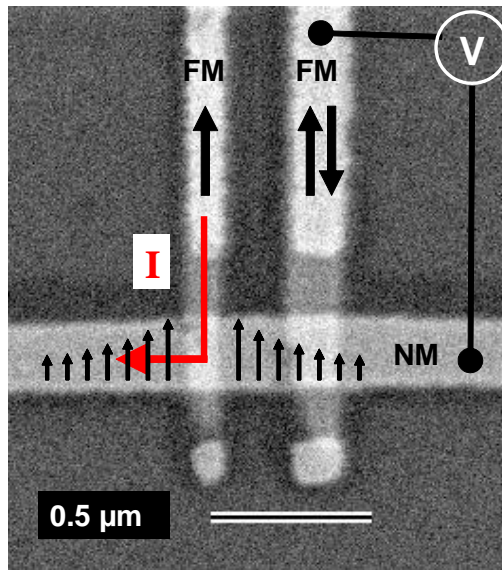


Figure 1. Scanning electron microscope image of a lateral spin valve with a schematic illustration of spin injection, accumulation and detection in a non-local measurement.

**Horizontally aligned carbon nanotube networks:
a route toward highly conductive, flexible & controllably transparent electrodes, field emitters
and infra-red sensors**

M. T. Cole¹, Y. Zhang¹, P. Hiralal¹, M. Mann¹, C. Li^{1,2}, K. B. K. Teo³ & W. I. Milne¹

¹ Electrical Engineering Division, Engineering Department, University of Cambridge,
9 JJ Thomson Avenue, CB3 0FA, Cambridge, UK

² School of Electronic Science and Engineering, Southeast University, Nanjing 210096, China

³ Aixtron Nanoinstruments, Swavesey, Cambridge, CB24 4FQ, UK

mtc35@cam.ac.uk

Flexible, highly conductive and transparent electronic materials are critically important areas of active research. Metals, although being excellent conductors are largely brittle and have increasingly poor conductance when strained. Moreover, metals are optically opaque at the technologically relevant sub-100 nm node. Serpentine Au thin films embedded in elastomeric membranes have gone some way towards solving the flexibility problem. Transparent conducting metal oxides, such as increasingly expensive indium tin oxide, open up the field of optoelectronics. Simultaneously achieving high transparency and high conductivity is the ultimate goal. Conductive polymers including untreated, and poly-ethyl glycol enhanced, Poly(3,4-ethylenedioxythiophene) poly(styrenesulfonate) have had some success, however sheet resistances require further improvement and the observed non-constant variation in optical transmission with wavelength across the NIR-vis spectra result in an undesirable characteristic blue hue in most PEDOT:PSS derivatives. Carbon-based materials show significant promise and solve many of these problems. Here we report on the fabrication, characterisation and application of thin films comprised of random and aligned horizontal carbon nanotube (H-CNTs).

Figure 1 (a)-(d) illustrates a CNT shearing and transferral process for the fabrication of aligned H-CNT films on polycarbonate substrates, such as polypropylene carbonate (PPC) and polyethylene terephthalate (PET), developed by us [1]. We have also successfully demonstrated the ability to pattern and control the transparency of these films by O₂ reactive ion etching (Fig. 3(b), (c), (d)) [1]. An alternative approach to transparency control has been investigated. By reducing the length of the source CNT material we have shown that it is possible to control the transferred H-CNT films conductivity and optical transmissivity. For CNTs of length > 50 μm we find that the aligned MWNTs adhere strongly to the untreated PC substrates. Whilst for lengths < 50 μm an adhesion promoter (aminopropyl-triethoxysilane, APTS) largely improves the transferred films uniformity, especially when transferring onto ITO, SiO₂, and other natively hydrophobic surfaces (Fig. 3(a)). Our most opaque and highly conductive films have sheet resistances of the order of 1.2 Ω/□ with an optical transmission of 10%. We have also investigated the use of these rolled CNT films as field emitters, which have been compared to vacuum filtrated random networks, and screen printed networks [2].

Free-standing aligned H-CNT networks have also been fabricated (Fig. 2 (a)-(d)). These suspended networks are structurally maintained by inter-CNT Van der Waals forces and can be pulled to span significant lengths. CNTs are known to be strongly absorbing in the infra-red (IR) spectrum making them ideal as IR sensors. Figure 2(e) shows a typical current response of the suspend H-CNT films when irradiated with IR radiation [3].

In this presentation the results outlined above will be developed and an overview of some of the ongoing work taking place within Cambridge's Electronic Devices & Materials group will be discussed.

Keywords: Carbon nanotubes, flexible, horizontally alignment, transparent, field emission, infra-red sensors

References

- [1] M. T. Cole, P. Hiralal, Y. Zhang, C. Li, R. Weatherup, K. B. K. Teo & W. I. Milne, *Submitted*, July 2010.
- [2] M. T. Cole, C. Li, Y. Zhang, M. Mann, K. B. K. Teo, & W. I. Milne, *Submitted*, Aug. 2010
- [3] M. T. Cole, X. Xu, Y. Zhang, K. B. K. Teo, A. Ferrari, & W. I. Milne, *Submitted*, Aug. 2010

This work was supported by the Schiff Studentship, University of Cambridge. We would also like to acknowledge the EC funded NanoICT project and St John's College Cambridge.

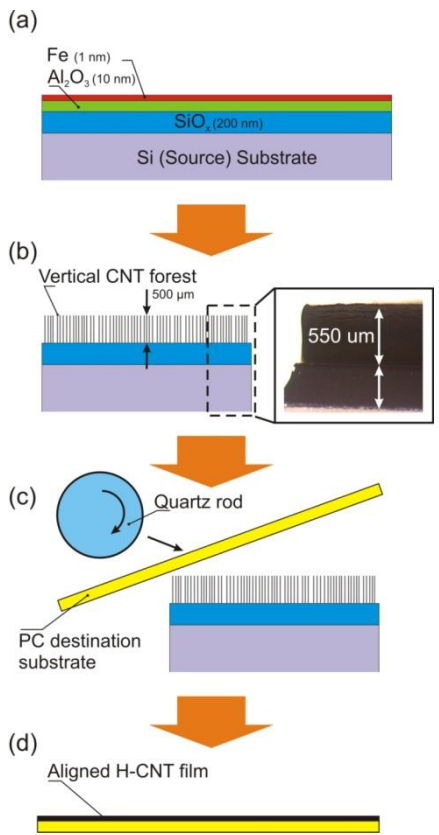


Figure 1. (a)-(d) Horizontally aligned sheared H-CNT film fabrication and transferral process onto PC destination substrates [1].

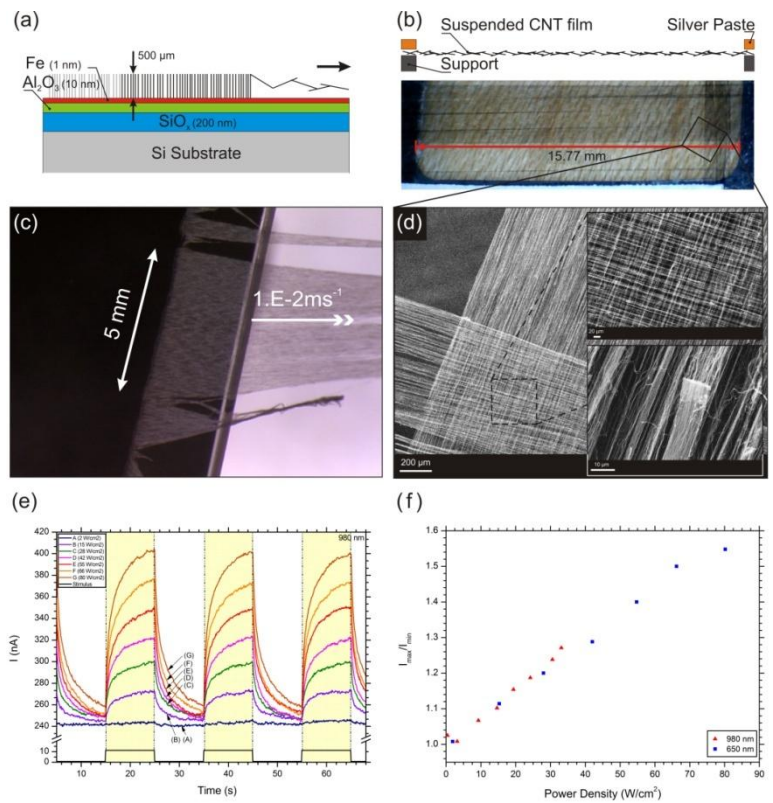


Figure 2. (a)-(c) Fabrication process of suspended H-CNT films for planar IR sensor [3]. (d) SEM micrographs of suspended CNT array. (e) 980 nm IR response (power density, 2-80 W/cm²). (f) Emission current showing a strong dependence on the incident power density at 650 nm and 980 nm excitation [3].

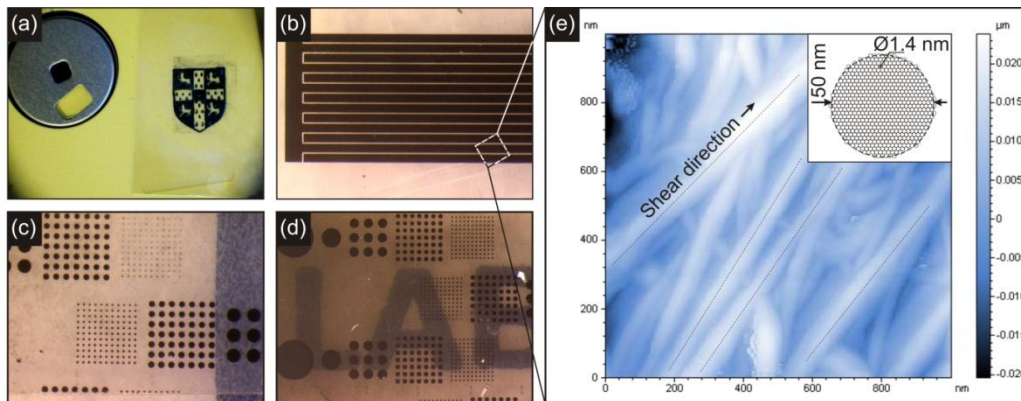


Figure 3. LEFT. (a)-(d) Optical micrographs of shear aligned H-CNT films on PET/ITO/APTS, PET and PPC, where O₂ RIE patterning and transparency control have been used. (e) AFM of H-CNT film [1].

Superlattice of resonators on monolayer graphene created by intercalated gold nanoclusters

Marion Cranney¹, L.Simon¹, F. Vonau¹, D. Aubel¹, P. Pillai², M.M. De Souza²

¹ Institut de Sciences des Matériaux de Mulhouse LRC 7228-CNRS, 4, rue des Frères Lumières, 68093 Mulhouse, France

² Department of Electronic and Electrical Engineering, Mappin Building, Mappin Street, Sheffield S1 3JD, UK

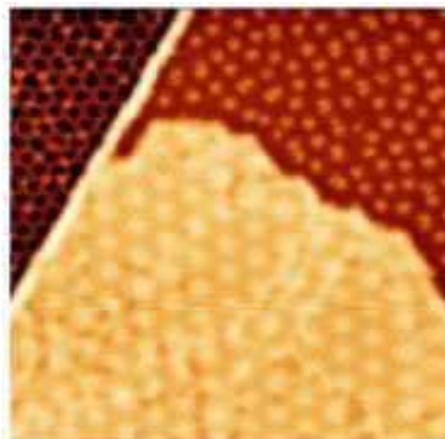
Laurent.Simon@uha.fr

Since the pioneering investigations on graphite formation on 6H-SiC(0001) and 6H-SiC(000-1) [1], the possibility to grow a few epitaxial layers of graphene on silicon carbide substrates, as demonstrated by C. Berger et al [2], appears to be a promising approach for practical electronic applications. The studies of electronic properties of epitaxial graphene reveal the existence of a n-type doping with a charge transfer from the substrate to the epitaxial graphene layer. In a recent report, a simple way to shift the Fermi level and induce p-type doping by deposition of gold atoms on top of graphene was proposed [3]. The authors proposed that gold atoms are covalently bonded to the epitaxial graphene. However, in a deeper insight study by STM, we have revealed that gold atoms intercalate in between the buffer layer and the graphene monolayer. Depending on the preparation procedure we have obtained intercalated quasi “free standing” gold monolayer and small Au clusters [4]. We report here a detailed study of the intercalated “free standing” gold clusters. These clusters create on the upper monolayer graphene locally screened regions where quasi particles are perturbed as revealed by a strong standing waves pattern. This results in each cluster acting as a quantum dot creating a superlattice of resonators on graphene which has not been observed before. Furthermore a deeper insight of the standing waves pattern using Fourier Transform Scanning Tunneling Spectroscopy indicates strong localization at the Van Hove singularity corresponding to a band crossover and a nodal-antinodal dichotomy as observed for a “Van-Hove scenario” in the case of high Tc superconductors.

References

- [1] A. J. Van Bommel et al, Surf.Sci. 48 (1975) 463, I. Forbeaux et al, Phys. Rev. B, 58 (1998) 16396, L. Simon et al, Phys. Rev. B, 60 (1999) 11653.
 [2] C. Berger et al, J. Phys. Chem., 108 (2004) 19912.
 [3] I. Gierz et al, Nano Letters, 8 (2008) 4603. [4] B. Premlal et al, APL, 94 (2009) 263115.

Figure



STM picture (40x40 nm², -1.0 V, 0.9 nA, 77 K) of the surface of epitaxial graphene obtained after gold deposition. It shows the pristine monolayer graphene and two new domains due to the intercalation of gold atoms between the monolayer graphene and the buffer layer. The first domain consists in the intercalation of gold clusters and the other one is formed by a freestanding monolayer of gold [4].

Analysis of Carbon- and other Nano-Structures using Si Drift Detectors in Energy Dispersive X-ray Spectroscopy

M. Falke, A. Käppel, R. Terborg, R. Krömer and M. Rohde

Bruker Nano GmbH, Schwarzschildstraße. 12, 12489 Berlin, Germany

meiken.falke@bruker-nano.de

We want to explain the silicon drift detector (SDD) technology briefly and show examples of nanoanalysis using SDD for SEM and TEM. Peltier cooled Silicon drift detectors, originally developed for space research where the use of liquid nitrogen was impossible, have been introduced for energy dispersive X-ray spectroscopy (EDS) in scanning electron microscopy (SEM) more than a decade ago [1]. Now they are about to revolutionize nanoanalysis of element composition using EDS in SEM and transmission electron microscopy (TEM) [2].

SEM at low voltages is suitable to analyse surfaces of bulk structures and to investigate electron transparent samples with nm-resolution. Image resolution of up to atomic level is now routinely available using aberration corrected TEM. Brukers liquid nitrogen free EDS for element mapping is suitable for both SEM and aberration corrected TEM. Using one 30mm² SDD at 0.12sr solid angle for x-ray collection, atom column EDS in case of an aberration corrected instrument [3] and nm resolution EDS for a conventional TEM [2] have been shown. In TEM atom column EDS is seen as a directly interpretable important complement to the well established electron energy loss spectroscopy [4] used for chemical analysis of nano-structures on atomic level. Multiple detectors achieving a much higher solid angle for x-ray collection can be used for very fast elemental mapping and to detect small amounts of matter in the nanostructure [5].

Our first example of SDD-EDS is a combined SEM- and TEM-study of an array of multiwall carbon nanotubes (MWCNT). Fig. 1 shows the MWCNT array in the SEM and a signal mixed of transmitted and back scattered electrons, which reveals the whereabouts of the catalyst nanoparticles used for the CNT growth. Element mapping by EDS in a transmission electron microscope distinguishes between Ni and Co catalyst particles remaining inside the tubes and shows the successful Cu coating of the multiwall carbon nanotubes [6,7]. The Z-contrast in high angle annular dark field (HAADF) imaging clearly distinguishes between the heavier matter of the coating and catalyst particles and the lighter carbon of the tubes.

Figure 2 shows data on magnetic nanostructures, achieved using a combination of electron energy loss spectroscopy and EDS in TEM. The study of the element composition on the nm-scale helped to explain the magnetic behaviour of these hedgehog like nanospheres [8].

The third example deals with the compositional analysis of quantum well samples used for the development of laser diodes (Figure 3). Utilising TEM EDS the element composition can be analysed within minutes [9].

In summary, SDD-technology is a valuable addition to the analytical tools provided for analysis of nanostructures on atomic level. The low interference, low noise and good light element performance as well as the robustness and capability to deal with high exposure rates as well as low x-ray input makes this technology particularly interesting for the use in high end aberration corrected microscopes and in combination with high brightness sources. Successful data analysis on atom column level is possible.

References

- [1] L. Strüder, et al., *Microsc Microanal* 4 (1999) 622.
- [2] M. Falke, et al., *Imaging & Microscopy* 11 (2009) 35; *Microsc Microanal* 15, Suppl2 (2009). [3] M.-W. Chu, et al., *Phys. Rev. Lett.* (2010).
- [4] A.J. D'Alfonso et al., *Phys. Rev. B* 81 (2009) 100101(R).
- [5] H.S. von Harrach et al., *Microsc Microanal* 15, suppl.2 (2009) 208.
- [6] T. Waechtler, et al., *J. Electrochem. Soc.* 156 (6), (2009) H453-H459.
- [7] S. Hermann, et al., *Microelectronic Engineering* 87 (3), (2010) pp.438-442.
- [8] C. Brombacher, M. Albrecht, Institute of Physics, Technical University Chemnitz, Germany [9] G. Tränkle, A. Mogilatenko, Ferdinand Braun Institute of High Frequency Technology, Berlin

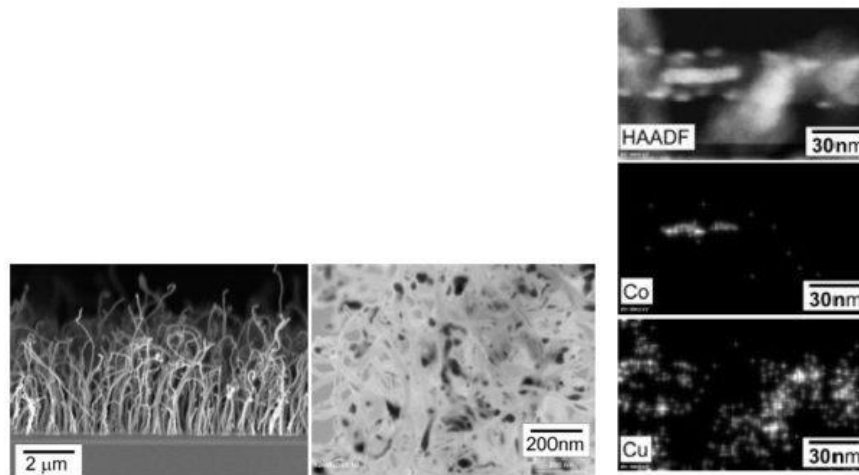


Figure 1. Left: Array of MWCNTs on a Si/Ta- substrate in SEM. The mixed transmission and BSE signal of disordered MWCNTs reveals the where about of the catalyst nanoparticles. Right: EDS of multiwall carbon nanotubes on a lacy carbon gold grid: HAADF, Co-map and Cu-map. The Co-catalyst particle, and the oxidized Cu-coating, all just few nm in size, were clearly revealed during this 1 min EDS-map.

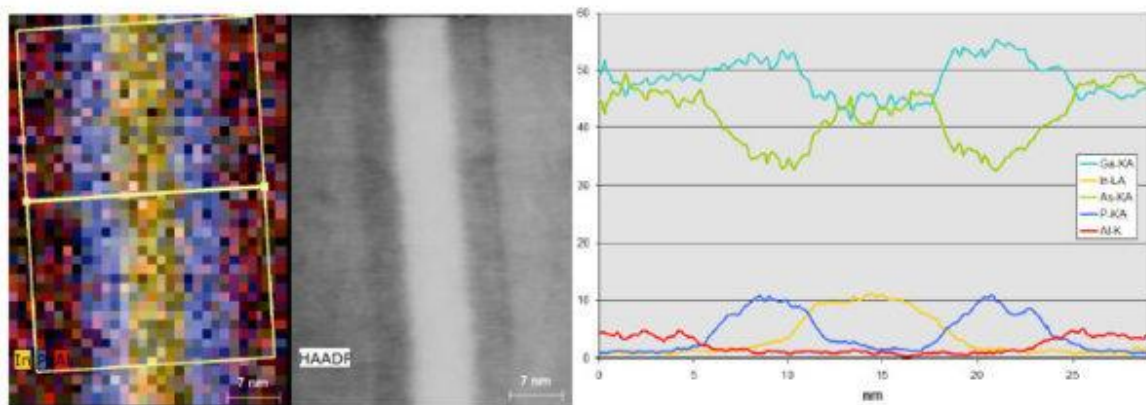


Figure 2. The element profile of a sample from research on laser diodes: The Indium distribution resembles the bright features in the HAADF signal showing heavier elements. The element profile was generated using 8by8 binning and adding up all spectra perpendicular to the layers in the indicated area. Even the nm-sized kink on the right side of the light element P-profile is reproduced in EDS as visible in the HAADF signal.

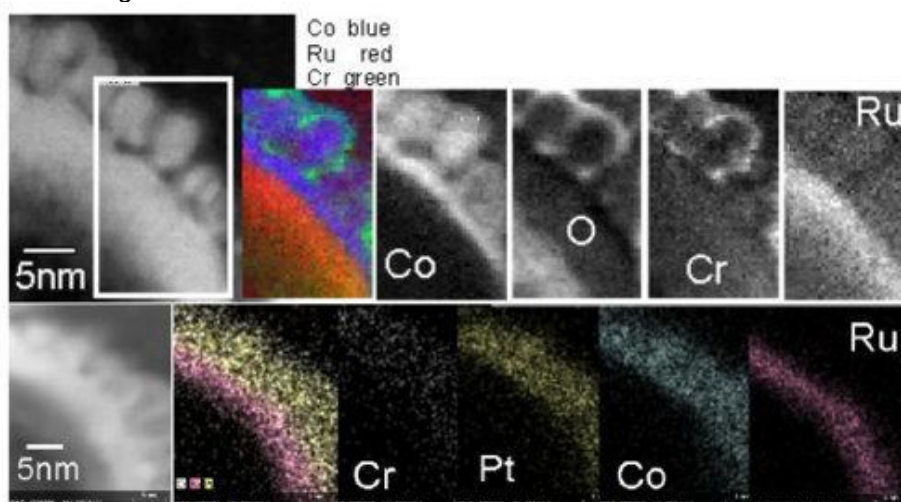


Figure 3. Upper part: HAADF and element map using EELS spectrum imaging in a NION Cs-corrected dedicated STEM. Lower Part: Liquid nitrogen free EDS map of the same sample area in an uncorrected conventional Jeol STEM, the second frame shows Ru, Pt and Cr. Pt appears with Co. Ru is part of the seed layer.

Combining Scanning Probe Microscopy and X-Ray Spectroscopy to Obtain Simultaneously Surface Topography and Chemical Mapping

C. Fauquet, M. Dehlinger, F. Jandard, S. Ferrero¹⁾, S. Larcheri²⁾, F. Rocca²⁾, J. Purans³⁾, A. Bjeoumikhov⁴⁾, A. Erko⁵⁾, D. Tonneau

Université de la Méditerranée, CNRS-CINaM, Faculté des Sciences de Luminy, case 913, 13288 Marseille cedex 09, France

- 1) Cie AXESS TECH, 750 Chemin de Beaupré, 13760 Saint Cannat, France
- 2) CNR, Ist Foton & Nanotecnol, Sez FBK CeFSA Trento, I-38123 Trento, Italy
- 3) Latvian State Univ, Inst Solid State Phys, LV-1063 Riga, Latvia
- 4) IFG GmbH, Rudower Chaussee 29/31, 12489 Berlin, Germany
- 5) HZB-Synchrotron Bessy, Albert Einstein Strasse, 15, 12489 Berlin, Germany

fauquet@cinam.univ-mrs.fr

Non destructive tools providing elemental and chemical analysis at high resolution are necessary for life and physical sciences. For example electronics or glass industry needs in-lab tools for material processing and control (RRAM, FeRAM, smart materials, solar cells) [1].

Near Field Microscopes are powerful tools for surface topography analysis at nanometric lateral resolution. But, these equipments cannot provide chemical mapping of the analysed surface.

X-Ray Spectroscopies are fine analysis techniques providing chemical and structural properties of a material, based on the spectroscopy of the emitted photons or photoelectrons. They require a high brightness excitation X-Ray source, synchrotron beam, to irradiate the sample. The lateral resolution is about 1 μm , but it is not possible to image simultaneously the sample surface neither to position the X-Ray beam on a peculiar micro or nano object. Among these techniques, XEOL spectroscopy (X-Ray Excited Optical Luminescence) deals with the analysis of visible photons emitted from the surface of the sample.

We have designed and fabricated a new characterization tool combining X-Ray Spectroscopy and Shear Force Microscopy and working at ambient conditions, allowing surface topography measurement simultaneously to chemical mapping [2,3]. The probe of the microscope is a sharp and low aperture optical fiber used to detect the XEOL signal of the sample under synchrotron irradiation. Simultaneously, it is possible to obtain the topography of the sample surface. Thus, the instrument is able to image the surface and to localize a peculiar object that can be further chemically analyzed by XEOL analysis.

In this work, we present the results obtained on the ID03 line at ESRF. First experiments were performed on a ZnO layer deposited on a silicon sample. Figure 1a) shows the conventional XEOL spectra acquired on ZnO powder and on the ZnO layer. Figure 1b) shows the XEOL spectrum of the same layer recorded in near field using our apparatus. The spectra acquired either in far or in near field are in good agreement with the ZnO powder reference spectrum. Moreover, collecting the XEOL signal in near field increases significantly the lateral resolution of the XEOL technique, which is now limited only by the aperture of the optical fiber.

Further characterizations were performed on ZnWO₃-ZnO layer co-sputtered on a silicon sample. Figure 2 shows both topography and luminescence cartography of this layer recorded simultaneously. In the upper figures (a, b, c, d) the sample topography is presented. We show in the figures (e, f, g, h) the corresponding luminescence cartography obtained respectively, from the left to the right, before and after the Zn-K edge, as well as before and after the W-K edge. The acquisition time was 45 minutes per twin image topography-light. From (f) and (h) images, chemical mapping of the sample, i.e. regions rich in Zn or W can be defined.

Replacing the optical fiber of our microscope by an X-ray monocabillary, it is possible to collect the X-Ray Fluorescence (XRF) in near field instead of the XEOL signal. An Energy Dispersive X-Ray analyser is thus used to carry out the spectrometry of the fluorescence signal. Up to now, we have demonstrated the feasibility of this concept and that a resolution of 1 μm can be reached using a laboratory X-ray excitation source (rotating anode), while a resolution of less than 100 nm is expected using a brighter source (synchrotron environment). Of course the sample topography can be obtained simultaneously to chemical analysis.

References

- [1] http://www.itrs.net/Links/2007ITRS/2007_Chapters/2007_ERM.pdf
- [2] D. Pailharey et al. Journal of Physics: Conference Series 93, Functional Materials and Nanotechnologies, 2007
- [3] S. Larcheri et al. Review of Scientific Instruments **79**, 2008

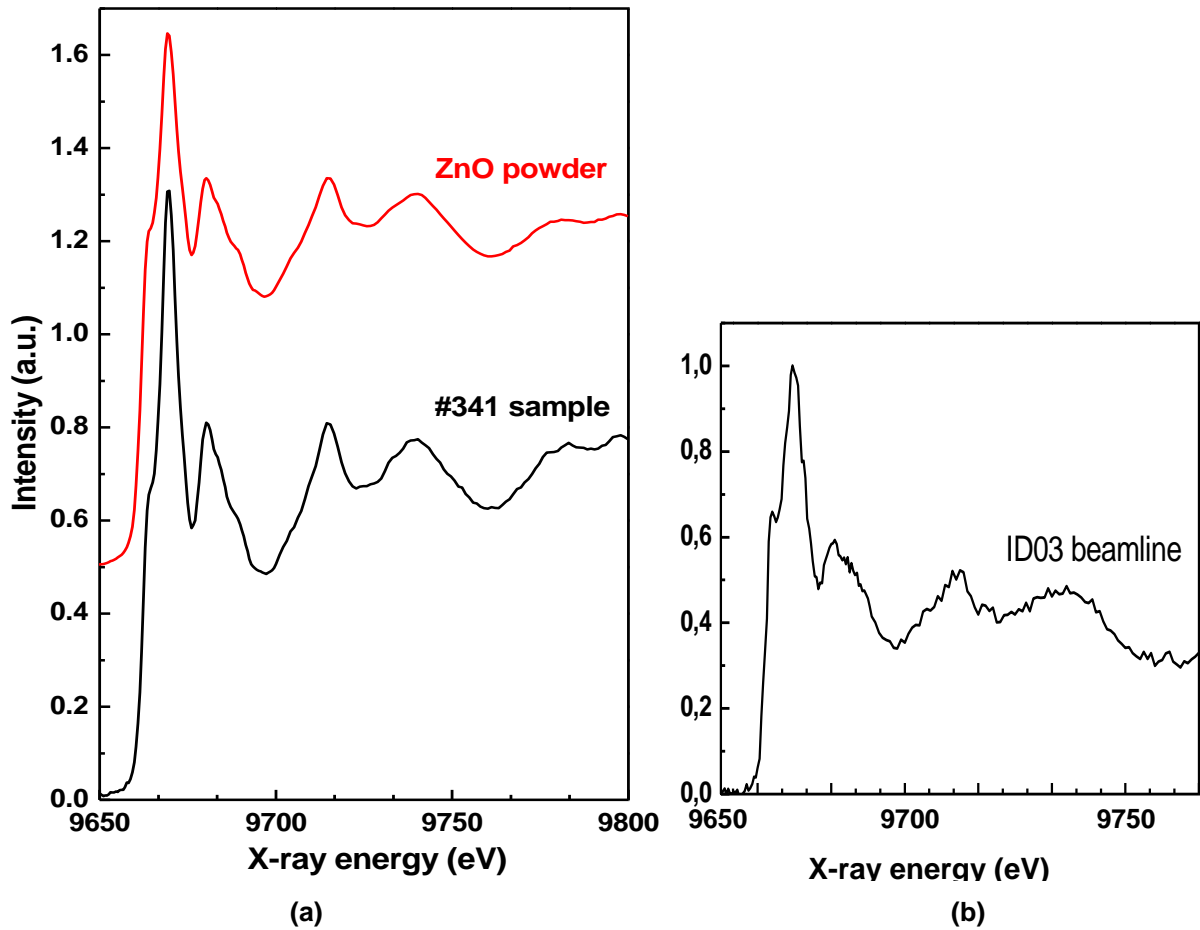


Figure 1. (a) XEOL spectra of ZnO powder (top) and of a ZnO layer sputtered on silicon sample (bottom). (b) XEOL spectrum of the same ZnO layer recorded in near field with the sharp and low aperture optical fiber, probe of our shear force microscope.

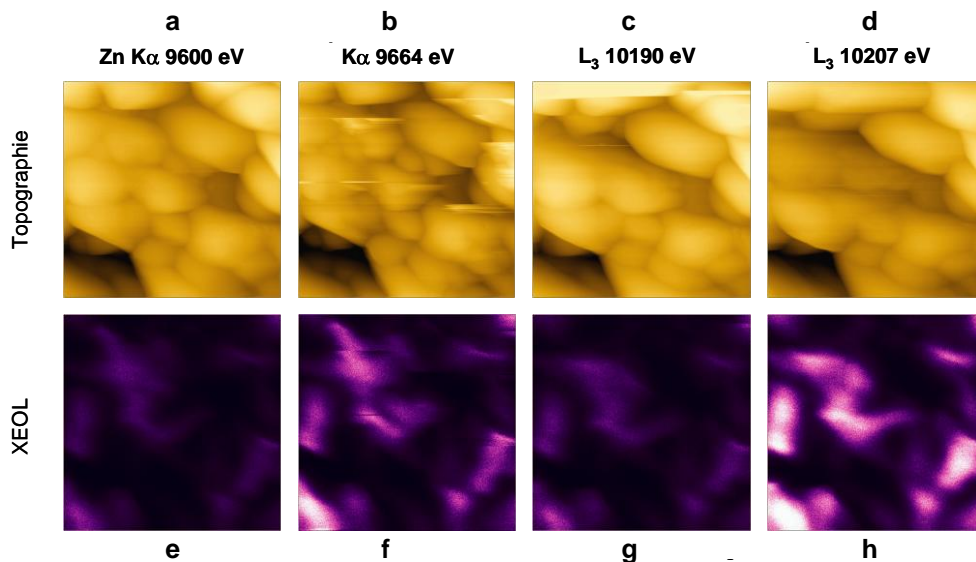


Figure 2. (a-d) topography of a sample coated with the ZnWO₃ + ZnO layer (2 x 2 μm^2). (bottom) corresponding visible light image under illumination by X-ray beam from left to right below (e) and above (f) the Zn threshold (9.6 keV) and below (g) and above (h) W threshold (10.2 keV).

Structural modification of MgO/CoFeB using a low energy ion beam from an assisted deposition source

Ricardo Ferreira^{1,2}, Susana Cardoso^{1,3}, Paulo P. Freitas^{1,2,3}

¹ INESC-Microsistemas e Nanotecnologias (INESC-MN) and Institute for Nanosciences and Nanotechnologies (IN), Rua Alves Redol, 9, 1000-029 Lisbon – Portugal

² International Iberian Nanotechnology Laboratory (INL), Braga -Portugal

³ Instituto Superior Técnico (IST), Departamento de Física, Lisbon - Portugal

rferreira@inesc-mn.pt

Ion Beam Assisted Deposition (IBAD) was already proposed as an alternative to the more conventional Physical Vapor Deposition (PVD) as a method to produce MgO/CoFeB MTJs in the range $RxA \sim 1 \Omega \mu m^2$ [1]. This deposition method has two main advantages over PVD :

- 1) The plasma is generated far from the sample being deposited, thus limiting the damage of deposited stack induced by energetic species in the plasma.
- 2) The energy of the ions and the number of ions are uncoupled parameters that can be controlled independently.

Despite the advantages of IBAD, PVD is still the deposition method producing better MgO/CoFeB MTJs. Still, transport results in stacks obtained by both methods are strongly system dependent and far from the theoretically predicted values for TMR (>1000% [2]).

For this work, MgO was deposited in a dual Ion Beam deposition system starting from an MgO ceramic target and using one of the ion beam guns to assist the deposition. The base deposition rate of MgO in the absence of an assistance beam was changed between 0.1Å/s and 0.3Å/s, using different parameter sets for the deposition gun. For each of these deposition conditions, the parameters of the assist gun were changed as well. The deposition rate of for each set of deposition and assist gun parameters was measured (Figure 1). The obtained results can be quantitatively understood with a simple model of the ion beam guns.

Both guns are Ion Beam Kaufman sources with an RF antenna being used to create the plasma inside a reactor (with Xe as process gas in the deposition gun and Ar as process gas in the assistance gun) biased with a positive voltage (V^+). The ions are then extracted from the reactor with a second negatively charged grid (V^-), as shown in Figure 1. It can be assumed that the number of ions per unit of time is proportional to I^+ and the energy of each incoming ion is proportional to V^+ . Experimental values show that the base deposition rate, in the absence of an assistance beam, is proportional to the deposition gun ion beam power [$I^+ \times V^+$]_{deposition}. When the assist gun power is large, a similar relation can be found. In this regime, the deposition rate during an Ion Beam Assisted Deposition decreases proportionally to the assistance gun ion beam power [$I^+ \times V^+$]_{assistance}, as expected with an ion beam etching away a fraction of the deposited material. A new regime is found when the number of ions per unit of time is increased and the energy per ion is decreased (high I^+ and low V^+). This regime can only be achieved using relatively large extraction voltages (V^-) and results in a reduced etching rate, signaling a change in the energy transfer process between the assistance ion beam and the deposited atoms (Figure 1).

The MgO layers deposited in the two assisted regimes were characterized by x-ray diffraction in samples made of glass // Ta 30Å / CoFeB 300Å / MgO 300 Å / CoFeB 300Å / Ta 30 Å. The experimental results show that the texture of MgO and CoFeB can be enhanced by carefully choosing the parameters of the assistance ion beam for each set of deposition parameters. Furthermore, the lattice constant of MgO can be tuned between 2.09Å and 2.12Å depending on the ratio between the deposition gun beam power and the assist gun beam power (Figure 2). A decrease in the width of the CoFeB peak observed when the MgO lattice constant is decreased indicates that the lattice mismatch at the MgO/CoFeB can be minimized by carefully choosing the ion beam assisted deposition conditions (Figure 2).

The impact of these structural modifications on the transport properties of MgO/CoFeB MTJs is currently being assessed.

References

- [1] "Ion Beam Assisted Deposition of MgO barriers for Magnetic Tunnel Junctions", S.Cardoso, R.J.Macedo, R.Ferreira, A.Augusto, P.Visniowsky, and P.P.Freitas, J.Appl.Phys., vol.103, pp.07A905-07A907, April 2008.
- [2] "Spin-dependent tunneling conductance of Fe|MgO|Fe sandwiches" Butler et al., Phys. Rev. B 63, 056614 (2001).

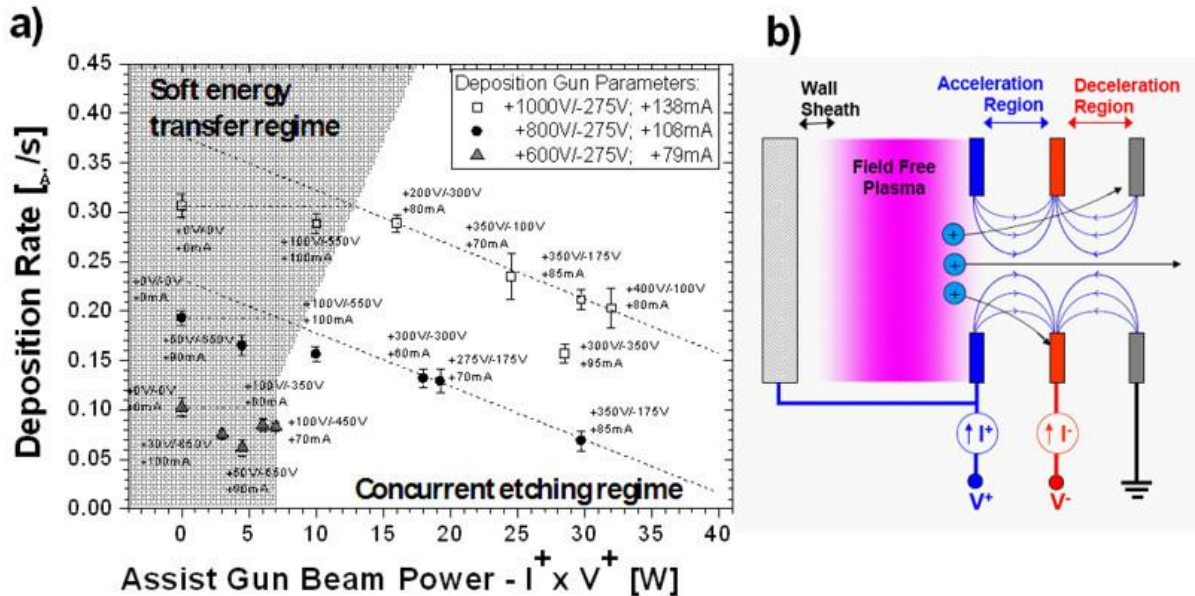


Figure 1 – Left : Deposition rate of MgO as a function of the assistance beam power for selected conditions of the deposition gun. The transition between the etching regime and a soft energy transfer mechanism is indicated. Right : schematic of the assist gun grids. The positive voltage V^+ is a measure of the ions kinetic energy and the positive current I^+ is a measure of the ion flux.

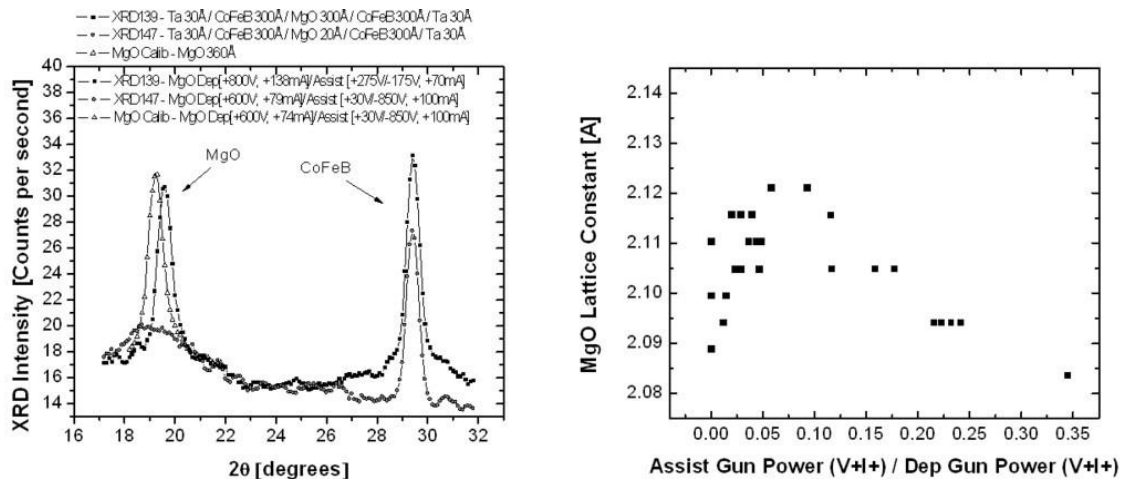


Figure 2 – Left : XRD diffraction spectrum of three different structures containing MgO and CoFeB for different deposition conditions of MgO. Notice the change in the MgO peak position as a function of the deposition conditions. The CoFeB peak width also depends on the CoFeB deposition conditions. Right : MgO lattice constant as a function of the ratio between the assist gun power and the deposition gun power.

Malaria Diagnostics based on Antibody-Functionalized Gold Nanoparticles and *Plasmodium falciparum* Hsp70

Ricardo Franco¹, Inês Gomes^{1,2}, Bassem Shenouda^{1,3}, Cláudia Sá e Cunha², Hassan Azzazy³, Maria Mota², Miguel Prudêncio²

¹ REQUIMTE, Departamento de Química, Faculdade de Ciências e Tecnologia, Universidade Nova de Lisboa, 2829-516 Caparica, Portugal

² Malaria Unit, Instituto de Medicina Molecular, Faculdade de Medicina da Universidade de Lisboa, 1649-028 Lisboa, Portugal

³ Department of Chemistry, SSE # 1194, AUC Avenue, 74, New Cairo, 11835, Egypt

r.franco@dq.fct.unl.pt

Biomedical nanotechnology presents revolutionary opportunities in the detection of pathogenic microorganisms. Despite its huge burden, with forty percent of the world's population at risk of infection, the diagnosis of malaria is often not straightforward and there is an urgent need to develop rapid, sensitive, and cost-effective tests for both high- and low-resource settings. We aim to design a gold nanoparticle (AuNP)-based rapid detection test (RDT) using specific antibodies to detect *Plasmodium falciparum* (malaria parasite) antigens in clinical specimens. The characteristics of the proposed malaria RDTs include reproducibility, acceptable high sensitivity and specificity, rapidity, ease of performance and interpretation, stability when stored, and capability of species differentiation, all at an affordable price [1].

Our approach is based on the utilization of mercaptoundecanoic acid (MUA)-capped AuNPs conjugated with 2E6 antibodies. These antibodies specifically recognize *Plasmodium falciparum* Heat Shock Protein 70 (PfHsp70). Heat Shock Proteins are immunodominant antigens recognized by the host immune system in various infectious diseases. In particular, PfHsp70 which possesses chaperone and anti-apoptotic activity has recently drawn attention as a novel therapeutic target [2]. The presence of parasitic Hsp70 in the pellet of saponin treated red blood cells of infected mice (and not uninfected mice or humans) was confirmed by Western blot (Figure 1). This result suggests that this antibody-antigen set could be used in the development of an RDT for malaria in clinical samples. PfHsp70 antigens purified from an overexpressing *E. coli* system using His-tag chromatography [3], were targeted by the 2E6 antibodies, as proven by Western blotting analysis. Such antibody-antigen system was used as proof-of-concept for the detection method.

The formation of the 2E6-MUA-AuNP bionano-conjugates was assessed using a previously established method based on ζ -potential measurements [4], indicating that stable bionano-conjugates can be obtained with ca. 150 molecules of antibody per each MUA-AuNP (Figure 2). The bionano-conjugates were produced by simple incubation of the MUA functionalized AuNPs with the 2E6 antibody, suggesting electrostatic and van der Waals forces are involved in formation of the bionano-conjugates. On the other hand, agarose gel electrophoresis showed the formation of more compact 2E6-MUA-AuNP bionano-conjugates in the presence of the cross-linking agents EDC/NHS. We propose cross-linking of the antibody to the MUA-AuNP allows bionano-conjugates that are more robust and appropriate for detection in comparison with their non-crosslinked counterparts.

References

- [1] D. Bell and R. W. Peeling, Nat Rev Microbiol, **4** (2006) S34.
- [2] G. Misra and R. Ramachandran, Biophys Chem, **142** (2009) 55.
- [3] T. S. Matambo, O. O. Odunuga, A. Boshoff, G. L. Blatch, Protein Expr. Purif. **33** (2004) 214.
- [4] I. Gomes, N.C. Santos, L.M.A. Oliveira, A. Quintas, P. Eaton, E. Pereira, R. Franco, J. Phys. Chem. C, **112** (2008) 16340.

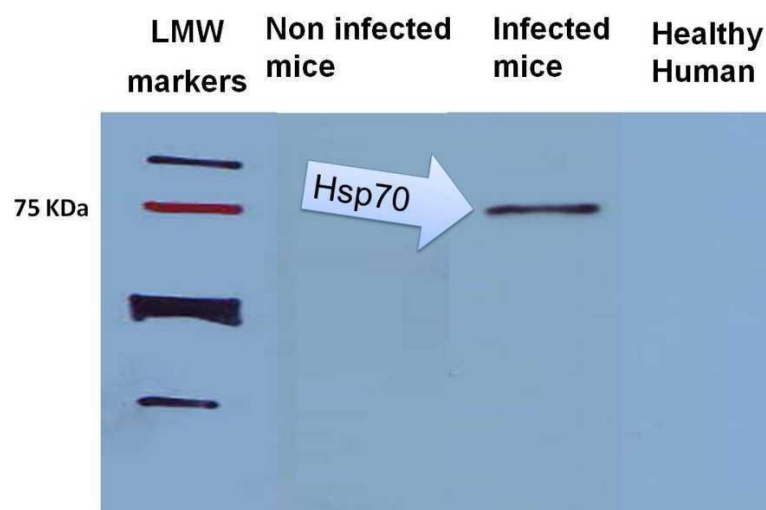


Figure 1. Western blot analysis, using 2E6 antibody, of saponin-treated pellets of red blood cells from mice infected with *Plasmodium berghei*; non infected mice; or a healthy human donor.

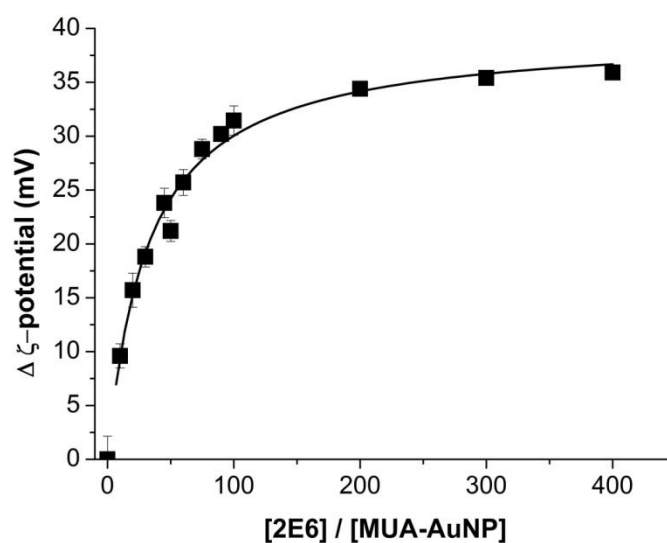


Figure 2. Variation of ζ -potential for each bionano-conjugate in relation to the ζ -potential value for MUA-AuNP alone, determined as a function of the $[2E6] / [MUA-AuNP]$ ratio. The solid line represents the fitting to a Langmuir adsorption isotherm.

Acknowledgments: FLAD (Luso-American Foundation), Portugal, is gratefully acknowledged for financial support to this work. Professor Gregory L. Blatch (Rhodes University, South Africa) is kindly acknowledged for supplying the *PfHsp70* over-expressing plasmid.

Increasing the modulation depth in Au/Co/Au magnetoplasmonic interferometers

D. Martín-Becerra¹, J. B. González-Díaz¹, V. V. Temnov², A. Cebollada¹, G. Armelles¹, T. Thomay³,
A. Leitenstorfer³, R. Bratschitsch³, A. García-Martín¹, **M. U. González**¹

¹IMM-Instituto de Microelectrónica de Madrid (CNM-CSIC), Isaac Newton 8, PTM,
E-28760 Tres Cantos, Madrid, Spain.

²Department of Chemistry, Massachusetts Institute of Technology, Cambridge (MA), USA

³Department of Physics and Center for Applied Photonics, University of Konstanz, Germany

mugonzalez@imm.cnm.csic.es

The ability of surface plasmon polaritons (SPP) to confine optical fields beyond the diffraction limit makes them very attractive for the development of miniaturized optical devices. Several passive plasmonic systems have been successfully demonstrated in the last decade, but the achievement of nanophotonic devices with advanced functionalities requires the implementation of active configurations. This necessitates the capability to manipulate the surface plasmon polaritons with an external agent. Among the different control agents considered so far, the magnetic field holds a robust promise since it is able to directly modify the dispersion relation of SPPs [1]. This modification lies on the non-diagonal elements of the dielectric tensor, ϵ_{ij} . For noble metals, the ones typically used in plasmonics, these elements are unfortunately very small at reasonable field values. On the other hand, ferromagnetic metals have sizeable ϵ_{ij} values at small magnetic fields (proportional to their magnetization), but they are optically too absorbent. Thereby, a smart system to develop magnetic field sensitive plasmonic devices could be multilayers of noble and ferromagnetic metals [2, 3].

Based on these hybrid multilayers, magnetoplasmonic modulation has been recently demonstrated [4]. The implementation of these modulators has been performed through micro-interferometers consisting on a slit paired with a tilted groove, as sketched in Fig. 1. Illumination with a p -polarized laser beam at normal incidence results in the excitation of SPPs at the groove, which propagate towards the slit, where they are reconverted into free-space radiation (I_{SP}) and interfere with light directly transmitted through the slit (I_T). The interference term is given by $\sqrt{I_{SP}}\sqrt{I_T} \cos(k_{SP}d + \phi_0)$, with k_{SP} the SPP wavevector and d the groove-slit distance. In our tilted groove configuration, d varies for each slit position, creating a pattern of maxima and minima in the light transmitted through the slit (see optical image in Fig. 1). When we apply an external periodic magnetic field high enough to saturate the sample (about 20 mT) in the direction parallel to the slit axis, k_{SP} is modified therefore shifting the interference pattern. Thus, at each slit position we detect a variation of the intensity synchronous with the applied magnetic field (see graph in Fig. 1). The full intensity modulation depth of the system is given by the product $\Delta k \times d$, where Δk is the SPP wavevector modification induced by the magnetic field.

The modulation obtained in this basic configuration of the magnetoplasmonic interferometers made of Au/Co/Au multilayers in air is of the order of 2% at a wavelength of $\lambda_0 = 800$ nm and for a mean slit-groove distance of 20 μm , corresponding to $\Delta k \sim 0.5 \times 10^{-3} \mu\text{m}^{-1}$ [4]. This modulation value is reasonable although slightly low for practical applications, and thus the optimization of the geometrical parameters to increase the modulation of the surface plasmon wavevector will provide a higher flexibility in the design of the magnetoplasmonic active devices. A straightforward approach entails the coverage of the metallic multilayer with a dielectric media with higher ϵ_d , since the modulation Δk is proportional to $(\epsilon_d)^2$. We have then covered our magnetoplasmonic interferometers with a thin layer of PMMA ($\epsilon_d = 2.22$). Figure 2 shows the measured Δk for systems with 60 nm PMMA at $\lambda_0 = 633$ nm as compared to identical reference samples without PMMA. A fourfold enhancement of the Δk value, in excellent agreement with the theoretical predictions, has been obtained. Nevertheless, the propagation distance of the plasmon, L_{SP} , decreases with the addition of dielectric overlayers, which will prevent the use of interferometers with large d and the intensity modulation depth will then be limited. Thus, a compromise between the Δk enhancement and the SPP propagation distance has to be achieved. The relevant figure of merit in this case is the product $\Delta k \times L_{SP}$. Our theoretical results show that, with the right thickness of polymer cover, this product can be almost doubled. A detailed analysis of the behaviour of the magnetoplasmonic interferometers when covered with dielectric overlayers, both in terms of modulation enhancement and propagation distance, will be presented. The dependence of these two parameters with the thickness of the dielectric overlayer allows us to obtain information on the SPP electromagnetic field distribution in our system.

References

- [1] R. F. Wallis, J. J. Brion, E. Burstein, and A. Hartstein, Phys. Rev. B **9** (1974) 3424.
 [2] J. B. González-Díaz, A. García-Martín, G. Armelles, J. M. García-Martín, C. Clavero, A. Cebollada, R. A. Lukaszew, J. R. Skuza, D. P. Kumah and R. Clarke, Phys. Rev. B **76** (2007) 153402.
 [3] E. Ferreiro-Vila, J. B. González-Díaz, R. Fermento, M. U. González, A. García-Martín, J. M. García-Martín, A. Cebollada, G. Armelles, D. Meneses-Rodríguez and E. Muñoz-Sandoval, Phys. Rev. B **80** (2009) 125132.
 [4] V. V. Temnov, G. Armelles, U. Woggon, D. Guzatov, A. Cebollada, A. Garcia-Martin, J. Garcia-Martin, T. Thomay, A. Leitenstorfer, and R. Bratschitsch, Nat. Photonics **4** (2010) 107.

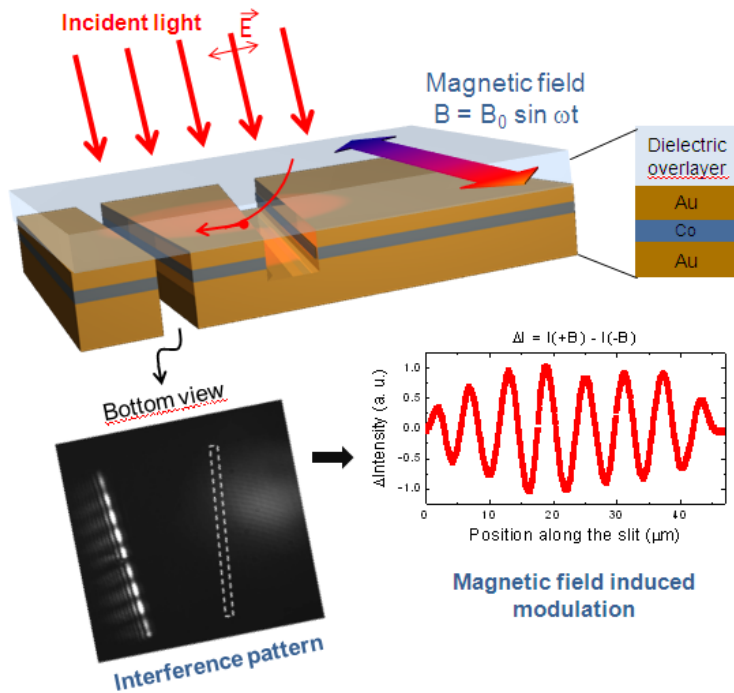
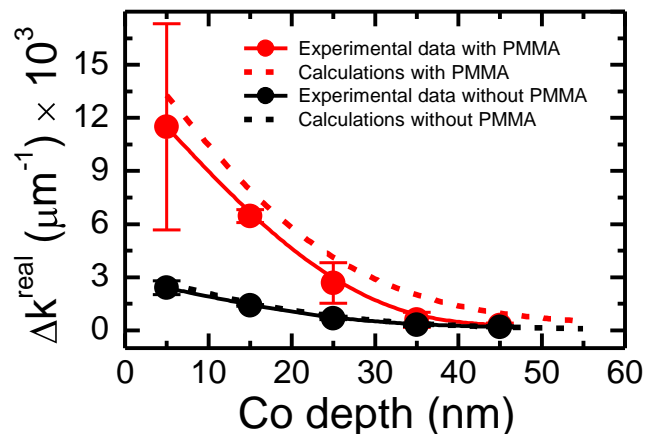


Figure 1. Sketch of the magnetoplasmonic micro-interferometer.

Figure 2. Comparison of the SPP wavevector modulation as a function of the Co layer position for Au/Co/Au micro-interferometers without dielectric overlayer and with 60 nm PMMA overlayer. The values correspond to $\lambda_0 = 633$ nm.



Fast and wavelength selective photoresponse from QD/CNT hybrid

Chang-Soo Han, Hyung Cheoul Shim, Sohee Jeong

Korea Institute of Machinery & Materials, 171 Jang Yousung, Daejeon, South Korea

cshan@kimm.re.kr

QDs absorb lights of all wavelengths less than their own band energy, as well as emit the light according to their specific wavelength [1]. It can be used for several applications such as LED, solar cell, photodetector and so on. Even though QDs has great ability to produce charges from phonon injection, it is not easy to carry the extracted charges to the specific position in order to make the current. Therefore, carbon nanotube (CNT) as carrier transporter have been tried to use, while preserving optical characteristics of QDs [2]. There are several issues in QD/CNT hybrid structure such as dependency of CNT type (Multi-wall CNT, MWNT and single walled CNT, SWNT), linking agent between QD and CNT and the relation between wavelength of the incident light and QD size.

We firstly introduced pyridine as a linking ligand between QD and CNT. It has very short molecular length so that the interference by the light is minimized. Secondly, the difference between MWNT and SWNT as a carrier transporter has been investigated in view of the charge transfer. Finally, we measured the photo response according to the size change of QDs [3]. We fabricated FET (Field Effect Transistor) structure of QD/CNT hybrid material by using dielectrophoresis. After taking the assembled images from SEM and fluorescence microscope, we measured photo excitation of the device by using Ar laser varying its wavelength. Pyridine molecules were used as a short, non-covalent linker allowing assemblies more efficient carrier transfer without deleteriously altering the electronic structure of NQDs and SWNTs.

Figure 1 explains how pyridine molecule combines the QD with SWNT. As the result, we demonstrate that the electron of QD occurred from photoexcitation delivered to carbon nanotube via photoluminescence measurement. In addition, QDs were firmly attached to SWNT as shown in Figure 1c. Photoexcitation studies of resulting assemblies support the efficient carrier transfer in CdSe-py-SWNTs unlike in the CdSe/ZnS-py-SWNTs.

In Figure 2, the fabricated FET device shows that the electron transfer from QD to SWNT definitely was achieved. Our observation in photocurrent, resistivity, and gate dependence characteristics along with the optical measurements suggest the efficient electron transfer from photoexcited NQDs to SWNTs.

As the result, we found that SWNT/QD hybrid structure offered rapid response as a photodetector for specific wavelength of light. In addition, we found that the size of QDs definitely determined the detectable band spectrum of the incident light. For example, the QD with 543nm emission wavelength almost could not detect the light over 600nm wavelength.

References

- [1] Alivisatos A P, Science, Vol. 1271, pp.933-937, 1996. Ritchie, G.S., Trans. ASME, J. Lub. Tech.,1 (1983), 375-376.
- [2] Hu L, Zhao Y L, Ryu K, Zhou C, Stoddart J F and Gruner G J. Adv. Mater., **20** (2008), 939-945.
- [3] S. Jeong, H. Shim, S. Kim, C. -S. Han, ACS Nano, **4** (2009), 324-330.

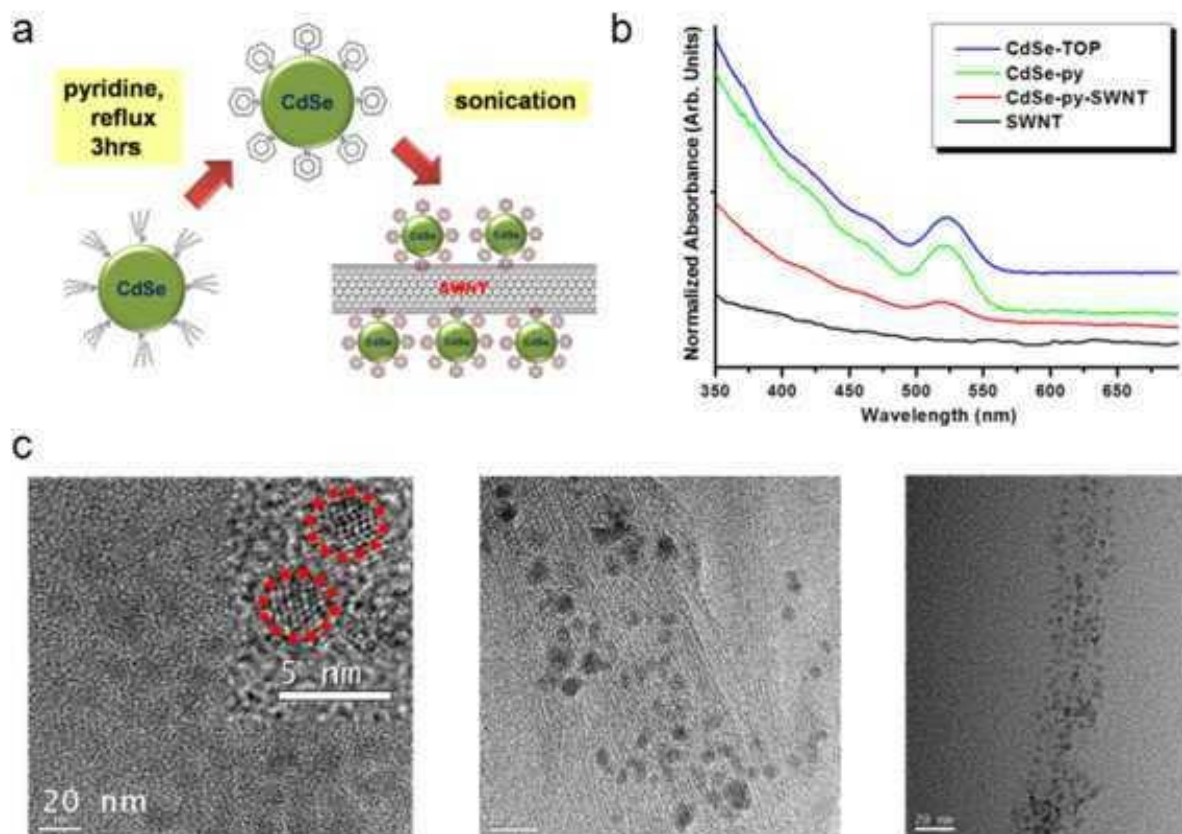


Figure 1. a) A schematic diagram illustrates the non-covalent approach used to fabricate the NQD-SWNT hybrid structures. b) UV/VIS absorption spectra show the optical transitions of synthesized CdSe particles prior to surface modification (trioctylphosphine-capped CdSe in toluene), CdSe-py, CdSe-py-SWNT hybrid nanostructure, and SWNT. The 1S transition of CdSe at 522 nm was retained throughout the process. c) TEM images show the CdSe nanocrystals (left, average size ~ 2.8 nm) and the hybrid CdSe-py-SWNT (middle and right)

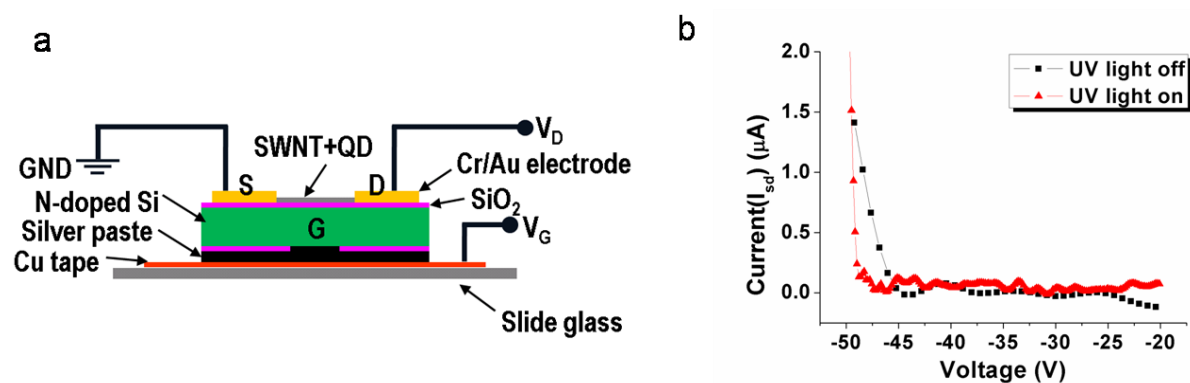


Figure 2. a) A schematic diagram shows the configuration of a CdSe-py-SWNT FET for measurements of gate dependence. b) The gate dependence curve of a CdSe-py-SWNT FET is shown with illumination on and off; $\lambda = 365$ nm, $I = 1.2$ mW/cm²

Protein Adsorption to Biomaterials - Atomic Force Microscopy & Radioactive Labeling Analysis

Maria Holmberg & Xiaolin Hou Technical

University of Denmark, Department of Micro- and Nanotechnology, Frederiksborgvej 399, Roskilde, Denmark

maria.holmberg@nanotech.dtu.dk

In this study protein adsorption onto biomaterials is investigated using Atomic Force Microscopy (AFM) and radioactive labeling. Biomaterials are defined as artificial materials that interact with a biological system and are used in implants, biosensors, biomedical devices etc. Protein adsorption onto these biomaterials can result in dysfunctional or less efficient devices and can evoke unwanted response from the biological system the material is introduced onto [1-5].

By labeling proteins with different radioactive isotopes that emit gamma radiation with different energies we have developed a unique protocol for detection of several proteins onto a surface simultaneously [6-8]. Combining this quantitative technique with AFM measurements in liquid makes it possible to monitor formation of protein layers onto biomaterials in an environment similar to that, the materials are designed to function in. The setup combining AFM and radioactive labeling gives an opportunity to study interaction between artificial materials and biomolecules on nano-, micro- and macro-scale.

Figure 1 shows results from radioactive labeling where three different blood proteins (albumin, IgG and fibrinogen) are detected simultaneously on a polyethylene terephthalate (PET) polymer surface as a function of adsorption time. It is observed that the protein adsorption is increasing with adsorption time and that different proteins dominate the surface at different times. The concentrations used correspond to a protein level of 0.25 % blood and the amount protein adsorbed in Figure 1 indicates monolayer adsorption at this concentration level.

Figure 2 shows AFM Tapping Mode images (5x5 μm) obtained in cPBS (citrate Phosphate Buffered Saline) buffer of a) a clean PET surface, b) the same PET surface after introduction of 1 mg/ml albumin and c) the same PET surface after performing a scratching experiment. The roughness obtained before and after proteins are introduced is rather similar, indicating that the adsorbed albumin is homogeneously distributed over the surface. After performing a scratching experiment, where contact mode imaging with a rather high force is performed in a restricted area of the surface (700x700 nm), one can clearly observe that material is removed from the scanned area (see arrow in Figure 2c).

Figure 3 shows an AFM Tapping Mode image (10x10 μm) of a PET surface to which 10 mg/ml albumin has been introduced. The image is obtained in cPBS buffer and the different areas on the surface have had more or less contact with the scanning tip. Most scans and scratching experiments have been performed in area A, while area B only has been scanned once or twice. Area C is an area on the surface that never has been scanned before obtaining the image. The degree of impact on the protein layer from scanning gives valuable information about strength and character of interaction between protein and surface.

References

- [1] B.D. Ratner, S.J. Bryant, *Annu. Rev. Biomed. Eng.*, 6 (2004) 41.
- [2] D.F. Williams, *Biomaterials*, 30 (2009) 5897
- [3] N. Huebsch, D. Mooney, *Nature*, vol 462 (2009) 426.
- [4] J.M. Anderson, A. Rodriguez, D.T. Chang, *Seminars in Immunology*, 20 (2008) 80.
- [5] T.S. Tsapikouni, Y.F. Missirlis, *Material Science and Engineering B*, 152 (2008) 2
- [6] M. Holmberg, K.B. Stibius, N.B. Larsen, X.L. Hou, *J. Mat. Science. Mat. in Med.*, 19 (2008) 2179
- [7] M. Holmberg, X.L. Hou, *Langmuir*, 25 (2009) 2081
- [8] M. Holmberg, X.L. Hou, *Langmuir*, 26 (2010) 938

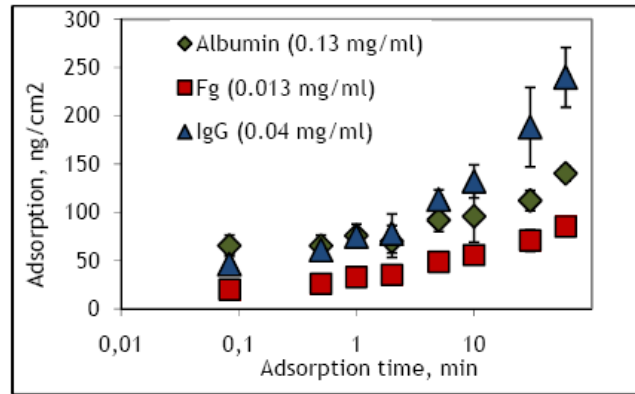


Figure 1. Albumin, fibrinogen (Fg) and IgG adsorption onto PET surface as a function of adsorption time. Proteins are added to the surface simultaneously with the concentrations shown in the figure and which corresponds approximately to the concentrations in 0.25 % blood.

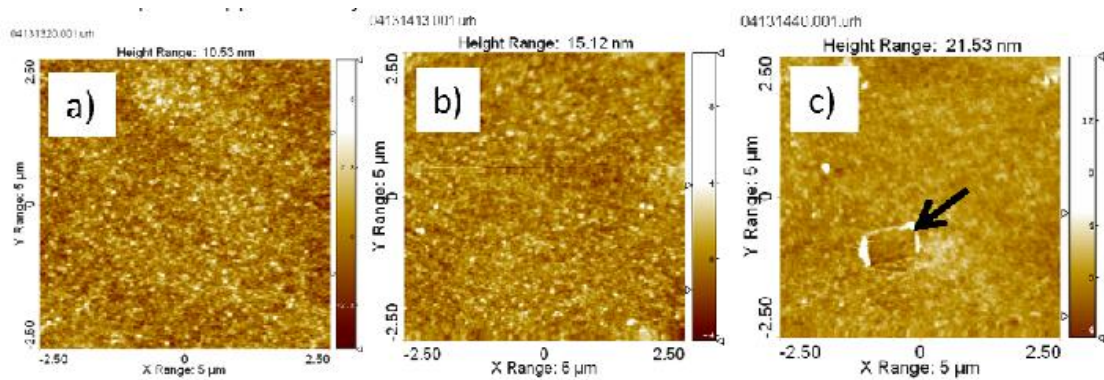


Figure 2. AFM Tapping Mode images (5x5 μm) of a) clean PET in cPBS, b) the same PET surface after introduction of 1 mg/ml albumin and c) the same PET surface after performing a scratching experiment.

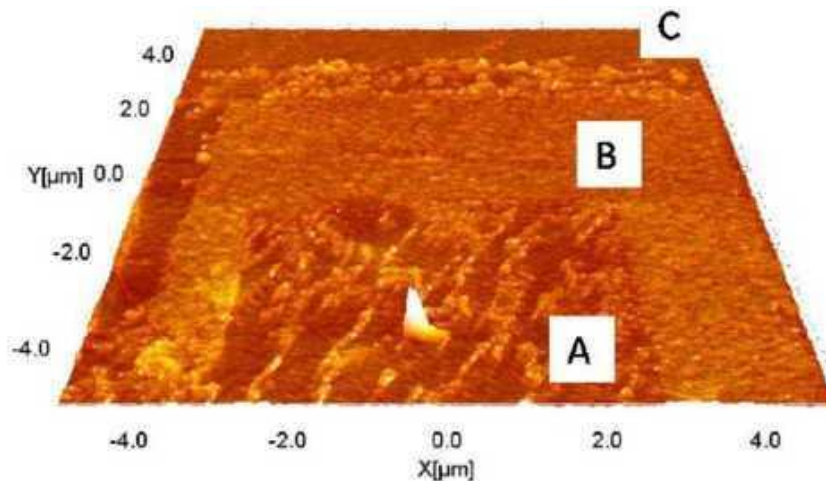


Figure 3. AFM Tapping Mode image of a 10x10 μmeter large area where a protein layer (10 mg/ml albumin) has been more or less disturbed by the scanning cantilever and tip. Most scans and scratching experiments have been performed in area A, while area B only has been scanned once or twice. Area C is an area on the surface that has never been scanned before.

Symmetry breaking and on-tube modulated surface potentials in hybrids of Single-Walled Carbon Nanotubes with encapsulated inorganic nanostructures

Adelina Ilie¹, James S. Bendall², Katsumi Nagaoka³, Tomonobu Nakayama³, Stefan Egger⁴, and Simon Crampin¹

¹Department of Physics & Centre for Graphene Science, University of Bath, Bath BA2 7AY, UK

²University of Cambridge, 11. J J Thomson Avenue, Cambridge CB3 0FF, UK

³Nano System Functionality Centre, MANA, National Institute for Materials Science, 1-1, Namiki, Tsukuba, Ibaraki 305-0044, Japan

⁴EMPA, Überlandstrasse 129, CH-8600 Dübendorf, Switzerland

a.ilie@bath.ac.uk

Templated confinement in carbon nanotubes has emerged in recent years as a successful route towards producing low dimensional hybrid nanomaterials with new and diverse nanoscale properties and applications, from nanothermometers, to nanofluidic attogram mass transport, to chemical sensors with enhanced sensitivity, to transport phenomena such as negative differential resistance (NDR) or spin-related, or vectors for drug delivery. It also generates phases of materials inaccessible otherwise. Effects are particularly rich when confining inorganic materials in Single-Walled Carbon Nanotubes (SWCNTs), with theoretical predictions and increasing experimental evidence of unique morphologies forming inside [1-3]: inorganic nanotubes (INTs), twisted structures, with lowered symmetry and high anisotropy, or with strong structural relaxation.

To ultimately exploit these hybrid nanomaterials controllably one needs to be able to correlate structure with physical properties, and then with functionality down to the *local (atomic) level*. This approach is essential at this degree of lateral confinement where few atom morphological variations can dramatically affect properties.

For this, we combine high resolution transmission electron microscopy (HRTEM), scanning tunnelling microscopy /spectroscopy (STM/STS), and ab-initio calculations to study structural phases of SWCNT-templated silver iodide (AgI) nanowires [4]. We show that symmetry breaking of the nanotube's surface wavefunction correlates with the electrostatic/polarization interaction from the ionic component of AgI filling (which has a mixed ionic-covalent character). This is the first direct demonstration of the capability of inorganic nanostructures to be unique sources of non-bonding on-tube *surface potentials where symmetry and magnitude can be controllably modulated*, with strong implications for electronic transport.

Here, low-dimensional AgI nanowires formed inside SWCNTs provided the first opportunity to use STM/STS to reveal more generic local effects on nanotubes caused by a long-range, non-bonding, electrostatic/polarization interaction potential. AgI is a good study system as its polymorphic nature helps select the symmetry of the resulting SWCNT-encapsulated phases. Fig.1 shows such an AgI phase with strong charge anisotropy, where charges of alternating sign are separated in rows (see Fig. 3a): 1(a) is an HRTEM image of two structural configurations stemming from the same crystallization phase, i.e. in a narrower nanotube, and a larger nanotube where structural relaxation occurred; 1(c) are associated structural models derived from Density Functional Theory (DFT) simulations; 1(b) are HRTEM image simulations using the structural models from 1(c). Figure 2 shows STM/STS from AgI-filled SWCNTs. A stripe-like superstructure breaks the usual symmetry of the nanotube's wavefunction. We found that its overall characteristics and energy dependence is consistent with the ionic/polarization perturbation potential at the nanotube wall generated by the phases in Fig. 1 (and different from known superstructures). This potential has a stripe-like surface distribution, shown in Fig. 3(a); its amplitude magnitude is sizeable, of several tenths of eV, as obtained from both Discrete Dipole Approximation (DDA) and DFT calculations. Fig. 3(b) shows that the potential's distribution / symmetry and its magnitude is governed crucially by the type of encapsulated AgI phase: a different phase, with fast charge alternation and thus less anisotropic charge distribution, produces a different symmetry and a strongly reduced modulation of the potential.

This leads to the generalization that *well-chosen* encapsulated inorganic structures with regulated, "quantized" number of atomic rows can be unique sources of interaction potentials with the nanotubes where symmetry and magnitude can be controllably selected and modulated. Adding to the results of another study of ours, where permanent dipoles in the chain of a SWCNT-encapsulated KI nanocrystal were invoked to explain Negative Differential Resistance phenomena [5], such potentials can have

strong implications for the electronic transport through carbon nanotube-based hybrids. Moreover, they can provide a potential way to dominate and uniformize the nanotube's response in respect to its (n,m) type; as well as an additional, charge-based assembly mechanism for nanotube functionalization.

References

- [1] C.L. Bishop, M. Wilson, *J. Mat. Chem.* **19**, 2929 (2009); M. Wilson, *Nano Lett.* **4**, 299 (2004).
 [2] E. Philp, J. Sloan, A.I. Kirkland, R.R. Meyer, S. Friedrichs, J.L. Hutchinson, M.L.H. Green, *Nat. Mater.* **2**, 788 (2003).
 [3] M. Baldoni, S. Leoni, A. Sgamellotti, G. Seifert, and F. Mercuri, *Small*, **3**, 1730 – 1734 (2007).
 [4] A. Ilie, J. S. Bendall, K. Nagaoka, T. Nakayama, S. Egger, and S. Crampin, submitted, (2010).
 [5] A. Ilie, S. Egger, S. Friedrichs, D.-J. Kang, M.L.H. Green, *Appl. Phys. Lett.* **91**, 253124 (2007).

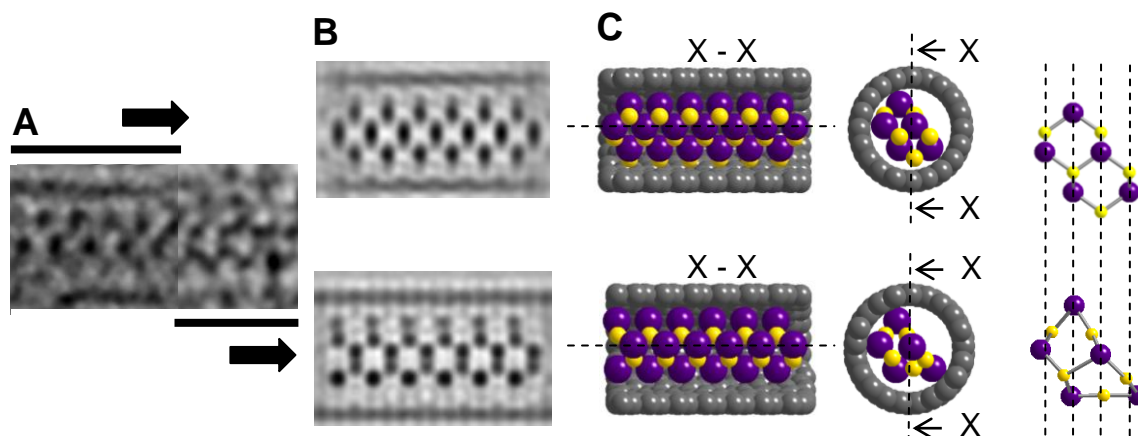
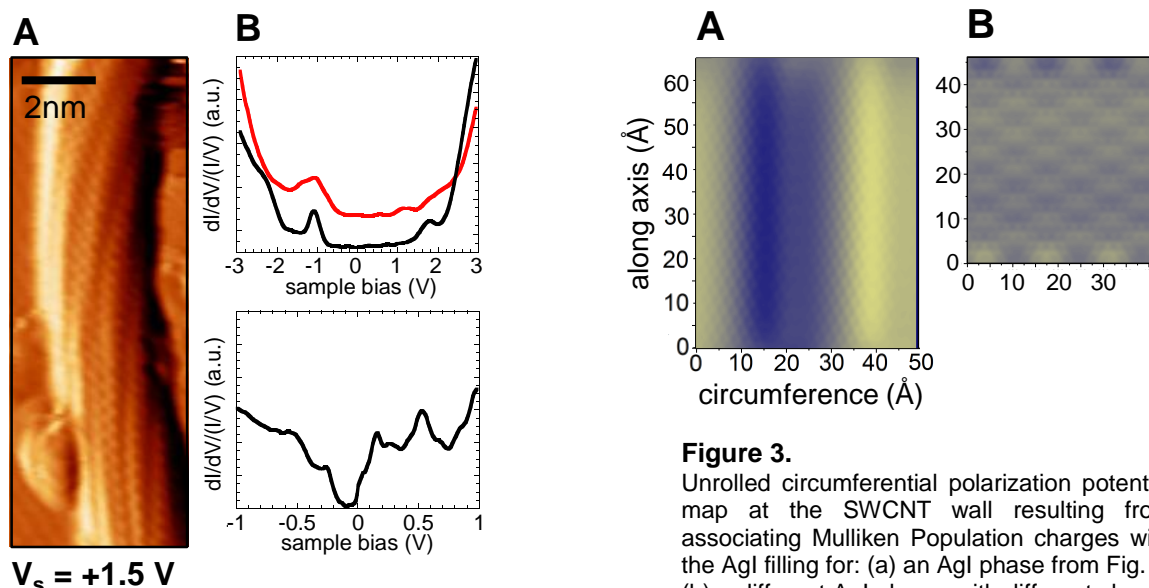


Figure 1.

(a) HRTEM of same AgI phase, without (left) and with (right) structural relaxation in a narrower (1.45 nm diameter) / larger (~1.65 nm diameter) SWCNT, respectively; (b) HRTEM image simulations using structural models from (c); (c) structural models for unrelaxed (top) / relaxed (bottom) AgI phases. DFT simulations were used to determine relaxation.



$V_s = +1.5 \text{ V}$

Figure 2.

(a) Bias-dependent STM showing a stripe-like superstructure; (b) Example of associated STS spectroscopy. Both STM/STS are consistent with proposed models.

Figure 3.

Unrolled circumferential polarization potential map at the SWCNT wall resulting from associating Mulliken Population charges with the AgI filling for: (a) an AgI phase from Fig. 1; (b) a different AgI phase, with different charge distribution (see text). The maps have been obtained by unrolling the AgI@SWCNTs structures.

Dynamical Mean-Field Theory for Electronic Structure and Transport Properties of Nanoscopic Conductors

David Jacob¹, Gabriel Kotliar²

¹Max-Planck-Institut für Mikrostrukturphysik, Weinberg 2, 06120 Halle, Germany

²Dept. of Physics & Astronomy, Rutgers University, Piscataway, NJ-08854, USA

djacob@mpi-halle.de

Dynamic correlations due to strong electron interactions can play a crucial role in determining the electronic structure and transport properties of nanostructures containing magnetic atoms. This has been most impressively demonstrated by the recent observation of Kondo effect in ferromagnetic nanocontacts[1]. Other recent examples demonstrating the importance of dynamic correlations in nanoscopic systems are the observation and manipulation of the Kondo effect in magnetic adatoms and molecules on metal surfaces[2-4].

We present a novel approach that allows to predict the electronic structure and transport properties of nanoscopic conductors taking fully into account the strong dynamic correlations arising from the strong electron-electron interactions of d-or f-electrons of transition metal atoms. Our approach combines ab initio electronic structure calculations with the Dynamical Mean-Field Theory (DMFT) in order to treat the dynamic correlations originating from the strongly interacting d- and f-electrons properly. This work extends upon our previous work considering a single magnetic impurity in a nanocontact [5] to the case of several magnetic atoms.

We demonstrate the importance of dynamic correlations for several experimentally relevant systems: A single magnetic impurity in a nanocontact (Fig.1a), a single magnetic atom adsorbed on a graphene sheet (Fig.1b), and a magnetic nanocontact consisting of several magnetic atoms(Fig.1c).The examples show that dynamic correlations in these systems are indeed important and can give rise to Kondo effect which shows up as Fano features in the conductance vs. bias voltage characteristics similar to those observed in experiments. Incontrast, conventional ab initio transport calculations based on density functional theory(DFT) can not describe the dynamic correlations that lead to Kondo effect and the corresponding Fano features in the conductance as can be seen in Fig.2.

References

- [1]M.R.Calvo,J.Fernández-Rossier, J.J.Palacios, D.Jacob, D.Natelson and C.Untiedt, Nature 458 (2009) 1150
- [2]N.Neeletal., Phys. Rev. Lett. 98 (2007) 016801
- [3]P.Wahletal., Phys. Rev. Lett. 98 (2007) 056601
- [4]A.Zhaoetal., Science 309 (2005) 1542
- [5]D.Jacob, K.Haule and G.Kotliar, Phys. Rev. Lett. 103 (2009) 016803

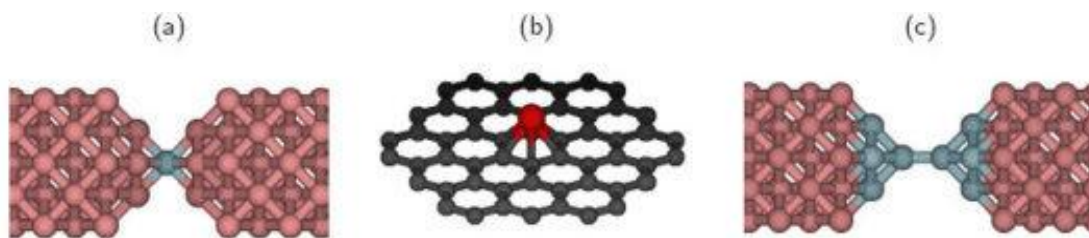


Figure1. (a) Single magnetic impurity in the contact region of a Cu nanocontact. (b) Single Co atom adsorbed at the hollow site of graphene sheet.(c) Ni nanocontact bridging two semi-infinite Cu nanowires.

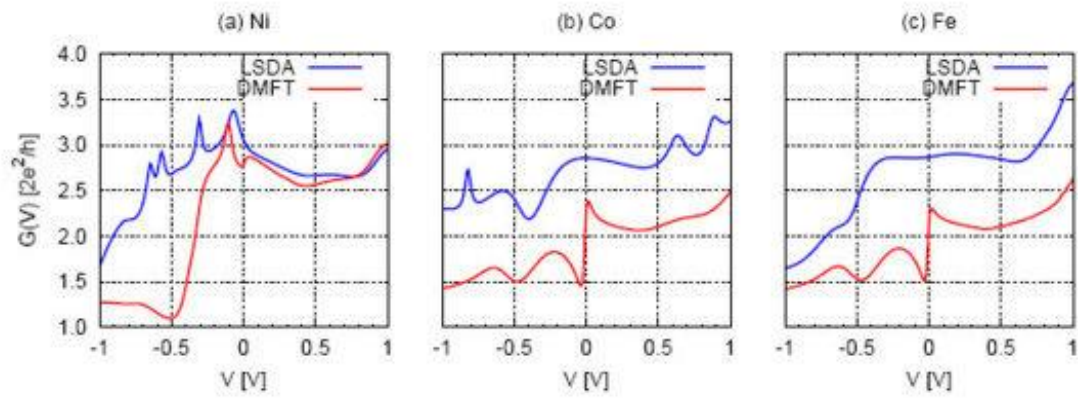


Figure 2. Conductance vs. bias voltage of a Cu nanocontact hosting a single magnetic impurity calculated with the novel DMFT nanotransport method (red curves) on the one hand and with the conventional DFT based transport method (blue curves) with in the local spin density approximation (LSDA) on the other hand.

Small sub-nm metal clusters: the key missing point in many catalytic processes?

M.A. López-Quintela & J. Rivas

University of Santiago de Compostela, NANOMAG Lab., Research Technological Institute, University of Santiago de Compostela. E-15782 Santiago de Compostela. Spain

malopez.quintela@usc.es/jose.rivas@usc.es

The discovery of Haruta et al. (T. Hayashi, et al. *J. Catal.* 1998, 178, 566) showing the catalytic activity of oxide-supported gold nanoparticles opened a very exciting field of research in nanocatalysis. Since then much effort was devoted to the understanding of such surprising catalytic activity (see e.g. M. M. Schubert et al. *J. Catal.* 2001, 197, 113). But, it was not until recently that it was recognized that most of the activity of catalysts synthesized by standard chemical procedures (deposition-precipitation, impregnation, etc.) can be attributed to the presence of small gold clusters containing only a few atoms, with large nm-sized particles being mostly spectators (A. A. Herzing et al. *Science*, 2008, 321, 1331).

Small metal clusters, are considered to be one of the most exciting areas in the next generation of catalysts (H. Häkkinen et al. *Angew. Chem. Int. Ed.* 2003, 42, 1297). However, although different experimental and theoretical results seem to support this idea, there are until now no conclusive evidences for this claim. The main reason for this uncertainty is the difficulty to prepare such tiny entities, which depend very much on the type of preparation, the functional groups attached to them and the supporting material. In the last years we have developed several soft wet-chemical techniques to control the growth of very small sub-nm metal clusters of different materials (Pt, Au, Ag, Cu, ...) down to 2-3 atoms (Guillén-Villafuerte et al. *Angew. Chem. Int. Ed.* 2006, 45, 4266 ; Ledo-Suárez et al. *Angew. Chem. Int. Ed.* 2007, 46, 8823; Rodríguez-Vázquez et al. *Langmuir*, 2008, 24, 12690; Selva et al. *J. Am. Chem. Soc.* 2010, in press). These methods allow, in a simple way, to select and scale up the production of clusters (M.A. López Quintela and J. Rivas. *Stable Atomic Quantum Clusters, Production Method Thereof and Use of Same*. Patent Applications PCT/ES2006/070121, 2006; WO2007017550A1, 2007), without using strong-binding ligands, like thiols, phosphines, etc, which may inhibit, in some cases, their catalytic properties. In this talk we will summarize the catalytic properties of small metal clusters (< 10-13 atoms) mainly focused on two specific areas: their electrocatalytic properties and also their ability to catalyze and direct the growth of anisotropic structures (rods, prisms, ...).

Organic photonic devices by soft nanopatterning on active materials and nanofluids

E. Mele, L. Persano, A. Camposeo, G. Potente, R. Cingolani and D. Pisignano

National Nanotechnology Laboratory of CNR-INFM and Italian Institute of Technology, Università di Lecce, via Arnesano I-73100, Lecce, Italy

dario.pisignano@unisalento.it

Methods for nanopatterning active materials and nanocomposites on surfaces play a fundamental role in the fabrication of functional devices. In organic nano- and optoelectronics, a current challenging issue is the research of cheap, parallel-patterning approaches for fabricating addressable matrix arrangements of spatially discrete elements, and high-quality emissive features with sub-100 nm size, to be employed as nanoscale light sources. In this frame, high-resolution soft lithographic technologies are able to fulfill these requirements, and particularly approaches based on nanofluidic transport of molecules. Recently, researchers began to investigate the potential of fluidics at the 10–100 nm scale because of its unequalled manipulation, separation, and delivery accuracy at molecular scale, and due to the availability of flexible lithographic techniques for fabricating structures with sub-micrometer resolution.

We report on our results demonstrating (i) nanofluidics as sub-100 nm technology for building emissive organic nanofeatures with precise control of their cross-section and spatial arrangement, and (ii) nanopatterning of materials composite at nanoscale, made by nanoparticles and polymers. We realise emissive arrays and optically active dots and fibers with lateral dimensions of features down to a few tens of nanometers. Moreover, vertically moving nanofluids can be exploited to overcome hard polymer transport in materials incorporating nanocrystals. Rheology, fluorescence, quantum yield, and emission directionality of the nanostructures are investigated. The obtained results open new perspectives for the realization of light-sources for nanophotonics, based on hybrid organic-inorganic systems by combining nanofluidic and optoelectronic materials properties.

Microsensors based on multi-wall decorated carbon nanotubes and few-layer graphene

S. A. Moshkalev, F. P. Rouxinol, C. Verissimo, R. V. Gelamo, A. R. Vaz, M.B. Moraes

Center for Semiconductor Components, University of Campinas – UNICAMP, P.O Box 6061, 13083-870, Campinas, SP, Brazil

stanisla@ccs.unicamp.br

Nanoscale graphitic carbon materials like carbon nanotubes (CNT) and, more recently, few-layer graphite (graphene) have attracted much interest due to unique combination of electrical, mechanical, chemical properties and many potential applications. However, for successful applications of these materials in microdevices like gas sensors, reliable and compatible technologies of controlled synthesis or deposition, manipulation, functionalization, decoration, integration and others, comprising specific technological platforms, should be developed.

In this work, multi-wall carbon nanotubes and few-layer graphene have been utilized to fabricate gas sensors with extremely low power consumption. The technologies of processing and manipulation have been established first for multi-wall carbon nanotubes. To provide selective sensitivity to different gases, the nanotubes were decorated by various metal or metal oxide (Ti, Sn, Ni, TiO₂, SnO₂, CePrOx, etc.) nanoparticles (NP) using several chemical or physical processes. Then, decorated nanotubes were deposited from liquid solutions precisely over pairs of metal (Ti, W, Au) electrodes with micron scale gaps using ac di-electrophoresis, to form a chemical resistor configuration, Fig. 1. After deposition, thermal annealing in vacuum was used for electrical contact improvement. Both suspended and supported (over SiO₂ substrate) nanotubes were tested. To obtain suspended nanotubes, FIB milling was used to make deep trenches between electrodes, before nanotubes deposition.

The samples (CNT/NP) were characterized using various microscopy techniques (SEM, TEM, EDX, EELS, confocal Raman, Raman imaging, AFM). Electrical measurements were carried out to evaluate performance of CNT/NP based sensors in the presence of various gases (Ar, N₂, O₂, H₂S) in a gas chamber. Two different effects during CNT/NP-gas interaction were observed: i) electrothermal (change of the nanotube resistances due to their cooling by gas, as nanotubes can be heated up strongly in vacuum by current - Joule effect), ii) chemical interaction between nanoparticles and the injected gas. The characteristic times differ very strongly for these two processes, that helps to distinguish between their contributions. The Joule effect (self-heating) was found to heat up suspended nanotubes up to 300-400 C at applied biases as low as 0.5 V (microwatt power consumption), while much smaller heating was observed for supported CNTs, due to unexpectedly high heat dissipation to the SiO₂ substrate.

On the other hand, self-heating of nanotubes by current was found to increase dramatically the reactivity of nanoparticles towards reactive gases. In particular, this effect allowed to obtain high sensitivity in detection of oxygen by Ti decorated nanotubes at room temperature, which is impossible for conventional thin film sensors, Fig. 2. For comparison, with supported nanotubes, measurable signals were obtained only when substrate was heated to 150-200 C.

Similar technologies have been applied here also to fabricate few-layer graphene (FLG) based gas sensors. These sensors can have some advantages over CNT base ones, for example much bigger area can be exposed to gases, resulting in increased sensitivity. Utilizing an ac di-electrophoresis method, we were able to deposit FLG in suspended or supported configurations, Fig. 3. Some samples were studied using confocal Raman spectroscopy to study spatial distribution of the FLG flake properties (not shown). The annealing performed in a high vacuum (< 5x10⁻⁶ Torr) at 850 oC, was found to dramatically reduce electrical resistance down to a few hundreds of kΩ. Preliminary results of tests carried out with gases like O₂ and propanol vapor and Sn-decorated FLG have shown the possibility of using such devices as highly-sensitive gas or pressure sensors in a suspended chemi-resistor configuration, see Fig. 3.

References

- [1] R.V. Gelamo F. Rouxinol, C. Verissimo, A. Vaz, M. B. Moraes, S. Moshkalev, Chem. Phys. Lett., 482 (2009) 302.
- [2] R.V. Gelamo, F. Rouxinol, C. Verissimo, S. Moshkalev, Sensor Letters, 8 (2010), 488
- [3] F. P. Rouxinol, et al, to be published.

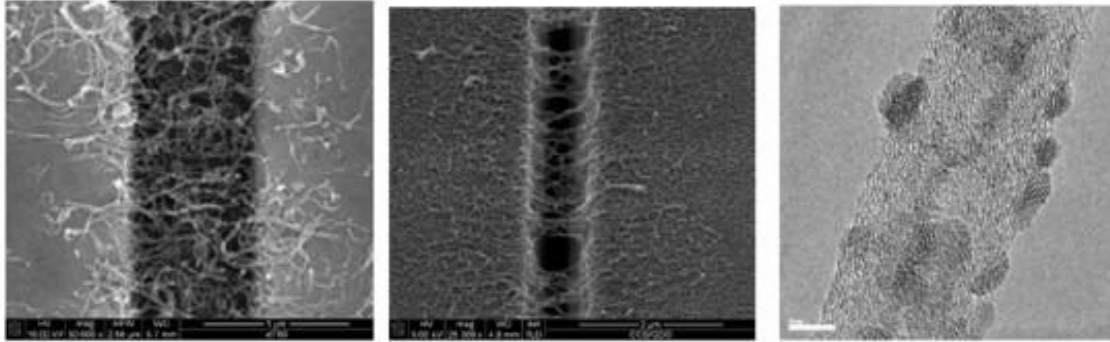


Figure 1. SEM images of multi-wall carbon nanotubes in supported (left) or suspended (center) sensor configuration, and TEM image of SnO₂ decorated nanotube (right)..

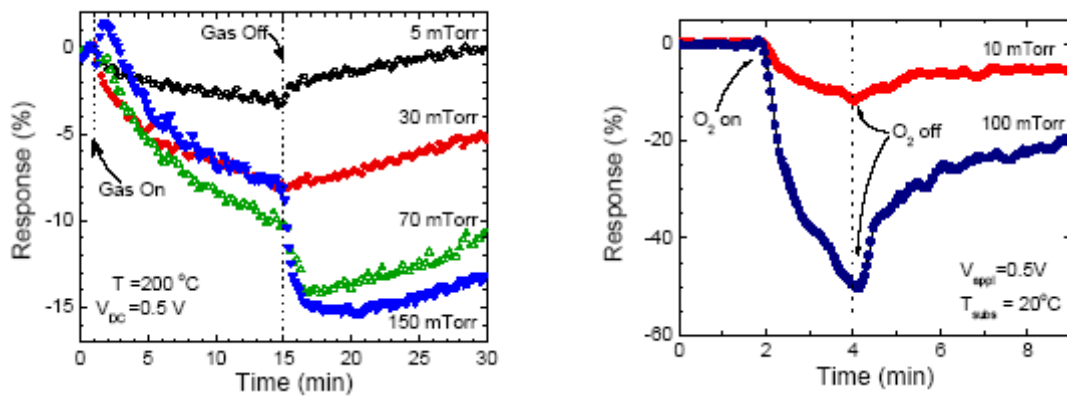


Figure 2. Sensor response for O₂ pulses in the vacuum chamber for Ti-decorated multi-wall carbon nanotubes in supported (left) or suspended (right) sensor configuration.

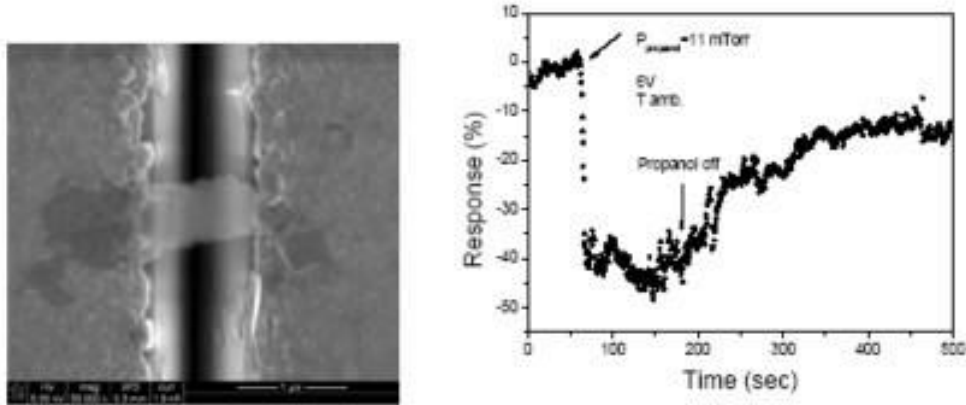


Figure 3. Suspended FLG flake deposited over electrodes (left) and sensor response for Sn-decorated FLG when propanol vapor is injected in the vacuum chamber.

Kinetics underlying the switching time of a silver sulfide atomic switch

Alpana Nayak, Kazuya Terabe, Tohru Tsuruoka, Tsuyoshi Hasegawa, and Masakazu Aono

WPI Center for Materials Nanoarchitectonics (MANA), National Institute for Materials Science,
1-1 Namiki, Tsukuba, Ibaraki 305-0044, Japan.

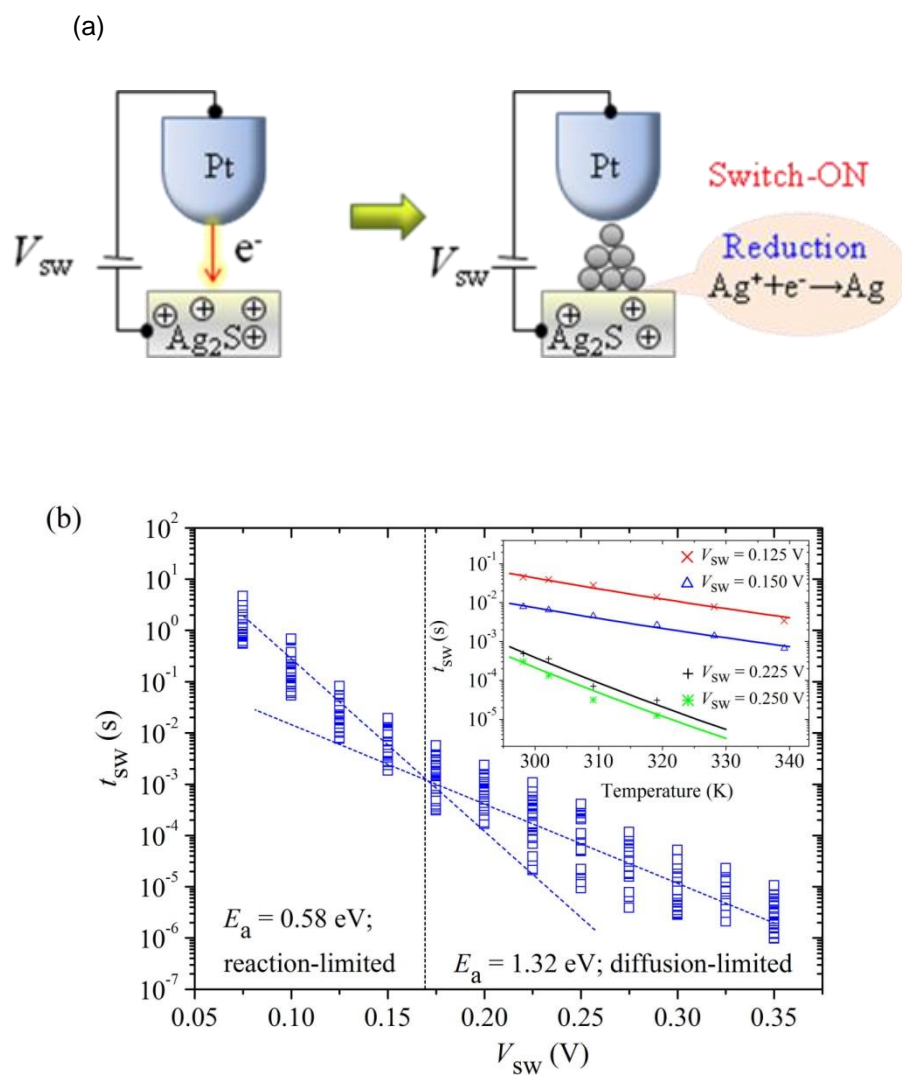
NAYAK.Alpana@nims.go.jp

Nanoionics based atomic switches have been attracting much attention in recent years to overcome the limitations of conventional semiconductor technology. Prior to their use in actual devices, a fundamental understanding of the switching mechanism is necessary. Accordingly, we investigated the switching time of a Ag_2S atomic switch as a function of bias voltage and temperature. A Ag_2S atomic switch¹, in which the formation and annihilation of Ag atomic bridge is controlled by a solid-electrochemical reaction, is realized across a nanogap between a solid-electrolyte electrode (Ag_2S) and a counter metal electrode (Pt tip of STM). Increasing the bias voltage decreases the switching time exponentially² with a greater exponent for the lower range of bias than that for the higher range. The two distinct exponential decay components indicate an existence of different rate-limiting processes for lower and higher bias voltages. Furthermore, the switching time shortens with raising temperature, following the Arrhenius relation. The activation energy extracted from the Arrhenius plots yielded values of 0.58 eV and 1.32 eV for the lower and higher bias ranges, respectively. On the basis of these results, we infer that, there are two main processes which govern the switching mechanism; first, the electrochemical reaction $\text{Ag}^+ + \text{e}^- \rightarrow \text{Ag}$, and second, the diffusion of Ag^+ ions, and that the rate-limiting process depends on the range of bias applied. We believe that the switching time is reaction-limited for lower bias voltages and diffusion-limited for higher bias voltages. This investigation advances the fundamental understanding of the switching mechanism of the atomic switch which is essential for its successful device application.

References

- [1] K. Terabe, T. Hasegawa, T. Nakayama, and M. Aono, *Nature*, **433** (2005), 47.
- [2] A. Nayak, T. Tamura, T. Tsuruoka, K. Terabe, S. Hosaka, T. Hasegawa and M. Aono, *The Journal of Physical Chemistry Letters* **1** (2010), 604.

Figure1. (a) Schematic representation of the operation of an electrochemically controlled Ag_2S atomic switch with a nanogap, (b) Switching time t_{sw} measured as a function of bias V_{sw} at room temperature for an initial off-resistance of $1 \text{ M}\Omega$. The dashed lines show the two distinct exponential decay components with different activation energy E_a . The temperature dependence of t_{sw} is shown in the inset.



Coupling of photonic nanowires to k-mismatched waveguides and resonators

Paulo Taveres^a, Manfred Niehus^{a,b}

^aISEL|DEETC, Rua Conselheiro Emídio Navarro 1, 1959-007 Lisboa, Portugal

^bInstituto de Telecomunicações, Campus Universitário de Santiago, 3810-193 Aveiro, Portugal

mniehus@av.it.pt

We present results concerning the coupling of EM guided waves between dielectric photonic nanowires and k-mismatched waveguides and/or resonators.

We begin by describing the coupling between two identical cylindrical nanofibers. A coupling model based on the evanescent field overlap is compared to a full three-dimensional finite-difference time-domain simulation obtained with the MEEP software package. The results are compared to those of other authors [1], and special emphasis is given to identify the limits of coupled mode theory based on perturbation theory in the present context. We find strong similarities with fiber mode coupling in tapered optical fibers [2].

Subsequently, a k-mismatch is introduced into the coupling scheme, and the first order impact on coupling efficiency and beating length is investigated.

Care is taken to permit a direct comparison with an experimental setup, where the waist region of adiabatically tapered optical nanofibers represent the initial waveguide.

Next, we studied and analysed the coupling from a photonic nanowire to a single ring resonator, both in tapping and add/drop configuration. Through the conventional transmission spectra, we analyzed coupling efficiencies for the experimental parameter space, also in function of the k-mismatch. Also, we paid special attention to the evanescent field enhancement effect in the space between waveguide and resonator in the propagation direction. Fundamental and technical coupling limits are discussed.

Finally, we will discuss the important problem coupling efficient between cylindrical photonic nanowires and high index materials and photonic crystals, and will present simulation results for these configurations.

References

- [1] Keji Huang, Shuangyang Yang, and Limin Tong, "Modeling of evanescent coupling between two parallel optical nanowires", *Appl. Opt.* **46**, 1429-1434 (2007).
- [2] M. Niehus, G.M.Fernandes, A.N.Pinto, "Design of a tunable single photon interferometer based on modal engineered tapered optical fibers", SPIE Proc. Photonics Europe 2010.



Figure 1. One-to-four nanofiber beamsplitter simulated with FDTD

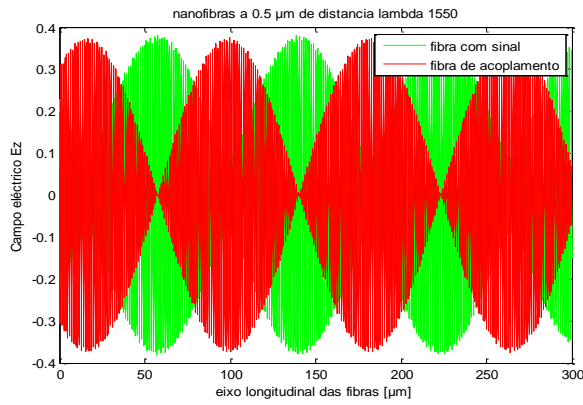


Figure 2. Periodic energy exchange between nanofibers due to evanescent field overlap-result of simulation

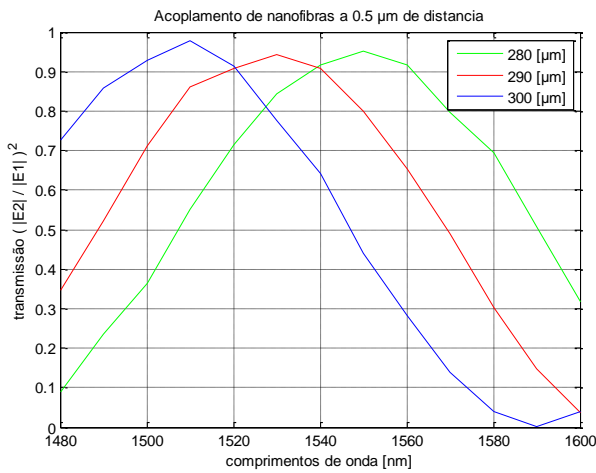


Figure 3. Spectral transmission of coupled nanofibers

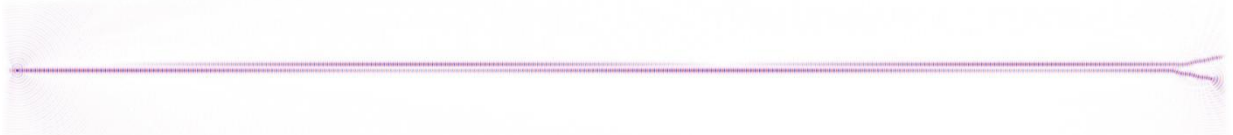


Figure 4. Periodic energy exchange between nanofibers due to evanescent field overlap- simulation

Green Photocatalytic Synthesis of Au and Ag Nanoparticles: Size and Shape Control

Eulália Pereira,¹ Patrícia A. Carvalho,² Eliana Malheiro,¹ Adelaide Miranda,¹ Pedro Quaresma,¹ Leonor Soares,¹ Armando Silva¹

1) REQUIMTE/Departamento de Química e Bioquímica, Faculdade de Ciências, Universidade do Porto, 4169-007 Porto, Portugal

2) Departamento de Engenharia de Materiais, Instituto Superior Técnico, 1049-100 Lisboa, Portugal

eulalia.pereira@fc.up.pt

Green chemistry synthetic approaches must be designed for reduced environmental impact; waste reduction; process safety; materials, and energy efficiency. This is seldom the case in the synthesis of nanoparticles, since the need for a high control of size and size dispersion is usually achieved through the use of high temperatures, and toxic materials. The development of bulk solution synthetic methods in water that can save energy and reagents while allowing high yields of NPs with low size dispersion is of paramount importance for the full implementation of a green chemistry synthetic strategy in NPs, specially intended for biological applications. One promising way to achieve it is to control the formation of nanoparticles by use of a catalyzed reaction.

Herein, we describe a method that relies on a photocatalytic reaction to produce gold and silver NPs with enhanced mono-dispersion in an aqueous medium, at pH 7 and room temperature. [1,2] The use of a photocatalyst allows fast formation of seeds in solution, leading to superior size-dispersion of the final NPs (Figure 1). This one-pot seeding method engages the following green chemistry principles: *(i)* low energy consumption, the reaction is carried out at room temperature and uses a low-power halogen bulb for photocatalysis; *(ii)* short reaction time, the complete synthesis takes in most cases less than 4 minutes; *(iii)* non-toxic reagents, triethanolamine (TEA) is the electron donor and toxic surfactants that are commonly used as capping agents are replaced by water soluble polymers that are physiologically compatible: poly(N-vinyl pyrrolidone) (PVP), starch, acacia gum, and cellulose; *(iv)* no purification is necessary; a mono-dispersed NPs solution is readily obtained. Furthermore, the NPs can be easily functionalized with a thiolated ligand, imparting new functionalities to the NPs that can be explored for biological applications. In comparison to other methods using the same type of capping agents, the present methodology yields a significantly better size dispersion.

A similar strategy was used to control the shape of the nanoparticles. In this case, a shape-directing capping agent was used (CTAB) in conjunction with a stringent control of the reaction kinetics to prepare Au triangular nanoplates (Figure 2) and nanocubes (Figure 3). Adjustment of the experimental conditions, such as concentration of the photocatalyst and concentration of capping agent allows control of the average size of the anisometric nanoparticles. In particular, for the synthesis of triangular nanoplates, it is possible to control the average edge length in the range 50-150 nm by changing the concentration of the photocatalyst. In addition, for each concentration of photocatalyst used it is possible to fine-tune the edge length of the nanoplates by changing the concentration of capping agent. Preliminary kinetic studies show that the photocatalyst and the capping agent influence both the rate of nucleation and the rate of growth of the nanoparticles, but with opposing actions. This behavior may be advantageously used to control the size/size dispersion of the nanoparticles, keeping high yields of the selected shape. In addition, these kinetic studies are useful to further understand the basic principles underneath the control of size and shape in the synthesis of nanoparticles, which represents one of the major challenges in the chemical synthesis of nanoparticles.

References

- [1] Y. J. Song, Y. Yang, C. J. Medforth, E. Pereira, A. K. Singh, H. F. Xu, Y. B. Jiang, C. J. Brinker, F. van Swol and J. A. Shelnutt, *J. Am. Chem. Soc.* **126** (2004) 635.
[2] P. Quaresma, L. Soares, L. Contar, A. Miranda, I. Osório, P. A. Carvalho, R. Franco, E. Pereira, *Green Chem.* **11** (2009) 1889.

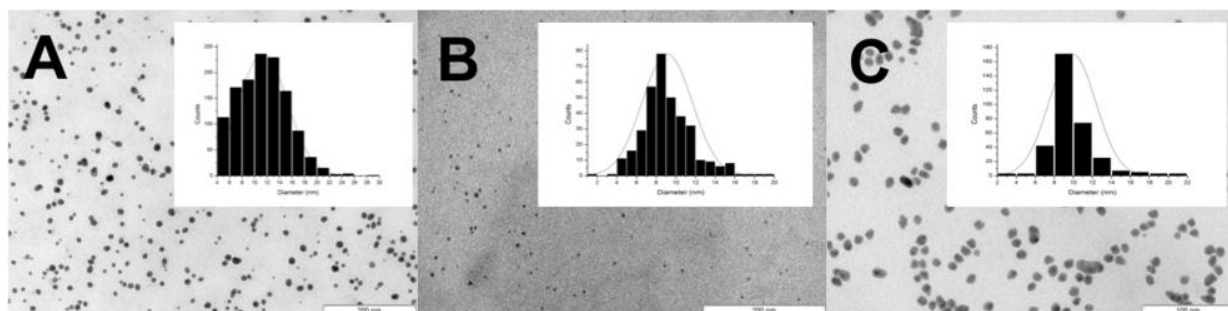


Figure 1. Representative TEM images of A) Au NPs synthesized with acacia gum as capping agent (mean diameter 11.3 ± 3.9 nm); B) Ag NPs synthesized with starch as a capping agent (mean diameter 9.1 ± 2.5 nm); and Au/Ag alloy NPs synthesized with acacia gum as capping agent (mean diameter 9.8 ± 2.5 nm). The insets are the corresponding histograms of size distribution obtained with more than 200 nanoparticles.

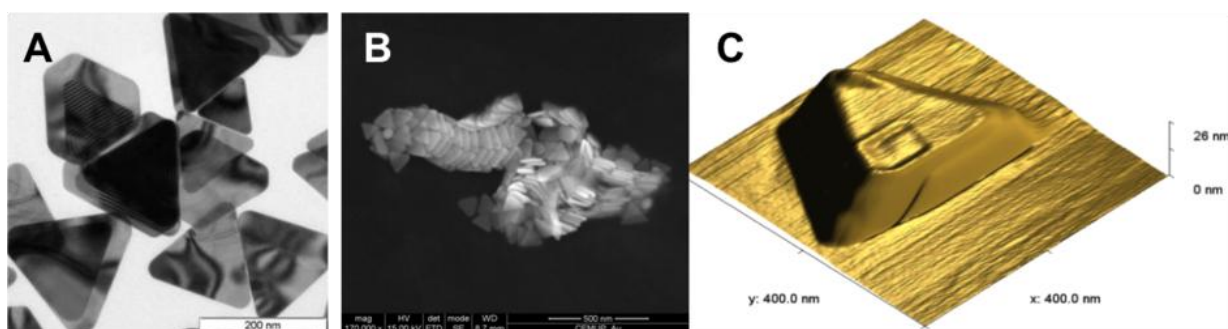


Figure 2. A) TEM, B) SEM, and C) AFM images of gold nanotriangles synthesized photocatalytically.

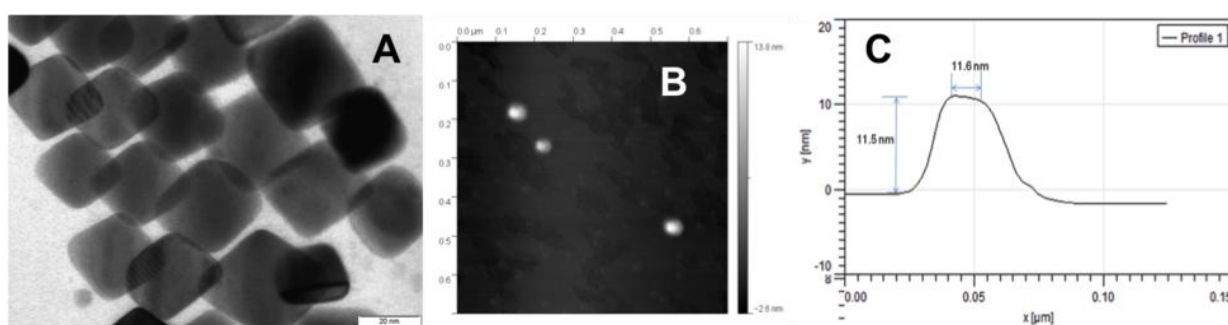


Figure 3. A) TEM image, B) AFM image, and C) AFM height profile of gold nanocubes synthesized photocatalytically.

Polymer Electrospun Nanofibers as Building Blocks for Nanotechnology

Alessandro Polini, Stefano Pagliara, Elisa Mele, Luana Persano, Roberto Cingolani, Andrea Camposeo
and **Dario Pisignano**

National Nanotechnology Laboratory of CNR-INFM and Italian Institute of Technology,
Università di Lecce, via Arnesano I-73100, Lecce, Italy

dario.pisignano@unisalento.it

Polymeric nanofibers realized by electrospinning technology are very advantageous nanostructures by virtue of their ultra-high surface to volume ratio, offering the opportunity to easily control the surface topography and chemical composition for many nanotechnological applications.

In biomedical engineering, the research of new scaffold design is addressed by nanomaterials mimicking fibrous extracellular matrix micro-environments. Tailoring polymer nanofibers is made possible by means of specific biological functions incorporating molecules in the electrospinning solution, or functionalizing the external surface of nanofibers by linking molecules, such as cell adhesive proteins and peptides.

On the other hand, active nanofibers are also interesting for their confinement effects on electronic and optical properties. In particular, active, flexible, fully organic nanofibers, realized by light emitting polymers and composites, show tunable emitting properties, and are attracting building blocks as low-cost photon sources. The integration of active organic nanostructures in microfluidic devices is especially relevant for high-sensitivity diagnostic applications. In this context, the main challenge is to dispose of miniaturized light-sources integrated into lab-on-chips, involving very tiny needed liquid volumes for ultimately single reaction diagnostic.

References

- A. Polini et al. *Soft Matter* 6, 1668 (2010).
- A. Camposeo et al. *Appl. Phys. Lett.* 90, 143115 (2007);
Small 5, 562 (2009); *Appl. Phys. Lett.* 94, 043109 (2009).
- F. Di Benedetto et al., *Adv. Mater.* 20, 314 (2008);
Nature Nanotechnol. 3, 614 (2008).
- S. Pagliara et al. *Lab Chip* 9, 2851 (2009),
Appl. Phys. Lett. 95, 263301 (2009).

Magnetic Edges Current and Disorder in Graphene Nano-Ribbons

B. Raquet¹, J-P Poumirol¹, A. Cresti², S. Roche³, R. Ribeiro¹, W. Escoffier¹, M. Goiran¹,
X. Wang⁴, X. Li⁴, H. Dai⁴

¹LNCMI, UPR 3228, Université de Toulouse, 31400 Toulouse, France

²CEA, LETI, MINATEC, F38054 Grenoble, France

³CIN2 (CSIC-ICN), Campus UAB, E-08193 Barcelona, Spain

⁴Dpt of Chemistry and Lab. of Advanced Materials, Stanford University, California USA

bertrand.raquet@lncmi.cnrs.fr

The control of the current flow in graphene nanoribbons (GNRs) constitutes a fascinating challenge for the future of carbon-based electronic devices. However, non-perfect edges, bulk vacancies, charge trapped in the oxide or structural deformations are potential sources of backscattering. Their respective contribution remains debated and seems to be sample dependent.

This work presents compelling evidences of the 1D transport character in the first generation of chemically derived GNRs with smooth edges and the possibility of tuning backscattering effects by means of an external magnetic field [1]. Bandstructure calculations allow some assignment of the measured gate-dependent conductance modulations to the underlying van Hove singularities, and hence some estimation of the likely ribbon edge symmetry. The application of perpendicular high magnetic field on narrow ribbons, in the range of 11-30nm, further induces a marked enhancement of the conductance, irrespective of the applied gate voltage and in large contrast to the magneto-fingerprints of graphene flakes. Close to the charge neutrality point, the measured large positive magnetoconductance is attributed to the formation of the first Landau state, responsible for the closing of the energy gap and of a marked reduction of backscattering processes. Landauer-Buttiker conductance simulations convincingly support the scenario of an entangled interplay between the magnetic bands formation and a disorder-induced interband scattering suppression. Both smooth edge disorder and long range Coulomb scatters yield similar conclusions.

Finally, a comparative magneto-transport study between chemically derived GNRs and patterned GNR by oxygen plasma reactive ion etching will be addressed.

References

[1] J-M Poumirol et al., arXiv:1002.4571

Diffusion of DNA polymer molecules in nanochannels

R. Sczech¹, S. Howitz², M. Mertig¹

¹ Technische Universität Dresden, 01062 Dresden, Germany.

² GeSiM, Bautzner Landstrasse 45, 01454 Großerkmannsdorf, Germany

DNA molecules can be transported in a nanochannel with help of electrophoretic and hydrodynamic flow. Transport experiments and theoretical considerations point to an interaction of electrophoresis, electro-osmosis, and the unique statistical properties of confined polymers. The confinement of the device also plays a crucial role by influencing the electric fields in the nanochannel [1].

Nanofluidic channels in polydimethylsiloxane (PDMS) were formed by classical nanoimprinting technology combining micro- and nanofluidic features. We circumvent small aspect ratios by superimposing a permanent layer of the heat curable varnish SU-8 for the micrometer wide entrance channels. The utility of the hybrid micro- and nanofluidic PDMS structures for single molecule observation and manipulation was demonstrated by introducing single molecules of λ -DNA into the channels using optimized conditions for the applied potential and flow [2].

Manipulation of transport was successfully demonstrated with PDMS nanochannels with a cross section $\leq 1 \mu\text{m}$ observed by using epifluorescence video microscopy. Once stabilized inside a nanochannel the free diffusion of individual λ -DNA molecules could be observed. Diffusivity was compared with previous studies that concentrated on nanoslits and checked for adaptability to blob theory and reflecting rod theory [3].

References

- [1] Stein, D.; Deurvorst, Z.; van der Heyden, F. H. J.; Koopmans, W. J. A.; Gabel, A. and Dekker, C., *Nano Letters*, 10, 765-772 (2010)
- [2] Gast, F.; Dittrich, P.; Schwille, P.; Weigel, M.; Mertig, M.; Opitz, J.; Queitsch, U.; Diez, S.; Lincoln, B.; Wottawah, F.; Schinkinger, S.; Guck, J.; Käs, J.; Smolinski, J.; Salchert, K.; Werner, C.; Duschl, C.; Jäger, M.; Uhlig, K.; Geggier, P. and Howitz, S., *Microfluidics and Nanofluidics*, 2, 21-36 (2006)
- [3] Strychalski, E. A.; Levy, S. L. & Craighead, H. G., *Macromolecules*, 41, 7716-7721 (2008)

Suppression of thermal conduction and enhanced thermoelectric figure of merit in disordered carbon systems

Haldun Sevinçli¹, Wu Li^{1,2}, Stephan Roche^{1,3,4}, Gianaurelio Cuniberti¹

¹ Institute for Materials Science and Max Bergmann Center of Biomaterials, Dresden University of Technology, D-01062 Dresden, Germany.

² Institute of Physics, Chinese Academy of Sciences, 100190 Beijing, China.

³ Institute for Nanoscience and Cryogenics INAC/SP2M/L_Sim, CEA, 38054 Grenoble Cedex 9, France.

⁴ Centre d'Investigació en Nanociència i Nanotecnologia (CSIC-ICN), 08193 Bellaterra, Barcelona, Spain

haldun.sevincli@nano.tu-dresden.de

Graphitic allotropes of carbon are known to have extremely high mechanical strength and stiffness which give rise to ultra high thermal conduction through these materials [1]. Isotopic or Anderson-type disorder can reduce thermal conductivity in quasi-one-dimensional forms of carbon, namely carbon nanotubes and graphene nanoribbons, which are of special importance because of their potential in device applications [2]. Using non-equilibrium Green function methods and also developing an order-N method for phonons we investigate thermal transport properties of graphene nanoribbons with edge-disorder. We find that edge-disorder suppresses phonon transport very strongly so that elastic mean free paths are considerably short (Figure 1) and thermal conduction can be reduced by orders of magnitude [3,4]. Of special importance is graphene nanoribbons with zigzag edges where the outstanding electronic transport properties are weakly affected by edge-disorder [5]. We show that edge-disorder can separate electronic and phononic degrees of freedom very effectively in zigzag graphene nanoribbons and a “phonon glass-electron crystal” is achievable for narrow systems. We also show that thermoelectric figure of merit (ZT) can be enhanced at the edge of the first conduction plateau and can reach the values up to 4 at room temperature [3].

References

- [1] A. A. Balandin et al., Nano Lett. 8, 902 (2008), Y. M. Zuev, W. Chang, and P. Kim, Phys. Rev. Lett. 102, 096807 (2009), J. H. Seol et al., Science 328, 213 (2010).
- [2] I. Savić, N. Mingo, and D. A. Stewart, Phys. Rev. Lett. 101, 165502 (2008).
- [3] H. Sevinçli and G. Cuniberti, Phys. Rev. B 81, 113401 (2010).
- [4] W. Li, H. Sevinçli, G. Cuniberti and S. Roche, submitted.
- [5] D. A. Areshkin, D. Gunlycke, and C. T. White, Nano Lett. 7, 204 (2007).

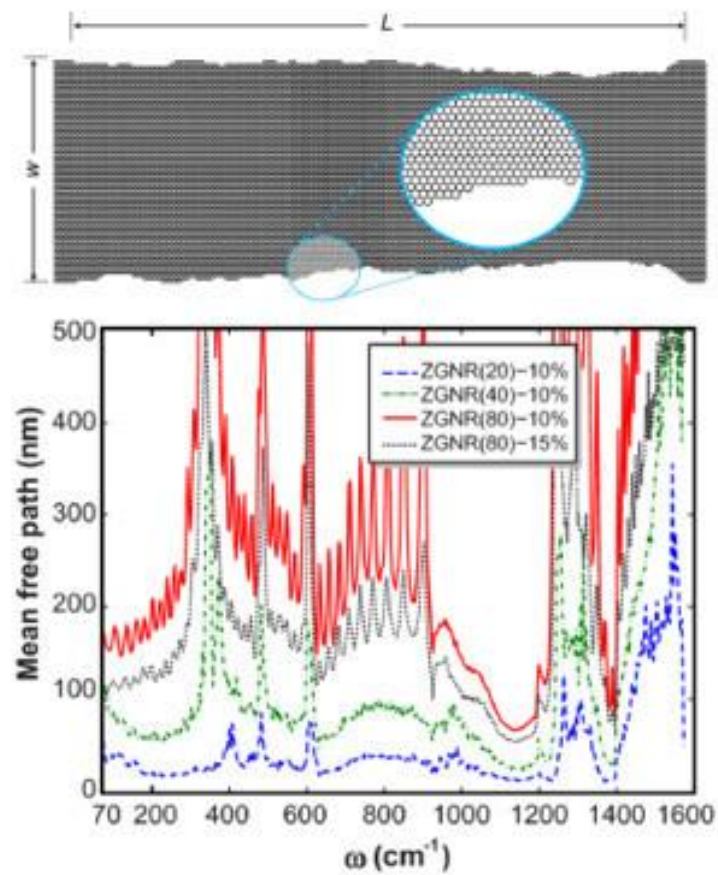


Figure 1. Upper panel: short portion of an edge disordered GNR (width $w=17.04$ nm, length $L\sim 50$ nm and disorder density of 10%). Lower panel: elastic MFP for ZGNR of widths $Nz=20, 40,$ and 80 (4.26, 8.52, and 17.04 nm, respectively) with disorder density of 10%, and also for the $Nz=80$ and 15% disorder for comparison.

A Compact Model for the Magnetic Tunnel Junction Switched by Thermally Assisted Spin Transfer Torque (STT+TAS)

Julien Duval^{1,2}, Weisheng Zhao^{1,2}, Jacques-Olivier Klein^{2,1} and Claude Chappert^{1,2}

¹ IEF, CNRS, UMR8622, Orsay, France-91405

² Univ. Paris-Sud 11, Orsay, France-91405

weisheng.zhao@u-psud.fr

Thanks to its non-volatility, high write/read speed and easy integration with CMOS process, Magnetic Tunnel Junctions (MTJ) has become a cornerstone of spin electronics such as the Magnetic RAM (MRAM) [1] and Magnetic logic [2-3]. The current research in MTJ nanopillar focus on the high performance (power efficient, high speed and high reliability) switching approaches, as the two high currents used in the conventional methods limit the power and die area of MTJ based circuits. Thermally Assisted Switching [4] was proposed to improve the data stability and reduce the power dissipation but it cannot overcome the miniaturization limits (~65nm). Spin Transfer Torque [5] is one of the most potential approaches to overcome these limits, as it requires only one low current for the switching. However, STT brings new problem: the degradation of thermal stability. Recently, a new approach: Thermally Assisted Spin Transfer Torque (STT+TAS) combining the advantages of both two technologies has been proposed [6], which promises low power, high density and high data stability.

The MTJ stack in Fig 1.a is slightly modified to be adapted to the TAS operation: the storage layer is coupled with an anti-ferromagnetic (AF2) layer with low blocking temperature ($T_{b2} \approx -150^\circ$, $T_{b1} \approx -300^\circ$) [7]. Contrary to the STT-MTJ, the storage stability is no longer based on the shape anisotropy but on the exchange bias [8], the shape of the STT+TAS MTJ is thus circular as we can see in Fig 1.b. Therefore, this stability does not depend on the volume of the MTJ which is very interesting in order to improve the scalability of the MTJ. For the writing process, a low current I_{switch} passes through the MTJ and heats the stack. When the MTJ is heated at a temperature above the blocking temperature T_{b2} , the exchange bias effect disappears and the same low current I_{switch} can switch the magnetization of storage layer. By changing the current direction of I_{switch} , shown in Fig.1c and d, the state of MTJ can be switched from P (low resistance, logic '0') to AP (high resistance, logic '1') and from AP to P. After the switching, the temperature of MTJ is reduced below T_{b2} and the exchange bias effect reappears for the storage layer but with new magnetization direction. In order to prevent any switching of the reference layer, the blocking temperature T_{b1} of the AF1 layer should be much higher than T_{b2} . In order to develop the MTJ based memory and logic circuits, a compact model compatible with the standard IC CAD tools is necessary. Based on our previous STT-MTJ model [9], this new compact model integrates the thermal variations activated by the current or voltage pulses, temperature dependence of the MTJ switching threshold and duration [10].

In our model, a RC circuit shown in Fig.2 has been implemented in parallel with the MTJ to present the temperature evaluation. By using a multiplier (M_0) and an adder (A_0), the temperature T can be observed by the V_{temp} voltage. This TAS+STT compact model has been developed in Verilog-A language and implemented on Cadence Virtuoso platform [11]. A number of experimental parameters are integrated in this model to improve the simulation accuracy. To demonstrate the expected behaviors of STT+TAS switching approach transient simulations have been done. Fig.3 shows the simulation results of the heating and switching operations of the compact model. Only one low current I_{switch} is used for the heating and switching of MTJ ($a=b=65\text{nm}$, $\text{TMR}=120\%$). The heating period for the MTJ in P to AP state is about 6.3ns and can be reduced by increasing the switching current value. As the temperature T of MTJ reaches to the blocking temperature T_{b2} , the model will compare the I_{switch} with the critical switching current. In the simulation shown in Fig.3, I_{switch} is superior to the critical current I_{C0} and the switching can be done in about 5ns thanks to the spin dynamic behaviors [12].

We presented the compact model for STT+TAS switching approach based MTJ, which integrates the heating/cooling phenomena and STT dynamic switching behaviours. The model is compatible to the standard CAD tools and can be simulated directly with the CMOS design kit. The simulations and calculation of hybrid MTJ/CMOS circuit based on this model are under investigation in our laboratory.

References

- [1] B. N. Engel et al., IEEE TMAG, Vol. 41, pp. 132--136, 2005.
- [2] J.-P. Wang and X. Yao, Journal. of Nanoelectronics and Optoelectronics, Vol.3, pp.12--23, 2008.
- [3] W.S. Zhao et al., ACM TECS, Vol.9, No.2, article 14, October 2009.
- [4] I. L. Prejbeanu et al., IEEE TMAG, Vol. 40, pp. 2625--2627, 2004.
- [5] J. C. Slonczewski, JMMM, Vol. 159, 1996.
- [6] H. Xi et al., IEEE TMAG, Vol.46, 2010, pp.860-866.
- [7] I.L. Prejbeanu et al., Journal of Physics: CM. Vol. 19, 165218, 2007.
- [8] J.Nogues et al., JMMM . Vol 192, pp.203-232. 1999.
- [9] W.S. Zhao et al., Proc. of IEEE-BMAS, USA, pp.40-43, 2006. L.B. Faber et al., Proc. of DTIS, Tunis, 2009.
- [10] RC.Souca et al. Journal of Applied Physics, 95, pp.6783-6785, 2004.
- [11] Virtuoso Spectre Circuit Simulator User Guide, 2004.
- [12] J.Nogues et al., JMMM . Vol 192, pp.203-232. 1999.

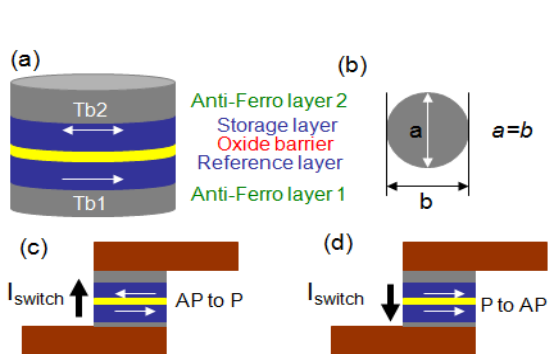


Figure 1. (a) STT+TAS switching approach: MTJ is composed of 5 layers (two anti-ferromagnetic layers, two ferromagnetic layers and one oxide barrier). (b) The shape of STT+TAS MTJ is circular. (c) and (d) The current I_{switch} passing through the STT+TAS MTJ heats it up to the blocking temperature (T_{b2}) and then, the same current changes the magnetization of the storage layer and programs the state of the STT+TAS MTJ.

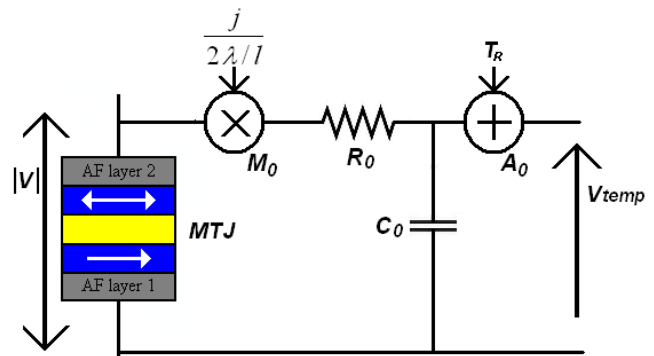


Figure 2. Electrical equivalent circuit to implement the temperature on the model.

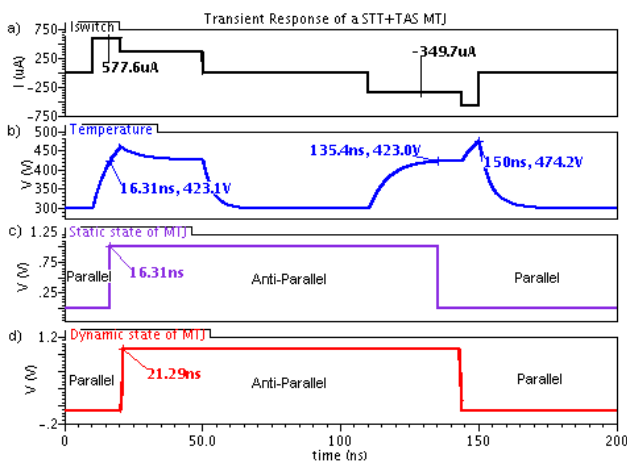


Figure 3. Transient simulation of the STT+TAS MTJ compact model. (a) The heating-switching current (400mv voltage pulse duration: 40ns and period: 100ns), the I_{switch} value is as low as 577.6uA for both heating and switching the MTJ from P to AP state in about 11ns. In order to switch the MTJ from AP to P state, the current direction is negative and the current value is about 349.7uA. (b) The temperature the MTJ increases with the current pulse. The MTJ in P state can be heated more rapidly than the MTJ in AP state thanks to the higher current. (c) The static switching of STT+TAS MTJ, the switch can be done as the temperature of MTJ reaches up to the blocking temperature. (d) The dynamic switching of STT+TAS MTJ, taking into account the spin dynamic behaviors [9].



ORAL CONTRIBUTIONS

(PhD - Parallel Sessions)

Room Temperature Sputtered Ta₂O₅ for Solid State Biosensors

R. Branquinho^{1,2}, J. V. Pinto¹, P. Barquinha¹, L. Pereira¹, P. Estrela³, P. Baptista⁴, R. Martins¹, E. Fortunato¹

¹ CENIMAT, I3N and CEMOP/UNINOVA, Faculdade de Ciência e Tecnologia da Universidade Nova de Lisboa (FCT-UNL), Campus de Caparica, 2829-516 Caparica, Portugal

² INL, International Iberian Nanotechnology Laboratory, Braga, Portugal

³ Department of Electronic and Electrical Engineering University of Bath, BA2 7AY, UK

⁴ CIGMH/Departamento de Ciências da Vida, FCT-UNL, 2829-516 Caparica, Portugal

ritasba@fct.unl.pt

Since the enzyme modified electrode was invented by Clark in 1962 this area of research has been ever growing. Biosensors have application in many areas of interest from agriculture to industrial control, pharmaceutical to health care. Consequently much effort is put into new and improved materials for device optimization and sensitivity enhancement.

Ion sensitive field effect transistors (ISFETs) based biosensors have a fast response and are suitable for miniaturization, since the signal-to-noise ratio is independent of the device area. It is also possible to integrate several ISFET sensors to allow the simultaneous measurement of various parameters by coating each gate dielectric with a specific biological agent.

High-k dielectrics that are used as the gate oxide, such as Ta₂O₅, show sensitivity to pH so the optimization of this sensitive layer is crucial.

An advantageous technique for oxide thin films deposition is radiofrequency (rf) magnetron sputtering because it permits good quality films to be obtained at room temperature and the use of low cost disposable substrates such as plastic and even paper.

We present a study of Ta₂O₅ thin films deposition conditions and their influence on pH sensitivity. The films were produced by varying some deposition parameters, such as argon and oxygen partial pressure ratio and deposition pressure. The influence of post-production treatments such as annealing temperature and plasma surface treatments with argon and oxygen, performed under several conditions, were also studied in order to assess their contribution to pH sensitivity. The films were deposited on p-doped Si/SiO₂ substrates in an electrolyte-insulator-semiconductor (EIS) capacitive structure that was used to evaluate the sensors' response to pH (Fig.1). EIS devices mimic the gate structure of the ISFET and have the advantage of being easier to fabricate. Capacitance measurements were performed in a standard three electrode configuration (Fig.2).

An enzyme modified sensor was successfully constructed by adsorptively immobilizing penicillinase onto the surface of the Ta₂O₅ film that yielded the optimal pH sensitivity. The underlying pH sensor detects the variation in H⁺ concentration resulting from the catalyzed hydrolysis of penicillin G by penicillinase, which is dependent on the penicillin concentration in the solution.

The application of the studied sensitive Ta₂O₅ films to ISFET biosensor structures was also studied and will be discussed.

References

- [1] Turek, M., M. Keusgen, et al., Journal of Contemporary Physics-Armenian Academy of Sciences, 43(2) (2008) 82-85.
- [2] Pan, T. M. and J. C. Lin., Sensors and Actuators B-Chemical, 138(2) (2009) 474-479.
- [3] Yan, F., P. Estrela, et al., Sensors, 5(4-5) (2005) 293-301.

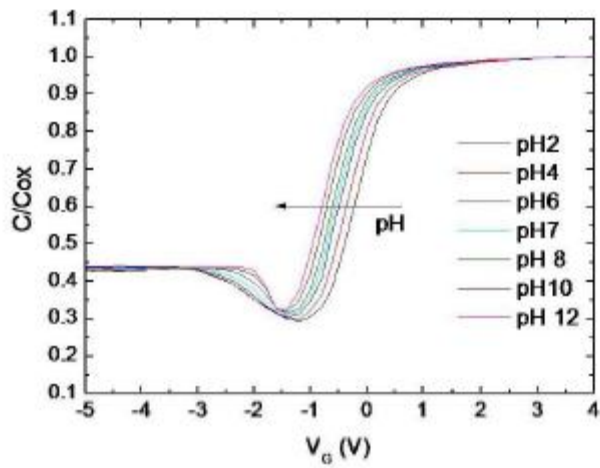


Figure 1. EIS device's capacitance vs voltage characteristics variation due to pH.

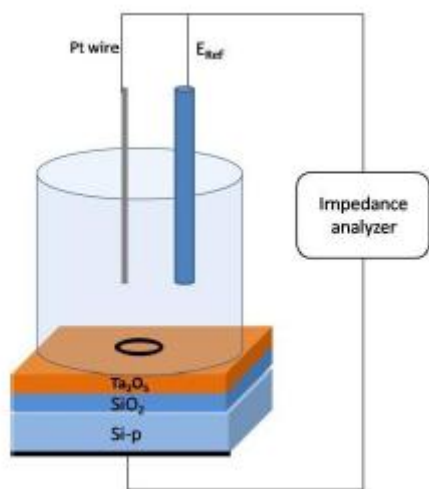


Figure 2. Experimental set-up used for EIS structure capacitance measurements

Modulation of Localized Surface Plasmons and SERS Response in Gold Dumbbells through Silver Coating

M. Fernanda Cardinal^{1,2}, Benito Rodríguez-González¹, Ramón A. Alvarez-Puebla¹, Jorge Pérez-Juste¹, and Luis M. Liz-Marzán^{1*}

¹ Departamento de Química Física, Unidad Asociada Universidade de Vigo-CSIC, Vigo, Spain.

² International Iberian Nanotechnology Laboratory, Braga, Portugal.

mfcardinal@uvigo.es

In this work, we describe the modulation of localized surface plasmons in gold dumbbell-like nanoparticles through step-wise silver coating. We analyse and compare the experimental and calculated optical response of the obtained nanoparticles. Additionally, we discuss on the near-field distributions and their relevance in surface-enhanced Raman scattering (SERS) and demonstrate the improved efficiency of these bimetallic nanoparticles as SERS substrates.

Gold dumbbells were formed through seeded growth of preformed nanorods (average aspect ratio ~ 4), by reduction of HAuCl₄ with ascorbic acid in the presence of hexadecyltrimethylammonium bromide (CTAB), AgNO₃ and small amounts of iodide ions. The selective tip growth leads to a controlled red-shift of the longitudinal surface plasmon resonance of the nanorods.¹ The as-prepared Au dumbbells were coated with silver in an aqueous solution containing CTAB, AgNO₃, NaOH and ascorbic acid.² Opposite to tip growth, deposition of the silver shell caused the longitudinal plasmon band to significantly blue-shift, but additionally a new plasmon band arose and its intensity increased with reaction time and silver salt concentration.

Characterization of the samples performed with transmission (TEM and HRTEM) and scanning transmission electron microscopy (X-ray spectrometer coupled to a STEM) showed that conformal growth is only obtained for rather low silver concentration, whereas for intermediate and high silver salt concentration, the final nanoparticles have rod-like and/or irregular faceted morphologies as a consequence of anisotropic silver growth (Figure 1).

The experimental UV-visible spectra were analyzed and compared with simulations based on the boundary element method (BEM),^{3,4} which allows numerical resolution of Maxwell's equations in frequency space. Since HRTEM images showed well-defined interfaces between the two metals, each metal was described in simulations by tabulated dielectric functions that depend only on the frequency of light applying the local approximation. Calculations of the extinction cross section and near-field maps were carried out for gold dumbbells and Au@Ag core-shell nanoparticles of different morphologies. Additionally, assignment of transverse and longitudinal plasmon modes was achieved by simulating the extinction cross sections for incident light with different polarizations and comparing these data with experimental spectra from measurements on aligned nanorods.

Finally, we carried out average SERS on the dilute colloids using 1-naphthalenethiol (1NAT) as a Raman active probe and compared the efficiency between the bimetallic Au@Ag with those of the starting nanoparticles (AuNRs and AuDBs). The results for the different samples upon excitation with two visible lasers are depicted in Figure 2.

References

- [1] Grzelczak M., Sánchez-Iglesias A., Benito Rodríguez-González, Alvarez-Puebla R., Pérez-Juste J. and Liz-Marzán L.M., *Adv. Funct. Mater.*, 18 (2008) 3780.
- [2] Rodríguez-González, B., Burrows, A., Watanabe, M., Kiely, C. J. and Liz-Marzán, L. M., *J. Mater. Chem.*, 15 (2005) 1755.
- [3] García de Abajo, F. J.; Howie, A. *Phys. Rev. Lett.*, 80 (1998) 5180.
- [4] Myroshnychenko V., Rodríguez-Fernández J., Pastoriza-Santos I., Funston A. M., Novo C., Mulvaney P., Liz-Marzán L.M., García de Abajo F. J., *Chem. Soc. Rev.* 37 (2008) 1792.

Figures

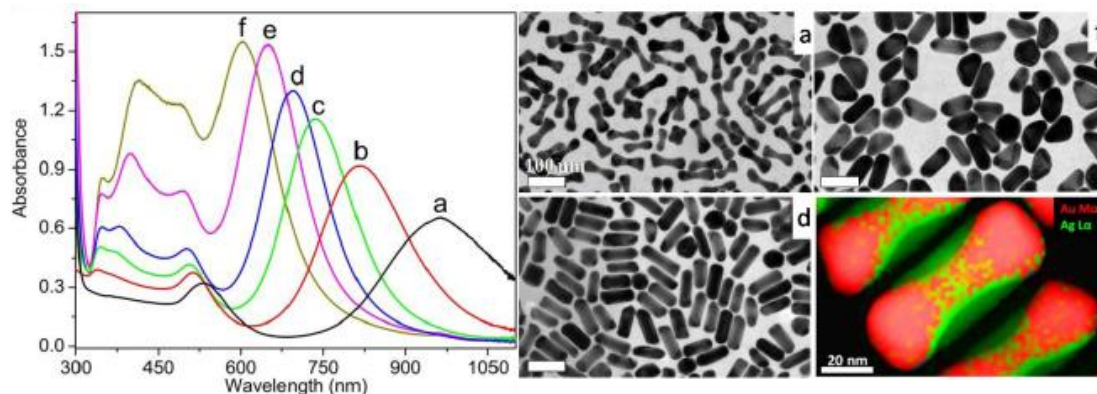


Figure 1. Left: UV-visible spectra of Au dumbbells (a) and bimetallic NPs grown with increasing $[Ag^+]/[Au^0]$ molar ratios from b to f. Right: Representative TEM images corresponding to samples a, d and f (scale bars: 100nm) and STEM-XEDS elemental map of sample d.

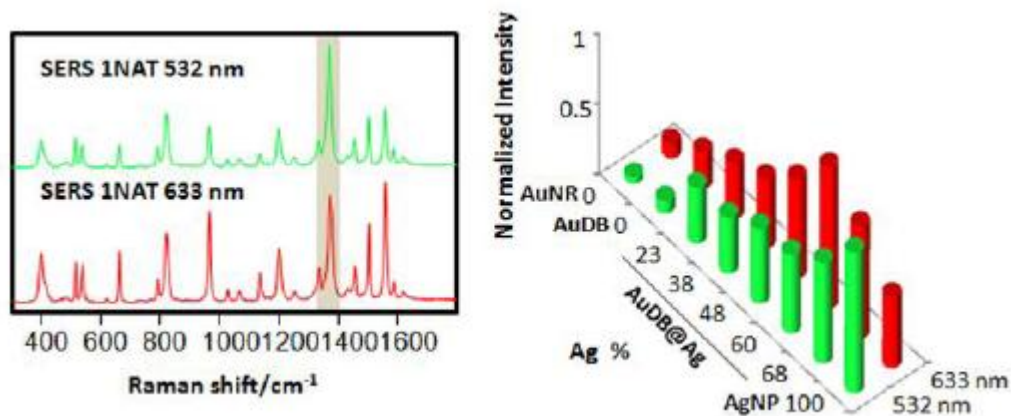


Figure 2. Left: Average SERS spectra of 1NAT on AuDB@Ag, acquired in solution with green and a red laser lines. Right: Intensities of the ring stretching (1368 cm⁻¹) band as a function of silver molar percentage in the particles (AuNR and AuDB: 0%; AuDB@Ag b, c, d, e: 23, 38, 48, 60, 68%, respectively; Ag-citrate: 100%).

Development of core/shell superparamagnetic iron oxide/silica nanorods

Daniel Carmona, Nuria Miguel, Alejandro G. Roca, Francisco Balas and Jesús Santamaría

Instituto de Nanociencia de Aragon, Edificio I+D, Mariano Esquillor 18, 50018 Zaragoza Internacional
Iberian nanotechnology Laboratory, Avda central nº100, Edificio dos Congregados, 4710-229 Braga,
Portugal

Centro de Investigaciones Biomedicas en Red (CIBER BBN), campus Rio Ebro,
c/ Maria de Luna 18, 50018, Zaragoza

[danielcarmona @unizar.es](mailto:danielcarmona@unizar.es)

Aqueous suspensions of iron oxide nanoparticles (MNPs) have been shown to be promising materials for diagnose and treatment of several illnesses[1,2]. Drug delivery carriers, NMR contrast agents and nano heat power sources are typical apical application where MNPs has gained attention due to their magnetic properties or low toxicity. However, one of the best problems of these suspensions is the lack of colloidal stability at physiological pH because magnetic particles tend to agglomerate and coagulate causing thrombus in blood vessels and veins. An accurate surface treatment that involves the hydrolysis and condensation of silica alcoholoxide precursors onto the particle surface provides several advantages over other surface treatments[3]. Silica not only provides an electrostatic repulsion between particles at pH 7 but also chemical stability, low toxicity and a very reactive surface composed by silanol groups for further amine, carboxylic or thiol functionalization. Moreover, silica matrix has shown to present a great potential for their adsorption capacity and integration of other type of particles or fluorescent probes[4]. Final properties of silica-coated iron oxide nanoparticles will depend on the type of aggregate that they form apart from their intrinsic properties.

In this work, we have studied the particle structure that is synthesized between the magnetic iron oxide nanoparticles and silica using magnetite/maghemite particles with different size, aggregation degree and surface nature. The final properties of these particles will be strongly depending on the particle shape and encapsulation degree. Magnetic nanoparticles were synthesized by thermal decomposition of iron acetylacetonate in triethyleneglycol (TREG). Using this strategy, high-quality one-step biocompatible particles could be obtained. TREG acts as solvent, reductor and capping agent providing hydroxyl groups to the surface[5]. Carboxylic moiety was easily incorporated to the particles by adding DMSA (dimercaptosuccinic acid) to the suspension. Naked nanoparticles of maghemite were obtained by classical coprecipitation from iron salts. Silica coating was performed to the three suspensions using well known Stöber method[6] in very dilute concentrations at different hydrolysis times.

Transmission Electron Microscopy studies are used for description of the real structure of silica/iron oxide nanoparticles. When maghemite nanoparticles synthesized by coprecipitation were used for silica coating, spherical silica particles with spherical aggregates of iron oxide nanoparticles inside were formed. Particle size increases from 20 nm to 300 nm when the hydrolysis time goes from 1 to 6 hours. For suspensions that consist on maghemite nanoparticles coated by TREG, unexpected rod shape maghemite aggregates embedded in silica rods of around 700 nm were obtained. When TREG molecules were exchanged by DMSA from the maghemite nanoparticles, individual particles or clusters formed by less than 5 were coated by a thin silica layer that growth with the hydrolysis time leading to spherical particles of 50-200 nm of average size. Aggregate size of the starting suspension, medium ionic strength and pH, hydrolysis time but specially particle surface functional groups seems to be responsible for the final particle structure.

These results indicate that by selection of the synthesis conditions, the morphology of iron oxide/silica nanocomposites can be tailored from nanoparticles to nanorods. Also, the relative positions of silica and iron oxide nanoparticles can be determined at will. This is of particular relevance for the design of drug magnetic carriers or magnetic separation devices because magnetic properties of the material can be tuned by changing particle density and aggregate shape inside the silica particle and adsorption/release capacity can be tuned by changing the silica matrix size and their shape.

References

- [1] Roca, A. G.; et al. *Journal of Physics D: Applied Physics* 2009, 42, 224002.
- [2] Arruebo, M.; Fernández-Pacheco, R.; Ibarra, M. R.; Santamaría, J. *Nanotoday* 2007, 2, 22-32.
- [3] Philipse, A. P.; Nechifor, A. M.; Pathmamanoharan, C. *Langmuir* 1994, 10, 4451.
- [4] Tartaj, P.; Serna, C. J. *Journal of the American Chemical Society* 2003, 125, 15754-15755.
- [5] Wan, J.; W.Cai; Meng, X.; Liu, E. *Chem. Commun.* 2007, 5004-5006.

[6] Stöber, W.; Fink, A.; Bohn, E. Journal of Colloid And Interface Science 1968, 26, 62-69.

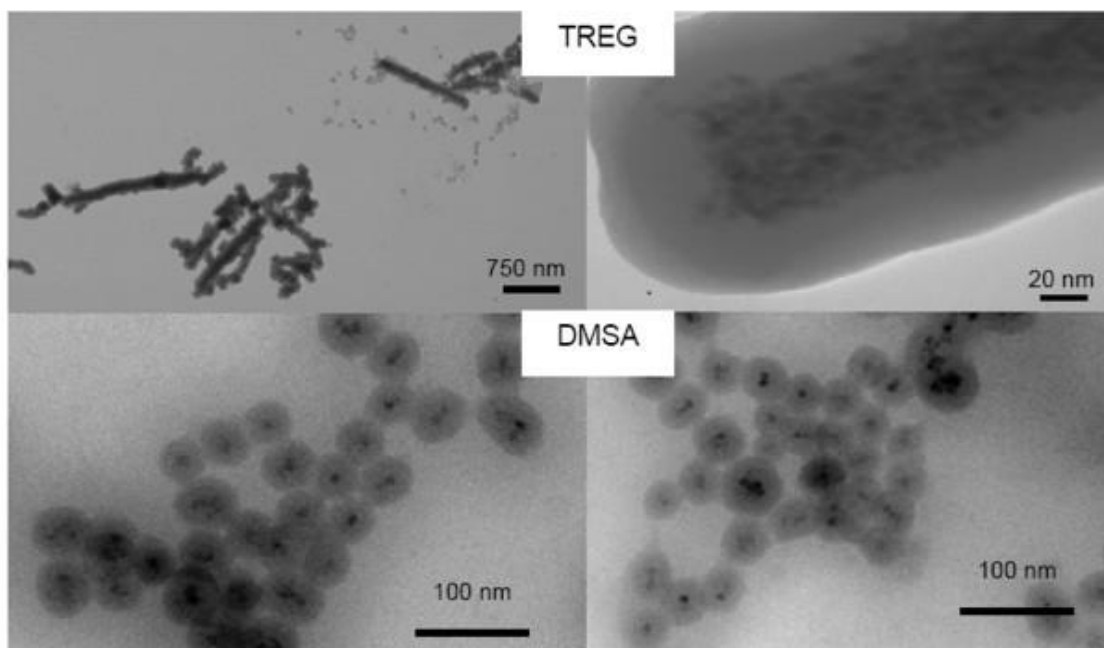


Figure 1. TEM mages of different silica-iron oxide composite nanoparticles obtained using different preparation procedures.

Observation of polarized multiphoton emission from resonant Al, Ag and Au nanoantennas

Marta Castro-Lopez¹, Daan Brinks¹, Riccardo Sapienza¹ and Niek van Hulst^{1,2}

¹ICFO – Institute of Photonic Sciences, Mediterranean Technology Park,
08860 Castelldefels (Barcelona), Spain

²ICREA - Inst. Catalana de Recerca i Estudis Avançats, 08015, Barcelona, Spain

marta.castro@icfo.es

Optical antennas have gained major importance as coupling elements between near and far field in nanoscale photonics. Although nanoantennas are already widely being used, their fabrication and characterization are still challenging and no systematic experimental comparisons between antennas of different metals have been made.

We present an experimental study of optical rod antennas of three different metals: Aluminum, Silver and Gold. We identify the first and third resonance modes by two-photon luminescence (TPL) analysis and their relative shift due to their different plasmon characteristics. Whereas plasmonic studies are usually performed on gold, here we show that Al is a suitable metal for the fabrication of optical antennas due to its strong resonances.

Furthermore, a polarization analysis gives new insights into the nature of optical resonances of nanostructures. We see the TPL signal is unpolarized in the case of gold, while aluminum follows the polarization of the excitation (along the rod). On the other hand, when the polarization of the incident light is orthogonal (perpendicular to the rod) the TPL signal drops to almost zero for the three metals.

We expect that a better understanding of the properties of different metallic antennas will lead to more efficient designs for nanooptical elements and plasmonic structures.

References

- [1] P. Muhlschlegel, H. J. Eisler, O. J. F. Martin, B. Hecht and D. Pohl, *Science*, **308** (2005) 1607-1609.
- [2] J. N. Farahani, D. W. Pohl, H-J. Eisler and B. Hecht, *PRL*, **Vol. 95** (2005) 017402.
- [3] T. H. Taminiau, R. J. Moerland, F. B. Segerink, L. Kuipers and N. F. van Hulst, *Nanoletters*, **Vol. 7 No. 1** (2007) 28-33.
- [4] P. Ghenuche, S. Cherukulappurath, T. H. Taminiau, N. F. van Hulst and R. Quidant, *PRL*, **Vol. 101** (2008) 116805.
- [5] T-D. Onuta, M. Waegele, C. C. DuFort, W. L. Schaich and B. Dregnea, *Nanoletters*, **Vol. 7 No. 3** (2007) 557-564.

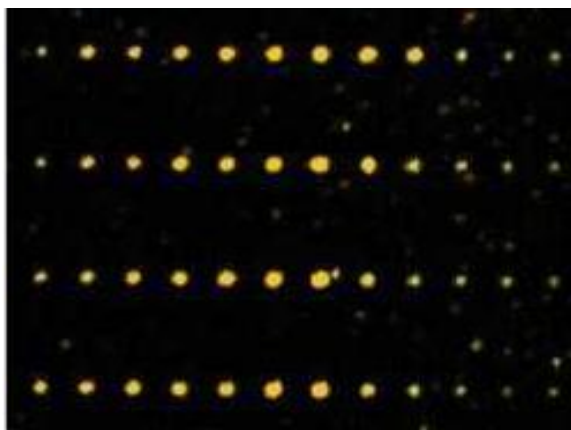


Figure 1. TPL image of four identical rows of gold nanoantennas with lengths between 50 nm (left) and 160 nm (right). The structures exhibit a clear resonance upon excitation with an ultrashort pulse at central wavelength 780 nm.

Bioadhesive mannosamine-loaded nanoparticles for an effective ocular vaccination against animal brucellosis

R. Da Costa Martins¹, C. Gamazo¹, M. Sánchez², I. Peñuelas², J.M. Irache¹

¹ Immunoadjuvant Unit, Department of Pharmaceutics and Pharmaceutical Technology and Department of Microbiology and Parasitology, University of Navarra, Pamplona, Spain

² Radiopharmacy Unit, Department of Nuclear Medicine, Clínica Universitaria de Navarra, University of Navarra, 31008 Pamplona, Spain

rmartins@alumni.unav.es

Introduction: Animal brucellosis is one of the major bacteriological diseases worldwide, and constitutes an important socioeconomic and sanitary problem. The current commercial vaccine used against this zoonosis is the *Brucella melitensis* Rev 1 vaccine, which, due to its live attenuated characteristics, displays a large number of drawbacks. Subcellular vaccines exhibit important advantages to face these handicaps. In this context, the hot saline (HS) subcellular antigenic extract from *B. ovis* has been proved to be highly immunogenic. However, due to its non-replicant nature, adequate adjuvants have to be associated. The need of an adequate adjuvant capable of increasing the mucosal immune response and protection, lead us to suggest the use of poly(anhydride) nanoparticles. To exploit the potential of these systems, nanoparticles were surface decorated with mannosamine, in order to specifically target mannose receptors highly expressed on the immune system cells.

Our purpose was to study the biopharmaceutical properties of HS loaded poly(anhydride) mannosylated (MAN-NP-HS) and conventional (NP-HS) nanoparticles, and evaluate their *in vivo* protective efficacy and biodistribution after ocular immunization.

Methods: Nanoparticles were prepared by the solvent displacement method, freeze-dried and characterized by PCS, ELDA, TEM, SEM, SDS-PAGE, Western-Blot and BCATM assay. The *in vitro* release and the stability in mucosal fluids were also evaluated. For the TLR's activation study, free HS, nanoparticles and adequate controls, were tested in duplicate on recombinant HEK-293 cell lines. An ocular immunization was performed in mice and, during this time, blood, faecal samples and spleens were recovered for IgG1, IgG2a, IgA, IL-2, IL-4, IFN- γ quantification. Eight weeks after vaccination animals were challenged against *B. ovis*, and 3 weeks later were slaughtered for bacteriological examinations. Moreover, 99mtechnetium radiolabelled nanoparticles were ocular administered, and, at 2 and 24 hours, animals were slaughtered for *in vivo* biodistribution examinations.

Results: All freeze-dried formulations displayed a size of around 200-300 nm, with negative surface charge and low polydispersion (PDI<0.2), with a loading of about 30 μ g HS per mg of nanoparticle with high entrapment efficiency (see Table 1). The mannosamine content, for MAN-NP-HS, was 32.1 ± 4.7 μ g/mg nanoparticle. SEM analysis demonstrated the spherical and highly homogeneous nature of the nanoparticles (Figure 1). Figure 2 indicates that the protein profile, structural integrity and antigenicity of the entrapped HS in both nanosystems were maintained after preparation. Concerning to HS release, Figure 3 shows that both NP-HS and MAN-NP-HS showed a biphasic release pattern characterized by a burst effect followed by a continuous release of the antigen for at least 30 days. Furthermore, both systems were also highly stable in the mucosal environment, since after 2 h of incubation in lachrymal fluid, the remaining nanoparticles were of about 80%. The TLR's activation study demonstrated that both nanoparticles and free HS, clearly induced hTLR2, hTLR4 and hTLR5 expressing cell lines (Figure 4).

Interestingly, the elicited specific levels of IgG1, IgG2a, IgA, IL-2, IL-4 and IFN- γ levels showed a correlation with the bacteriological results. The degree of infection, expressed by the log mean \pm SD CFU/spleen, was: i) MAN-NP-HS: 3.7 ± 0.1 ; ii) NP-HS: 4.9 ± 0.4 ; iii) Rev 1: 4.2 ± 0.3 and iv) control unvaccinated animals: 6.7 ± 0.3 (expressed by the log mean \pm SD CFU/spleen, n=6). The *in vivo* biodistribution revealed that 99mTc-MAN-NP-HS were mainly located in the gastrointestinal tract, nasal and ocular mucosa and lymph nodes, probably due to their specific target and strong bioadhesive performance, thus enhancing the antigen delivery to the mucosal associated lymphoid tissue (MALT).

Conclusions: MAN-NP-HS revealed excellent characteristics as antigenic delivery systems throughout the ocular mucosa, by improving mucosal delivery and enhancing immune response. Their effective protection and intrinsic avirulence, make them a suitable anti-*Brucella* vaccine candidate.

Acknowledgments: "Fundação para a Ciência e a Tecnologia" (SFRH/BD/41703/2007) in Portugal, "Fundación Caja Navarra: Nanotecnología y Medicamentos" (nº 10828) and "Departamento de Salud, Gobierno de Navarra" in Spain.

References

[1] Da Costa Martins R, Gamazo C, Irache, JM. Eur J Pharm Sci, 37 (2009) 563–572.

Vaccine formulation	Size (nm)	Zeta potential (mV)	Man content ($\mu\text{g}/\text{mg NP}$)	HS loading ($\mu\text{g}/\text{mg NP}$)
NP-HS	186 \pm 2	-37.7 \pm 0.7	-	33.5 \pm 0.4
MAN-NP-HS	306 \pm 11	-34.6 \pm 1.3	32.1 \pm 4.7	27.9 \pm 0.2

Table 1. Physicochemical characteristics of nanoparticles. NP-HS: HS loaded conventional nanoparticles; MAN-NP-HS: HS loaded mannoseylated nanoparticles (data expressed as mean \pm SD, n=10).

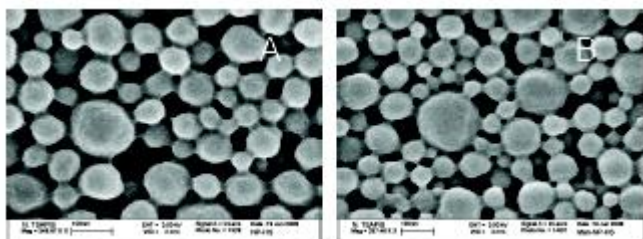


Figure 1. SEM microphotographs of NP-HS (A) and MAN-NP-HS (B).

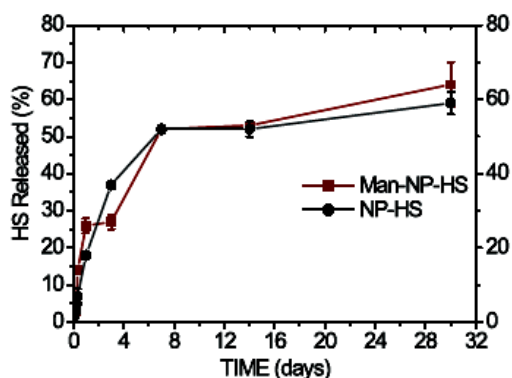


Figure 3. Antigenic release properties from HS containing nanoparticles. These graphs express in percentage the cumulative HS release from the formulations tested (BCATM protein assay): NP-HS (●) and MAN-NP-HS (■). Data express the mean \pm SD, n=3.

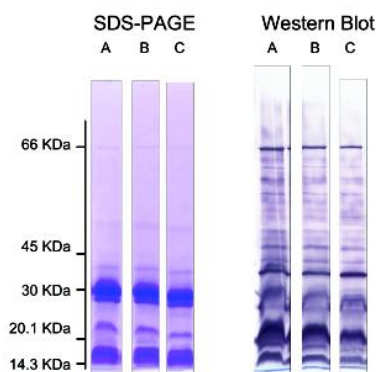


Figure 2. SDS-PAGE and Coomassie blue stain profiles of free and entrapped HS and Western blot against a pool of sera from *B. ovis* experimentally infected rabbits. A: Free HS (40 μg); B: NP-HS; C: MAN-NP-HS.

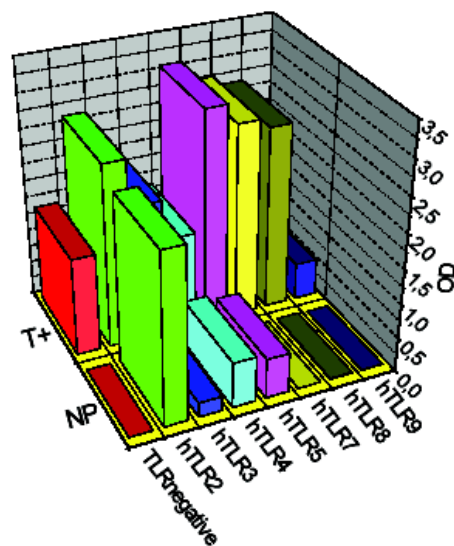


Figure 4. Effects of nanoparticles on the activation of TLR signaling. Bars represent engagement to TLR2, TLR3, TLR4, TLR5, TLR7, TLR8, and TLR9 after incubation with positive controls (T+) and poly(anhydride) nanoparticles (NP). TLR non expressing recombinant cell line also included (TLR-). HEK-293 cells stably co-transfected with TLR and NF- κ B-inducible, and secreted the alkaline phosphatase reporter gene. Results are given in optical density values (O.D.).

Nanodroplet deposition and manipulation with an AFM tip

Laure Fabié, Erik Dujardin, Thierry Ondarçuhu

Nanosciences group, CEMES-CNRS, 29 rue Jeanne Marvig, 31055 Toulouse, France

fabie@cemes.fr

Controlled deposition of individual molecules on a surface is an important challenge in many studies in nanosciences. In this context, a liquid nanodispensing technique (NADIS) was recently conceived to answer the new need of efficient techniques of molecule deposition. Indeed, this direct deposition method enables to pattern substrates on the nanometer scale by combining the resolution of the SPM-based lithographic methods like Dip pen lithography and the flexibility of liquid manipulation.

The principle of this technique consists in using a modified AFM tip to deposit nanodroplets (Figure 1)[1]. For that purpose, a standard hollow tip is drilled by Focused Ion Beam (FIB) to create a narrow channel at its apex (figure2a). The deposit is performed by transferring liquid from a reservoir droplet, containing the particles of interest placed onto the cantilever, to the surface through the channel during an approach-retract of the tip in force spectroscopy mode.

Channel diameters down to 35nm have been obtained enabling to dispense ultra small volumes in the femto- (10^{-15} l) to atto-liter (10^{-18} l) range which can lead to lateral dimensions below 100nm [2]. Such nanodroplets contain, for standard dilutions, only few solute molecules, opening the way to single molecules deposition. Different kinds of particles (nanoparticles, proteins...) have been deposited to create various patterns (dots arrays, lines) on different surfaces proving the flexibility of this method (figure2b and 2c).

On a more fundamental side, this technique is a unique tool to study capillarity and wetting dynamics at the sub-micrometric scale.

The analyze of the capillary forces exerted on the tip during the liquid deposition demonstrated a wide range of behaviors depending on the experimental conditions and provides a real time monitoring of the process. Moreover the simulation of these force curves with the software "Surface evolver"[3] gives a great insight on the dispensing mechanism and the capillarity at the nanoscale[4].

We also showed that the deposition of lines, realized with a nanopositioning table incorporated in an AFM, is an original method to study the dynamics of spreading at sub-micrometric dimensions and millisecond timescale. A model, developed for constant pressure, describes this injection mechanism.

In conclusion, besides its performances as a nanopatterning tools, the NADIS technique is a very efficient to probe nanofluidics phenomena.

References

- [1] A. Meister, M. Liley, J. Brugger, et al., Applied Physics Letters **85** (2004) 6260.
- [2] A. P. Fang, E. Dujardin, and T. Ondarçuhu, Nano Letters, **6** (2006) 2368.
- [3] K. A. Brakke, Experimental Mathematics **1** (1992) 141.
- [4] L. Fabie, H. Durou, and T. Ondarçuhu, Langmuir **26** (2010) 1870.

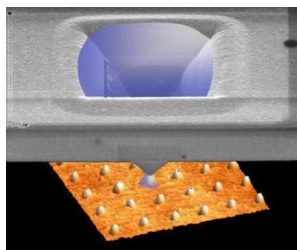


Figure 1: illustration of the deposition method NADIS

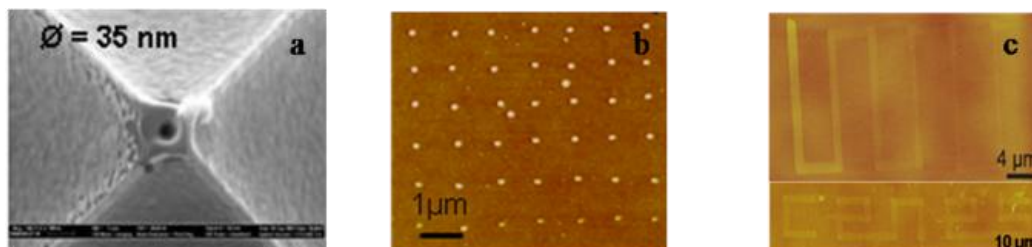


Figure 2. (a) SEM image of a NADIS tip, (b) AFM image of proteins dots array, (c) AFM images of Ruthenium complex lines

Self-assembly of oligothiophenecarboxylic acid monolayer by Scanning Tunneling Microscope (STM)

Chaoying Fu¹, Oleksandr Ivashenko¹, Jennifer M. Macleod^{2#}, Tyler Taerum¹, Dmitrii F. Perepichka¹ and Federico Rosei²

¹Department of Chemistry, McGill University, 801 Sherbrooke Street West, Montréal, QC, Canada H3A 2K6

²INRS-ÉMT, Université du Québec, 1650 Boulevard Lionel-Boulet, Varennes, QC J3X 1S2 Canada

[#]Current address: Dipartimento di Fisica, Università degli Studi di Trieste, Trieste, Italy

chaoying.fu@mail.mcgill.ca

Thiophene-containing molecules and polymers comprise a very important class of electronic materials. Among various candidates, fullerene/polythiophene have shown the best performance in solar cell applications. However, the difficulties arise from significantly uncontrolled morphologies; namely, polydispersity of polythiophenes and uncontrolled agglomeration of fullerenes. In this work, H-bonding has been used to control the self-organization of oligothiophene semiconductors. By means of Scanning Tunneling Microscopy (STM), the study has demonstrated formation of highly ordered 2D networks of the COOH-substituted oligothiophene TTBTA (**Figure 1a**) and TTATA (**Figure 2**) as well as monolayers of oligothiophene and fullerene molecular semiconductors (**Figure 1b**). Thus, the results have revealed details of the molecular-scale phase separation and ordering with potential implications for the design of organic electronic devices, in particular future bulk heterojunction solar cells.

Oligothiophenecarboxylic acid (TTBTA and TTATA) self-assembles at the solution/graphite interface into either a porous network linked by dimeric hydrogen bonding associations of COOH groups (R_2^2 (8)) or a close-packed network linked in a novel hexameric (R_6^6 (24)) or tetrameric (R_4^4 (12)) hydrogen binding motifs. Analysis of high-resolution STM images shows that the pore cavities can efficiently host C60 molecules, which form ordered domains with number of fullerenes per cavity varying from one to four. The observed monodisperse filling and long-range co-alignment of fullerenes is described in terms of a combination of an electrostatic effect and the commensurability between the graphite and molecular network, which leads to differentiation of otherwise identical adsorption sites in the pores.

References

- [1] J.M. MacLeod, O. Ivashenko, C. Fu, T. Taerum, F. Rosei, and D.F. Perepichka, *J. Am. Chem. Soc.* 2009, 131(46), 16844.
- [2] T. Taerum, O. Lukyanova, R. Wylie, D. F. Perepichka, *Org. Lett.* 2009, 11(15), 3230.
- [3] J. L. Brusso, O. Hirst, A. Dadvand, S. Ganesan, F. Cicoira, C. M. Robertson, R. T. Oakley, F. Rosei, D. F. Perepichka, *Chem. Mater.* 2008, 20, 2484.
- [4] D. F. Perepichka, F. Rosei, *Science* 2009, 323, 216.

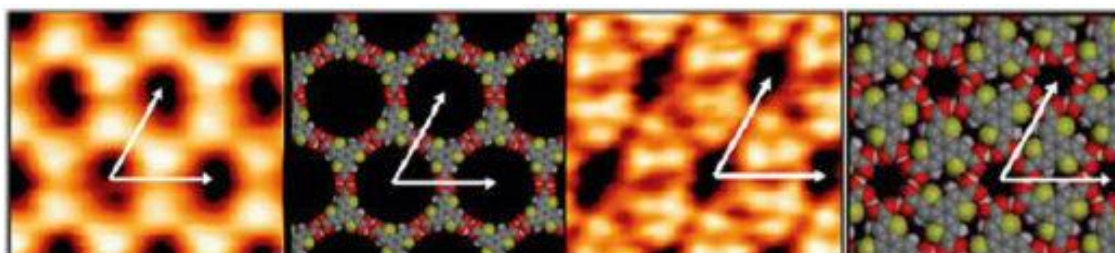


Figure 1a STM image and model of the TTBTA chicken wire and close-packed structures, formed at the HOPG/heptanoic acid interface. Lattice vectors are indicated in white.

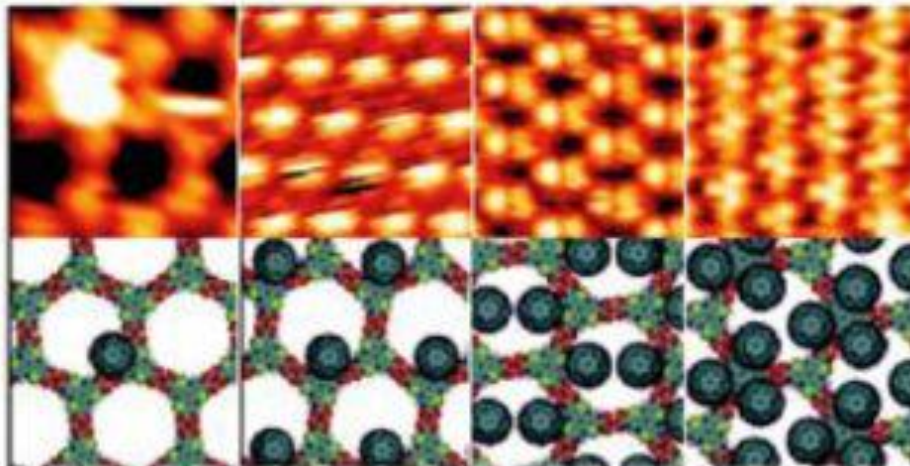


Figure 1b STM image and model of the TTbTA-C60 chicken wire host-guest architectures with sparse fullerene coverage and one, two, and three fullerenes per chicken wire unit cell.

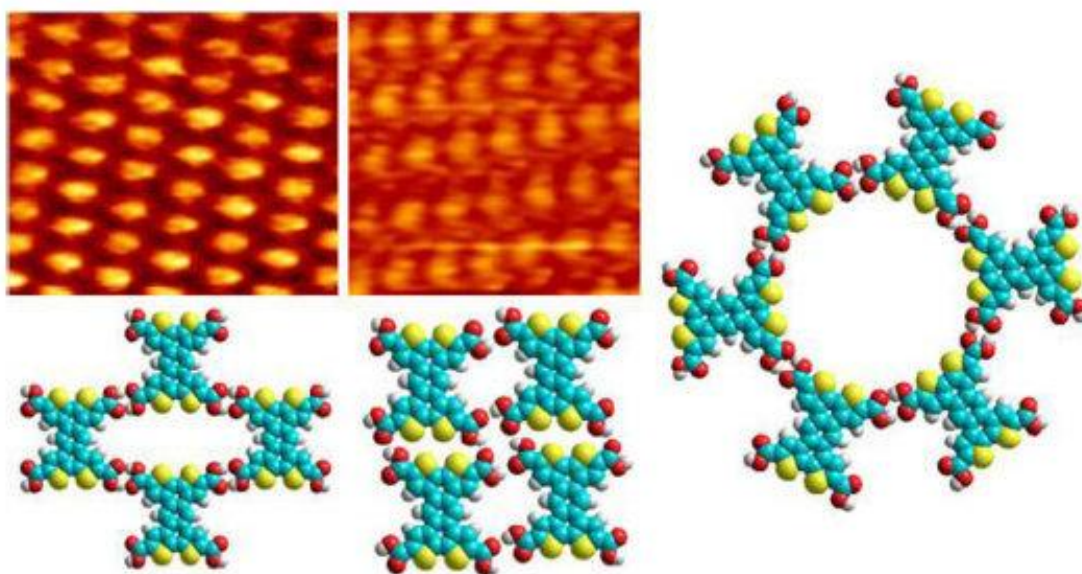


Figure 2 STM image and model of the TTATA rectangular and close-packed structures, formed at the HOPG/Octanoic acid/Trichlorobenzene interface. The last model of Kagome structure is purely theoretically modeled but waiting for experimental observation in near future.

Tunneling-current-induced light emission from PTCDI-C7 thin films on the graphite and the Au(111) surfaces

A. Fujiki¹, Y. Miyake¹, M. Kasaya-Akai¹, A. Saito^{1,2}, and Y. Kuwahara¹

¹ Department of Precision Science and Technology, Graduate School of Engineering, Osaka University, 2-1 Yamada-oka, Suita, Osaka 565-0871, Japan

² PRESTO, Japan Science and Technology Agency (JST), 4-1-8 Honcho, Kawaguchi, Saitama 332-0012, Japan

fujiki@ss.prec.eng.osaka-u.ac.jp

We have investigated the emission properties of N,N'-diheptyl-3,4,9,10-erylenebiscarboximide (PTCDI-C7) thin films on the highly oriented pyrolytic graphite (HOPG) and the Au(111) surfaces using tunneling electrons from a scanning tunneling microscope (STM). The STM-induced light emission (STM-LE) analysis is a useful tool for characterizing the optical and electrical properties of nanoscale materials such as not only metal and semiconductor nanostructures but also organic single molecules. It involves, however, analytical difficulties of extremely weak signal. The combination of STM-LE analysis and plasmon enhancement effects is quite promising for overcoming the difficulties. Surface plasmons in the interface between a metallic and a dielectric medium generate an intense electromagnetic field on the metal surface, which provides an efficient enhancement field for some optical processes, such as fluorescence/phosphorescence emission and optical absorption of organic molecules on the metal surface. Indeed, we have first observed metal enhanced fluorescence of Cu phthalocyanine with the assistance of enhancement effect utilizing tip-induced plasmon (TIP) [1]. Liu et al. [2] reported that they observed molecular fluorescence from porphyrin thin films on the Au and Ag substrates but not on the HOPG and indium tin oxide substrates. In this work, we prepared PTCDI-C7 films on conducting

substrates using a simple spin-casting method, and studied by STM-LE in air and at room temperature. To examine effects of surface plasmons on the substrates, we employed HOPG and Au(111) as the substrates. We observed molecular fluorescence from PTCDI-C7 on Au(111) in company with plasmon-mediated light emission from the Au substrate. We also observed a significant intensity of fluorescence from PTCDI-C7 on the HOPG substrate in contrast to the previous reports.

The HOPG and the Au(111) substrates show different surface plasmon modes, therefore, plasmon-mediated fluorescence resulting from the TIP excitation could be observed only on the Au(111) in our previous studies[1,3]. We prepared the Au(111) substrate by an evaporation of Au onto a cleaved mica substrate heated at 300 degrees centigrade to produce atomically flat terraces of Au(111). The PTCDI-C7 (Fig.1) thin films on HOPG and on Au(111) were prepared by spin-casting method with 2 mg/5 ml solution of PTCDI-C7 in 1-tetradecene at a spin velocity 1000 rpm under ambient condition. The STM-LE measurements were performed in air and at room temperature by using a commercial STM (Nanoscope IIIa of Digital Instrument). Mechanically sharpened Pt/Ir tip was used as an STM tip in all measurements. A schematic drawing of whole STM-LE system is shown in Fig. 2. By using this system we obtained a photon integration mapping (photon counting signals synchronized with every pixel of an STM topographic image) with a photon counting detector and emission spectra with a CCD spectrometer.

The light emission was observed from PTCDI-C7 thin films both on HOPG and Au(111). The reason which we could observe the molecular fluorescence on HOPG substrate in contrast to the previous reports[1,2] is seemed to a large quantum yield of fluorescence emission of PTCDI-C7 and/or crystal characteristics less subject to quenching effect from the substrate than those of phthalocyanine and porphyrin cases. Figure 3 shows (a) an STM topographic image, (b) a photon integration map and (c) optical spectra at four bias voltages from 1.0 to 2.2 V obtained from PTCDI-C7 thin films on the HOPG substrate. A photon mapping image (Fig. 3(b)) showed that the homogeneous emission was obtained from whole

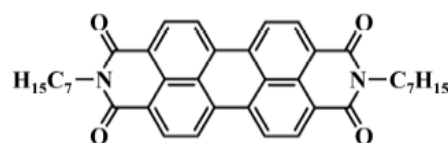


Figure 1. Molecular structure of PTCDI-C7.

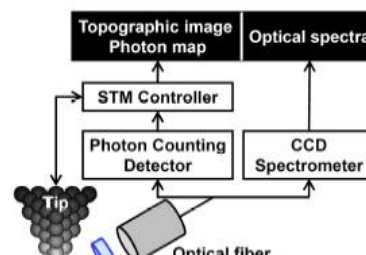


Figure 2. Schematic diagram of the photon detection system equipped with an STM working in ambient condition.

scan area. Note that the STM tip contacted with the thin films under our current condition, that is, the tunneling electrons pass through the thin film to the substrate. In the emission spectra (Fig. 3(c)), one can see peaks at ~ 660 nm, ~ 750 nm and ~ 890 nm. As no emission was observed from a bare HOPG surface and the peak positions didn't shift by changing the bias voltages, these peaks were originated from PTCDI-C7. Compared with the absorption spectra, these peaks are attributed to the fluorescence from PTCDI-C7 with its vibronic progression with large Stokes shift [4]. Figure 4 shows the results of STM-LE obtained from PTCDI-C7 thin films on the Au(111) substrate. A photon mapping image was similar to that on the HOPG substrate. In the emission spectra (Fig.4 (c)), three kinds of emission peaks at ~ 750 nm, ~ 880 nm and ~ 960 nm were observed and the peak intensity of PTCDI-C7 films on Au(111) was ~ 5 fold larger than that on HOPG. This is due to the plasmon enhancement effect in which molecular emission originated from PTCDI-C7 could be observed in company with plasmon-mediated light emission on the Au substrate. Peak-positions on the Au(111) substrate seemed to coincide with those on the HOPG substrate, where the peaks at ~ 750 nm, ~ 880 nm and ~ 960 nm were effectively enhanced by the TIP, on the other hand, the peak at ~ 660 nm observed on HOPG was not well resonated with TIP.

In conclusion, we investigated the STM-LE of PTCDI-C7 thin films on HOPG and Au(111). Both STM-LE of the fluorescence with its vibronic progression from PTCDI-C7 on the HOPG and on the Au(111) substrate including large Stokes shifts. It was interesting that we could observe a significant intensity of fluorescence on the HOPG substrate. Obtained results indicated that the light emission from PTCDI-C7 in this case was due not to the isolated molecular condition but to the thin-film structure although the highly localized TIP enabled STM-LE analysis to evaluate a single molecular level interaction, which was in contrast to our previous study [1].

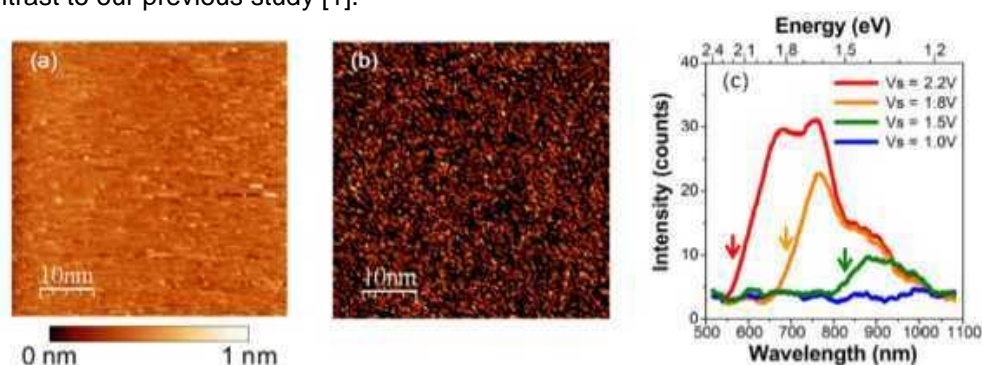


Figure 3. (a) Topographic image, (b) photon map, and (c) emission spectra of PTCDI-C7 thin film on HOPG. Tunneling current, 20 nA; bias voltage, 2.2 V in (a) and (b), and at 1.0 V \sim 2.2 V for 15 min in (c).

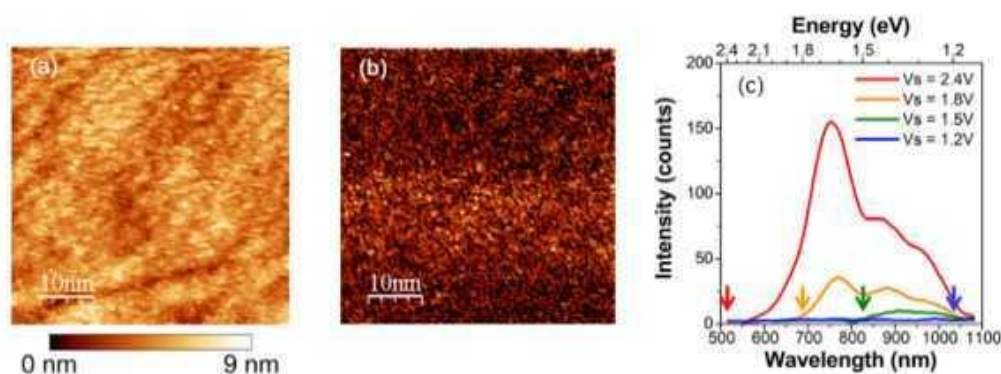


Figure 4. (a) Topographic image, (b) photon map and (c) emission spectra of PTCDI-C7 thin film on Au(111). Tunneling current, 20 nA; bias voltage, 2.2 V in (a) and (b), and at 1.2 V \sim 2.4 V for 15 min in (c).

References

- [1] T. Uemura, M. Furumoto, T. Nakano, M. Akai-Kasaya, M. Aono, A. Saito and Y. Kuwahara, Chem. Phys. Lett. 448 (2007) 232.
- [2] H.W. Liu, Y. Ie, T. Yoshinobu, Y. Aso, H. Iwasaki, R. Nishitani, Appl. Phys. Lett. 88 (2006) 061901.
- [3] T. Uemura, M. Furumoto, T. Nakano, M. Akai-Kasaya, M. Aono, A. Saito and Y. Kuwahara, e-Journal of Surf. Sci. and Nanotech. 4 (2006) 559.
- [4] P. Schouwink, A. H. Schaefer, c. Seidel, and H. Fuchs, Thin solid films 372 (2000) 163.

**Non-volatile memory using Optically-Gated Carbon Nanotube FET:
Description of carrier mobility model in P3OT and hopping mechanism at SiO₂-P3OT interface**

Si-Yu Liao, Cristell Maneux, Sebastien Fregonese, and Thomas Zimmer

Laboratoire IMS, CNRS-UMR 5218, Université Bordeaux 1, 351 Crs de la Libération, TALENCE, France

siyu.liao@ims-bordeaux.fr

The operation of Optically-Gated CNT field effect transistor (OG-CNTFET) has been demonstrated by using photo-generated electrons density to modulate the channel potential as well as the electric gate [1]. This device (Fig. 1) which presents non-volatile memory property is particularly interesting for neuromorphic network design to build the learning circuit [2]. To answer the requirement of CAD simulation, a compact model is developed to describe the OG-CNTFET operation using a physical and behavioral mixed approach [3]. Recently, Schottky metal-CNT contacts have then been taken into account in this model because of the importance of the remarkable barrier height at source and drain contacts [4]. In this paper, the physical meaning of the model is further enhanced. Since the relaxation recombination mechanism of the photo-charged OG-CNTFET is modeled by the P3OT conductivity expression while in [3, 4], it was modeled through an empirical current source. By developing the P3OT conductivity expression, we provide a detailed physical based model of the OG-CNTFET which more accurately describes the carrier relaxation mechanism.

Photo-generated electrons are held in deep traps at the SiO₂-P3OT interface when the electric gate bias is null. We assume that the relaxation of OG-CNTFET is associated with the electron hopping mechanism from deep traps to the CNT channel. To model the relaxation, we calculate the intrinsic conductance between interface traps and the channel. Two general methods have been reported to describe the carrier mobility of P3OT and P3HT which are widely used in solar cells: Pool-Frenkel model (PF) and Gaussian disorder model (GDM) [5]. We integrate PF mobility (μ_{P3OT}) into the expression of P3OT conductivity (σ_{P3OT}) thanks to the good fitting in the low electric field range [5] corresponding to the non-volatile memory operation condition.

$$\mu_{P3OT} \approx \mu_0 \exp\left(-\frac{E_0}{kT} \cdot \frac{T_R - T}{T_R}\right) \Rightarrow \sigma_{P3OT} \approx N_{trap} e \mu_0 \exp\left(-\frac{E_0}{kT} \cdot \frac{T_R - T}{T_R}\right)$$

The expression of mobility is simplified from ref [5]. The field dependence in the exponential is negligible because the channel potential supposes to be uniform to present a ballistic transport in our compact model. Therefore, in the P3OT layer, the electric field doesn't take place as well as in the CNT channel. E_0 is the activation energy of interface traps without electric field. T_R is the empirical reference temperature for associated known P3OT mobility. N_{trap} represents the density of occupied traps. We use optimized values from ref. 5: E_0 is equal to 0.165 eV; T_R is equal to 700 K; μ_0 is equal to $2.7 \times 10^{-3} \text{ cm}^2/(\text{V}\cdot\text{s})$.

The recombination of trapped electron supposes that a tiny part of trapped electrons can be released thanks to hopping mechanism at the SiO₂-P3OT interface and finally evacuates through the nanotube [4]. We simplify this mechanism by a relaxation probability Rate_{relax} , which depends only on the temperature. Hence, the relaxation current results from the product of the voltage bias $V_{Laseri,CNT}$ times P3OT conductor Y_{P3OT} times Rate_{relax} .

$$I_{relax} = V_{Laseri,CNT} \cdot Y_{P3OT} \cdot \text{Rate}_{relax} = V_{Laseri,CNT} \cdot \sigma_{P3OT} \frac{area}{length} \cdot \text{Rate}_{relax}$$

$$\text{with } N_{trap} \cdot e = Q_{trap} = V_{Laseri,CNT} C_{Optic1}$$

$$\Rightarrow I_{relax} = V_{Laseri,CNT}^2 C_{Optic1} \cdot \mu_0 \exp\left(-\frac{E_0}{kT} \cdot \frac{T_R - T}{T_R}\right) \frac{L_G d_{CNT}}{w_{eff}} \cdot \text{Rate}_{relax}$$

C_{Optic1} represents the trap capacitance [3]; L_G , d_{CNT} , and w_{eff} are device geometries [4].

In fig. 2, we compare chronograms of simulation results to experimental measurements of OG-CNTFET non-volatile memory operation [2]. The programming [3] and the gate-protected [4] programming mechanisms have been reported. The two chronograms in the first line present V_{DS} memory programming commands. The programming voltage is 4 V in the simulation, 5.5 V in measurements. The memory reading voltage is -0.4 V in both case. In the middle line, V_{DS} programs successively the photo-charged OG-CNTFET from the high to low conductivity state without the gate protection ($V_G=0V$).

In the third line, the V_{DS} programming is stopped by a gate positive pulse of 6 V, and the devices keep their high conductivity state. Here, we focus on the states from a programming pulse to another: the drain current levels I_D are almost unchanged; i.e. they keep the last programmed state. In simulated chronograms, the slight decrease of I_D represents the SiO_2 -P3OT interface traps relaxation. The simulated device behavior is very close to the experience, but the I_{on} - I_{off} level is remarkable different. Because the measurements were achieved on a nanotube network-based OG-CNTFET [2], the I_{on} - I_{off} ratio was lower than the device with the single CNT channel [1].

References

- [1] J. Borghetti, V. Derycke, S. Lenfant, P. Chenevier, A. Filoramo, M. Goffman, D. Vuillaume, J.-P. Bourgoin, *Adv. Mat.*, **18** (2006) 2535-2540.
- [2] W.-S. Zhao, G. Agnus, V. Derycke, A. Filoramo, J.-P. Bourgoin, and C. Gamrat, *Nanotechnology*, **21** (2010) 175202.
- [3] S.-Y. Liao, C. Maneux, V. Pouget, S. Fregonese, and T. Zimmer, *Phys. Stat. Sol.*, (2010) in press.
- [4] S.-Y. Liao, M. Najari, C. Maneux, S. Fregonese, T. Zimmer, H. Mnif, and N. Masmoudi, *IEEE DTIS* 2010, (2010).
- [5] V. Kazukauskas, M. Pranaitis, V. Cyras, L. Sicot, and F. Kajzar, *Eur. Phys. J. Appl. Phys.*, **37** (2007) 247-251.

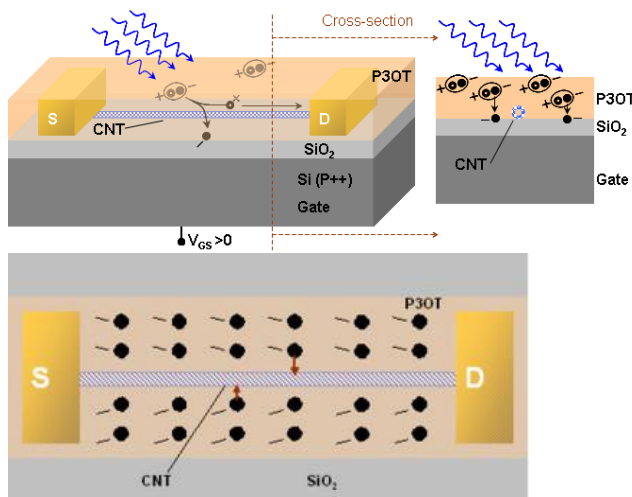


Figure 1. OG-CNTFET description: **Left**, the OG-CNTFET structure scheme with the optical gating mechanism; **Right**, the device relaxation resulted by the electron hopping mechanism.

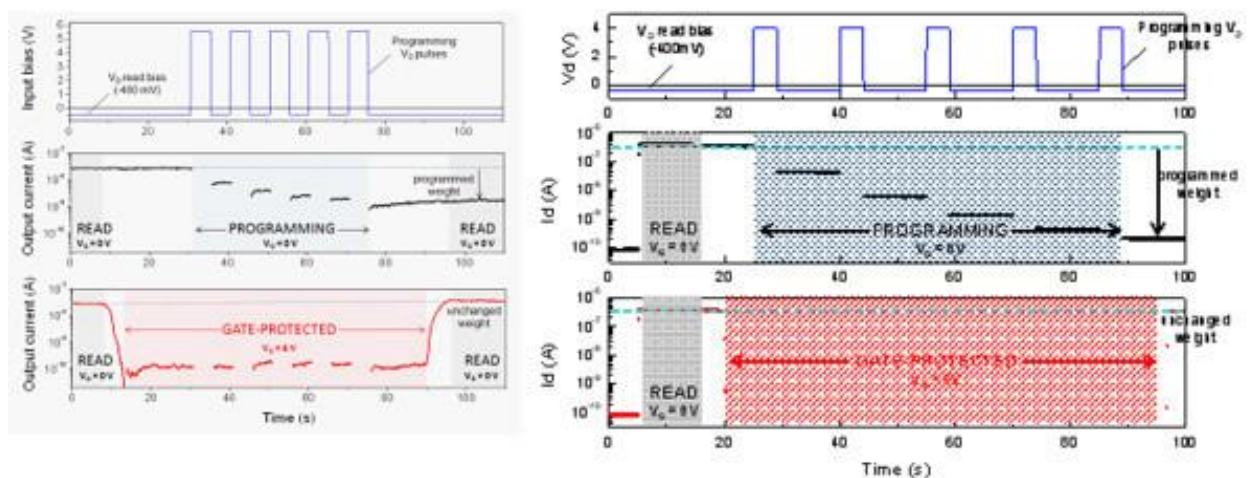


Figure 2. OG-CNTFET operation: Chronograms of the non-volatile memory programming. **Left**, the experimental measurement data with and without gate protection [5]; **Right**, the associated simulation results. The programmed weight in the simulation is greater than the one in the experience since the programming in the simulation is more efficient.

Development of nanostructured 3D matrices to direct mesenchymal stem cells behaviour

F.R. Maia^{1,2,3}, K. Fonseca^{1,3}, P.L. Granja^{1,3}, C.C. Barrias¹

¹ INEB – Instituto de Engenharia Biomédica, Divisão de Biomateriais, R. Campo Alegre 823, 4150-180 Porto, Portugal.

² INL – International Iberian Nanotechnology Laboratory, Avda Central 100, 4710-229 Braga, Portugal.

³ Universidade do Porto, Faculdade de Engenharia, Departamento de Engenharia Metalúrgica e de Materiais. Rua Dr. Roberto Frias, 4200-465 Porto, Portugal.

raqmaia@ineb.up.pt

Introduction

New strategies for bone regeneration therapies evoke the development of improved biomaterials that reproduce key functions of the natural extracellular matrix (ECM), which serves both as a structural support for cells and as a dynamic biochemical network that directs cellular activities.

In this study, chemical functionalization of alginate hydrogels with an osteogenic signaling peptide was investigated. The selected peptide is based in the C-terminal sequence of OGP (Osteogenic Growth Peptide), known to increase bone mass and fracture healing in vivo, and to regulate cell proliferation and osteogenic differentiation in vitro [1]. Generally designated by OGP₁₀₋₁₄ (Tyr-Gly-Phe-Gly-Gly), this five amino-acid sequence retains full bioactivity, being responsible for binding to the OGP receptor [1]. OGP-alginate was further combined with alginate modified with a cell-adhesion peptide (RGD-alginate), previously shown to enhance the viability and osteogenic differentiation of cells in the entrapped state [2] and with alginate modified with a protease-sensitive peptide (PVGLIG-alginate) to allow cells to partially remodel the hydrogel and spread within the matrix. Alginate hydrogels containing the three peptides were used as a 3D matrix for culturing human mesenchymal stem cells (hMSC), and the effect of these multifunctional microenvironments in cell behaviour, namely on osteogenic differentiation was investigated.

Materials and Methods

Alginate (Protanal LF 20/40, FMC Biopolymers) was bulk-functionalized with the peptide sequence GGGYGFGG (OGP₁₀₋₁₄ with a poly-glycine spacer, GenScript) using standard aqueous carbodiimide chemistry [2]. Different amounts of peptide (10, 50 and 100 mg) per gram of alginate were used. The amount of coupled peptides was analyzed by UV spectroscopy and by using the bicinchoninic acid (BCA) assay. 3D cultures of hMSC within multifunctional alginate hydrogels were established by combining cells with gel precursor solutions prior to polymerization.

Cells inside the discs were cultured under basal and osteogenic induction conditions for up to 16 days. Osteogenic differentiation was analyzed by assaying alkaline phosphatase activity (ALP) using a cytochemical staining in situ.

Results and Discussion

UV spectroscopy and the BCA acid assay showed that the osteogenic peptide sequence was effectively grafted to alginate, and that the coupled amount increased with the amount of peptide initially available for reaction. The reaction yields varied from 84±3% (10 mg/g alginate) to 46±4% (100 mg/g alginate) (Figure 1). hMSC were cultured within RGD-alginate, PVGLIG/RGD-alginate and OGP/PVGLIG/RGD-alginate discs. Cells entrapped within alginate discs were only able to remodel the hydrogel matrix and spread when PVGLIG-alginate was used in combination with RGD-alginate.

The osteogenic differentiation of 3D cultured hMSC was analysed through ALP activity along the time of culture in cells entrapped in RGD-alginate, PVGLIG/RGD-alginate and OGP/PVGLIG/RGD-alginate discs, under basal and osteogenic induction conditions. In figure 2 is possible to observe that ALP activity increase along the time, especially under osteogenic induction conditions and in the presence of OGP₁₀₋₁₄. Moreover, under the same conditions, the degradation of the hydrogels was accelerated;

References

- [1] Chen Y-C et al. J Peptide Res 2000;56:147-156;
 [2] Evangelista MB et al. Biomaterials 2007;28:3644-3655;

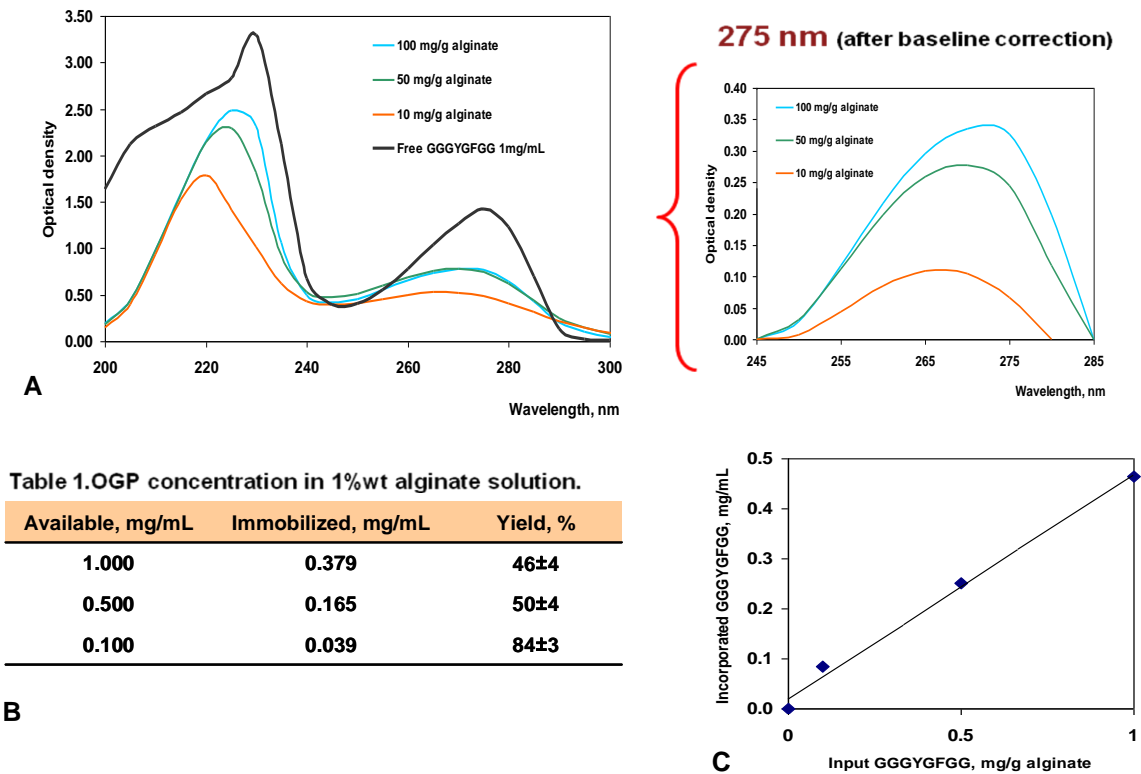


Figure 1. (A) The presence of peaks around 230/275 nm was observed, which indicates that the peptide was effectively grafted to the polymer backbone. (B) Table 1. lists the amount of immobilized OGP10-14 obtained using different initial amounts of peptide and the respective reaction yields. (C) A linear relationship between the amount of immobilized peptide and that initially available for reaction was obtained.

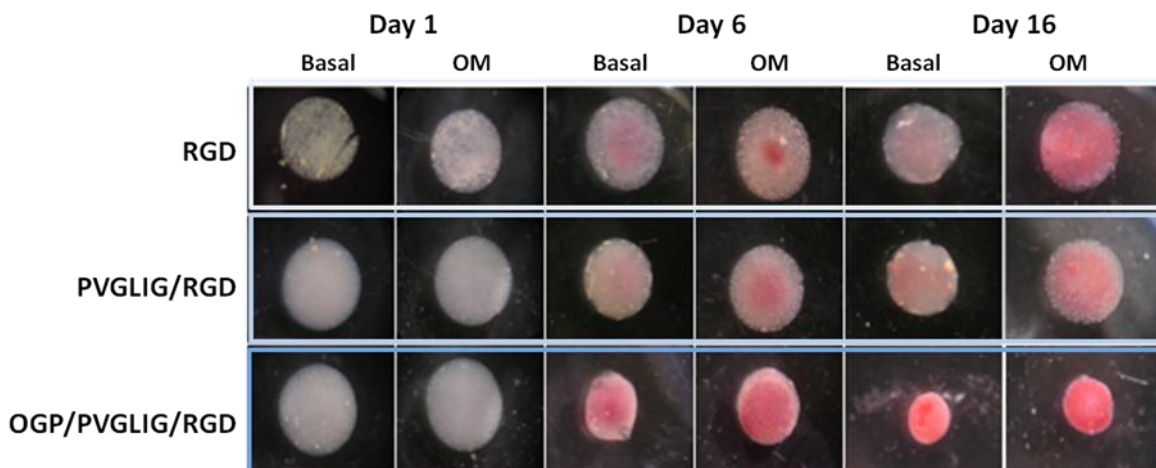


Figure 2. Expression of ALP activity along the time in cells entrapped in RGD-alginate, PVGLIG/RGD-alginate and OGP/PVGLIG/RGD-alginate discs, under basal and osteogenic induction conditions. ALP activity increase along the time, especially under osteogenic induction conditions, and in the presence of OGP₁₀₋₁₄. Moreover, in the presence of OGP₁₀₋₁₄ the degradation of the hydrogels was faster (original magnification 25x).

Wavelength dependence of the SPP wavevector magnetic modulation in Au/Co/Au films

D. Martín-Becerra^{‡,1}, J. B. González-Díaz¹, V. V. Temnov², A. Cebollada¹, G. Armelles¹, T. Thomay³, A. Leitenstorfer³, R. Bratschitsch³, A. García-Martín¹, M. U. González¹

¹IMM-Instituto de Microelectrónica de Madrid (CNM-CSIC), Isaac Newton 8, PTM, E-28760 Tres Cantos, Madrid, Spain.

²Department of Chemistry, Massachusetts Institute of Technology, Cambridge (MA), USA

³Department of Physics and Center for Applied Photonics, University of Konstanz, Germany

[‡]diana.martin@imm.cnm.csic.es

Surface plasmons polaritons (SPP) are evanescent waves that propagate along a dielectric-metal interface. They can be confined in subwavelength metal structures, i.e. below the diffraction limit, which leads to many possible applications, including miniaturized optical devices. Within that context, the development of active plasmonics is important to achieve nanophotonic devices with advanced functionalities. This requires a system where the plasmon properties can be manipulated using an external agent. Among the different control agents considered so far, the magnetic field seems a promising candidate, since it is able to modify the dispersion relation of SPP [1] at reasonable magnetic field strengths, and with a high switching speed. This modulation comes from the non-diagonal elements of the dielectric tensor, ϵ_{ij} , appearing when the magnetic field is turned on. For noble metals, the ones typically used in plasmonics, these elements are proportional to the applied magnetic field but, unfortunately, very small at field values reasonable for developing applications. On the other hand, ferromagnetic metals have sizeable ϵ_{ij} values at small magnetic fields (proportional to their magnetization), but are optically too absorbent. A smart system to develop magnetic field tunable plasmonic devices is the use of multilayers of noble and ferromagnetic metals [2, 3].

That is the framework of the present work, where we analyze the magnetic field induced SPP wavevector modulation (Δk) in Au/Co/Au films as a function of the wavelength and the position of the Co layer inside the trilayer.

The experimental analysis of the SPP wavevector modulation has been performed via surface plasmon interferometry with tilted slit-groove microinterferometers [4]. A sketch of a magneto-plasmonic interferometer is shown in Fig. 1. Illumination with a p-polarized laser beam at normal incidence results in the excitation of SPPs at the groove that propagate towards the slit, where they are reconverted back into free-space radiation (I_{SP}) and interfere with light directly transmitted through the slit (I_r). The total intensity collected from the slit is:

$$I_{DC} = I_r + I_{SP} e^{-2k_{SP}^i d} + 2\sqrt{I_{SP}} e^{-k_{SP}^i d} \sqrt{I_r} \cdot \cos(k_{SP}^r \cdot d + \varphi_0),$$

where k_{SP}^r and k_{SP}^i are the real and imaginary part of the SPP wavevector respectively, φ_0 is an arbitrary phase and d is the groove-slit distance.

When the light intensity transmitted through the slit is recorded by scanning a photodiode along the slit axis (see optical interferogram in Fig. 2), a series of maxima and minima appears as a consequence of the different slit-groove distance for each slit position. To detect the magnetic modulation, we apply an external periodic magnetic field high enough to saturate the sample (about 20 mT) in the direction parallel to the slit axis. This generates a variation in the SPP wavevector, therefore shifting the interference pattern. Then, at each point of the slit, we measure the variation of intensity associated with this pattern shift, I_{MP} , with a lock-in amplifier. This constitutes the magnetoplasmonic interferogram, also shown in Fig. 2. Actually, when applying the magnetic field, both the real and the imaginary part of the SPP wavevector k_{SP} are modified and the I_{MP} signal can be expressed, up to a first order approximation, as:

$$I_{MP} = I(M) - I(-M) \approx (-2 \cdot \Delta k_{SP}^r \cdot d) \sqrt{I_{SP}} e^{-k_{SP}^i d} \sqrt{I_r} \cdot \sin(k_{SP}^r \cdot d + \varphi_0 + \Phi), \text{ with } \tan \Phi = \frac{\Delta k_{SP}^i}{\Delta k_{SP}^r}$$

Here Δk_{SP} represents the k_{SP} modulation with the sample magnetization and it is defined as $\Delta k_{SP} = k_{SP}(M) - k_{SP}(-M)$. As we can see in the equation, the modulation of k_{SP}^r (Δk_{SP}^r) is related to the amplitude of the magnetoplasmonic signal, while the modulation of k_{SP}^i (Δk_{SP}^i) induces a phase shift (Φ) between the optical and the magnetoplasmonic signal. We would like to notice here that for $\Delta k_{SP}^i = 0$; the optical and magnetoplasmonic interferograms are shifted by exactly 90° due to the cosine and sine dependence of each magnitude, and according to our definition Φ is zero in that case.

Thus, through the analysis of both interferograms we are able to determine the modulation of both the real and imaginary part of k_{SP} . We have performed this analysis as a function of the wavelength and Co position. Figure 3 shows the behaviour of $\text{Re}k_{SP}$ as a function of Co depth for three different wavelengths.

We have observed that Δk_{SP}^r decays exponentially as the position of the cobalt layer goes deeper in the trilayer, a behaviour that can be correlated with the exponential decay of the SPP field inside the metal [4]. Regarding the wavelength dependence, $\text{Re}k_{SP}$ decreases as the wavelength increases. We associate this behaviour with the dispersion relation of the plasmon, since the higher the wavelength, the closer the plasmon is to the light line, and the more its electromagnetic field is spread on the dielectric. For lower wavelengths, on the other contrary, the SPP electromagnetic field appears more squeezed at the interface, probing more inside the metal layer, where the magnetic activity lies.

The behaviour of the imaginary part is not so directly related with the extension of the SPP electromagnetic field in the interface, and the value of the $\text{Im}k_{ij}$ and its dependence with the wavelength seem to be the relevant parameters in this case.

References:

- [1] R. F. Wallis, J. J. Brion, E. Burstein, and A. Hartstein, Phys. Rev. B **9** (1974) 3424.
- [2] J. B. González-Díaz, A. García-Martín, G. Armelles, J. M. García-Martín, C. Clavero, A. Cebollada, R. A. Lukaszew, J. R. Skuza, D. P. Kumah and R. Clarke, Phys. Rev. B **76** (2007) 153402.
- [3] E. Ferreiro-Vila, J. B. González-Díaz, R. Fermento, M. U. González, A. García-Martín, J. M. García-Martín, A. Cebollada, G. Armelles, D. Meneses-Rodríguez and E. Muñoz-Sandoval, Phys. Rev. B **80** (2009) 125132.
- [4] V. V. Temnov, G. Armelles, U. Woggon, D. Guzatov, A. Cebollada, A. Garcia-Martin, J. M. Garcia-Martin, T. Thomay, A. Leitenstorfer, and R. Bratschitsch, Nat. Photonics **4** (2010) 107.

Figures:

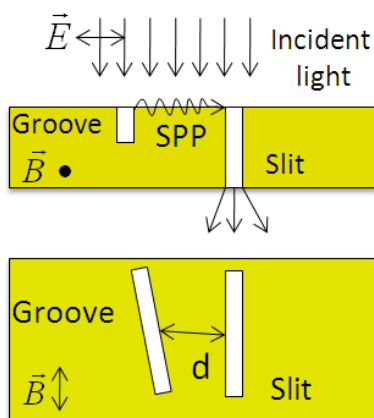


Figure 1: Interference pattern and sketch of the magnetoplasmonic micro-interferometer.

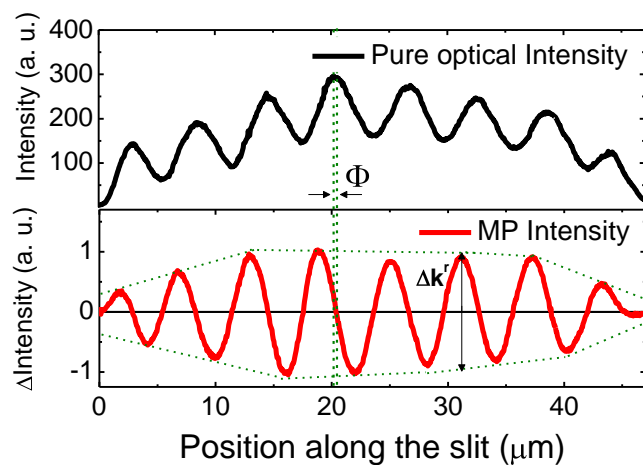


Figure 2: Optical and magnetoplasmonic interferogram

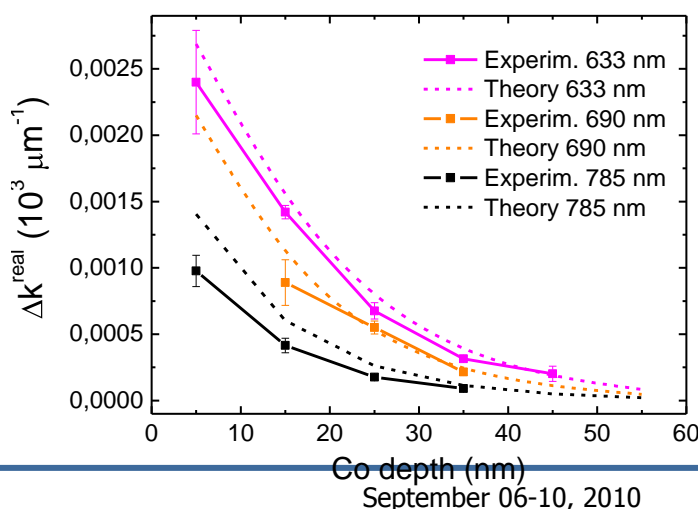


Figure 3: Dependence of the modulation of the real part of k_{SP} with the position of the cobalt layer and the incident wavelength.

Synthesis, Nanostructural and Electronic Characterization of Anthracenedicarboximide Derivatives.

Matthew K. Morantz, Afshin Dadvand, Dmitrii F. Perepichka

McGill University Department of Chemistry, 801 Sherbrooke St. W., Montreal, Quebec, Canada

matthew.morantz@mail.mcgill.ca

Since the discovery of the first semiconducting organic molecules, great interest has been paid to the field of organic semiconductors. Intended to complement, rather than to replace their inorganic counterparts, organic molecules have several important advantages, not least of which is their tunability. Indeed: colour, morphology, solid-state packing as well as many other properties can be finely modulated in target molecules by slightly varying their structure. What is more, it is usually possible to cheaply process these materials at low temperature (typically below 250°C), allowing for a wide range of potential applications and avoiding the costly microfabrication rooms now eponymous with the semiconductor industry.

Despite a host of suitable p-channel candidates (which conduct charge via holes), organic n-channel materials (where charge carriers are electrons) are rare and usually suffer from electron-trapping defects, particularly when exposed to air. One strategy to circumvent this trapping has been the incorporation of strongly electron-withdrawing groups along a semiconductor's π -conjugated core, in order to stabilize electrons as they traverse the material. Anthracenedicarboximides (ADCIs) are one such n-type semiconducting material, in which carboximide groups at either end provide the electron-withdrawing effect necessary for a low LUMO. ADCIs are an ideal candidate for an organic semiconductor, thanks to their flat core (allowing efficient packing in space) and their symmetry (allowing for easy functionalization) [1].

We have thus completed a Density Functional Theory computational study of the ADCI class of molecules, in order to calculate electronic levels and reorganization energies of several compounds. As a result, we have identified and synthesized a considerable number of ADCI derivatives.

We will present synthesis, TFT performance and self-assembly properties of the parent (unsubstituted) ADCI **1** (*cf.* figures 2 and 3) in addition to that of several novel derivatives, complemented by DFT calculations of the electronic levels and reorganization energies. The specific goal of the study is to probe the effects of ADCI side groups on surface nanostructure and, therefore, on molecular packing and charge mobility. We will also investigate whether alkyl chain length parity plays a role in this system.

Significantly, the results of this study will develop a new type of n-type semiconductor. Additionally, we will advance the current understanding of the relationship between molecular structure/crystal packing and device performance in n-channel materials, allowing for more rational design.

References

[1] Wang, Z.; Kim, C.; Facchetti, A.; Marks, T. J. *J. Am. Chem. Soc.* **44** (2007), 13.

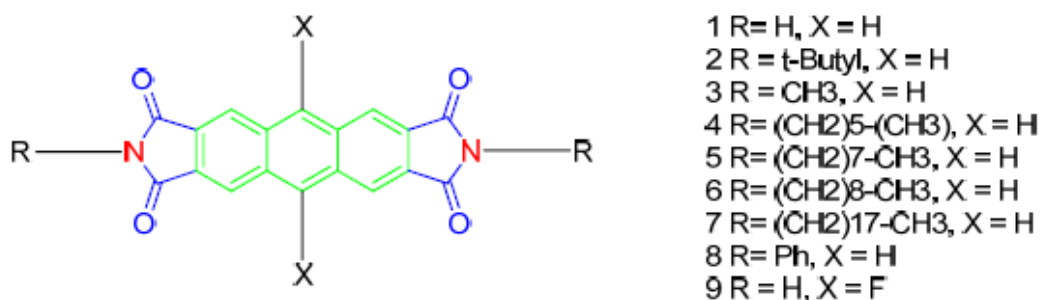


Figure 5. Summary of compounds synthesized and studied

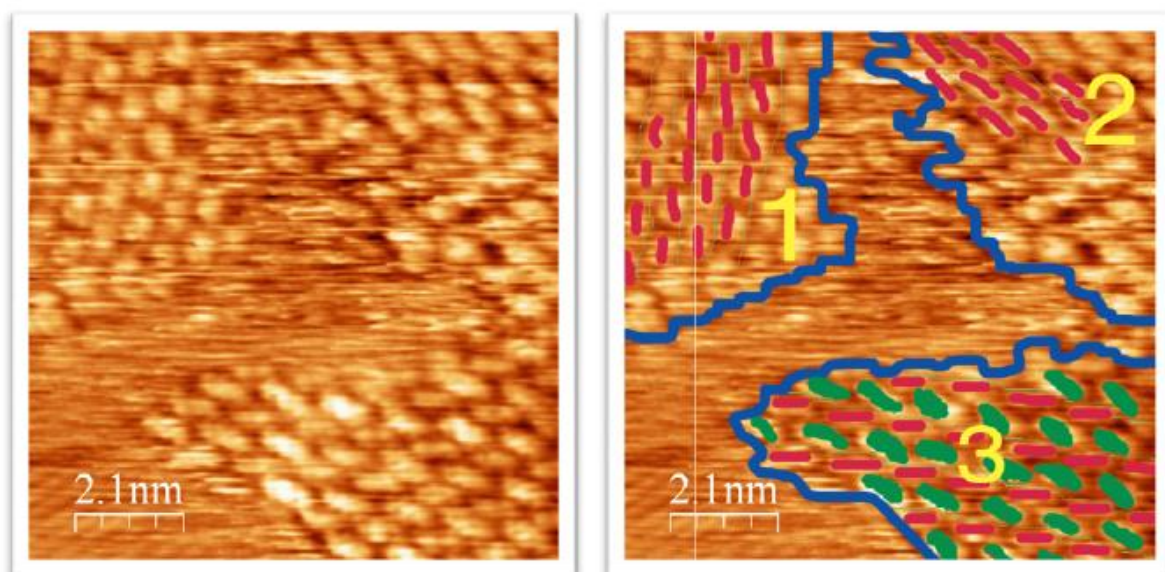


Figure 6. STM image of 2-D SAMN formed from compound 1 at the heptanoic acid/HOPG surface. The processed image at right was marked up to show distinct domains.

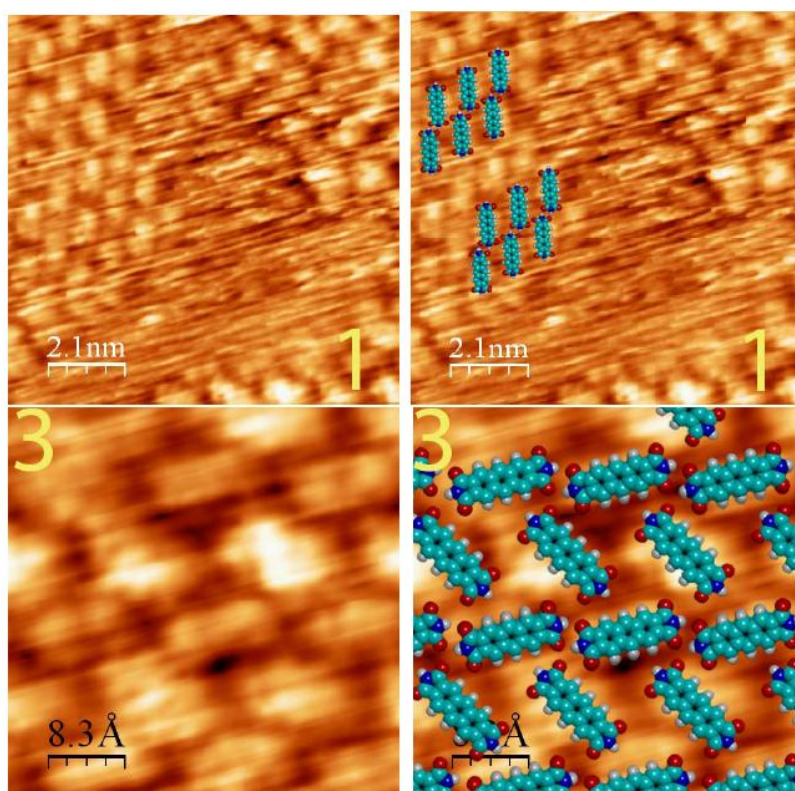


Figure 7. Enlargements of domains 1 and 3 of the STM images from Figure 2, with DFT-optimized molecular models of the molecules superimposed on the image.

Effects of asymmetric dipolar interactions between elliptical ferromagnetic nanomagnets in artificial spin-ice structures

J.M.Porro¹, M.Grimsditch^{1,2}, V.Metlushko³, O.Idigoras¹, A.Berger¹, P.Vavassori¹

¹ CIC nanoGUNE Consolider, Tolosa Hiribidea 76, E-20018, Donostia-San Sebastián

² Materials Science Division, Argonne Natl. Lab., 9700 South Cass Ave., Argonne, IL 60439

³ Department of Electrical and Computer Engineering, University of Illinois at Chicago, Chicago IL 60607

t.porro@nanogune.eu

At the present time, arrays and networks of closely-spaced, dipole-coupled, single-domain nanomagnets are being intensively studied. For applications of nanomagnets in hard disk drives and magnetic random access memories the challenge is generally to avoid magnetic dipole interactions between the individual elements in such arrays, because they are a limiting factor for the achievable data storage density. Contrary to these application related aspects, the dipolar interaction between nanomagnets can be utilized to form a so-called 'artificial spin-ice' structure, which has been recently offered a novel approach to understanding and exploiting the properties of disordered systems, such as liquids, glasses and disordered magnets that are governed by competing interactions leading to frustration effects [1]. Moreover, dipolar interactions have been utilized to realize magnetic quantum-dot cellular automata systems, which are networks of dipole-coupled nanomagnets designed for digital computation [2]. In our studies we demonstrate that dipolar interactions in such arrays can be exploited to induce and control magnetization states and reversal paths in nanomagnets that are completely different from those occurring in isolated nanomagnets.

We fabricated and studied arrays of elliptical ferromagnetic (material Py 25 nm thick) nanomagnets of 700 nm length and 200 nm width, arranged in groups of four to form square units. The square units are organized in a checkerboard pattern (see scanning electron micrograph in Fig. 1). The characterization of the magnetization reversal process in our sample was performed by means of our home-built Magneto-Optical Kerr Effect (MOKE) setup and magnetic force microscopy (MFM) for different orientations and intensities of the applied magnetic field. The experimental results are compared to those obtained from micromagnetic simulations.

In general, the magnetic measurements show that the magnetization reversal process in the nanomagnets changes substantially by applying the external magnetic field parallel to (within $\pm 0.2\sigma$) or at an angle from one of the sides of the squares forming the array (see hysteresis loops in the bottom panel of Fig. 2). The simulations performed on a unit cell of the spin-ice array confirm this behavior (see hysteresis loops in the top panel of Fig. 2): when the magnetic field is applied away from the symmetry axes of the ferromagnetic nanomagnets the formation and rotation of a so-called 'S' single domain state is observed in all the nanomagnets, whereas when the field is applied parallel to their symmetry axis the formation of a so-called 'C' state, which evolves into a single vortex state, is observed in the two elliptical nanomagnets having their short axis parallel to the field (see micromagnetic configurations in Fig. 3).

We analyzed the role played by each of the ferromagnetic nanomagnets in the magnetization reversal process, finding that the formation of the vortex state in the two nanomagnets with short axis parallel to the field is due to the asymmetry of the stray field generated by the other two nanomagnets in the spin-ice unit cell.

Confirmation of the existence of these intermediate metastable states was obtained using magnetic force microscopy after applying a suitable field sequence (see magnetic force micrographs in Fig. 3).

Our studies demonstrate that it is indeed possible to control the magnetization states in elliptical ferromagnetic nanoislands by placing localized magnetic field sources in their proximity, and that such localized field sources can be easily facilitated within an appropriate array structure.

We acknowledge funding of the Department of Industry, Trade, and Tourism of the Basque Government and the Provincial Council Gipuzkoa under the ETORTEK Program, Project No. IE06-172, as well as the Spanish Ministry of Science and Education under the Consolider-Ingenio 2010 Program, Project CSD2006-53. P.V. also acknowledges support through the Marie Curie International Reintegration Grant within the 7th European Community Framework Programme, (Grant Agreement No. PIEF-GA-2008-220166) and finally the Basque Government for the Formación de Investigadores fellowships No. BFI09.284 and BFI09.289.

References

- [1] R. F. Wang et al., Nature 439, 303 (2006)
- [2] A.Imre et al., Science 311, 205 (2006)

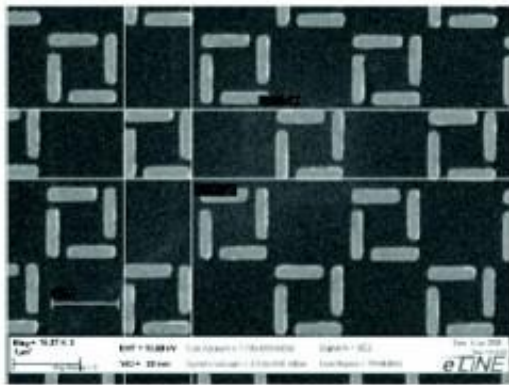


Figure 1. SEM image of the fabricated and analyzed sample.

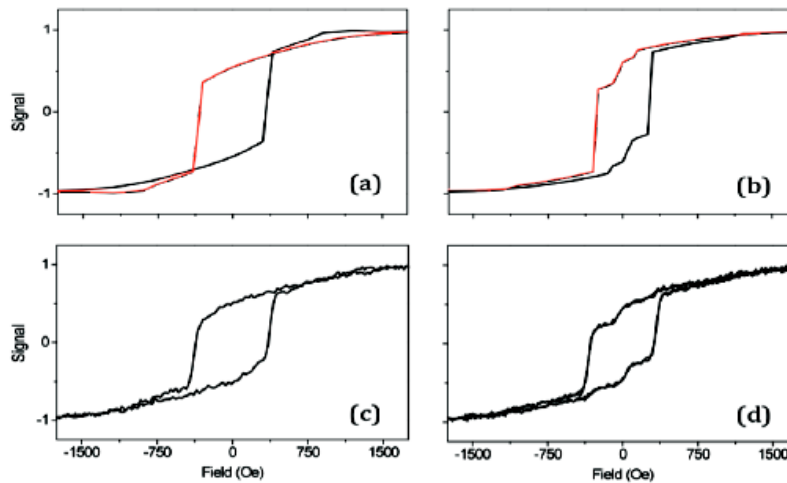


Figure 2. Calculated longitudinal-MOKE hysteresis loops for the off-axis (a) and on-axis (b) external applied magnetic field, and the corresponding measured hysteresis loops for the off-axis (c) and on-axis (d) cases.

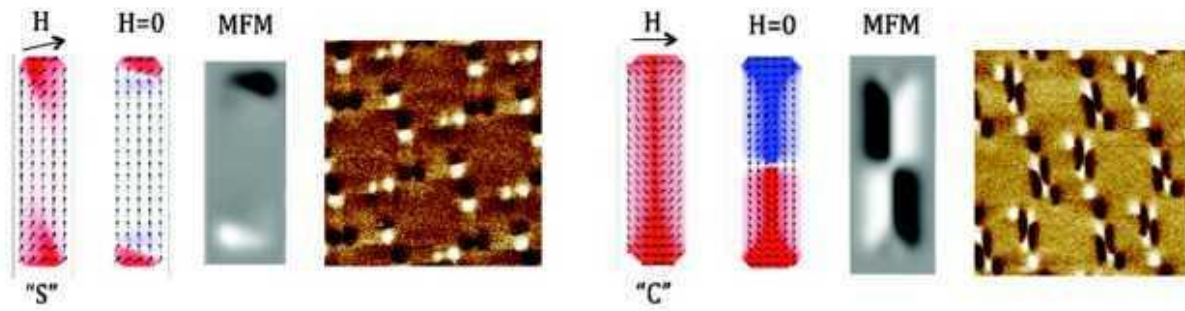


Figure 3. Calculations of the seed and remanent ($H = 0$) magnetization states in an interacting nanomagnet and the corresponding calculated and measured MFM images for the off-axis (left) and on-axis (right) directions of the applied magnetic field.

Development of Nano-Bio hybrid material based on CdTe Quantum Dots and Bacteriorhodopsin protein for future technologies

Aliaksandra Rakovich¹, Alyona Sukhanova^{2,3}, Evgeniy Lukashev⁴, Nicolas Bouchonville³, Vladimir Oleinikov⁵, Mikhail Artemyev⁶, Nikolai Gaponik⁷, Michael Molinari³, Michel Troyon³, Yury P. Rakovich¹, John F. Donegan¹ and Igor Nabiev^{2,3,8}

¹ School of Physics and CRANN, Trinity College Dublin, Dublin 2, Ireland,

² Université de Reims Champagne-Ardenne, 51100 Reims, France,

³ CIC nanoGUNE Consolider, E-20018 San Sebastian - Donostia, Spain,

⁴ Department of Biophysics, Lomonosov Moscow State University, 119992 Moscow, Russian Federation

⁵ Shemyakin-Ovchinnikov Institute of Bioorganic Chemistry, Russian Academy of Sciences, 117987 Moscow, Russian Federation,

⁶ Institute of Physico-Chemical Problems, Belarusian State University, Minsk, Belarus

⁷ Technical University of Dresden, 01062 Dresden, Germany

⁸ IKERBASQUE, Basque Foundation for Science, 48011 Bilbao, Spain

rakovica@tcd.ie

Many technologies rely on the properties of “pure” semiconductor materials for operation. It has been proposed that future technologies will be based on hybrid materials, developed as a result of multidisciplinary studies combining the expertise in Physics, Chemistry and Biology. The interface between nano- and bio-technology, for example, has enormous potential to supply such hybrid materials.

Protein-based devices, for example has received considerable attention during the last few decades [1]. However, most of the light-sensitive proteins investigated for such purposes are not able to deal with the high energy of the UV photons [2]. In fact, most do not absorb UV photons at all, resulting in overall efficiencies of less than 1% [3]. Nanotechnology opens the way to improve the performance of these proteins. For example, semiconductor QDs are able to absorb photons over a wide spectral region [4] and then transfer the harvested energy to the chromophores of such proteins [5], while down converting the absorbed energy so the damage to the chromophores is minimized.

Here the development of a nano-/bio- hybrid material based on photochromic protein bacteriorhodopsin (bR) and CdTe semiconductor quantum dots (QDs) is described. CdTe QDs of carefully selected photoluminescence colours were attached to the purple membranes (PMs) of bacteria *Halobacterium salinarum* (containing photochromic membrane protein bacteriorhodopsin in its natural environment) by utilizing either electrostatic assembly or covalent conjugation (Fig.1).

When such hybrids were assembled electrostatically, QDs self-assembled on the surface of PMs in such a way that efficient Förster Resonance Energy Transfer (FRET) from QDs to bR was realized (Figs. 1 and 2). Results demonstrate significant quenching of QDs' PL due FRET from QDs (donors) to the protein-linked bR retinal (acceptor), with a corresponding decrease in the fluorescence lifetime of the QDs (Fig.2). Quenching of QDs PL in electrostatically-assembled complexes was found to be strongly dependent on both QDs' radii and their surface functionalization [7]. A 3-fold enhancement in FRET efficiency was observed when QDs were attached to PMs by chemical conjugation, due to a reduced donor-acceptor separation distance.

Most importantly, it was shown that attachment of QDs to PMs does not disturb the biological function of bR – the pumping of a proton (H^+) from cytoplasmic side to the extracellular side of the membrane did not cease. In fact, an upto 20% enhancement in its function was observed upon addition of QDs to the system.

The described nano-bio hybrid material, with advanced optical and biological functions, will allow the development of devices with unique electronic and photonic properties, paving the way to novel nanophotonic and photovoltaic applications.

References

- [1] Birge, R. R. *et al.*, J. Phys. Chem. B, **103** (1999) 10746-10766
- [2] Lao, K. & Glazer, A. N., Proc. Natl. Acad. Sci. USA, **93** (1996) 5258–5263
- [3] Archer, M. D., Barber, J. in Molecular to Global Photosynthesis (ed. Archer, M. D. & Barber, J.), Imperial College Press, London (2004) pp. 1-41
- [4] Resch-Genger, U., Grabolle, M., Cavaliere-Jaricot, S., Nitschke, R. & Nann, T., Nature Meth., **5** (2008) 763-775
- [5] Nabiev, I., Sukhanova, A., Artemyev, M. & Oleinikov, V. in Colloidal Nanoparticles in Biotechnology (ed. Elaissari, A.), Ch. 6, Wiley & Sons Inc. (2008) 133-168
- [6] Nabiev, I., Efremov, R. G. & Chumanov, G. D., J. Biosciences, **8** (1985) 363-373
- [7] Rakovich, A., Sukhanova, A., Bouchonville, N., Molinari, M., Troyon, M., Cohen, J. H. M., Rakovich, Y., Donegan, J. F., Nabiev, I., Proc. of SPIE, **7366** (2009) 736620-1

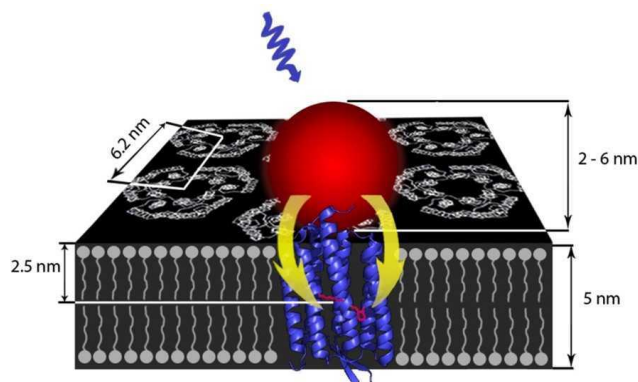


Figure 1. Structure of QD-bR hybrid material. Each bR protein extends from one side of the purple membrane to the other, and contains one retinal molecule (shown in purple) [6]. Photon energy is absorbed by a QD immobilized on the surface of the PM. This energy is then transferred to the retinal by FRET mechanism, resulting in strong quenching of QDs' PL.

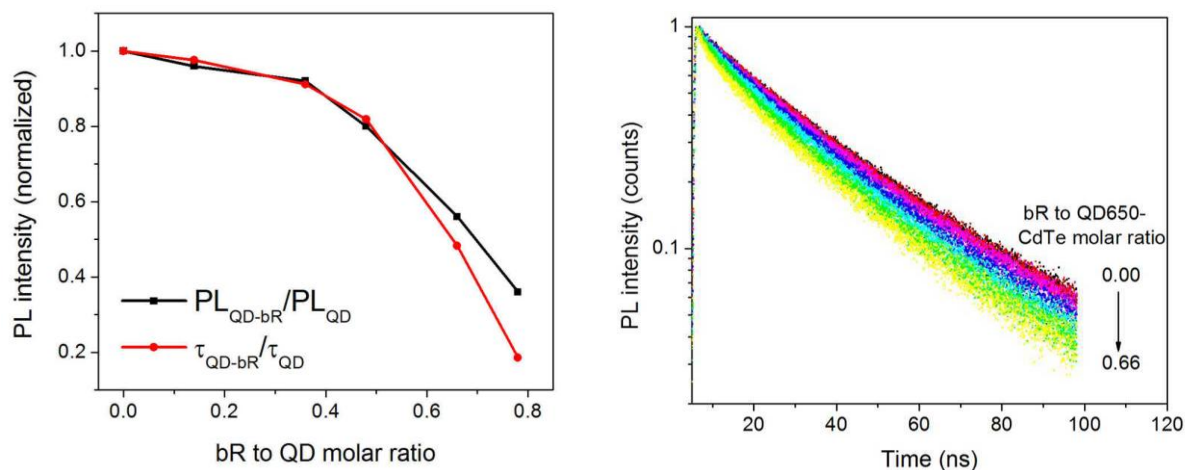


Figure 2. Integrated photoluminescence and time-resolved photoluminescence decay as a function of bacteriorhodopsin to quantum dots molar ratios. Panel a: PL quenching of QD650 at different bR to QD molar ratios. There is very good agreement between the integrated PL measurements (\blacksquare) and lifetime data (\blacktriangleright), calculated as $1 - (\text{FRET efficiency})$, suggesting that FRET is the main mechanism of quenching of QDs' PL. Panel b shows time-resolved data for bR-QD hybrids in which bR to QD molar ratios were changed from 0 to ~0.7.

1D polymer/CNT composite : elaboration and transport properties

F. Roussel^{1,2}, T. Souier³, M. Pinault¹, J. Cousty³, M. Mayne l'Hermite¹, J.-E. Wegrowe²

1. CEA, IRAMIS, SPAM, Laboratoire Francis Perrin (CEA-CNRS URA 2453), 91191 Gif-sur-Yvette, France.
2. Laboratoire des Solides Irradiés, Ecole Polytechnique, CNRS UMR 7642, CEA/DSM/IRAMIS, Palaiseau, France
3. Service de Physique et Chimie des Surfaces et Interfaces, CEA/DSM/IRAMIS - CEA Saclay, France

florent.roussel@cea.fr

Multi-Walled Carbon Nanotubes (MWNTs) can be aligned directly during their synthesis, forming carpets and thus 1D anisotropic networks. Aerosol-assisted Catalytic Chemical Vapour Deposition (CCVD) process is, for instance, one technique used to produce aligned MWNTs[1,2]. Such aligned MWNTs can be impregnated in a polymer matrix, forming a 1D composite. Few papers[3,4] reports the preparation and the electrical property measurements of such composites. The conductivity is macroscopically measured by a two probe method, both along the axial direction of MWNTs and perpendicularly to this direction. The authors report interesting values of conductivities, in particular in the 1D direction, which are higher in comparison to conductivities measured on randomly oriented CNT composites[4]. However, little information is given in terms of conductivity contribution at the nanotube scale.

In this context, our motivation is to study the electrical properties of 1D composite materials taking into account their fabrication parameters. In this presentation, a particular attention will be paid to the physical-chemical analysis of the samples and the electrical property measurements at the nanoscale level.

1D composites are produced with a four step process : first, MWNT carpets are synthesized by an aerosol-assisted CCVD process on quartz substrates ; then the carpets are annealed at 2000°C under argon atmosphere[5] ; and then they are impregnated in an epoxy polymer matrix and cured ; finally they are polished in order to adjust the thickness of the composite.

At each step of the preparation process, the MWNTs and the composites are characterized. MWNT carpets are observed by Scanning Electron Microscopy (SEM) (Fig. 1.a) in order to measure their thickness (corresponding to the CNTs' length) and to qualitatively estimate their alignment. Some of the MWNT carpets are dispersed before and after the annealing operation in an ethanol solution and observed by Transmission Electron Microscopy (TEM) with the purpose of measuring their internal and external diameters by statistical analysis. Typically, MWNT carpets used in this study exhibit a thickness of 1 mm and MWNT external mean diameter is 50 nm. The surface of each side of the composite sample which has been mirror-polished, is observed by SEM (Fig. 1.b), showing that MWNTs sections are protruding. A statistical measurement of the protruding MWNTs gives an average density value of the tubes which is around $4 \cdot 10^9$ MWNT/cm².

Atomic Force Microscope (AFM) equipped with a special Current-Sensing (CS) device has been used to analyse the composite surface at room temperature, which allows a simultaneous mapping of the topography (Fig. 2.a) and of the local resistivity of the surface. These combined measurements provide a clear identification of the MWNTs on the composite surface, supporting the information from the SEM observations (Fig. 2.b). They allow not only to calculate the MWNT density with a result consistent with the one provided by SEM, but also to measure how much the MWNTs protrude from the polymer, which is found to be around a few nanometres. The distribution of the resistivity along the composite surface is studied quantitatively. Statistical analysis of the resistivity clearly reveals the presence of MWNTs protruding from the surface. Low resistivity such as 10^4 ohms has been measured in several areas of the composite surface. Some I/V spectroscopy curves were measured on different points of the surface ; they show two kinds of electrical behaviour when MWNTs are occurring in these areas : ohmic and non-ohmic ones. Some hypothesis of explanations will be given in order to explain the non-ohmic behaviour which is similar with previous measurements performed at the Laboratoire des Solides Irradiés on nano-objects[6] with the same geometry. Complementary AFM measurements are currently in progress in order to confirm such a non-ohmic behaviour at room temperature.

References

- [1] M. Pinault, M. Mayne-L'Hermite, C. Reynaud, V. Pichot, P. Launois, and D. Ballutaud, *Carbon*, **5 (12)** (2005) 2968-2976.
- [2] M. Pinault, V. Pichot, H. Khodja, P. Launois, C. Reynaud, and M. Mayne-L'Hermite, *Nano Letters*, **5 (12)** (2005) 2394-2398.
- [3] H. Peng, and X. Sun, *Chemical Physics Letters*, **471** (2009) 103-105.
- [4] H. Cebeci, R. Guzman de Villoria, A. John Hart, and B.L. Wardle, *Composites Science and Technology*, **69** (2009) 2649-2656.
- [5] M. Pinault, M. Mayne-L'Hermite, C. Reynaud, O. Beyssac, J.N. Rouzaud, and C. Clinard, *Diamond and Related Materials*, **13 (4-8)** (2004) 1266-1269.
- [6] J.-F. Dayen, T.L. Wade, G. Rizza, D.S. Golubev, C.-S. Cojocaru, D. Pribat, X. Jehl, M. Sanquer, and J.-E. Wegrowe, *The European Physical Journal Applied Physics*, **45** (2009) 10604.

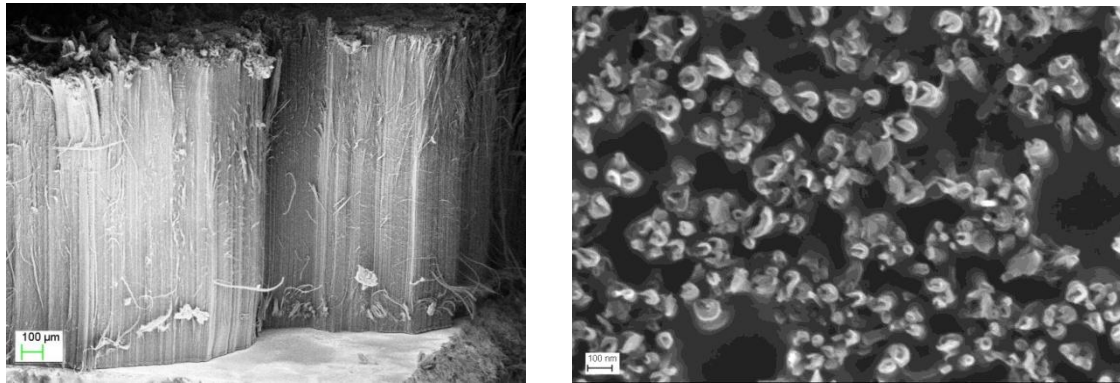


Figure 1. SEM observations ((a) CNT carpet on quartz substrate ; (b) CNT/Epoxy composite surface)

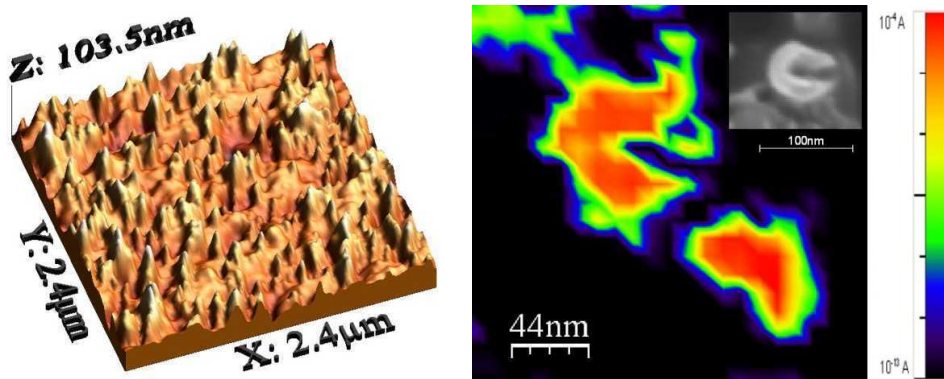


Figure 2. AFM images ((a) 3D view of the surface topography ; (b) comparison between zoomed CS-AFM and zoomed SEM pictures on the upper inset)



ORAL CONTRIBUTIONS

(Nanoresearch in Portugal - Parallel Session)

Optical performance of highly oriented nanofibers of very efficiency organic nonlinear materials

E. de Matos Gomes¹, D. Isakov¹, M. S. Belsley¹, M. M. Raposo², R. M.F. Baptista², S. P.G. Costa², M. Margarida R. Costa³, B. Almeida¹, S. Fernandes¹, P. Sá¹

¹Departamento de Física, Universidade do Minho, Braga, Portugal

²Departamento de Física, Universidade do Minho, Braga, Portugal

³Departamento de Física, Universidade de Coimbra, Coimbra, Portugal

emg@fisica.uminho.pt

The interest in organic chromophores having strong second harmonic generation (SHG) performances is related to their possible use in low cost electro-optic devices such as high-speed photonic switching and electro-optic modulators.

The basis for organic second-order nonlinear optical (NLO) materials are chromophores that exhibit large first hyperpolarizabilities, β , with a macroscopic organization of microscopic molecular building blocks into a noncentrosymmetric crystal packing. In general, dipolar second-order NLO chromophores consist of a π -conjugated bridge end-capped with strong electron donor and acceptor substituents (D- π -A).[1]

To achieve macroscopic departure from centrosymmetry, we report a simple and generic preparation of nanofibers of stable organic nanocrystals using the electrospinning technique,[2] consisting of highly efficient organic electrooptic and nonlinear optical materials and discuss their nonlinear optical performance. We demonstrate that electrospinning is a very effective tool for producing uniaxially aligned nanofibers of (D- π -A) organic chromophores with anisotropic properties. Highly aligned nanofibers of both well established organic NLO materials like 2-methyl-4-nitroaniline and of new arylthienyl- and bithienylbenzothiazoles [3,4] have been produced using a rotating drum collector and consist of organic NLO functional nanocrystals embedded in a polymeric matrix.

X-Ray diffraction studies show that the chromophores exhibit highly uniform orientations within the nanofibers having their dipole moment directed along the fibers axis behaving like a "single-crystal"-like layer.

Optical second harmonic generation polarimetry reveals a high degree of molecular alignment within the fibers and demonstrates the effectiveness of the nanofibers in generating second harmonic light. Benzothiazole heterocycles are also used for several optical applications in materials chemistry (eg OLEDs) due to their fluorescence.[5] Fluorescence studies of the fiber containing arylthienyl- and bithienylbenzothiazoles were also performed showing that these novel materials exhibit also fluorescence properties. Moreover the λ_{em} of the fiber compared to the λ_{em} of the benzothiazole solution showed a bathochromic shift of 34 nm.

A discussion about the influence of fiber morphology and structure on light propagation properties will be undertaken in view of its technological applications.

References

[1] He, G. S.; Tan, L.-S.; Zheng, Q.; Prasad, P. N., Chem. Rev. 108 (2008) 1245.

[2] Li, D.; Xia, X., Adv. Mater. 16 (2004) 1151

[3] Batista, R. M. F.; Costa, S. P. G.; Raposo, M. M. M., Tetrahedron Lett. 45 (2004) 2825.

[4] Costa, S. P. G.; Batista, R. M. F.; Cardoso, P.; Belsley, M.; Raposo, M. M. M. Eur. J. Org. Chem. 17 (2006) 3938.

[5] Pina, J.; Seixas de Melo, J.; Burrows, H. D.; Batista, R. M. F.; Costa, S. P. G.; Raposo, M. M. M. J. Phys. Chem. A 2007, 111, 8574.

Multiplex genetic characterization via noble metal nanoprobos

Gonçalo Doria¹, João Conde^{1,2}, Miguel Larguinho^{1,3} and Pedro Baptista¹

¹CIGMH/DCV, Faculdade de Ciências e Tecnologia, Universidade Nova de Lisboa, Caparica, Portugal;
Tel/Fax: (+351) 212 948 530;

² Instituto de Nanociencia de Aragón, Universidad de Zaragoza, Zaragoza, Spain;

³ BIOSCOPE/Physical-Chemistry Department, Faculty of Science, University of Vigo, Ourense, Spain;

doria_go@fct.unl.pt

Cancer is a multigenic complex disease where is usually required that multiple gene loci are characterized simultaneously and/or in association (e.g. tumor suppressor gene TP53, c-myc oncogene, BCR-ABL fusion oncogene, among others)[1,2]. Here, we present the use of noble metal nanoparticles with different compositions in a one-pot multi-color DNA detection strategy for multiplex cancer diagnostic. Synthesis and functionalization with thiol-ssDNA of pure gold and gold-silver alloy nanoparticles was successfully achieved, yielding different nanoprobos with tunable colors and distinct absorption peaks, characteristic of each nanoparticles' surface plasmon resonance. These nanoprobos were combined in a one-pot reaction to allow for the simultaneous differential detection of different nucleic acids sequences related to cancer, following a non-cross-linking method that has been previously developed by our group using gold nanoprobos alone[3,4,5]. The method is based on the colorimetric comparison of solutions before and after salt-induced nanoprobe aggregation. Only the presence of a complementary target stabilizes the corresponding nanoprobe, preventing aggregation and colorimetric change after salt addition, while the absence of a complementary target leads to the aggregation of nanoprobos with a concomitant color change of solution (Figure 1)[6].

References

- [1] Afar DE et al., Science, 264 (1994) 424-6;
- [2] Ho JS et al., Mol Cell Biol, 25 (2005) 7423-31;
- [3] Baptista P et al., J Biotechnol, 119 (2005) 111-7;
- [4] Baptista P et al., Clin Chem, 52 (2006) 1433-4;
- [5] Doria G et al., IET Nanobiotechnol, 1 (2007) 53-7.
- [6] Doria G et al., Nanotechnology, 21 (2010) 255101;

Acknowledgements

We thank FCT/MCTES for financial support: PTDC/SAU-BEB/66511/2006; PTDC/EEA-ELC/74236/2006; Nanotruck-Action NanoSciEra+ and CIGMH.

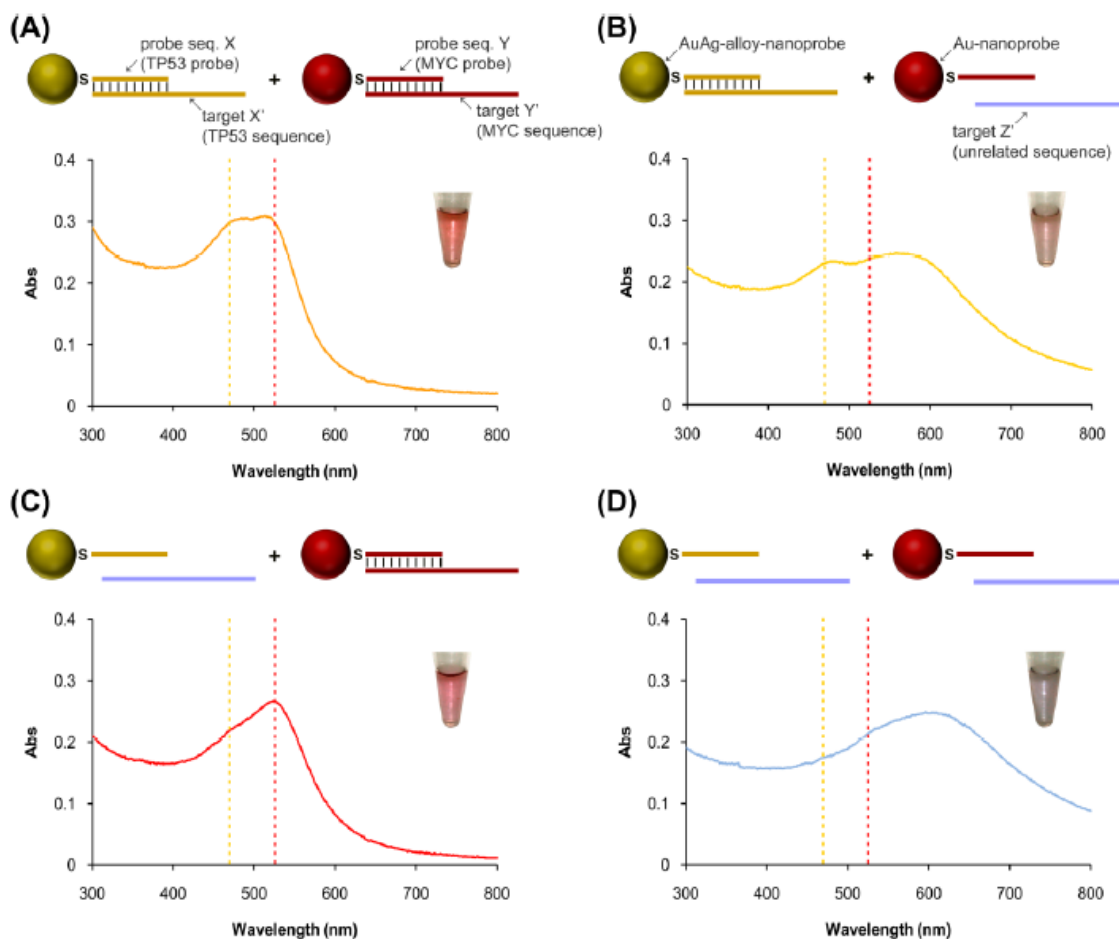


Figure 1. One-pot colorimetric multi-target detection [1]. UV-visible spectrum and digital photograph of AuAg-alloy- and Au-nanoprobe mix in the presence of: (A) complementary targets to both the AuAg-alloy- and Au-nanoprobe; (B) a complementary target to the AuAg-alloy-nanoprobe; (C) a complementary target to the Au-nanoprobe; (D) a non-complementary target to both AuAg-alloy- and Au-nanoprobes. Vertical dashed lines represent the absorption peaks of AuAg-alloy-nanoprobes (orange broken line; 470 nm) and Au-nanoprobes (red broken line; 526 nm) when dispersed in solution.

Effect of Eu-implantation and annealing on the GaN QDs excitonic recombination

M. Peres¹, S. Magalhães^{1,2}, V. Fellmann³, B. Daudin³, A. J. Neves¹, E. Alves^{2,4},
K. Lorenz^{2,4}, **T. Monteiro**¹

¹ Departamento de Física e I3N, Universidade de Aveiro, Campus de Santiago,
3810-193 Aveiro, Portugal

² Instituto Tecnológico e Nuclear,
Estrada Nacional 10, 2685-953 Sacavém, Portugal

³ CEA/CNRS Group, "Nanophysique et Semiconducteurs", Dépt. de Recherche Fondamentale
sur la Matière Condensée, CEA/Grenoble, 17 rue des Martyrs, 38054 Grenoble Cedex 9, France

⁴ CFNUL, Av. Prof. Gama Pinto, 1649-003 Lisboa, Portugal

tita@ua.pt

Self-assembled GaN quantum dots (QDs) stacked in superlattices (SL) with AlN spacer layers were implanted with several fluences of Europium ions. The as-implanted samples were further submitted to thermal annealing treatments between 800°C to 1200°C and Eu³⁺ optical activation is achieved in all the analyzed superlattices.

Due to the combined effects of quantum confinement of the carriers, strain state of the stacked heterostructures and quantum confined Stark effect, the excitonic recombination in the as-grown samples can be observed above and below the bulk GaN bandgap for small and larger GaN QDs as shown in Figure 1.

In order to analyse the effects of Eu-implantation on the GaN QDs excitonic recombination we have performed a detailed photoluminescence (PL) and photoluminescence excitation (PLE) study in the as-grown and implanted and annealed SL structures. In addition to the SL samples individual as-grown and Eu-implanted GaN and AlN hosts were also considered for comparison.

The peak position of the GaN QDs excitonic recombination is known to be very sensitive to the dots size, shape and thermal annealing treatments [1-3]. The effects of thermal annealing are also evidenced in Figure 1 where a high energy shift of the band maxima is identified for the SL samples annealed at the temperature of 1200°C.

The PLE spectra monitored at the band maxima of the different as-grown and annealed SL samples are characterized by a broad absorption band peaked nearby 253 nm with a sample dependent onset absorption band, extending to wavelengths higher than 300 nm. For comparison we have plotted in Figure 1 the PLE spectra monitored at 415 nm luminescence band in AlN layers. As observed, the peak position of the absorption band occurs at the same wavelength of the GaN QDs. However, in this case no shoulder is observed on the low energy side of the onset absorption. As the peak position and shape of the absorption band is equal for the as-grown and annealed samples we believe that they represent the main population mechanism of the GaN QDs excitonic recombination.

After Eu-implantation and annealing we identify by PLE that the GaN QDs excitonic recombination is also populated by an Eu-related defect absorption band peaked at ~265 nm, the X₂ absorption band [4]. The presence of the multiple excitation paths and their influence on the thermal quenching of the GaN QDs excitonic recombination in the Eu-doped SL is discussed.

We acknowledge funding from FCT, Portugal (PTDC/CTM/100756/2008). M. Peres and S. Magalhães thanks to FCT for their PhD grants SFRH/BD/45774/2008 and SFRH/BD/44635/2008, respectively.

References

[1] T. Steiner, (ed.), Semiconductor Nanostructures for Optoelectronic Applications (Artech House Inc., Boston, London, 2004), and references therein.

- [2] H. Morkoc, (ed.), Handbook of Nitride Semiconductors and Devices (Wiley-VCH, Weinheim, Berlin, 2008), and references therein.
- [3] M. Peres, A. J. Neves, T. Monteiro, S. Magalhães, E. Alves, K. Lorenz, H. Okuno-Vila, V. Fellmann, C. Bougerol, B. Daudin, Phys. Status Solidi B, 1–4 (2010) / DOI 10.1002/pssb.200983674.
- [4] H. J. Lozykowski, W. M. Jadwisienczak, phys. stat. sol. (b), **244** (2007) 2109.
- [5] K. Wang, K. P. O'Donnell, B. Hourahine, R. W. Martin, I. M. Watson, K. Lorenz, E. Alves, Phys. Rev. B, **80** (2009) 125206.

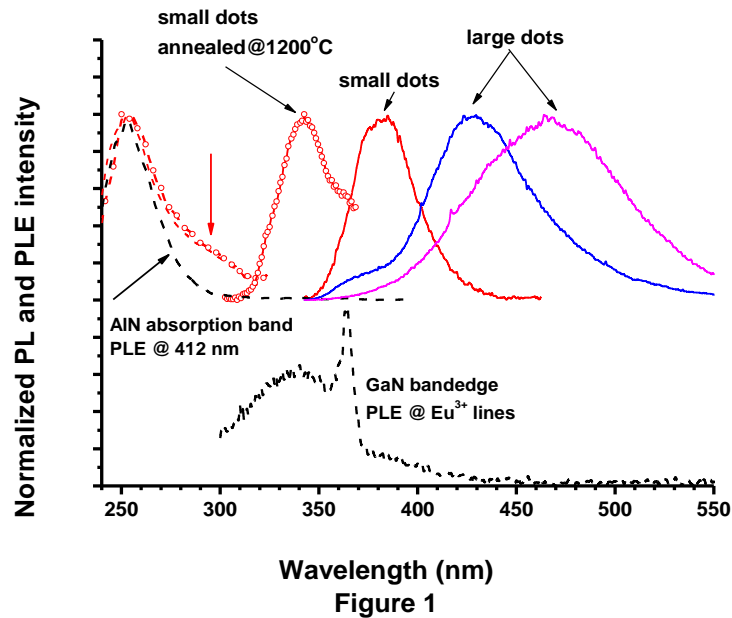


Figure 1. RT PL (full lines) and PLE spectra (dashed lines) of as-grown and annealed at 1200°C (line and symbols) SL samples. For comparison, the RT PLE spectra of an undoped AlN sample (upper black dotted line) and the 14 K PLE spectra of a GaN:Eu (lower black dotted line) samples are shown.

Fabrication of silica hollow microcoils with mesoporous walls

Carlos Rodríguez-Abreu^{1,2}, Neus Vilanova², Conxita Solans², Masaki Ujihara³,
Toyoko Imae³, and Seiji Motojima⁴

¹ International Iberian Nanotechnology Laboratory (INL), Avda. Central nº100, Edifício dos Congregados, 4710-229, Braga, Portugal

² Instituto de Química Avanzada de Cataluña. Consejo Superior de Investigaciones Científicas (IQAC-CSIC) Jordi Girona 18-26, 08034 Barcelona, Spain

³ Graduate Institute of Engineering, National Taiwan University of Science and Technology, 43 Keelung Road, Section 4, Taipei, Taiwan

⁴ Toyota Physical & Chemical Research Institute, Nagakute, Aichi 480-1192, Japan

crodriguez@inl.int

Hollow silica microcoils have been prepared by using functionalized carbon microcoils (CMCs) as hard templates [1,2] and surfactant aggregates as soft templates. The obtained materials have been characterized by electron and optical microscopy, small angle X-ray scattering, thermogravimetry and porosimetry (gas sorption analysis). The obtained hollow microcoils resemble the original hard templates in shape and size. Moreover, they have mesoporous walls (pore size ≈ 3 nm) with some domains where pores are ordered in a hexagonal array, originated from surfactant micelles. As a result the surface area of the silica microcoils is much higher than that of the original CMCs used as templates. The obtained silica microcoils also show preferential adsorption of cationic fluorescent dyes. A mechanism for the formation of silica microcoils is proposed.

References

[1] Motojima, S.; Chen, X., Bull. Chem. Soc. Jpn. **80** (2007) 449.

[2] Adhikari, P.D.; Tai, Y.; Ujihara, M.; Chu, C-C. ; Imae, T.; Motojima, S., J. Nanosci. Nanotechnol. **10** (2010) 833.

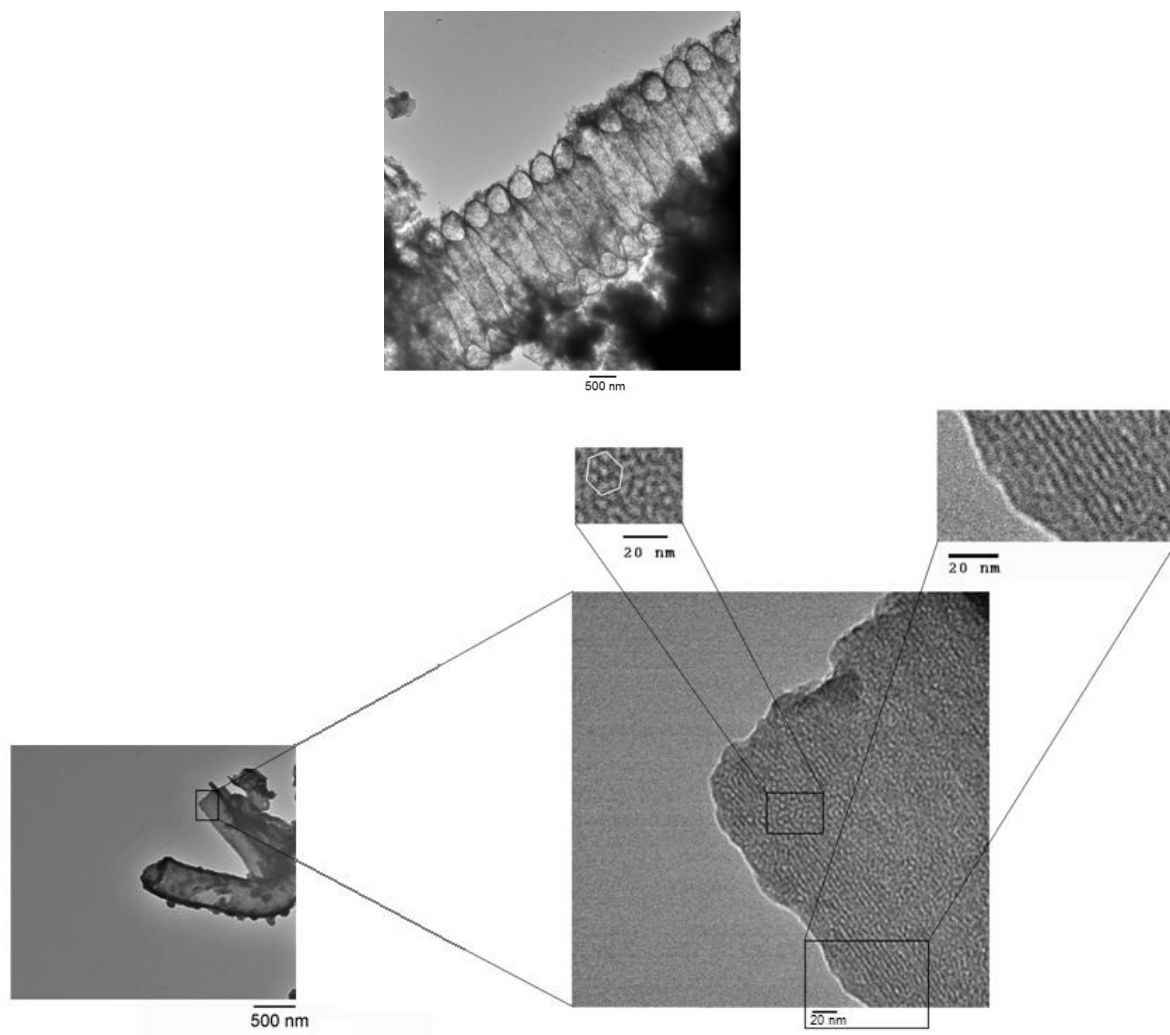


Figure 1. TEM images of sections of silica hollow microcoils.

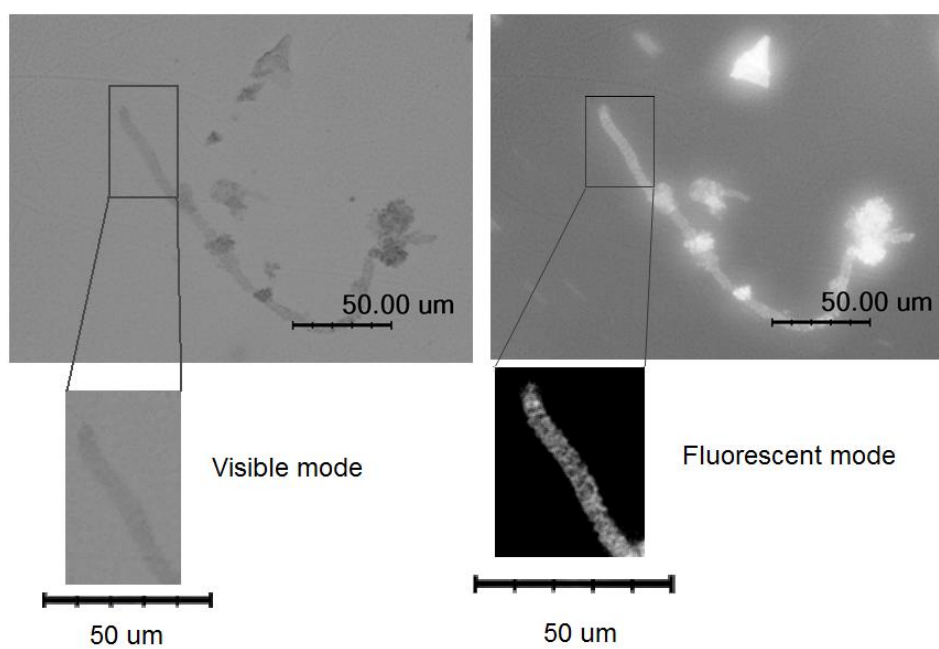


Figure 2. Visible and fluorescent microscopic images of hollow silica microcoils after soaking them in aqueous solutions of rhodamine B

Visibility enhancement of Graphene on multiple substrates

Peter Schellenberg¹, Michael Belsley¹, Hugo Gonçalves¹, Cacilda Moura¹, Tobias Stauber²

¹Center of Physics, University of Minho, Campus de Gualtar, 4710-057 Braga, Portugal

²Department of Condensed Matter Physics, University Autónoma of Madrid, Campus of Cantoblanco, E-28049Madrid, Spain

peter.schellenberg@fisica.uminho.pt

In order to take advantage of the enormous potential of graphene for future electronic micro-circuits, nanophotonic assemblies, coatings and other microstructured graphene based devices, it is essential to develop graphene visualization techniques, which reliably and rapidly deliver images of graphene and graphene based structures.

A multitude of optical techniques have been put forward to this end, for example based on the exploitation of refractive index differences. Several imaging methods are based on Raman and Rayleigh scattering, or on fluorescence quenching of dyes by graphene layers. Generally these methods require relatively complex equipment or an optimized substrate coating. Here, we report on two novel and easy to use techniques for the identification of potential graphene flakes.

One technique aims to increase the contrast of the graphene and multilayer graphene structures by reducing background intensity by using immersion microscopy. The second technique exploits hydrophobicity differences between substrate and graphene structures to enhance their visibility. This second method can be employed to quickly and easily visualize graphene and few-layer graphite on a wide variety of substrates without the need for any specific surface modification or preparation. To our knowledge, there is no other currently available method that is capable of readily visualizing graphene flakes on plastic surfaces, untreated dielectrics and uncoated metals.

On the rule of disorder in the conductivity of high aspect ratio carbon filled composites in the framework of complex networks

J. Silva^{1,2}, R. Simões^{2,3}, S. Lanceros-Mendez¹, R. Vaia⁴

¹- Center of Physics, University of Minho, Campus de Gualtar, 4710-057 Braga, Portugal

²- Institute for Polymers & Composites IPC/I3N, University of Minho, 4800-058 Guimarães, Portugal

³- School of Technology, Polytechnic Institute of Cavado and Ave, 4750-820 Barcelos, Portugal.

⁴- Air Force Research Laboratories, Wright-Patterson AFB, OH 45433-7750, USA

rsimoes@dep.uminho.pt / rsimoes@ipca.pt

The inclusion of high aspect ratio fillers like carbon nanotubes (CNT) or vapour grown carbon nanofibers (VGCNF) in a polymeric matrix enhances the electric and mechanical properties [1] of the matrix. The filler concentration, aspect ratio (AR) and dispersion are expected to affect the material response [1]. Both for CNT/polymer or VGCNF/polymer composites a divergence is expected in the composite conductivity for a critical volume fraction, which is usually discussed in the framework of the percolation theory [2].

In a recent review [3] the experimental percolation thresholds for CNT composites revealed the existence of a wide range of values for the same type of CNT/polymer composites, a deviation from the bounds predicted by the excluded volume theory and a dispersion for the values of the critical exponent (t) [2]. The later exponent is expected to be independent of filler geometry or matrix, taking a value that depends on the system dimension.

In this work it is demonstrated that the conductance of carbon nanotube composites can be described in the context of complex network theory, providing interesting insights into the nature of the physical phenomena behind the conductance behavior. Using the complex network framework, by mapping fillers to vertices and edges to the gap between fillers, we are able to describe the percolation threshold and relate the composite conductance with a weak disorder regime. The theoretical arguments are validated by experimental results from the literature.

References

[1] E. T. Thostenson, C. Li, and T.-W. Chou, *Composites Science and Technology* 65, 491 (2005).

[2] D. Stauffer and A. Aharony, *Introduction to Percolation Theory* (Taylor and Francis, London, 1992); A. Celzard, E. McRae, e.a., *Physical Review B* 53, 6209 (1996).

[3] W. Bauhofer and J. Z. Kovacs, *Composites Science and Technology* 69, 1486 (2009)

Acknowledgments

Effort sponsored by the Air Force Office of Scientific Research, Air Force Material Command, USAF, under grant number FA8655-06-1-3009. We acknowledge also the Foundation for Science and Technology, Lisbon, through the 3° Quadro Comunitario de Apoio, the POCTI and FEDER programs, the PTDC/CTM/69316/2006 grant and the NANO/NMed-SD/0156/2007 project. JS thank the FCT grant SFRH/BD/60623/2009.

Comparison of the results of the microbiologic quality of an untreated water sample using conventional culture media and a DNA chip for simultaneous detection of microorganisms

Vale, F.F.¹, Saraiva, K.¹, Fontes, M.¹, Vieira, H.²

¹ Faculty of Engineering, Catholic University of Portugal, Estrada Octavio Pato, 2635-631 Rio de Mouro, Portugal;

² BIOALVO SA, Edificio ICAT, Campus da FCUL, Lisbon, Portugal.

filipavale@fe.ucp.pt

Consumption of contaminated drinking water heavily contributes to the burden of gastrointestinal waterborne diseases. This is of particular importance in developing countries. Indeed, the World Health Organization (WHO) states that almost one tenth of the global disease burden could be prevented by improving water supply, sanitation, and hygiene and water resources management. The same organization estimates that around 1.5 million deaths per year could be avoided if these measures were implemented [1].

Conventional detection methodologies present several shortcomings, such as representativity of indicator species (on which absence water quality relies), low throughput and increasing resources as more species are to be detected and time consuming. DNA chips have the potential to serve as surveillance systems for the simultaneous detection of pathogens, overcoming these limitations. DNA chips have the advantage of being high throughput (simply to increase the number of testing probes in the chip), quick (does not rely on time consuming bacterial growth) and may detect stressed bacteria (that does not develop in a Petri dishes but still can infect the human host). Considering this we have developed a DNA chip (AQUACHIP®) for simultaneous detection of multiple waterborne pathogens.

Species specific DNA probes were implemented on a microarray, allowing detection of which sample is positive for which microorganism. The selected microorganisms were the Portuguese and European Community mandatory microbiological parameters and indicator parameters required in water intended for human consumption, delivered by public distribution systems, trucks or cistern-ships, or used in the alimentary industry (coliform bacteria group, *Escherichia coli*, Enterococcus and *Clostridium perfringens*, including spores); and a group of non-mandatory microorganisms selected according to their impact on public health [2, 3].

In the present study one untreated water sample was analyzed by conventional methods and by the DNA Chip. The results were concordant for the mandatory organisms using both methods, which reinforces the utility and the proof-of-concept of the DNA chip. However, we have obtained discordant results for *Pseudomonas* spp. and *Salmonella* spp., which can be represent a DNA chip false positive or a conventional method false negative. Indeed, stressed bacteria may be unable to growth using culture media, and DNA probes implemented in the DNA chip for these microorganisms may not be sufficient specific to correctly detect them. For instance, for the *Salmonella* probe, which has 95% homology to *E. coli* DNA, according to BLAST [4] (E-value 3E-28), so a positive signal was expected. In conclusion, the chip appears to be correctly identifying mandatory bacteria, but the probes for some of the non-mandatory microorganisms should be further evaluated. These results should be further confirmed increasing the number of analyzed water samples.

References

- [1] Prüss-Üstün, A., R. Bos, F. Gore, and J. Bartram. World Health Organization, Geneva, 2008.
- [2] Vale, F.F., A.M. Silva, A.T. Granja, M.J. Vale, and H. Vieira. Phys Status Solidi C 6 (2009) 2184.
- [3] Martins, N., Vale, F.F., Vieira, H. Phys Status Solidi C (In press).
- [4] Altschul, S.F., T.L. Madden, A.A. Schaffer, J. Zhang, Z. Zhang, W. Miller, and D.J. Lipman. Nucl. Acids Res. **25** (1997) 3389.



INDEX - POSTERS

Only Posters submitted by registered participants are listed below. Last update (23/08/2010)

(Please, find your final poster number by looking up your name in the Author Index displayed in the Registration and the Poster Exhibition Areas)

Alphabetical Order (173)

Presenting Author		Country	Topic	Poster Title	Student/ Senior
Abd El Fattah	Zakaria	Spain	Nanostructured and nanoparticle based materials	<i>Fermi Gap Engineering By Au doping of The Ag/Cu(111) Dislocation Network</i>	Student
Abreu	Ana Sofia	Portugal	Nanobiotechnologies	<i>Nanoliposomes for encapsulation and delivery of the potential antitumoral methyl 6-methoxy-3-(4-methoxyphenyl)-1H-indole-2-carboxylate</i>	Student
Aguilo-Aguayo	Noemv	Spain	Nanostructured and nanoparticle based materials	<i>Correlation between current applied and crystallinity of carbon in Fe@C nanoparticles obtained by plasma arc</i>	Student
Altenburg	Simon	Germany	Graphene / Carbon nanotubes based nanoelectronics and field emission	<i>Scanning tunneling microscopic investigations into electron transport through graphene</i>	Student
Alubaidy	Mohammed-Amin	Canada	Nanobiotechnologies	<i>Fabrication of nanofiber reinforced polymer microstructures through two photon polymerization</i>	Student
Alzina	Francesc	Spain	Graphene / Carbon nanotubes based nanoelectronics and field emission	<i>Probing electron dynamics in ozone-doped graphene by Raman spectroscopy</i>	Senior
Ambrosini	Stefano	Italy	Low dimensional materials (nanowires, clusters, quantum dots, etc.)	<i>Self catalyzed GaAs nanowires on GaAs (100): growth and characterization</i>	Student
An	Taechang	Korea	Nanofabrication tools & nanoscale integration	<i>Fabrication of Functional Micro- and Nanoneedle electrodes using Template of Carbon Nanotube Nanoneedle and Electrodeposition</i>	Student
Anaraki	Azam	Iran	NanoChemistry	<i>High photocatalytic activity of Zn₂SnO₄ among various structures of Zn₂xSn_{1-x}O₂ prepared by a hydrothermal method</i>	Student
Aranburu	Nora	Spain	Nanostructured and nanoparticle based materials	<i>Organoclay reinforced compatibilized nanocomposites of polypropylene with an amorphous polyamide</i>	Student
Arroyo-Hernandez	Maria	Spain	Low dimensional materials (nanowires, clusters, quantum dots, etc.)	<i>Catalytic growth of ZnO nanowires by rf magnetron sputtering</i>	Senior
Asedegbega Nieto	Esther	Spain	NanoChemistry	<i>Preparation and Surface Functionalization of MWCNTs: study of the composite materials produced by interaction with a iron phthalocyanine complex</i>	Senior
Asokan	Vijayshankar	Norway	Nanostructured and nanoparticle based materials	<i>Structural transformation of carbon black using a metal catalyst</i>	Student
Bache	Michael	Denmark	Nanobiotechnologies	<i>Pesticide detection using a surface stress micro cantilever system</i>	Student
Badylevich	Mikhail	Belgium	Low dimensional materials (nanowires, clusters, quantum dots, etc.)	<i>Ellipsometry study of SiGe nanocrystals embedded in SiO₂</i>	Senior
Balasubramanian	Vimalkumar	Switzerland	Nanostructured and nanoparticle based materials	<i>Polymeric nanoreactors: a new way to improve antioxidant therapy</i>	Student

Presenting Author		Country	Topic	Poster Title	Student/ Senior
Bañobre	Manuel	Spain	Nanostructured and nanoparticle based materials	<i>The influence of colloidal parameters on the specific power absorption of magnetite nanoparticles with core-shell structure.</i>	Student
Baptista	Pedro	Portugal	Nanobiotechnologies	<i>Gold-Nanoprobes for specific targets enrichment</i>	Senior
Batista	Carlos	Portugal	Other	<i>Synthesis and Characterisation of VO₂-based ThermoChromic Thin films for Energy Efficient Windows</i>	Student
Benedicto Cordoba	Marcos	Spain	Nanostructured and nanoparticle based materials	<i>Fabrication of HfO₂ patterns by nanoscale lithography methods and selective dry etching for III-V CMOS application</i>	Student
Benedicto Cordoba	Marcos	Spain	Nanostructured and nanoparticle based materials	<i>Nucleation of SrTiO₃ (STO) nanostructures on Si substrates prepared by metalorganic decomposition (MOD)</i>	Student
Berindan	Ioana	Romania	NanoChemistry	<i>Developing nanotechnology based cancer therapeutics: RNA interference as a powerful tool in gene silencing for p53</i>	Senior
Bosch-Navarro	Concha	Spain	Graphene / Carbon nanotubes based nanoelectronics and field emission	<i>Influence of the pH on the Hydrothermal-Assisted Synthesis of Graphene</i>	Student
Boutinguiza Larosi	Mohamed	Spain	Nanobiotechnologies	<i>Production of nanoparticles from natural and synthetic hydroxylapatite by laser ablation</i>	Senior
Branquinho	Rita	Portugal	Nanobiotechnologies	<i>Room Temperature Sputtered Ta₂O₅ for Solid State Biosensors</i>	Student
Cangueiro	Maguie	Portugal	Other	<i>In vitro transdermal delivery of caffeine-loaded alginate particles</i>	Student
Carabineiro	Sonia	Portugal	Nanostructured and nanoparticle based materials	<i>Gold nanoparticles supported on magnesium oxide for CO oxidation</i>	Senior
Carabineiro	Sonia	Portugal	Nanostructured and nanoparticle based materials	<i>Effect of the carbon nanotube surface characteristics on the percolation threshold and conductivity of carbon nanotube/poly(vinylidene fluoride) composites</i>	Senior
Carbo-Argibay	Enrique	Spain	NanoChemistry	<i>Tuning the Gold Nanorods Morphology</i>	Student
Cardinal	Maria Fernanda	Spain	NanoOptics & NanoPhotonics	<i>Modulation of Localized Surface Plasmons and SERS Response in Gold Dumbbells through Silver Coating</i>	Student
Carmona	Daniel	Spain	Nanomagnetism and Spintronics	<i>Silica rod-shape capsules embebing superparamagnetic iron oxide nanoparticles</i>	Student
Castanheira	Elisabete	Portugal	Nanobiotechnologies	<i>New potential antitumoral fluorescent tetracyclic thieno[3,2-b]pyridine derivatives: Interaction with DNA and encapsulation in nanoliposomes</i>	Senior
Castro	Eduardo	Spain	Graphene / Carbon nanotubes based nanoelectronics and field emission	<i>Temperature dependent resistivity due to flexural phonons in single and bilayer graphene</i>	Senior
Castro Lopez	Marta	Spain	NanoOptics & NanoPhotonics	<i>Observation of polarized multiphoton emission from resonant Al, Ag and Au nanoantennas</i>	Student
Cernohorsky	Ondrej	Czech Republic	Nanostructured and nanoparticle based materials	<i>Palladium nanoparticles on InP for hydrogen detection</i>	Student
Choi	WooSeok	Korea	Graphene / Carbon nanotubes based nanoelectronics and field emission	<i>Organic Electrochemical Transistors Based on Dielectrophoretically Aligned Nanowire Array</i>	Student

Presenting Author		Country	Topic	Poster Title	Student/ Senior
Clauzier	Stephanie	France	NanoChemistry	<i>Enhanced hydrogen solubility in nanosized ethanol and n-hexane confined in a silica aerogel matrix</i>	Student
Coluci	Vitor Rafael	Brazil	Theory and modelling at the nanoscale	<i>Carbon nanotube oscillators driven by thermophoresis</i>	Senior
Coluci	Vitor Rafael	Brazil	Nanobiotechnologies	<i>Modulation mechanisms of the genotoxicity of organic pollutants by carbon nanotubes</i>	Senior
Costa Lima	Sofia	Portugal	Nanobiotechnologies	<i>Pegylated nanoparticles for encapsulation of bisnaphthalimidopropyl derivatives against Leishmania infantum</i>	Senior
Coutinho	Paulo J. G.	Portugal	Nanostructured and nanoparticle based materials	<i>CdSe/TiO₂ core-shell nanoparticles produced in AOT reverse micelles: applications in pollutant photodegradation using visible light</i>	Senior
Cveticanin	Jelena	Yugoslavia	Nanostructured and nanoparticle based materials	<i>Studies on carbon nanotubes/silver clusters composites</i>	Student
Da Costa Martins	Raquel M.	Spain	Nanobiotechnologies	<i>Bioadhesive mannosamine-loaded nanoparticles for an effective ocular vaccination against animal brucellosis</i>	Student
Dadvand	Afshin	Canada	Low dimensional materials (nanowires, clusters, quantum dots, etc.)	<i>NIR Photoresponce in New Up-Converting CdSe/NaYF₄:Yb,Er Nano-Heterostructures</i>	Student
de la Escosura	Andres	Spain	Nanobiotechnologies	<i>Virus-Based Assemblies as Nanocontainers and Nanoreactors</i>	Senior
de Oliveira	Thales	Spain	Nanomagnetism and Spintronics	<i>Biotemplated polyaniline nanowires as building blocks for spin-valves</i>	Student
Diaz	Jordi	Spain	SPM	<i>Characterization of morphology, crystallization and melting behaviour of films of ethylene-vinyl acetate (EVA) by means of AFM and DSC</i>	Senior
Dieste	Oliver	Spain	Low dimensional materials (nanowires, clusters, quantum dots, etc.)	<i>Analysis of the process variables in Laser Spinning controlling the geometry of nanofibers</i>	Student
Domenech	Berta	Spain	NanoChemistry	<i>Polymer-stabilized Palladium Nanoparticles for catalytic membranes: ad hoc polymer fabrication.</i>	Student
Doria	Goncalo	Portugal	Nanobiotechnologies	<i>Multiplex genetic characterization via noble metal nanoprobos</i>	Senior
Drbohlavova	Jana	Czech Republic	Nanostructured and nanoparticle based materials	<i>TiO₂ highly ordered quantum dots prepared by anodization techniques on Si wafer</i>	Senior
Duarte	Abel J.	Portugal	NanoChemistry	<i>CdTe quantum dots based chemical nanosensors</i>	Student
Dubyanskiy	Sergey	Russia	Other	<i>Russian Nanotechnology Foresight and Roadmapping in Russian Corporation of Nanotechnologies (RUSNANO)</i>	Senior
Fabie	Laure	France	Nanofabrication tools & nanoscale integration	<i>Nanodroplet deposition and manipulation with an AFM tip</i>	Student
Fernandes	Sara	Portugal	Nanostructured and nanoparticle based materials	<i>Biosynthesis of silver nanoparticles by Aspergillus oryzae and Penicillium chrysogenum</i>	Senior
Ferreira	Tania	Portugal	Graphene / Carbon nanotubes based nanoelectronics and field emission	<i>Microinjection moulding of nanocomposites with modified carbon nanotubes: correlation between dispersion and electrical conductivity</i>	Student

Presenting Author		Country	Topic	Poster Title	Student/Senior
Flores	Raquel	Portugal	Nanomagnetism and Spintronics	<i>Serial MTJ sensors based on MgO in bridge configuration for in-chip current field detection</i>	Student
Fu	Chaoying	Canada	SPM	<i>Self-assembly of oligothiophenecarboxylic acid monolayer by Scanning Tunneling Microscope (STM)</i>	Student
Fujiki	Aya	Japan	NanoOptics & NanoPhotonics	<i>Tunneling-current-induced light emission from PTCDI-C7 thin films on the graphite and the Au(111) surfaces</i>	Student
Gallo	Juan	Spain	Nanobiotechnologies	<i>Core@Shell Fluorescent-Magnetic Glyco-ferrites as Specific Targeted Contrast Agents for Magnetic Resonance Imaging</i>	Student
Garcia	Cibeli	Portugal	Other	<i>Crystallographic Characterization of ZnO Thin Films by Electron Backscattered Diffraction</i>	Student
Garcia-Martin	Antonio	Spain	NanoOptics & NanoPhotonics	<i>Plasmon-Induced Magneto-Optical Activity in Nanosized Gold Disks</i>	Senior
Gnauck	Peter	Germany	Nanobiotechnologies	<i>High Resolution FIB-Nanotomography of biological cell tissue and investigation of interfaces between tissue and biocompatible materials</i>	Senior
Gomes	Raquel	Belgium	NanoChemistry	<i>NMR Studies on the Phosphonic Acid Oxide Capping of Colloidal Semiconductor Nanocrystals</i>	Senior
Gomes	Ines	Portugal	Nanobiotechnologies	<i>Tyrosinase-Gold Nanoparticles Bionanoconjugates on Nanostructured Gold Surfaces: Development of an Enzymatic Biosensor of Phenolic Compounds</i>	Senior
Gomes da Rocha	Claudia	Germany	Theory and modelling at the nanoscale	<i>Modelling nanosensor devices based on graphene ribbons</i>	Senior
Gomez	Virgina	Spain	Nanostructured and nanoparticle based materials	<i>One-step microwave synthesis and characterization of gadolinium-doped titania nanoparticles</i>	Student
Grueter	Raphael	Switzerland	Low dimensional materials (nanowires, clusters, quantum dots, etc.)	<i>Deposition and Modification of Nanowires by FluidFM technology</i>	Student
Grym	Jan	Czech Republic	Nanostructured and nanoparticle based materials	<i>Hydrogen Sensors Based on Electrophoretically Deposited Pd Nanoparticles onto InP</i>	Senior
Grym	Jan	Czech Republic	Nanofabrication tools & nanoscale integration	<i>Epitaxial growth of highly mismatched GaInAs layers on nanoporous GaAs substrates</i>	Senior
Guzman	Manuel	Spain	Nanostructured and nanoparticle based materials	<i>Reducing zinc oxide in rubber industry use through the development of mixed metal oxide nanoparticles</i>	Student
Hermosa	Cristina	Spain	NanoChemistry	<i>Towards alternative 2D polymers based on coordination polymers</i>	Student
Hosokawa	Yoshihiro	Japan	SPM	<i>Measurement of tip-sample interaction forces under infrared irradiation toward high-spatial-resolution infrared spectroscopy using FM-AFM</i>	Student
Hosseini	Ali A	Iran	Nanostructured and nanoparticle based materials	<i>The effects of Fe/Al₂O₃ preparation technique as a catalyst on synthesized CNTs in CVD method.</i>	Senior
Hrdy	Radim	Czech Republic	Nanostructured and nanoparticle based materials	<i>Electrochemical Perforation of the Aluminum Oxide Barrier Layer in Thin Film Micro Sensors</i>	Student
Hwang	Sung-Ho	Korea	Low dimensional materials (nanowires, clusters, quantum dots, etc.)	<i>Preparation and Gas Sensing Characteristics of Mesoporous In₂O₃ Nanofibers</i>	Senior

Presenting Author		Country	Topic	Poster Title	Student/ Senior
Imura	Ken-Ichiro	Japan	Graphene / Carbon nanotubes based nanoelectronics and field emission	<i>Zigzag edge modes of a Z2 topological insulator -- reentrance and completely flat spectrum</i>	Senior
Inestrosa	Maria Jose	Spain	Low dimensional materials (nanowires, clusters, quantum dots, etc.)	<i>Growth and structure of silicon clusters generated by low frequency square wave plasma modulation</i>	Student
Inglot	Michal	Poland	Graphene / Carbon nanotubes based nanoelectronics and field emission	<i>Local magnetic and electric state in pure and doped graphene</i>	Student
Janeiro	Ricardo	Portugal	Nanomagnetism and Spintronics	<i>MgO MTJ biosensors for immunomagnetic lateral lateral-flow detection</i>	Student
Justo	Yolanda	Belgium	Nanostructured and nanoparticle based materials	<i>The use of Langmuir-Blodgett films of PbSe/CdSe quantum dots for the determination of the PbSe/CdSe band alignment</i>	Student
Justo	Yolanda	Belgium	Nanostructured and nanoparticle based materials	<i>Langmuir-Blodgett films of lead chalcogenide quantum dots</i>	Student
Kadari	Belkacem	Canada	Nanostructured and nanoparticle based materials	<i>Luminescence of Silicon Nanocrystals</i>	Student
Kamal	John Sundar	Belgium	Low dimensional materials (nanowires, clusters, quantum dots, etc.)	<i>Anisotropic local field factors determine the absorption coefficient of colloidal quantum rods.</i>	Student
Kamal	John Sundar	Belgium	Low dimensional materials (nanowires, clusters, quantum dots, etc.)	<i>Size dependent optical properties of zinc blende CdTe nanocrystals</i>	Student
Khan	Abid Ali	Spain	Nanobiotechnologies	<i>Plant Virus Drug Delivery</i>	Student
Kim	Duckjong	Korea	Graphene / Carbon nanotubes based nanoelectronics and field emission	<i>Physical Change of Transparent Film Heaters Based on Single-Walled Carbon Nanotubes in High Temperature Environment</i>	Senior
Kolar	Petr	Czech Republic	Nanobiotechnologies	<i>Cell adhesion study to new endosteal implant by atomic force microscopy</i>	Student
Kumar	Shishir	Ireland	Graphene / Carbon nanotubes based nanoelectronics and field emission	<i>Lithographic Processing for Large Area CVD Graphene</i>	Student
Leconte	Nicolas	Belgium	Graphene / Carbon nanotubes based nanoelectronics and field emission	<i>Damaging Graphene with Ozone Treatment : a Chemically Tunable Metal-Insulator Transition</i>	Student
Lee	Soo-Keun	Korea	Nanostructured and nanoparticle based materials	<i>Preparation and characterization of coordination polymer particles with various aspect ratio</i>	Senior
Lepage	Dominic	Canada	NanoOptics & NanoPhotonics	<i>Hyperspectral imaging of surface plasmon resonance effects induced by uncollimated semiconductor radiation</i>	Student
Li	Wu	Germany	Theory and modelling at the nanoscale	<i>Phonon Transport in Large Scale Carbon-Based Disordered Materials: Implementation of an Efficient Order N and Real Space Kubo Methodology</i>	Student
Liao	Si-Yu	France	Graphene / Carbon nanotubes based nanoelectronics and field emission	<i>Non-volatile memory using Optically-Gated Carbon Nanotube FET: Description of carrier mobility model in P3OT and source-drain Schottky barrier</i>	Student
Lim	Sang Kyoo	Korea	Nanostructured and nanoparticle based materials	<i>Preparation and characterization of ZnO Nanofibers by Electrospinning</i>	Senior

Presenting Author		Country	Topic	Poster Title	Student/Senior
Lopez	Kenia	Spain	Nanostructured and nanoparticle based materials	<i>Squaramide Magnetic Iron Nanoparticles for the Selective Removal of Hg²⁺ Ions in Water</i>	Student
Lukman	Audra	Australia	Low dimensional materials (nanowires, clusters, quantum dots, etc.)	<i>Synthesis of Silver and Gold Nanoparticles in Aqueous Solutions Mediated by Naturally Occurring Compounds in Common Sprouting Seed Exudates</i>	Student
Madurga	Vicente	Spain	Nanofabrication tools & nanoscale integration	<i>Generating and measuring anisotropic elastic behavior of Co thin films with oriented surface nano-strings on micro-cantilevers</i>	Senior
Maftouni	Negin	Iran	Nanobiotechnologies	<i>Comparative Molecular dynamics simulation study of interaction of two cytotoxins and POPC nanobio membrane</i>	Student
Maia	Raquel	Portugal	Nanostructured and nanoparticle based materials	<i>Development of nanostructured 3D matrices to direct mesenchymal stem cells behaviour</i>	Student
Makk	Peter	Hungary	Low dimensional materials (nanowires, clusters, quantum dots, etc.)	<i>Identifying stable atomic configurations by the correlation analysis of conductance traces</i>	Student
Marinho	Zita	Portugal	Nanomagnetism and Spintronics	<i>Improving Magnetic Field Detection Limits of Spin Valve Sensors Using 3D Magnetic Flux Guide Concentrators</i>	Student
Marques	Leonel	Portugal	Nanostructured and nanoparticle based materials	<i>Carbon clathrates from fullerite under high pressure</i>	Senior
Martin	Jose I.	Spain	Nanomagnetism and Spintronics	<i>Magnetic force microscopy characterization of the magnetization reversal processes in high density arrays of Co bars with strong dipolar interactions</i>	Senior
Martin Becerra	Diana	Spain	NanoOptics & NanoPhotonics	<i>Wavelength dependence of the SPP wavevector magnetic modulation in Au/Co/Au films</i>	Student
Martinez	Gerardo	Spain	NanoChemistry	<i>Modification of Carbon Nanotubes and Graphene with 1-octadecylalcohol for Polymer Nanocomposites</i>	Senior
Martin-Martinez	Francisco	Spain	Theory and modelling at the nanoscale	<i>Energetic destabilization causes in carbon nanotubes with topological defects</i>	Student
Martins	Manuel	Portugal	Nanobiotechnologies	<i>Multifunctional nanocomposite particles for bio-labeling</i>	Student
Martin-Sanchez	Javier	Portugal	Low dimensional materials (nanowires, clusters, quantum dots, etc.)	<i>Morphological and structural characterization of Ge nanoparticles produced by Pulsed Laser Deposition</i>	Senior
Medina	Jose M.	Portugal	NanoOptics & NanoPhotonics	<i>Multispectral Imaging of Natural Photonic Nanostructures</i>	Senior
Miyake	Yusuke	Japan	SPM	<i>Tunneling-current-induced light emission from chiral binaphthylene-<i>perylenebiscarboxydiimide</i> dimer</i>	Senior
Mohiuddin	Mohammad	Canada	Nanostructured and nanoparticle based materials	<i>Electrical resistance of CNT-peek composites under temperature and compression</i>	Student
Molina Brito	Bertha	Mexico	Theory and modelling at the nanoscale	<i>Theoretical Analysis of the Electronic Properties of the Endohedral Clusters M@Al₁₂ (M= B, Al, Si, N, P) and their ions</i>	Senior
Morantz	Matthew	Canada	Nanostructured and nanoparticle based materials	<i>Synthesis, Nanostructural and Electronic Characterization of Anthracenedicarboximide Derivatives.</i>	Student
Morey	Jeroni	Spain	Nanostructured and nanoparticle based materials	<i>Novel Hybrid Nanoparticles Based on Squaramides</i>	Senior

Presenting Author		Country	Topic	Poster Title	Student/ Senior
Mostofi	Mehdi	Iran	Theory and modelling at the nanoscale	<i>Variable Physical Properties Effect on Velocity and Potential Distribution in a Nanotube with Large Zeta Potential</i>	Student
Moya	Sergio	Spain	NanoChemistry	<i>Confocal Raman Microscopy for the study of cell uptake of nanoparticles and toxicity</i>	Senior
Najari	Montasar	France	Graphene / Carbon nanotubes based nanoelectronics and field emission	<i>Design of 6T SRAM memory cell using a SB-CNTFET compact model</i>	Student
Nikolova	Liliya	Canada	Nanostructured and nanoparticle based materials	<i>In-situ Observations of Amorphous Germanium Nucleation and Nanocrystallization by Dynamic Transmission Electron Microscopy</i>	Student
Novais	Rui	Portugal	Nanostructured and nanoparticle based materials	<i>Chemical functionalization of carbon nanotubes and its influence on composite properties</i>	Student
Novosad	Valentyn	United States	Nanobiotechnologies	<i>Magneto-Mechanical Actuation: A Novel Approach to Targeted Cancer Cell Destruction</i>	Senior
Nuansing	Wiwat	Spain	NanoChemistry	<i>p-p Stacking in the Aromatic Peptides Electrospun Fibers</i>	Student
Olesen	Mikkel	Denmark	Graphene / Carbon nanotubes based nanoelectronics and field emission	<i>Electrical Measurements on Graphene Inside Scanning Electron Microscope Using Four Point Probes</i>	Student
Paiva	Diana	Portugal	Nanostructured and nanoparticle based materials	<i>Fluorinated Cholesterol based system with DOTAP for DNA Transfection</i>	Student
Paleo	Antonio J.	Portugal	Nanostructured and nanoparticle based materials	<i>Nanoparticle induced phase transformation and dielectric response of core/shell Fe/MgO-poly(vinylidene fluoride) nanocomposites</i>	Student
Pantis	Dan	Romania	Nanobiotechnologies	<i>The radio frequency systems to potentate the therapeutic properties of nanostructures and nanosystems as carriers into the cell.</i>	Student
Paulo	Cristiana	Portugal	Nanostructured and nanoparticle based materials	<i>Antifungal nanoparticles</i>	Student
Peraza Hernandez	Jose F.	Spain	Nanostructured and nanoparticle based materials	<i>Up-conversion and down-shifting in sol-gel derived glass-ceramics containing rare-earth doped SnO₂ and LaF₃ nanocrystals</i>	Senior
Peraza Hernandez	Jose F.	Spain	Nanostructured and nanoparticle based materials	<i>Sol-gel derived nano-glass-ceramics comprising RE-doped KYF₄ nanocrystals</i>	Senior
Perez	Jorge	Spain	Theory and modelling at the nanoscale	<i>Melting temperature of icosahedral metallic nanowires</i>	Student
Piksova	katerina	Czech Republic	SPM	<i>SEM Imaging of Films of Metal Nanoparticles Deposited on Semiconductors</i>	Senior
Pinto	Sara	Portugal	Nanostructured and nanoparticle based materials	<i>Structural study of multilayers of Si_{1-x}Gex Nanocrystals embedded in SiO₂ matrix</i>	Student
Piñeiro	Yolanda	Spain	Nanostructured and nanoparticle based materials	<i>Remote magnetic heating of smart thermoresponsive PNIPAM-Fe₃O₄ nanocomposites</i>	Senior
Plenat	Thomas	France	Nanobiotechnologies	<i>A novel DNA chip for single molecule analysis</i>	Senior
Popoff	Sebastien	France	NanoOptics & NanoPhotonics	<i>Controlling Light Inside Disordered Matrial : Matrix Model and Applications</i>	Student

Presenting Author		Country	Topic	Poster Title	Student/ Senior
Porro Azpiazu	Jose Maria	Spain	Nanomagnetism and Spintronics	<i>Effects of asymmetric dipolar interactions between elliptical ferromagnetic nanomagnets in artificial spin-ice structures</i>	Student
Prasek	Jan	Czech Republic	Nanostructured and nanoparticle based materials	<i>Utilizing Vertically Aligned Carbon Nanotubes Based Working Electrodes for Detection of Heavy Metal Ions and Thiols</i>	Senior
Prieto Ruiz	Juan Pablo	Spain	Nanomagnetism and Spintronics	<i>Magneto-optical characterization of CrII3/2[CrIII(CN)6] Prussian Blue Analogue films performed by Kerr magnetometry</i>	Student
Proenca	Mariana	Portugal	Low dimensional materials (nanowires, clusters, quantum dots, etc.)	<i>Fast deposition of elongated Nickel nanowires inside nanoporous alumina templates</i>	Student
Quintero Martinez	Felix	Spain	Low dimensional materials (nanowires, clusters, quantum dots, etc.)	<i>Production of glass nanofibers from fragile melts by Laser Spinning</i>	Senior
Rakovich	Aliaksandra	Ireland	Nanobiotechnologies	<i>Development of Nano-Bio hybrid material based on CdTe Quantum Dots and Bacteriorhodopsin protein for future technologies</i>	Student
Reis	Catarina	Portugal	Nanostructured and nanoparticle based materials	<i>Design and transdermal delivery of indomethacin nanosystem</i>	Senior
Rivero	Pedro Jose	Spain	NanoOptics & NanoPhotonics	<i>Lossy-mode resonance based optical fiber pH sensors</i>	Student
Rivero Fuente	Pedro	Spain	Nanostructured and nanoparticle based materials	<i>An antibacterial coating based on silver loaded in a polymer/sol-gel hybrid matrix</i>	Student
Rodriguez-Abreu	Carlos	Portugal	Nanostructured and nanoparticle based materials	<i>Fabrication of silica hollow microcoils with mesoporous walls</i>	Senior
Roussel	Florent	France	Nanostructured and nanoparticle based materials	<i>1D polymer/CNT composite : elaboration and transport properties</i>	Student
Ruiz Nicolas	Patricia	Spain	Nanostructured and nanoparticle based materials	<i>Intermatrix synthesis: easy technique permitting preparation of polymer-stabilized nanoparticles with desired composition and structure.</i>	Student
Saenz-Arce	Giovanni	Spain	SPM	<i>Adhesion and Energy Dissipation on the Formation of One-Atom Contact on Au and Pb</i>	Student
Salavagione	Horacio Javier	Spain	Graphene / Carbon nanotubes based nanoelectronics and field emission	<i>Synthesis of Few Layer Graphene by Electrochemical Intercalation and Exfoliation Induced by a Polymeric Surfactant</i>	Senior
Samantilleke	Anura	Portugal	Nanostructured and nanoparticle based materials	<i>Cohesive strength of ZnO:Ga thin films deposited at room temperature</i>	Senior
Samantilleke	Anura	Portugal	Nanostructured and nanoparticle based materials	<i>Nanostructured hybrid ZnO thin films for energy conversion</i>	Senior
Santamaria	Pablo	Spain	Nanostructured and nanoparticle based materials	<i>Effects of draw ratio on the structure and properties of polycarbonate films reinforced by an amorphous polyamide nanocomposite</i>	Student
Schellenberg	Peter	Portugal	Graphene / Carbon nanotubes based nanoelectronics and field emission	<i>Visibility enhancement of Graphene on multiple substrates</i>	Senior
Schneider	Natalia	Germany	SPM	<i>Optical probe of quantum shot noise reduction at a single atom contact</i>	Student
Sedighi	Amir	Germany	Theory and modelling at the nanoscale	<i>Molecular simulation of dendritic core multi shell(CMS) nanotransporter</i>	Student

Presenting Author		Country	Topic	Poster Title	Student/ Senior
Sencadas	Vitor	Portugal	Nanobiotechnologies	<i>Thermal annealing induced crystallization and phase transformation in electrospun poly(lactic acid) nanofibers</i>	Student
Sergeyev	Daulet	Kazakhstan	Other	<i>4e transport of a supercurrent in two-contact SQUID with anharmonic by current - phase dependence</i>	Student
Serrano	Aida	Spain	NanoOptics & NanoPhotonics	<i>Itinerant and localized surface plasmons in annealed Au films</i>	Student
Shen	Jing	France	Theory and modelling at the nanoscale	<i>Formation and properties of iron nanoparticles for nucleating CNTs in floating-catalyst CVD process</i>	Student
Silva Oliveira	Liliana Filipa	Portugal	Nanostructured and nanoparticle based materials	<i>Development of photocatalytic nanomaterials for pollution control, using thin film deposition techniques (sol-gel, PVD)</i>	Student
Suarez Guevara	Jullieth	Spain	Nanostructured and nanoparticle based materials	<i>Hydrothermal Synthesis of Metal-Polymer Hybrid Nanostructures. Polypyrrole-coated Copper Nanocables</i>	Student
Tomankova	Katerina	Czech Republic	Nanobiotechnologies	<i>Photodynamic effect on cytomechanical and morphological properties of HeLa cell lines</i>	Senior
Trpkov	Djordje	Yugoslavia	Nanobiotechnologies	<i>Optimal 99mTc radiolabeling of fullereneol C60(OH)22 – 24, potential tracer for scintigraphic investigation of kidneys and urinary bladder</i>	Student
Valtr	Miroslav	Czech Republic	SPM	<i>Atomic force microscopy characterization of nanoparticles on rough surfaces</i>	Student
Vasconcelos	Helena	Portugal	NanoOptics & NanoPhotonics	<i>Er³⁺ as optical probe to detect order/disorder in SiO₂-TiO₂-PO_{2.5} sol-gel thin films</i>	Senior
Vega	Andres	Spain	Low dimensional materials (nanowires, clusters, quantum dots, etc.)	<i>Stability, electronic structure and conductivity of monoatomic Mo wires inside carbon nanotubes</i>	Senior
Veigas	Bruno	Portugal	Nanobiotechnologies	<i>A PCR-Au-nanoprobes combined approach for detection of mutations associated with antibiotic resistance in Mycobacterium tuberculosis</i>	Student
Veverkova	Lenka	Czech Republic	NanoChemistry	<i>Interactions of heparine with polymethinium salts capped gold nanoparticles in aqueous environment.</i>	Student
Vieira	Eliana	Portugal	Nanostructured and nanoparticle based materials	<i>Structural and electrical characterization of Si_{1-x}Gex nanocrystals embedded in Al₂O₃ matrix</i>	Student
Voinova	Marina	Sweden	Nanobiotechnologies	<i>Mechanics of lipid nanotube networks and microcontainers</i>	Senior
Xuriguera	Elena	Spain	Nanostructured and nanoparticle based materials	<i>Study on oxidation layer of single core Nickel nanobeads</i>	Senior
Zabaleta	Asier	Spain	Nanostructured and nanoparticle based materials	<i>Characterization and properties of polyamide 12 nanocomposites</i>	Student
Zvatora	Pavel	Czech Republic	Nanostructured and nanoparticle based materials	<i>Polytetrafluorethylene as a substrate for surface enhanced Raman spectroscopy</i>	Student

Poster Contributions by Topics (173)

Presenting Author	Country	Poster Title	
TOPIC: Carbon Nanotubes Based Nanoelectronics and Field Emission			
Altenburg	Simon	Germany	<i>Scanning tunneling microscopic investigations into electron transport through graphene</i>
Alzina	Francesc	Spain	<i>Probing electron dynamics in ozone-doped graphene by Raman spectroscopy</i>
Bosch-Navarro	Concha	Spain	<i>Influence of the pH on the Hydrothermal-Assisted Synthesis of Graphene</i>
Castro	Eduardo	Spain	<i>Temperature dependent resistivity due to flexural phonons in single and bilayer graphene</i>
Choi	WooSeok	Korea	<i>Organic Electrochemical Transistors Based on Dielectrophoretically Aligned Nanowire Array</i>
Ferreira	Tania	Portugal	<i>Microinjection moulding of nanocomposites with modified carbon nanotubes: correlation between dispersion and electrical conductivity</i>
Imura	Ken-Ichiro	Japan	<i>Zigzag edge modes of a Z2 topological insulator --- reentrance and completely flat spectrum</i>
Inglot	Michal	Poland	<i>Local magnetic and electric state in pure and doped graphene</i>
Kim	Duckjong	Korea	<i>Physical Change of Transparent Film Heaters Based on Single-Walled Carbon Nanotubes in High Temperature Environment</i>
Kumar	Shishir	Ireland	<i>Lithographic Processing for Large Area CVD Graphene</i>
Leconte	Nicolas	Belgium	<i>Damaging Graphene with Ozone Treatment : a Chemically Tunable Metal-Insulator Transition</i>
Liao	Si-Yu	France	<i>Non-volatile memory using Optically-Gated Carbon Nanotube FET: Description of carrier mobility model in P3OT and source-drain Schottky barrier</i>
Najari	Montasar	France	<i>Design of 6T SRAM memory cell using a SB-CNTFET compact model</i>
Olesen	Mikkel	Denmark	<i>Electrical Measurements on Graphene Inside Scanning Electron Microscope Using Four Point Probes</i>
Salavagione	Horacio Javier	Spain	<i>Synthesis of Few Layer Graphene by Electrochemical Intercalation and Exfoliation Induced by a Polymeric Surfactant</i>
Schellenberg	Peter	Portugal	<i>Visibility enhancement of Graphene on multiple substrates</i>
TOPIC: Low-Dimensional Materials			
Ambrosini	Stefano	Italy	<i>Self catalyzed GaAs nanowires on GaAs (100): growth and characterization</i>
Arroyo-Hernandez	Maria	Spain	<i>Catalytic growth of ZnO nanowires by rf magnetron sputtering</i>

Presenting Author		Country	Poster Title
Badylevich	Mikhail	Belgium	<i>Ellipsometry study of SiGe nanocrystals embedded in SiO₂</i>
Dadvand	Afshin	Canada	<i>NIR Photoresponce in New Up-Converting CdSe/NaYF₄:Yb,Er Nano-Heterostructures</i>
Dieste	Oliver	Spain	<i>Analysis of the process variables in Laser Spinning controlling the geometry of nanofibers</i>
Grueter	Raphael	Switzerland	<i>Deposition and Modification of Nanowires by FluidFM technology</i>
Hwang	Sung-Ho	Korea	<i>Preparation and Gas Sensing Characteristics of Mesoporous In₂O₃ Nanofibers</i>
Inestrosa	Maria Jose	Spain	<i>Growth and structure of silicon clusters generated by low frequency square wave plasma modulation</i>
Kamal	John Sundar	Belgium	<i>Anisotropic local field factors determine the absorption coefficient of colloidal quantum rods.</i>
Kamal	John Sundar	Belgium	<i>Size dependent optical properties of zinc blende CdTe nanocrystals</i>
Lukman	Audra	Australia	<i>Synthesis of Silver and Gold Nanoparticles in Aqueous Solutions Mediated by Naturally Occurring Compounds in Common Sprouting Seed Exudates</i>
Makk	Peter	Hungary	<i>Identifying stable atomic configurations by the correlation analysis of conductance traces</i>
Martin-Sanchez	Javier	Portugal	<i>Morphological and structural characterization of Ge nanoparticles produced by Pulsed Laser Deposition</i>
Proenca	Mariana	Portugal	<i>Fast deposition of elongated Nickel nanowires inside nanoporous alumina templates</i>
Quintero Martinez	Felix	Spain	<i>Production of glass nanofibers from fragile melts by Laser Spinning</i>
Vega	Andres	Spain	<i>Stability, electronic structure and conductivity of monoatomic Mo wires inside carbon nanotubes</i>
TOPIC: Nanobiotechnologies			
Abreu	Ana Sofia	Portugal	<i>Nanoliposomes for encapsulation and delivery of the potential antitumoral methyl 6-methoxy-3-(4-methoxyphenyl)-1H-indole-2-carboxylate</i>
Alubaidy	Mohammed-Amin	Canada	<i>Fabrication of nanofiber reinforced polymer microstructures through two photon polymerization</i>
Bache	Michael	Denmark	<i>Pesticide detection using a surface stress micro cantilever system</i>
Baptista	Pedro	Portugal	<i>Gold-Nanoprobes for specific targets enrichment</i>
Boutinguiza Larosi	Mohamed	Spain	<i>Production of nanoparticles from natural and synthetic hydroxylapatite by laser ablation</i>
Branquinho	Rita	Portugal	<i>Room Temperature Sputtered Ta₂O₅ for Solid State Biosensors</i>
Castanheira	Elisabete	Portugal	<i>New potential antitumoral fluorescent tetracyclic thieno[3,2-b]pyridine derivatives: Interaction with DNA and encapsulation in nanoliposomes</i>
Coluci	Vitor Rafael	Brazil	<i>Modulation mechanisms of the genotoxicity of organic pollutants by carbon nanotubes</i>
Costa Lima	Sofia	Portugal	<i>Pegylated nanoparticles for encapsulation of bisnaphthalimidopropyl derivatives against Leishmania infantum</i>
Da Costa Martins	Raquel M.	Spain	<i>Bioadhesive mannosamine-loaded nanoparticles for an effective ocular vaccination against animal brucellosis</i>
de la Escosura	Andres	Spain	<i>Virus-Based Assemblies as Nanocontainers and Nanoreactors</i>
Doria	Goncalo	Portugal	<i>Multiplex genetic characterization via noble metal nanoprobes</i>
Gallo	Juan	Spain	<i>Core@Shell Fluorescent-Magnetic Glyco-ferrites as Specific Targeted Contrast Agents for Magnetic Resonance Imaging</i>
Gnauck	Peter	Germany	<i>High Resolution FIB-Nanotomography of biological cell tissue and investigation of interfaces between tissue and biocompatible materials</i>

Presenting Author		Country	Poster Title
Gomes	Ines	Portugal	<i>Tyrosinase-Gold Nanoparticles Bionanoconjugates on Nanostructured Gold Surfaces: Development of an Enzymatic Biosensor of Phenolic Compounds</i>
Khan	Abid Ali	Spain	<i>Plant Virus Drug Delivery</i>
Kolar	Petr	Czech Republic	<i>Cell adhesion study to new endosteal implant by atomic force microscopy</i>
Maftouni	Negin	Iran	<i>Comparative Molecular dynamics simulation study of interaction of two cytotoxins and POPC nanobio membrane</i>
Martins	Manuel	Portugal	<i>Multifunctional nanocomposite particles for bio-labeling</i>
Novosad	Valentyn	United States	<i>Magneto-Mechanical Actuation: A Novel Approach to Targeted Cancer Cell Destruction</i>
Pantis	Dan	Romania	<i>The radio frequency systems to potentate the therapeutic properties of nanostructures and nanosystems as carriers into the cell.</i>
Plenat	Thomas	France	<i>A novel DNA chip for single molecule analysis</i>
Rakovich	Aliaksandra	Ireland	<i>Development of Nano-Bio hybrid material based on CdTe Quantum Dots and Bacteriorhodopsin protein for future technologies</i>
Sencadas	Vitor	Portugal	<i>Thermal annealing induced crystallization and phase transformation in electrospun poly(lactic acid) nanofibers</i>
Tomankova	Katerina	Czech Republic	<i>Photodynamic effect on cytomechanical and morphological properties of HeLa cell lines</i>
Trpkov	Djordje	Yugoslavia	<i>Optimal 99mTc radiolabeling of fullerene C60 (OH)22 – 24, potential tracer for scintigraphic investigation of kidneys and urinary bladder</i>
Veigas	Bruno	Portugal	<i>A PCR-Au-nanoprobes combined approach for detection of mutations associated with antibiotic resistance in Mycobacterium tuberculosis</i>
Voinova	Marina	Sweden	<i>Mechanics of lipid nanotube networks and microcontainers</i>
TOPIC: Nanochemistry			
Anaraki	Azam	Iran	<i>High photocatalytic activity of Zn₂SnO₄ among various structures of Zn₂xSn_{1-x}O₂ prepared by a hydrothermal method</i>
Asedegbega Nieto	Esther	Spain	<i>Preparation and Surface Functionalization of MWCNTs: study of the composite materials produced by interaction with a iron phthalocyanine complex</i>
Berindan	Ioana	Romania	<i>Developing nanotechnology based cancer therapeutics: RNA interference as a powerful tool in gene silencing for p53</i>
Carbo-Argibay	Enrique	Spain	<i>Tuning the Gold Nanorods Morphology</i>
Clauzier	Stephanie	France	<i>Enhanced hydrogen solubility in nanosized ethanol and n-hexane confined in a silica aerogel matrix</i>
Domenech	Berta	Spain	<i>Polymer-stabilized Palladium Nanoparticles for catalytic membranes: ad hoc polymer fabrication.</i>
Duarte	Abel J.	Portugal	<i>CdTe quantum dots based chemical nanosensors</i>
Gomes	Raquel	Belgium	<i>NMR Studies on the Phosphonic Acid Oxide Capping of Colloidal Semiconductor Nanocrystals</i>
Hermosa	Cristina	Spain	<i>Towards alternative 2D polymers based on coordination polymers</i>
Martinez	Gerardo	Spain	<i>Modification of Carbon Nanotubes and Graphene with 1-octadecylalcohol for Polymer Nanocomposites</i>
Moya	Sergio	Spain	<i>Confocal Raman Microscopy for the study of cell uptake of nanoparticles and toxicity</i>

Presenting Author		Country	Poster Title
Nuansing	Wiwat	Spain	<i>p-p Stacking in the Aromatic Peptides Electrospun Fibers</i>
Veverkova	Lenka	Czech Republic	<i>Interactions of heparine with polymethinium salts capped gold nanoparticles in aqueous environment.</i>
TOPIC: Nanofabrication Tools and Nanoscale Integration			
An	Taechang	Korea	<i>Fabrication of Functional Micro- and Nanoneedle electrodes using Template of Carbon Nanotube Nanoneedle and Electrodeposition</i>
Fabie	Laure	France	<i>Nanodroplet deposition and manipulation with an AFM tip</i>
Grym	Jan	Czech Republic	<i>Epitaxial growth of highly mismatched GaInAs layers on nanoporous GaAs substrates</i>
Madurga	Vicente	Spain	<i>Generating and measuring anisotropic elastic behavior of Co thin films with oriented surface nano-strings on micro-cantilevers</i>
TOPIC: Nanomagnetism and Spintronics			
Carmona	Daniel	Spain	<i>Silica rod-shape capsules embebing superparamagnetic iron oxide nanoparticles</i>
de Oliveira	Thales	Spain	<i>Biotemplated polyaniline nanowires as building blocks for spin-valves</i>
Flores	Raquel	Portugal	<i>Serial MTJ sensors based on MgO in bridge configuration for in-chip current field detection</i>
Janeiro	Ricardo	Portugal	<i>MgO MTJ biosensors for immunomagnetic lagteral lateral-flow detection</i>
Marinho	Zita	Portugal	<i>Improving Magnetic Field Detection Limits of Spin Valve Sensors Using 3D Magnetic Flux Guide Concentrators</i>
Martin	Jose I.	Spain	<i>Magnetic force microscopy characterization of the magnetization reversal processes in high density arrays of Co bars with strong dipolar interactions</i>
Porro Azpiazu	Jose Maria	Spain	<i>Effects of asymmetric dipolar interactions between elliptical ferromagnetic nanomagnets in artificial spin-ice structures</i>
Prieto Ruiz	Juan Pablo	Spain	<i>Magneto-optical characterization of CrI₃/2[Cr^{III}(CN)₆] Prussian Blue Analogue films performed by Kerr magnetometry</i>
TOPIC: NanoOptics & NanoPhotonics			
Cardinal	Maria Fernanda	Spain	<i>Modulation of Localized Surface Plasmons and SERS Response in Gold Dumbbells through Silver Coating</i>
Castro Lopez	Marta	Spain	<i>Observation of polarized multiphoton emission from resonant Al, Ag and Au nanoantennas</i>
Fujiki	Aya	Japan	<i>Tunneling-current-induced light emission from PTCDI-C7 thin films on the graphite and the Au(111) surfaces</i>
Garcia-Martin	Antonio	Spain	<i>Plasmon-Induced Magneto-Optical Activity in Nanosized Gold Disks</i>
Lepage	Dominic	Canada	<i>Hyperspectral imaging of surface plasmon resonance effects induced by uncollimated semiconductor radiation</i>

Presenting Author		Country	Poster Title
Martin Becerra	Diana	Spain	<i>Wavelength dependence of the SPP wavevector magnetic modulation in Au/Co/Au films</i>
Medina	Jose M.	Portugal	<i>Multispectral Imaging of Natural Photonic Nanostructures</i>
Popoff	Sebastien	France	<i>Controlling Light Inside Disordered Matrial : Matrix Model and Applications</i>
Rivero	Pedro Jose	Spain	<i>Lossy-mode resonance based optical fiber pH sensors</i>
Serrano	Aida	Spain	<i>Itinerant and localized surface plasmons in annealed Au films</i>
Vasconcelos	Helena	Portugal	<i>Er3+ as optical probe to detect order/disorder in SiO2-TiO2-PO2.5 sol-gel thin films</i>
TOPIC: Nanostructured and Nanoparticle Based Materials			
Abd El Fattah	Zakaria	Spain	<i>Fermi Gap Engineering By Au doping of The Ag/Cu(111) Dislocation Network</i>
Aguilo-Aguayo	Noemv	Spain	<i>Correlation between current applied and crystallinity of carbon in Fe@C nanoparticles obtained by plasma arc</i>
Aranburu	Nora	Spain	<i>Organoclay reinforced compatibilized nanocomposites of polypropylene with an amorphous polyamide</i>
Asokan	Vijayshankar	Norway	<i>Structural transformation of carbon black using a metal catalyst</i>
Balasubramanian	Vimalkumar	Switzerland	<i>Polymeric nanoreactors: a new way to improve antioxidant therapy</i>
Bañobre	Manuel	Spain	<i>The influence of colloidal parameters on the specific power absorption of magnetite nanoparticles with core-shell structure.</i>
Benedicto Cordoba	Marcos	Spain	<i>Fabrication of HfO2 patterns by nanoscale lithography methods and selective dry etching for III-V CMOS application</i>
Benedicto Cordoba	Marcos	Spain	<i>Nucleation of SrTiO3 (STO) nanostructures on Si substrates prepared by metalorganic decomposition (MOD)</i>
Carabineiro	Sonia	Portugal	<i>Gold nanoparticles supported on magnesium oxide for CO oxidation</i>
Carabineiro	Sonia	Portugal	<i>Effect of the carbon nanotube surface characteristics on the percolation threshold and conductivity of carbon nanotube/poly(vinylidene fluoride) composites</i>
Cernohorsky	Ondrej	Czech Republic	<i>Palladium nanoparticles on InP for hydrogen detection</i>
Coutinho	Paulo J. G.	Portugal	<i>CdSe/TiO2 core-shell nanoparticles produced in AOT reverse micelles: applications in pollutant photodegradation using visible light</i>
Cveticanin	Jelena	Yugoslavia	<i>Studies on carbon nanotubes/silver clusters composites</i>
Drbohlavova	Jana	Czech Republic	<i>TiO2 highly ordered quantum dots prepared by anodization techniques on Si wafer</i>
Fernandes	Sara	Portugal	<i>Biosynthesis of silver nanoparticles by Aspergillus oryzae and Penicillium chrysogenum</i>

Presenting Author		Country	Poster Title
Gomez	Virgina	Spain	<i>One-step microwave synthesis and characterization of gadolinium-doped titania nanoparticles</i>
Grym	Jan	Czech Republic	<i>Hydrogen Sensors Based on Electrophoretically Deposited Pd Nanoparticles onto InP</i>
Guzman	Manuel	Spain	<i>Reducing zinc oxide in rubber industry use through the development of mixed metal oxide nanoparticles</i>
Hosseini	Ali A	Iran	<i>The effects of Fe/Al₂O₃ preparation technique as a catalyst on synthesized CNTs in CVD method.</i>
Hrdy	Radim	Czech Republic	<i>Electrochemical Perforation of the Aluminum Oxide Barrier Layer in Thin Film Micro Sensors</i>
Justo	Yolanda	Belgium	<i>The use of Langmuir-Blodgett films of PbSe/CdSe quantum dots for the determination of the PbSe/CdSe band alignment</i>
Justo	Yolanda	Belgium	<i>Langmuir-Blodgett films of lead chalcogenide quantum dots</i>
Kadari	Belkacem	Canada	<i>Luminescence of Silicon Nanocrystals</i>
Lee	Soo-Keun	Korea	<i>Preparation and characterization of coordination polymer particles with various aspect ratio</i>
Lim	Sang Kyoo	Korea	<i>Preparation and characterization of ZnO Nanofibers by Electrospinning</i>
Lopez	Kenia	Spain	<i>Squaramide Magnetic Iron Nanoparticles for the Selective Removal of Hg²⁺ Ions in Water</i>
Maia	Raquel	Portugal	<i>Development of nanostructured 3D matrices to direct mesenchymal stem cells behaviour</i>
Marques	Leonel	Portugal	<i>Carbon clathrates from fullerite under high pressure</i>
Mohiuddin	Mohammad	Canada	<i>Electrical resistance of CNT-peek composites under temperature and compression</i>
Morantz	Matthew	Canada	<i>Synthesis, Nanostructural and Electronic Characterization of Anthracenedicarboximide Derivatives.</i>
Morey	Jeroni	Spain	<i>Novel Hybrid Nanoparticles Based on Squaramides</i>
Nikolova	Liliya	Canada	<i>In-situ Observations of Amorphous Germanium Nucleation and Nanocrystallization by Dynamic Transmission Electron Microscopy</i>
Novais	Rui	Portugal	<i>Chemical functionalization of carbon nanotubes and its influence on composite properties</i>
Paiva	Diana	Portugal	<i>Fluorinated Cholesterol based system with DOTAP for DNA Transfection</i>
Paleo	Antonio J.	Portugal	<i>Nanoparticle induced phase transformation and dielectric response of core/shell Fe/MgO-poly(vinylidene fluoride) nanocomposites</i>
Paulo	Cristiana	Portugal	<i>Antifungal nanoparticles</i>
Peraza Hernandez	Jose F.	Spain	<i>Up-conversion and down-shifting in sol-gel derived glass-ceramics containing rare-earth doped SnO₂ and LaF₃ nanocrystals</i>

Presenting Author		Country	Poster Title
Peraza Hernandez	Jose F.	Spain	<i>Sol-gel derived nano-glass-ceramics comprising RE-doped KYF4 nanocrystals</i>
Pinto	Sara	Portugal	<i>Structural study of multilayers of Si1-xGex Nanocrystals embedded in SiO2 matrix</i>
Piñeiro	Yolanda	Spain	<i>Remote magnetic heating of smart thermoresponsive PNIPAM-Fe3O4 nanocomposites</i>
Prasek	Jan	Czech Republic	<i>Utilizing Vertically Aligned Carbon Nanotubes Based Working Electrodes for Detection of Heavy Metal Ions and Thiols</i>
Reis	Catarina	Portugal	<i>Design and transdermal delivery of indomethacin nanosystem</i>
Rivero Fuente	Pedro	Spain	<i>An antibacterial coating based on silver loaded in a polymer/sol-gel hybrid matrix</i>
Rodriguez-Abreu	Carlos	Portugal	<i>Fabrication of silica hollow microcoils with mesoporous walls</i>
Roussel	Florent	France	<i>1D polymer/CNT composite : elaboration and transport properties</i>
Ruiz Nicolas	Patricia	Spain	<i>Intermatrix synthesis: easy technique permitting preparation of polymer-stabilized nanoparticles with desired composition and structure.</i>
Samantilleke	Anura	Portugal	<i>Cohesive strength of ZnO:Ga thin films deposited at room temperature</i>
Samantilleke	Anura	Portugal	<i>Nanostructured hybrid ZnO thin films for energy conversion</i>
Santamarva	Pablo	Spain	<i>Effects of draw ratio on the structure and properties of polycarbonate films reinforced by an amorphous polyamide nanocomposite</i>
Silva Oliveira	Liliana Filipa	Portugal	<i>Development of photocatalytic nanomaterials for pollution control, using thin film deposition techniques (sol-gel, PVD)</i>
Suarez Guevara	Jullieth	Spain	<i>Hydrothermal Synthesis of Metal-Polymer Hybrid Nanostructures. Polypyrrole-coated Copper Nanocables</i>
Vieira	Eliana	Portugal	<i>Structural and electrical characterization of Si1-xGex nanocrystals embedded in Al2O3 matrix</i>
Xuriguera	Elena	Spain	<i>Study on oxidation layer of single core Nickel nanobeads</i>
Zabaleta	Asier	Spain	<i>Characterization and properties of polyamide 12 nanocomposites</i>
Zvatora	Pavel	Czech Republic	<i>Polytetrafluorethylene as a substrate for surface enhanced Raman spectroscopy</i>
TOPIC: Other			
Batista	Carlos	Portugal	<i>Synthesis and Characterisation of VO2-based Thermochromic Thin films for Energy Efficient Windows</i>
Cangueiro	Maguie	Portugal	<i>In vitro transdermal delivery of caffeine-loaded alginate particles</i>
Dubyanskiy	Sergey	Russia	<i>Russian Nanotechnology Foresight and Roadmapping in Russian Corporation of Nanotechnologies (RUSNANO)</i>

Presenting Author		Country	Poster Title
Garcia	Cibeli	Portugal	<i>Crystallographic Characterization of ZnO Thin Films by Electron Backscattered Diffraction</i>
Sergeyev	Daulet	Kazakhstan	<i>4e transport of a supercurrent in two-contact SQUID with anharmonic by current - phase dependence</i>
TOPIC: Scanning Probes Methods			
Diaz	Jordi	Spain	<i>Characterization of morphology, crystallization and melting behaviour of films of ethylene-vinyl acetate (EVA) by means of AFM and DSC</i>
Fu	Chaoying	Canada	<i>Self-assembly of oligothiophenecarboxylic acid monolayer by Scanning Tunneling Microscope (STM)</i>
Hosokawa	Yoshihiro	Japan	<i>Measurement of tip-sample interaction forces under infrared irradiation toward high-spatial-resolution infrared spectroscopy using FM-AFM</i>
Miyake	Yusuke	Japan	<i>Tunneling-current-induced light emission from chiral binaphthylene-perylenebis(carboxy)diimide dimer</i>
Piksova	katerina	Czech Republic	<i>SEM Imaging of Films of Metal Nanoparticles Deposited on Semiconductors</i>
Saenz-Arce	Giovanni	Spain	<i>Adhesion and Energy Dissipation on the Formation of One-Atom Contact on Au and Pb</i>
Schneider	Natalia	Germany	<i>Optical probe of quantum shot noise reduction at a single atom contact</i>
Valtr	Miroslav	Czech Republic	<i>Atomic force microscopy characterization of nanoparticles on rough surfaces</i>
TOPIC: Theory and Modelling at the Nanoscale			
Coluci	Vitor Rafael	Brazil	<i>Carbon nanotube oscillators driven by thermophoresis</i>
Gomes da Rocha	Claudia	Germany	<i>Modelling nanosensor devices based on graphene ribbons</i>
Li	Wu	Germany	<i>Phonon Transport in Large Scale Carbon-Based Disordered Materials: Implementation of an Efficient Order N and Real Space Kubo Methodology</i>
Martin-Martinez	Francisco	Spain	<i>Energetic destabilization causes in carbon nanotubes with topological defects</i>
Molina Brito	Bertha	Mexico	<i>Theoretical Analysis of the Electronic Properties of the Endohedral Clusters M@Al₁₂ (M= B, Al, Si, N, P) and their ions</i>
Mostofi	Mehdi	Iran	<i>Variable Physical Properties Effect on Velocity and Potential Distribution in a Nanotube with Large Zeta Potential</i>
Perez	Jorge	Spain	<i>Melting temperature of icosahedral metallic nanowires</i>
Sedighi	Amir	Germany	<i>Molecular simulation of dendritic core multi shell(CMS) nanotransporter</i>
Shen	Jing	France	<i>Formation and properties of iron nanoparticles for nucleating CNTs in floating-catalyst CVD process</i>

NOTES

science • industry • society

IMAGINENANO

Bringing together
Nanoscience and Nanotechnology

April 11-14, 2011 - Bilbao Exhibition Centre (Spain)

www.imagenenano.com

ImagineNano will comprise 6 parallel international conferences,
a huge industrial exhibition and a social event where everyone
can meet and greet Nanotechnology side by side



- Graphene 2011
- nanoBio&Med 2011
- NanoSpain 2011 - NanoSudoe (Spain, Portugal & France)
- TNA Energy 2011 Trends in NanoApplications
- PPM 2011 Photonics/Plasmonics/Magneto-Optics
- HPC-NN2011 High-Performance-Computing



ONE Place: 6 Conferences, 1 Industrial Exhibition and Societal Activities.